

# ***Bohayella rodrigodiaz* sp. nov.: a new species from Ecuador with an updated key to the New World species of *Bohayella* Belokobylskij (Hymenoptera, Braconidae, Cardiochilinae)**

Ilgoo Kang<sup>1</sup>

<sup>1</sup> Department of Entomology, Louisiana State University Agricultural Center, 404 Life Sciences Building, Baton Rouge, LA, 70803 USA

Corresponding author: Ilgoo Kang ([ikang1@lsu.edu](mailto:ikang1@lsu.edu))

Academic editor: J. Fernandez-Triana | Received 5 November 2021 | Accepted 18 December 2021 | Published 28 February 2022

<http://zoobank.org/DB15BFFD-B4AC-419E-8FAB-8E74D8B08570>

**Citation:** Kang I (2022) *Bohayella rodrigodiaz* sp. nov.: a new species from Ecuador with an updated key to the New World species of *Bohayella* Belokobylskij (Hymenoptera, Braconidae, Cardiochilinae). Journal of Hymenoptera Research 89: 1–8. <https://doi.org/10.3897/jhr.89.77687>

## **Abstract**

The New World species of *Bohayella* Belokobylskij, 1987 are revised based on morphological data, and a new species of the genus from Ecuador is described: *Bohayella rodrigodiaz* Kang, **sp. nov.** This work includes an updated identification key to species of *Bohayella* in the New World along with images of diagnostic characters. The number of recorded *Bohayella* species in the New World is increased from two to three.

## **Keywords**

Melanism, Neotropical region, parasitoid wasp, taxonomy

## **Introduction**

Ecuador has 228 braconid species recorded (Yu et al. 2016), including two members of the subfamily Cardiochilinae Ashmead, 1900 recorded by Fischer (1958) as *Cardiochiles aterrimus* Fischer and *C. purpureus* Fischer. A small genus of

cardiochilines, *Bohayella* Belokobylskij (Belokobylskij 1987) contains eleven species worldwide. Among these species, two recently described new species occur in lowland and cloud forests of Costa Rica, *B. geraldinae* Kang and *B. hansonii* Kang (Kang et al. 2020). Host records of two Old World species, *B. adina* (Wilkinson) and *B. exiguura* (Huddleston & Walker), were provided by Beeson and Chatterjee (1935), Huddleston and Walker (1988), and Dangerfield et al. (1999). Unfortunately, nothing is known about biology of New World members of the genus. The validity of the genus was corroborated by phylogenetic data in Dangerfield et al. (1999), based solely on morphological data, and again by Murphy et al. (2008) based on molecular data. These data indicate that *Bohayella* species form a monophyletic group. A new species of Ecuadorian *Bohayella* is described herein, the key to species in the New World is updated, and a distribution map for the new species is provided.

## Materials and methods

### Specimens

Specimens for this project were borrowed from the Texas A&M University Insect Collection (TAMU; College Station, Texas, USA) and University of Wyoming Insect Museum (UWIM; Laramie, Wyoming, USA). Holotype and paratypes of the new species will be housed in TAMU.

### Morphological analysis and morphometric characters

Morphological characters were examined using a Leica MZ75 stereomicroscope. Morphometric characters were measured using Adobe Photoshop CS 6 (Adobe Systems, Inc). Numbers in parentheses in a species description indicate  $0.01 \times$  the actual size of each body part. The unit of length used in the current work is mm.

### Terminology

Morphological terms and terms for wing venation used are largely based on those of Dangerfield et al. (1999) and Sharkey and Wharton (1997). Terms for surface sculpturing follow Harris (1979). Most terms used in the current work can be also confirmed on the Hymenoptera Anatomy Ontology website (<http://portal.hymao.org/projects/32/public/ontology/>). The following acronyms are used throughout: POL: distance between posterior ocelli, T1: first metasomal tergite, T2: second metasomal tergite, T3: third metasomal tergite, T4: fourth metasomal tergite, and T8: eighth metasomal tergite.

### Imaging and image processing

Images were initially captured using a Visionary Digital BK Plus imaging system (Dun, Inc.), equipped with a Canon EOS 5DS DSLR camera. Image stacking was performed using Zerene Stacker v.1.04 (Zerene Systems LLC.). Images were edited using Adobe Photoshop CS 6 or Adobe Photoshop CC 2019 (Adobe Systems, Inc), and image plates were generated using the same software.

## Results

### Taxonomy

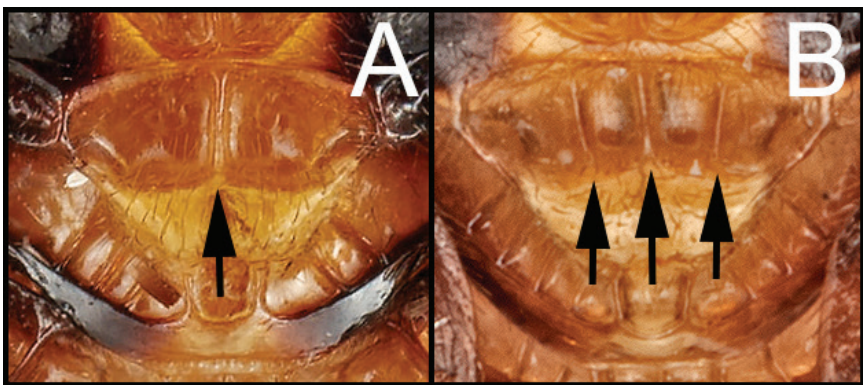
#### *Bohayella* Belokobylskij, 1987

**Type species.** *Bohayella tobiasi* Belokobylskij

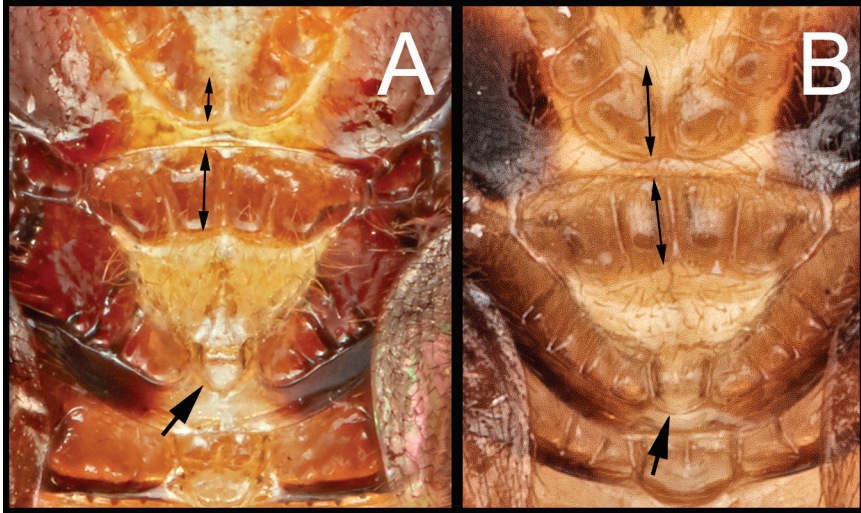
**Diagnosis.** Detailed diagnostic characters were described by Belokobylskij (1987), Dangerfield et al. (1999), and Kang et al. (2020). The genus is easily recognized by the following characters: Body small in size. Eyes with interommatidial setae, length and density of setae variable. Clypeal tubercles absent. Mouthparts short. Occipital carina absent. Mesonotum and mesopleuron strongly sculptured. Scutellum with apical cup-like pit. Epicnemial carina present. Median areola of propodeum fully developed. Metatibia without apical projection. Claws pectinate. Elongate and narrow T1 > 4.00 ×). T2 short and with a ball-like projection medio-basally. Hypopygium short and obtuse apically. Short ovipositor and ovipositor sheath (~0.20 × the length of metatibia).

#### Key to species of New World *Bohayella*

- 1        A. Scutellar sulcus with a median crenula..... *B. geraldinae*
- B. Scutellar sulcus with three crenulae ..... 2



- 2 A. Median crenula of notauli apparently shorter than median crenula of scutellar sulcus; apical cup-like pit of scutellum with V-shape posterior margin .....*B. hansonii*
- B. Median crenula of notauli slightly shorter than median crenula of scutellar sulcus; apical cup-like pit of scutellum with U-shape posterior margin .....  
..... *B. rodrigodiazii* Kang, sp. nov.



*Bobayella geraldinae* Kang, 2020

**Material examined.** *Holotype* Costa Rica • ♀; Heredia, 3 km S. Puerto Viejo OTS, La Selva; 100 m; Oct.1992; P. Hanson leg.; Huertos, Malaise trap set by G. Wright. *Paratypes* Costa Rica • 1 ♀; same data as for holotype; Nov. 1992 • 1 ♂; same collecting data as for preceding; 10°26'N, 84°01'W; 4, Apr. 1987; H. A. Hespeneide leg.

**Diagnosis.** Specimens of *B. geraldinae* are distinguished from Old World members by having angled RS and acute apical tooth on claws, and the members of *B. geraldinae* are distinct from the members of *B. rodrigodiazii* sp. nov. by having scutellar sulcus with one median crenula; apical maxillary palpomere as long as penultimate maxillary palpomere; median length of T1 ~5.10 × longer than apical width; T2 medially 0.21 × longer than T1; metasomal tergites generally pale but melanic apically.

**Description.** See Kang et al. (2020).

**Male.** See Kang et al. (2020).

**Host.** Unknown.

**Distribution.** Costa Rica (La Selva Biological Station).

*Bobayella hansonii* Kang, 2020

**Material examined.** *Holotype* Costa Rica • ♀; Puntarenas, San Vito, Estac. Biol., Las Alturas; 1,500 m; Jun. 1992; Paul Hanson leg.; traps #1 + #2, Malaise. *Paratypes*

Costa Rica • 2 ♀; same data as for holotype • 2 ♀; same collecting data as for preceding • 1 ♀; same collecting data as for preceding; 1,700 m; 11, Apr. 1993.

**Diagnosis.** Members of *B. hansonii* may be distinct from Old World members by having angled RS and acute apical tooth on claws and the members of *B. hansonii* are distinguished from the members of *B. rodrigodiazzi* sp. nov. by the following characters: median crenula of notauli shorter than median crenula of scutellar sulcus; apical cup-like pit of scutellum with V-shape posterior margin; metafemur  $\sim 0.31 \times$  longer than its length; metabasitarsus cylindrical; median length of T1  $4.00 \times$  longer than apical width; T2 melanic; T3  $\sim 2.55 \times$  longer than T2 medially.

**Description.** See Kang et al. (2020).

**Male.** Unknown.

**Host.** Unknown.

**Distribution.** Costa Rica (Las Alturas Biological Research Station).

***Bohayella rodrigodiazzi* Kang, sp. nov.**

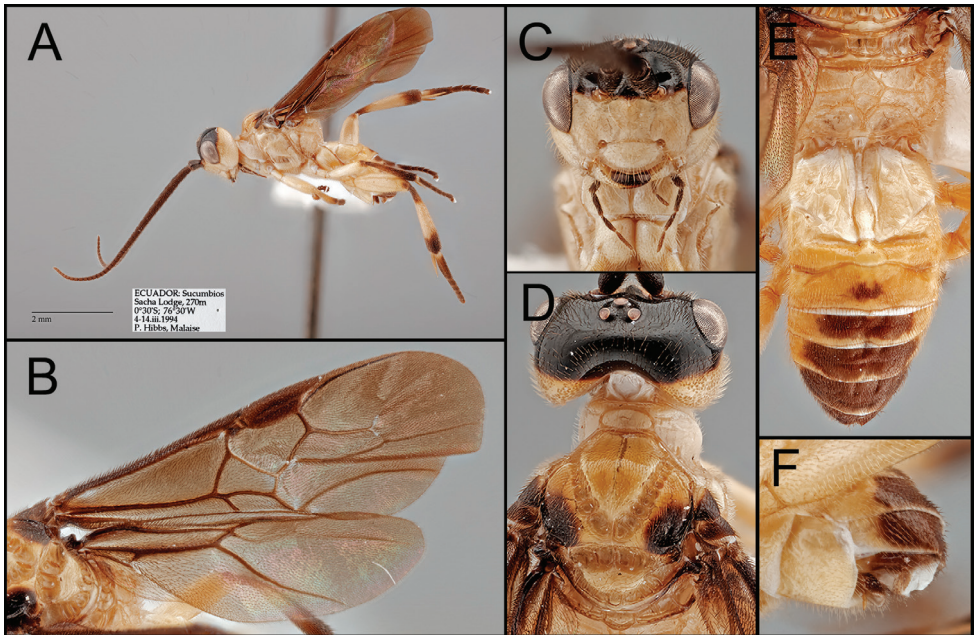
<http://zoobank.org/CD40E5E1-EF61-4F02-B960-100859706FEE>

Fig. 1A–F

**Material examined.** *Holotype* Ecuador • ♀; female, Sucumbíos, Rio Napo, Sacha Lodge;  $0^{\circ}30'S$ ,  $76^{\circ}30'W$ , 270 m; 4–14, Mar. 1994; Malaise trap; P. Hibbs leg. *Paratypes* Ecuador • 1 ♀; same data as for holotype;  $78^{\circ}30'W$ ; 220–230 m; 12–22, Jun. 1995. • 1 ♀; same collecting data as for preceding (Note: According to the GPS coordinates, Sacha Lodge is located near  $0^{\circ}30'S$ ,  $76^{\circ}30'W$ ).

**Diagnosis.** *B. rodrigodiazzi* sp. nov. can be distinguished from *B. geraldinae* by the following characters: apical maxillary palpomere slightly longer than penultimate maxillary palpomere; scutellar sulcus with three crenulae; median length of T1  $\sim 4.78 \times$  longer than apical width; T2 medially  $\sim 0.31 \times$  longer than T1; T4 medially melanic. *B. rodrigodiazzi* sp. nov. can be distinguished from *B. hansonii* by the following characters: median crenula of notauli as long as median crenula of scutellar sulcus (Fig. 1D); apical cup-like pit of scutellum with U-shape posterior margin (Fig. 1D); metabasitarsus antero-posteriorly slightly expanded; T1  $\sim 4.78 \times$  longer than apical width; ball-like projection of T2 pale (Fig. 1E); T3  $\sim 1.81 \times$  longer than T2 medially.

**Description.** Body  $\sim 4.95$ – $\sim 5.06$  mm. Forewing length:  $\sim 4.46$  mm. Hindwing length:  $\sim 3.50$  mm. Antenna length:  $\sim 4.84$ – $\sim 5.11$  mm. **Head.** Antenna 33–34-segmented. Interantennal space with median carina. POL  $\sim 1.31 \times$  longer than diameter of anterior ocellus (17:13). Eye sparsely setose with minute setae; length of eye  $0.78 \times$  longer than median width of gena in lateral view (39:50). Gena ventro-posteriorly extended into moderate prominence. Width of clypeus  $2.04 \times$  longer than height (49:24). Malar space  $\sim 1.83 \times$  longer than basal width of mandible (22:12). Mandible bidentate. Maxillary palpus five segmented; apical maxillary palpomere  $\sim 1.11 \times$  longer than penultimate maxillary palpomere (21:19). **Mesosoma.** Mesoscutum with sharp margin. Notauli broadly converging at base, with eleven crenulae; median crenula of notauli  $\sim 0.82 \times$  longer than median crenula of scutellar sulcus



**Figure 1.** *Bobayella rodrigidiazi* sp. nov. **A** lateral habitus **B** wings **C** anterior head **D** dorsal head and mesonotum **E** dorsal propodeum and metanotum **F** latero-ventral hypopygium.

(18:22). Scutellar sulcus with three crenulae. Apical cup-like pit of scutellum with U-shape posterior margin. Postscutellar depression present. Propodeum rugulose; median areola of propodeum apparent; median transverse carina of the propodeum reaching lateral margin. Pronotum anteriorly smooth and posteriorly crenulate. Mesopleuron dorsally and posteriorly with crenulate margin. Epicnemial carina present medially. Metapleuron anteriorly smooth and posteriorly crenulate. **Legs.** Basal spur on protibia  $\sim 0.76 \times$  longer than basitarsus (34:45). Basal spur on mesotibia  $\sim 0.89 \times$  longer than basitarsus (42:47). Width of metafemur  $\sim 0.34 \times$  longer than its length (46:135). Basal spur on metatibia  $\sim 0.82 \times$  longer than basitarsus (65:79). Metatarsal claw pectinate. **Wings.** Forewing second submarginal cell trapezoidal,  $\sim 0.35 \times$  longer than its maximum width (30:86); 3r absent; RS sharply angled at basal third; stigma  $\sim 3.31 \times$  longer than medial width (116:35); 1CUa short,  $0.26 \times$  longer than 1Cub (13:50). Hind wing 2–1A absent. **Metasoma.** T1 with a pair of lateral sutures posteriorly reduced, median length of T1  $\sim 4.78 \times$  longer than apical width (67:14). T2 with a ball-like projection, medially  $\sim 0.31 \times$  longer than T1 (21:67). T3  $\sim 1.81 \times$  longer than T2 medially (38:21). Protruded ovipositor sheath  $\sim 0.15 \times$  longer than Metatibia and apically setose (26:174).

**Color.** Body mostly pale; the following areas darker: antenna, vertex, frons, dorsal occiput, labrum, mandible apically, maxillary palpus, labial palpus, lateral mesonotal lobe posteriorly, tegula, margin of metanotum posteriorly, apical protibia, protarsus,

apical mesofemur, mesotibia, mesotarsus, apical metafemur, basal and apical metatibia, apical metatarsus mostly, T4–T8 (one specimen with melanic T3 medially), ovipositor sheath. Wings entirely infuscate, stigma darker.

**Male.** Unknown.

**Host.** Unknown.

**Distribution.** *B. rodrigodiaz* sp. nov. is known only from Sacha Lodge, Rio Napo, Sucumbíos, Ecuador at the elevations of 220m and 270m.

**Etymology.** This species is named in honor of Dr Rodrigo Diaz, Associate Professor of biological control in the Department of Entomology, Louisiana State University. He is the PhD advisor of the author of this paper (IK) and originally from Quito, Ecuador.

## Discussion

*Bohayella rodrigodiaz* sp. nov. is the third species of *Bohayella* recorded from the New World. The three species of New World *Bohayella* have similar body coloration, but their dorsal metasomal colors are diagnostic and may be correlated to the altitudes of their habitats. Specimens of *B. geraldinae* collected at altitudes of ~100m possess the palest tergites among the three species. Specimens of *B. rodrigodiaz* sp. nov. collected at the altitudes of ~250m have darker tergites than the members of *B. geraldinae* and paler tergites than specimens of *B. hansonii*. Specimens of *B. hansonii* collected at the altitudes above 1,500m possess the darkest tergites of the three species. This corresponds with the observations by Kang et al. (2020) that melanism of New World *Bohayella* species is associated with elevation. This pattern has been noted in other wasps by de Souza et al. (2020), Fernandez-Triana et al. (2014), and Mora and Hanson (2019). Also, melanism correlated with altitudinal gradient has recently been reported in dung beetles by Stanbrook et al. (2021). It is probable that there are a number of undescribed species of *Bohayella* as yet undiscovered in the neotropics.

## Acknowledgements

First of all, IK would like to thank Dr Michael Sharkey, academic father, for his continuous advice. Also, IK is grateful to Drs Scott Shaw in UWIM and Karen Wright in TAMU for specimen loans. Among people at LSU, IK would like to acknowledge PhD committee members, Drs Chris Carlton, Michael Kaller, and Qian “Karen” Sun, for their encouragement, the Department Head, Dr Michael Stout, for his support, Ms Victoria Bayless, for her invaluable advice, and Diaz’s lab members for their help and friendship. Lastly, IK is grateful to the Department of Entomology as well as LSU Agricultural Center for financial support.

## References

- Beeson CF, Chatterjee SN (1935) On the biology of the Braconidae (Hymenoptera). Indian Forest Records 1: 105–138.
- Belokobylskij SA (1987) A new genus of the subfamily Cardiochilinae (Hymenoptera, Braconidae) from the USSR Far East. Zoologicheskij Zhurnal 66(2): 302–304.
- Dangerfield PC, Austin AD, Whitfield JB (1999) Systematics of the world genera of Cardiochilinae (Hymenoptera: Braconidae). Invertebrate Systematics 13(6): 917–976. <https://doi.org/10.1071/IT98020>
- de Souza AR, Mayorquin AZ, Sarmiento CE (2020) Paper wasps are darker at high elevation. Journal of Thermal Biology 89: e102535. <https://doi.org/10.1016/j.jtherbio.2020.102535>
- Fernandez-Triana JL, Whitfield JB, Smith MA, Hallwachs W, Janzen DH (2014) Revision of the neotropical genus *Sendaphne* Nixon (Hymenoptera, Braconidae, Microgasterinae). Journal of Hymenoptera Research 41: 1–29. <https://doi.org/10.3897/JHR.41.8586>
- Hymenoptera Anatomy Consortium (2021) Hymenoptera Anatomy Consortium. <http://glossary.hymao.org> [Accessed on Oct 2021]
- Harris RA (1979) Glossary of surface sculpturing. Occasional Papers in Entomology 28: 1–31.
- Huddleston T, Walker AK (1988) *Cardiochiles* (Hymenoptera: Braconidae), a parasitoid of lepidopterous larvae, in the Sahel of Africa, with a review of the biology and host relationships of the genus. Bulletin of Entomological Research 78(3): 435–461. <https://doi.org/10.1017/S0007485300013201>
- Kang I, Shaw SR, Lord NP (2020) Two new species and distribution records for the genus *Bohayella* Belokobylskij, 1987 from Costa Rica (Hymenoptera, Braconidae, Cardiochilinae). ZooKeys 996: 93–105. <https://doi.org/10.3897/zookeys.996.59075>
- Mora R, Hanson PE (2019) Widespread Occurrence of Black-Orange-Black Color Pattern in Hymenoptera. Journal of Insect Science 19(2): 13: 1–12 <https://doi.org/10.1093/jisesa/iez021>
- Murphy N, Banks JC, Whitfield JB, Austin AD (2008) Phylogeny of the parasitic microgasteroid subfamilies (Hymenoptera: Braconidae) based on sequence data from seven genes, with an improved time estimate of the origin of the lineage. Molecular Phylogenetics and Evolution 47(1): 378–395. <https://doi.org/10.1016/j.ympev.2008.01.022>
- Sharkey MJ, Wharton RA (1997) Morphology and terminology. In: Wharton RA, Marsh PM, Sharkey MJ (Eds) Manual of the New World genera of the family Braconidae (Hymenoptera). Special Publication of the International Society of Hymenopterists, No 1, Washington DC, 19–37.
- Stanbrook RA, Harris WE, Wheeler CP, Jones M (2021) Evidence of phenotypic plasticity along an altitudinal gradient in the dung beetle *Onthophagus proteus*. PeerJ 9: e10798. <https://doi.org/10.7717/peerj.10798>
- Wilkinson DS (1930) New species and host records of Braconidae. Bulletin of Entomological Research 21: 481–487. <https://doi.org/10.1017/S0007485300024822>
- Yu DS, Achterberg C van, Horstmann K (2016) Taxapad, Ichneumonoidea. Vancouver, Canada. <http://www.taxapad.com>

# Inclusion of an alien species in the host range of the Neotropical parasitoid *Hymenoepimecis bicolor* (Brullé, 1846) (Hymenoptera, Ichneumonidae)

Marcelo O. Gonzaga<sup>1</sup>, Diego G. Pádua<sup>2</sup>, Adilson Quero<sup>3</sup>

**1** Instituto de Biologia, Universidade Federal de Uberlândia, Uberlândia, MG, Brazil **2** Programa de Pós-Graduação em Entomologia, Instituto Nacional de Pesquisas da Amazônia, Coordenação de Biodiversidade, Manaus, AM, Brazil **3** Pós-graduação em Ecologia e Conservação de Recursos Naturais, Universidade Federal de Uberlândia, Uberlândia, MG, Brazil

Corresponding author: Marcelo O. Gonzaga ([mogonzaga@yahoo.com.br](mailto:mogonzaga@yahoo.com.br))

---

Academic editor: Gavin Broad | Received 15 October 2021 | Accepted 8 February 2022 | Published 28 February 2022

---

<http://zoobank.org/88C6FAD0-F020-44BA-93E4-8915BE4E36E9>

---

**Citation:** Gonzaga MO, Pádua DG, Quero A (2022) Inclusion of an alien species in the host range of the Neotropical parasitoid *Hymenoepimecis bicolor* (Brullé, 1846) (Hymenoptera, Ichneumonidae). Journal of Hymenoptera Research 89: 9–18. <https://doi.org/10.3897/jhr.89.76620>

---

## Abstract

In this study we report the first case of an introduced alien host spider species being parasitized and manipulated by an ichneumonid wasp. *Hymenoepimecis bicolor*, previously described parasitizing exclusively *Trichonephila clavipes* (Araneidae), was observed parasitizing the European species *Cyrtophora citricola* (Araneidae) in southeastern Brazil. The cocoon web built by the parasitized spider is composed of a reduced horizontal sheet, which maintains the radial structure. The reduced number of radii and spirals probably reduce the chances of insect interception by these modified structures. In addition, the density of supporting threads is apparently very different between normal and modified webs. The cocoon web spun by *C. citricola* lacks the protective barrier structure usually observed in cocoon webs spun by parasitized females of *T. clavipes*. Our observations are in agreement with several predictions of the ecdysteroid hypothesis and represent an interesting opportunity for further investigation of interactions between these parasitoids and their spider hosts.

## Keywords

Host behavioral manipulation, host-parasitoid interactions, introduced species

## Introduction

*Hymenoepimecis* Viereck, 1912 is a genus of parasitoid wasps included in the *Polysphincta* group of genera, members of which are usually referred to as ‘polysphinctines’ (Hymenoptera, Ichneumonidae, Pimplinae) (Matsumoto 2016). The genus currently comprises 27 species, all of which are restricted to the Neotropical region (Yu et al. 2016; Pádua et al. 2020). Most species were previously reported to parasitize only one host species, but three species have been found to attack two host spiders each: *H. heidyae* Gauld, 1991: *Kapogea cyrtophoroides* (F. O. Pickard-Cambridge, 1904) and *K. sexnotata* (Simon, 1895) (Araneidae); *H. japi* Sobczak et al., 2009: *Leucauge roseosignata* Mello-Leitão, 1943 (Tetragnathidae) and *Mecynogea bigibba* Simon, 1903 (Araneidae); *H. veranii* Loffredo & Pentead-Dias, 2009: *Araneus omnicolor* (Keyserling, 1893) and *A. orgaos* Levi, 1991 (Araneidae) (Gonzaga and Sobczak 2007; Sobczak et al. 2014; Barrantes et al. 2018; Eberhard and Gonzaga 2019). The apparent specificity in the host-parasitoid interactions in the other cases, however, may be a consequence of a lack of information, since parasitoid behaviour has usually been described based on few observations. Conversely, host immobilization and manipulation during the egg laying process of polysphinctines usually involve specific approaching behaviors (see Gonzaga and Sobczak 2007; Takasuka et al. 2009; Kloss et al. 2016) and wasps seems to be very selective on host size (Gonzaga and Sobczak 2007). These factors may reduce the availability of the potential hosts. In addition, most reports of the interactions between *Hymenoepimecis* and their hosts indicate that spiders change their web-building behaviors because of the action of late instar wasp larvae, possibly through the inoculation of the hormone ecdysone or some precursor of this hormone (see Kloss et al. 2017; Eberhard and Gonzaga 2019). These changes result in modified cocoon webs with particular designs, and the survival of pupae of each parasitoid species may depend on specific designs obtained from their hosts. This may be another factor driving host specificity.

To date, all spiders reported as hosts of *Hymenoepimecis* are species native to the geographic range of the parasitoids. In this study we report the first case of a recently introduced host species (*Cyrtophora citricola* (Forsskål, 1775), Araneidae) that was attacked and had its web building behavior altered by a parasitoid previously reared only from a native host spider. We compared the structure of the cocoon web built by the parasitized host with that of normal webs. Additionally, we searched for egg parasitoids of *C. citricola* in two localities in Brazil, namely Uberlândia (MG) and Volta Redonda (RJ), in order to describe possible new interactions between other native parasitoids and this potential new host.

*Hymenoepimecis bicolor* has a wide geographical distribution, occurring from the Amazon basin (Pádua et al. 2015; Sobczak et al. 2018) to the southern region of Brazil (pers. obs.). This species was previously observed to attack *Trichonephila clavipes* (Linnaeus, 1767) (Araneidae) in Serra do Japi, state of São Paulo (Gonzaga et al. 2010), as well as in several other Brazilian localities, such as Uberlândia (MG), Palmas (TO) and Cascavel (RS) (pers. obs.). The wasp performs direct attacks (Sobczak 2013) after

hovering around the potential host, grasping the spider and introducing the ovipositor into the mouth of the host. The host is then paralyzed, while the wasp searches for and damages eggs previously attached by other individuals, finally depositing her own. The cocoon web spun by the spider shortly before being killed by the parasitoid larva is reduced, lacks spirals, and often presents barrier threads in a position close to that later occupied by the wasp cocoon.

The original distribution of *Cyrtophora citricola* includes Southern Europe, Africa, the Middle East, Pakistan, India, China, and Japan (World Spider Catalog 2022). Levi (1997) reported the first record of individuals collected in South America, in Valle del Cauca, Colombia. The first well-documented record of this species in Brazil was made by Álvares and De Maria (2004), who reported specimens collected in the municipalities of Belo Horizonte (19°52'S, 43°58'W) and Prudente de Morais (19°30'S, 43°07'W), both in the state of Minas Gerais. The specimens examined by these authors were collected in 2000 and 2001. Another possible previous record was made by Alves-Costa and Gonzaga (2001) during a study conducted in August 1998, in an area 80 km north of Manaus (2°30'S, 60°00'W), Amazonas State. These authors identified one of the species included in the study as *Cyrtophora* sp. (possibly *C. citricola*) based on juveniles and the shape of the webs. Later, Álvares and De Maria (2004) mentioned that they searched unsuccessfully for these specimens in the collection of the Instituto Nacional de Pesquisas da Amazônia (INPA) to confirm the identification.

## Methods

We found three cocoon webs of *C. citricola* in Volta Redonda, RJ. The first one was attached to the branches of a tree (*Anadenanthera colubrina*, Fabaceae), at a height of approximately 2.5 m from the ground, close to a small river within the urban area (22°31'24.17"S, 44°05'42.62"W). The other two were located within the area of the city zoo (Zoológico Municipal de Volta Redonda) (22°31'56.18"S, 44°06'12.74"W), attached to perennial shrubs (*Euphorbia milii*, Euphorbiaceae), both at heights of about 1 m. The first cocoon web was discovered on August 8, 2019 and the second on July 16, 2021. We located eight other webs of unparasitized individuals of *C. citricola* in a transect of 5 × 200 m from the site where we found the first cocoon web, on the same day. All egg sacs of these spiders were collected. The cocoon web was photographed and the cocoon was carefully removed and maintained in the laboratory until the emergence of the adult wasp. The second cocoon was collected from a damaged web and we kept the cocoon in the laboratory until the emergence of the adult, but no information was collected on the web structure. The third cocoon web had a larva in its last instar attached by its dorsal tubercles on a web thread. We observed the beginning of cocoon construction by the larva and collected the cocoon 24 hours later to rear the adult wasp in the laboratory.

The egg sacs of another 35 spiders were collected in Uberlândia (18°57'11.37"S, 48°17'15.70"W), MG. This additional sampling was conducted two weeks after col-

lecting the first cocoon (in August 2019), searching for parasitized individuals in another population of *C. citricola* (located about 1000 km from the first locality). All the egg sacs (77 from Uberlândia and eight from Volta Redonda) were opened in the laboratory and the egg masses were dissected to locate and identify possible egg parasitoids. We also counted the numbers of eggs inside 36 of those 77 egg sacs from Uberlândia ( $120.4 \pm 79.9$  [39 – 366] (mean  $\pm$  sd [min – max])).

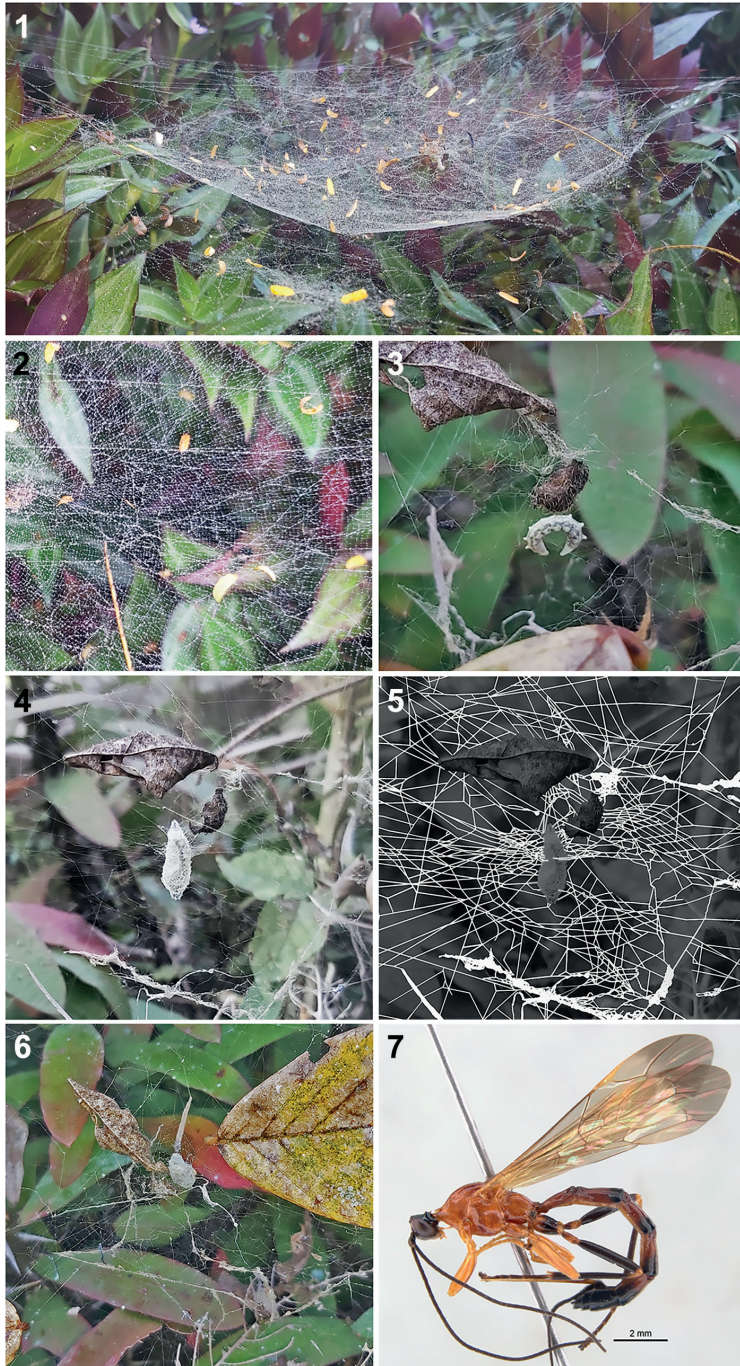
Photographs of normal and cocoon webs spun by *Trichonephila clavipes*, for comparison with webs spun by *C. citricola*, were previously obtained during studies conducted in 2010 in Serra do Japi, Jundiá, SP, Brazil. The *H. bicolor* images were taken using a Leica DMC4500 digital camera attached to a Leica M205A stereomicroscope and multiple layers were stacked by using the software Helicon Focus 5.3 Pro.

## Results

The general structure of the cocoon webs of *C. citricola* differs from those of normal webs, including the reduction of the fine meshed sheet of dry silk, which is always present in webs of unparasitized individuals (Figs 1, 2). The larva consumed the spider at the same location occupied by the host while in its resting position, just below the center of the horizontal radial structure. Its dorsal tubercles then attached to the supporting threads located just above this position (Fig. 3). The cocoon was constructed and remained connected to several radii (Figs 4–6). The *H. bicolor* collected just after cocoon construction emerged as an adult female 15 days later (Fig. 7). Females of *C. citricola* produced  $120.4 \pm 79.9$  eggs (mean  $\pm$  sd), but we did not find any egg parasitoids or egg predators within these egg masses.

## Discussion

The observation reported here is, as far as we know, the first record of a recently introduced alien host being parasitized by a species of *Hymenoepimecis* (Eberhard and Gonzaga 2019). One idiosyncrasy of the interaction between *H. bicolor* and its native host, *T. clavipes*, is that adult and sometimes subadult host females are much larger than the juveniles usually attacked (Sobczak 2013). Consequently, when most spiders within a population reach body sizes above the ideal, there is a pressure for wasps to attack unsuitable individuals (specifically large and potentially dangerous females or small adult males). In fact, Sobczak (2013) observed *T. clavipes* males carrying two larvae of *H. bicolor*. The same pressure may have directed the first attempts of *H. bicolor* to parasitize *C. citricola*, a new potential host within the size range usually selected for oviposition. In addition, individuals of both host species do not construct any form of shelter in their webs, remaining exposed during the day.



**Figures 1–7.** **1** normal web structure of *Cyrtophora citricola* **2** detail of the fine meshed sheet of dry silk of a normal web. **3** larva in its last instar, attached to the web by the dorsal hooks **4, 5** frontal view of a cocoon web with a cocoon attached (in **5** the web threads are highlighted) **6** upper view of the same cocoon web **7** female of *Hymenoepimecis bicolor*.

The selection of a new host species is an interesting occurrence because it has implications for our understanding of the plasticity of attacking and subduing behaviors of these wasps and in the mechanism of host behavior manipulation. New interactions between this introduced species and native egg parasitoids or predators, however, were not observed in the studied populations. Currently, records of egg parasitism of *C. citricola* are restricted to Europe (by *Philolema palanichamyi* Narendran, 1994 – Eurytomidae, and *Pediobius pyrgo* (Walker, 1839) – Eulophidae) (Chuang et al. 2019) and to Yemen (by *Eurytoma cyrtophora* Zerova et al., 2008 – Eurytomidae) (Zerova et al. 2008, but see Chuang et al. 2019 on this identification). Further sampling of Brazilian populations will be conducted to investigate the possibility of the establishment of such interactions.

Manipulation of host *T. clavipes* behavior by *H. bicolor* usually results in cocoon webs presenting barrier threads surrounding the position originally occupied by the spider (Gonzaga et al. 2010) (Figs 8, 9). In the two-dimensional normal orb webs of unparasitized individuals, this position is usually exposed (Fig. 8). The increased complexity of this region may be important to reduce cocoon susceptibility to predators and/or hyperparasitoids, and also to increase stability of the web during the wasp's development, as the cocoon is suspended from the web. This new protective component is absent from cocoon webs spun by *C. citricola*. In this case, however, the position occupied by the cocoon is already surrounded by several supporting threads in the normal webs and the connection of the cocoon to the radial threads ensures its stability. As in cocoon webs of *T. clavipes*, the reduction of web components associated with prey interception and retention is the main characteristic of cocoon webs spun by *C. citricola*. This alteration may reduce the risks of web destruction by struggling insects and is often observed in cocoon webs spun by several hosts of polysphinctines (e.g., Eberhard 2000; Gonzaga and Sobczak 2007, 2011; Korenko et al. 2015; Gonzaga et al. 2016).

Eberhard and Gonzaga (2019) listed eight theoretical predictions derived from the ecdysteroid hypothesis (i.e., modifications in web structure induced by parasitoids included in the *Polysphincta* genus group occur as an effect of the injection of ecdysteroids or some precursor of this substance). The case described here corroborates at least four of these predictions: i) strict host species specificity in the wasps should be rare; ii) the phylogenies of the wasps and the spiders that they parasitize should differ; iii) wasps of a single species should induce cocoon web designs that differ widely when they parasitize spiders with different natural histories; and iv) cocoon web design should be adjusted appropriately to the natural history of the spider species to provide protection. A fifth prediction is that cocoon webs should provide increased stability or protection for the cocoon of the wasp. We cannot be sure about this prediction based on a few observations, but the apparently stable structure of *C. citricola* webs likely requires little modification to offer protection to the cocoon (unlike the bidimensional design of *T. clavipes* webs). As previously mentioned, however, the cocoon remains suspended by several threads of the radial structure and probably is subject to a relatively reduced risk of damage or falling due to the action of intercepted insects. Further observation and experimental studies on this new system will clarify the generality of this finding and provide additional relevant information on the extension and limits of manipulation in this particular case.



**Figures 8–9.** 8 normal web of *Trichonephila clavipes* 9 cocoon of *H. bicolor* attached to a cocoon web spun by *Trichonephila clavipes* (photographs previously obtained in Serra do Japi, Jundiá, SP).

## Funding information

Conselho Nacional de Desenvolvimento Científico e Tecnológico (proc. 310477/2020-4)  
Fundação de Apoio à Pesquisa do Estado de Minas Gerais (APQ-02984-17)  
Instituto Nacional de Ciência e Tecnologia dos Hymenoptera Parasitoides (HYM-PAR - CNPq/CAPES/FAPESP)  
Programa de Pesquisas Ecológicas de Longa Duração (CAPES-CNPq-PELD: Proc. 441225/2016-0)  
Coordenação de Aperfeiçoamento de Pessoal de Nível Superior – Brasil (CAPES), Finance Code 001.

## Acknowledgements

We thank the Invertebrate Collection of INPA for the possibility to use the layer-photo equipment and Natália O. Leiner for assistance in field work. We also thank Almir Fraga Folly Júnior for allowing the samplings conducted in the area of the city zoo of Volta Redonda.

## References

- Álvares ESS, De Maria M (2004) First record of *Cyrtophora citricola* (Forsk.) in Brazil (Araneae, Araneidae). *Revista Brasileira de Zoologia* 21: 155–156. <https://doi.org/10.1590/S0101-81752004000100026>
- Alves-Costa C, Gonzaga MO (2001) Prey capture and spatial distribution of *Philoponella vittata* (Araneae, Uloboridae) in host webs. *Ethology Ecology & Evolution* 13: 239–246. <https://doi.org/10.1080/08927014.2001.9522773>
- Barrantes G, Segura-Hernández L, Solano-Brenes D, Hanson P (2018) When a little is enough: cocoon web of *Kapogea cyrtophoroides* (Araneae: Araneidae) induced by *Hymenoepimecis heidyae* (Ichneumonidae: Pimplinae). *Arachnologische Mitteilungen* 55: 30–35. <https://doi.org/10.30963/aramit5505>
- Chuang A, Gates MW, Grinsted L, Askew R, Leppanen C (2019) Two hymenopteran egg sac associates of the tent-web orbweaving spider, *Cyrtophora citricola* (Forsk., 1775) (Araneae, Araneidae). *ZooKeys* 874: 1–18. <https://doi.org/10.3897/zookeys.874.36656>
- Eberhard WG (2000) The natural history and behavior of *Hymenoepimecis argyraphaga* (Hymenoptera: Ichneumonidae) a parasitoid of *Plesiometa argyra* (Araneae, Tetragnathidae). *Journal of Hymenoptera Research* 9: 220–240.
- Eberhard WG, Gonzaga MO (2019) Evidence that *Polysphincta*-group wasps (Hymenoptera: Ichneumonidae) use ecdysteroids to manipulate the web-construction behaviour of their spider hosts. *Biological Journal of the Linnean Society* 127(2): 429–471. <https://doi.org/10.1093/biolinnean/blz044>

- Gonzaga MO, Sobczak JF (2007) Parasitoid-induced mortality of *Araneus omnicolor* (Araneae, Araneidae) by *Hymenoepimecis* sp. (Hymenoptera, Ichneumonidae) in southeastern Brazil. *Naturwissenschaften* 93: 223–227. <https://doi.org/10.1007/s00114-006-0177-z>
- Gonzaga MO, Sobczak JF (2011) Behavioral manipulation of the orb-weaver spider *Argiope argentata* (Araneae: Araneidae) by *Acrotaphus chedelae* (Hymenoptera: Ichneumonidae). *Entomological Science* 14(2): 220–223. <https://doi.org/10.1111/j.1479-8298.2010.00436.x>
- Gonzaga MO, Sobczak JF, Pentead-Dias AM, Eberhard WG (2010) Modification of *Nephila clavipes* (Araneae: Nephilidae) webs induced by the parasitoids *Hymenoepimecis bicolor* and *H. robertsae* (Hymenoptera: Ichneumonidae). *Ethology Ecology and Evolution* 22: 151–165. <https://doi.org/10.1080/03949371003707836>
- Gonzaga MO, Moura RR, Pêgo PT, Lee Bang D, Meira FA (2015) Changes to web architecture of *Leucauge volupis* (Araneae: Tetragnathidae) induced by the parasitoid *Hymenoepimecis jordanensis* (Hymenoptera: Ichneumonidae). *Behaviour* 152: 181–193. <https://doi.org/10.1163/1568539X-00003238>
- Gonzaga MO, Loffredo AP, Pentead-Dias AM, Cardoso JCFC (2016) Host behavior modification of *Achaearanea tingo* (Araneae: Theridiidae) induced by the parasitoid wasp *Zatypota alborhombarta* (Hymenoptera: Ichneumonidae). *Entomological Science* 19: 133–137. <https://doi.org/10.1111/ens.12178>
- Korenko S, Korenková B, Satrapová J, Hamouzová K, Belgers D (2015) Modification of *Tetragnatha montana* (Araneae, Tetragnathidae) web architecture induced by larva of the parasitoid *Acrodactyla quadrisculpta* (Hymenoptera, Ichneumonidae, Polysphincta genus-group). *Zoological Studies* 54(40): 1–7. <https://doi.org/10.1186/s40555-015-0119-6>
- Kloss TG, Gonzaga MO, Roxinol JAM, Sperber CF (2016) Attack behavior of two wasp species of the *Polysphincta* genus group (Hymenoptera, Ichneumonidae) on their orb-weaver spider hosts (Araneae, Araneidae). *Journal of Insect Behavior* 29: 315–324. <https://doi.org/10.1007/s10905-016-9560-6>
- Kloss TG, Gonzaga MO, Oliveira LL, Sperber CF (2017) Proximate mechanism of behavioral manipulation of an orb-weaver spider host by a parasitoid wasp. *PLoS ONE* 12(2): e0171336. <https://doi.org/10.1371/journal.pone.0171336>
- Levi HW (1997) The American orb weavers of the genera *Mecynogea*, *Manogea*, *Kapogea* and *Cyrtophora* (Araneae: Araneidae). *Bulletin of the Museum of Comparative Zoology* 155(5): 215–255.
- Matsumoto R (2016) Molecular phylogeny and systematics of the *Polysphincta* group of genera (Hymenoptera, Ichneumonidae, Pimplinae). *Systematic Entomology* 41(4): 854–864. <https://doi.org/10.1111/syen.12196>
- Pádua DG, Oliveira ML, Onody HC, Sobczak JF, Sääksjärvi IE, Gómez IC (2015) The Brazilian Amazonian species of *Hymenoepimecis* Viereck, 1912 (Hymenoptera: Ichneumonidae: Pimplinae). *Zootaxa* 4058(2): 175–194. <https://doi.org/10.11646/zootaxa.4058.2.2>
- Pádua DG, Sääksjärvi IE, Monteiro RF, Oliveira ML (2020) Seven new species of spider-attacking *Hymenoepimecis* Viereck (Hymenoptera, Ichneumonidae, Pimplinae) from Ecuador, French Guiana, and Peru, with an identification key to the world species. *ZooKeys* 935: 57–92. <https://doi.org/10.3897/zookeys.935.50492>

- Sobczak JF (2013) Estudos biológicos e ecológicos da interação entre *Nephila clavipes* (Araneae Nephilidae) e o parasitoide *Hymenoepimecis bicolor* (Hymenoptera, Ichneumonidae, Pimplinae). PhD Thesis. Universidade Federal de São Carlos, Brazil, 125 pp.
- Sobczak JF, Loffredo APS, Pentead-Dias AM, Gonzaga MO (2009) Two new species of *Hymenoepimecis* (Hymenoptera: Ichneumonidae: Pimplinae) with note on their spider hosts and behaviour manipulation. *Journal of Natural History* 43–44: 2691–2699. <https://doi.org/10.1080/00222930903244010>
- Sobczak JF, Sobczak JCMSM, Messas YF, Souza HS, Vasconcellos-Neto J (2014) A new record of a host-parasitoid interaction: *Hymenoepimecis veranii* Lofredo and Pentead-Dias, 2009 (Hymenoptera: Ichneumonidae) parasitizing *Araneus orgaos* Levi, 1991 (Araneae: Araneidae). *Journal of Insect Behavior* 27: 753–758. <https://doi.org/10.1007/s10905-014-9467-z>
- Sobczak JF, Loffredo APS, Pentead-Dias AM, Messas YF, Pádua DG (2018) Description of the male of *Hymenoepimecis bicolor* (Brullé, 1846) (Hymenoptera, Ichneumonidae, Pimplinae). *Brazilian Journal of Biology* 79(1): 154–157. <https://doi.org/10.1590/1519-6984.178889>
- Takasuka K, Matsumoto R, Ohbayashi N (2009) Oviposition behavior of *Zatypota albicoxa* (Hymenoptera, Ichneumonidae), an ectoparasitoid of *Achaearanea tepidariorum* (Araneae, Theridiidae). *Entomological Science* 12: 232–237. <https://doi.org/10.1111/j.1479-8298.2009.00338.x>
- World Spider Catalog (2022) World Spider Catalog, Version 23.0. Natural History Museum Bern. <https://doi.org/10.24436/2>
- Yu DS, van Achterberg C, Horstmann K (2016) World Ichneumonoidea 2015: Taxonomy, Biology, Morphology and Distribution. Taxapad 2016. Database on flash-drive.
- Zerova MD, Seryogina LY, van Harten A (2008) New and previously unknown Eurytomidae (Hymenoptera) species from Yemen. *Entomological Review* 87(8): 948–963. <https://doi.org/10.1134/S0013873808050096>

# Darwin wasps (Hymenoptera, Ichneumonidae) in Lower Eocene amber from the Paris basin

Alexandra Viertler<sup>1,2\*</sup>, Seraina Klopstein<sup>1,2\*</sup>,  
Corentin Jouault<sup>3,4,5</sup>, Tamara Spasojevic<sup>1,2\*</sup>

**1** Naturhistorisches Museum Basel, Augustinergasse 2, CH-4001 Basel, Switzerland **2** Institute of Ecology and Evolution, University of Bern, Baltzerstrasse 6, CH-3012 Bern, Switzerland **3** Institut de Systématique, Évolution, Biodiversité (ISYEB), Muséum national d'Histoire naturelle, CNRS, Sorbonne Université, EPHE, Université des Antilles, CP50, 57 rue Cuvier, 75005 Paris, France **4** Institut des Sciences de l'Évolution de Montpellier, CNRS, Place Eugène Bataillon, UMR 5554, 34095 Montpellier, France **5** Univ. Rennes, CNRS, Géosciences Rennes, UMR 6118, 35000 Rennes, France

Corresponding author: Tamara Spasojevic ([spasojevic.ta@gmail.com](mailto:spasojevic.ta@gmail.com))

Academic editor: Gavin Broad | Received 6 January 2022 | Accepted 8 February 2022 | Published 28 February 2022

<http://zoobank.org/AACD3DB7-8F69-4230-B12F-5E811CA88A15>

**Citation:** Viertler A, Klopstein S, Jouault C, Spasojevic T (2022) Darwin wasps (Hymenoptera, Ichneumonidae) in Lower Eocene amber from the Paris basin. *Journal of Hymenoptera Research* 89: 19–45. <https://doi.org/10.3897/jhr.89.80163>

## Abstract

Despite their ecological importance, Darwin wasps (Ichneumonidae) are among the most poorly studied groups of organisms. It is therefore not surprising that their fossil record is even more poorly understood than their extant diversity. The early Eocene seems rather fossil-poor regarding Ichneumonidae in amber and only one species, *Palaeometopius eocenicus* Menier et al., 2004, was described so far from Oise Amber from the Paris basin. Here, two new ichneumonid genera and species, *Madma oisella* **gen. et. sp. nov.** and *Pappous trichomatus* **gen. et. sp. nov.** are described and the placement of *Palaeometopius eocenicus* is revised. The three fossils are well-preserved and might represent stem taxa of Tryphoninae and Phygadeuontinae. They are a highly important addition to the early Palaeogene fossil record of Ichneumonidae that otherwise mainly consists of compression fossils, which yield far less detail of the specimens' morphology than amber pieces. Among the more than 1,000 Oise amber pieces examined, only three Ichneumonidae specimens have been found, versus about 60 Braconidae, a ratio very different from other amber deposits. Identification of additional ichneumonid specimens from this period (lowermost Eocene) is of particular importance for a better understanding of the subfamily and species compositions of this family after the K-Pg mass extinction.

\* These authors contributed equally.

**Keywords**

Amber deposit, Cenozoic, fossil, new genus, new species, Oise amber, parasitoids, plesiomorphic

**Introduction**

With around 25,000 described species (Yu et al. 2016) and between 60,000 and 100,000 estimated (Townes 1969; Rasnitsyn 1978), Ichneumonidae or “Darwin wasps” (Klopfstein et al. 2019) constitute one of the most diverse animal groups today and the largest family of parasitoid wasps. How these numbers compare to the past diversity of this group is largely unknown due to the poorly studied fossil record. In total, only 300 fossil species have been described, mostly from a few rather well-studied fossil localities, such as the latest Eocene Florissant Formation, which hosts one third of the known fossil species (PaleoBioDB 2021). This bias translates directly into a temporal bias in the ichneumonid fossils record, with more than half of the species known from the Eocene. Finally, the fossil record is strongly biased towards compression fossils, with only 31 species described from amber, most of which from the relatively poorly dated Baltic amber (for dating issues, see Sadowski et al. 2017).

The age of Darwin wasps has been estimated to the Early Jurassic, around 180 Ma (Spasojevic et al. 2021), but the oldest fossils are known from the Early Cretaceous (Kopylov 2009), resulting in a ghost lineage of around 60 Ma. The current evidence suggests that the Cretaceous ichneumonid fauna was dominated by extinct subfamilies, the earliest of which have been described from compression fossils: Tanychorinae, with uncertain placement in Ichneumonidae or Ichneumonoidea (Sharkey and Wahl 1992; Kopylov 2010a) and Palaeoichneumoninae (Kopylov 2009), the earliest unequivocal ichneumonids. Both subfamilies have been described from the Early Cretaceous of Transbaikalia and Mongolia. The more recently described Late Cretaceous subfamily Novichneumoninae is known from Burmese amber (Li et al. 2017; Kopylov et al. 2021), while Labenopimplinae have been described from the Late Cretaceous both from compression fossils from the Russian Far East (Kopylov 2010b), Botswana (Kopylov et al. 2010), Canadian (McKellar et al. 2013), and Taimyr amber (Kopylov 2012). Canadian amber also hosts the only Cretaceous ichneumonid described in an extant subfamily, *Albertocryptus dossenus* McKellar, Kopylov & Engel, 2013, but its placement in Labeninae is questionable (McKellar et al. 2013; Santos et al. in press).

In contrast to the Cretaceous, the Paleogene is dominated by extant ichneumonid subfamilies. Following a single ichneumonid from the Paleocene, *Phaenolobus arvenus* Piton, 1940, tentatively placed in Acaenitinae (Piton 1940), there is a rich ichneumonid fauna known from the Eocene and Oligocene. In total, 209 fossil species belonging to 19 extant and two fossil subfamilies were registered from this period (PaleoBioDB 2021), with the most significant deposits being the Florissant Formation and Green River Formation in the United States (Brues 1910; Spasojevic et al. 2018a), Aix-en-Provence in France (Theobald 1937), Rott Formation and Messel Pit in Germany

(Statz 1936; Spasojevic et al. 2018b), and Bembridge Marls from Bouldnor Formation in England (Cockerell 1921; Antropov et al. 2014). An early Eocene deposit, the Fur Formation in Denmark, also harbours numerous ichneumonid fossils (Rust 1998), although only a few have been described (Meier et al. 2022, Klopstein 2021) and a large number remains unstudied. Although not many ichneumonids are known from Eocene and Oligocene amber deposits, some have been described from Baltic amber, which appears to have preserved a much higher diversity of ichneumonid subfamilies than previously thought (Manukyan and Zhindarev 2021). Banchinae, Cryptinae (sensu Townes 1970a), Diplazontinae (only through a puparium with an emergence hole typical for the subfamily), Hybrizontinae, Stilbopinae, Tryphoninae, Orthocentrinae and Pimplinae are all found in Baltic amber, as well as the extinct Townesitinae and Pherombinae (Kasparyan 1988; Kasparyan 1994). Banchinae and Stilbopinae were also recorded in Rovno amber from Ukraine (Khalaim 2011). Although until now only a single ichneumonid has been described from early Eocene Oise amber, *Palaeometopius eocenicus* Menier et al., 2004 (Menier et al. 2004), it is an important deposit, as it provides more insights into the ichneumonid diversity close to the Cretaceous-Paleogene boundary.

Oise amber from several sites in the Paris Basin in France is a recently discovered deposit area from the early Eocene (Nel et al. 2004). It is dated back to the Ypresian, more precisely its sub-division Sparnacian (De Franceschi and De Ploëg 2003). In 1997 a new fossiliferous locality was discovered near the town of Creil and Houdancourt at the place known as 'Le Quesnoy' (Paris Basin, Oise, France) and dated to the lowermost Eocene, i.e., 55–53 Mya. This age was established by stratigraphy and confirmed by the presence of fossil remains of mammalian taxa, allowing a calibration against the mammalian layer reference. The amber was produced by angiosperms, most probably by *Aulacoxylon sparnacense* Combes, 1907 (Combretaceae or Caesalpiniaceae; De Franceschi and De Ploëg 2003). So far, many interesting inclusions have been found in this amber, ranging from different plant structures, feathers, hair, and coprolites from vertebrates, to a great diversity of insects. The composition of those fossils leads to the assumption of a subtropical environment, with a semi-deciduous or deciduous forest, and wet and dry seasons. In nearby sediments, fossils of amphibians and insect larvae that depend on aquatic habitats were found, suggesting a nearby freshwater source (Nel et al. 2004).

The preservation of some fossils in Oise amber, especially insects, is of high quality, with sometimes even internal soft tissues, like organs or musculature, clearly visible after the necessary scanning procedures (van de Kamp et al. 2014). It is in this respect comparable with Baltic amber (Grimaldi et al. 1994; Kehlmaier et al. 2014; Selden and Penney 2017). The insect diversity found in Oise amber was examined in 2009, and revealed about 17 insect orders with different family diversities (Brasero et al. 2009). While most orders are still poorly studied, others like the Psocoptera were examined rather well (Nel et al. 2005). The most diverse appear to be Coleoptera and Psocoptera, followed by Hymenoptera (Brasero et al. 2009). Within Hymenoptera eight families have been found so far, including both extant families of Ichneumonoidea; two species

of Braconidae have to date been described (Belokobylskij et al. 2010) and one species of Ichneumonidae (Menier et al. 2004).

We here conduct the first systematic study of Darwin wasps in Oise amber, based on the extensive collection of this amber at the Muséum Nationale d'Histoire Naturelle in Paris. We describe two new species and redescribe *Palaeometopius eocenicus*, while re-evaluating its subfamily placement. We find that all three examined fossils possess unique character combinations that require placing them in new genera. All three taxa combine plesiomorphic with derived character systems and are thus especially informative about character evolution in stem versus crown group Darwin wasps.

## Materials and methods

All fossil specimens studied here come from the Oise amber deposit (49°20'06.0"N, 2°40'28.9"E). The amber pieces were first polished on one side to screen their content and then completely polished with a diamond disk to remove the weathered surface for optimal study of all inclusions. Then, the thin polishing marks on the amber surface were removed using diatomite. Amber fragments were immersed in water plus sugar solutions or in maple syrup to minimize light scattering during study and image capture (Sadowski 2021). Specimens were examined and photographed under a Nikon SMZ25 stereomicroscope with a Nikon D800 attached or with the Keyence VHX 600 system at magnification 200×. Some overview images were digitally stacked using photomicrographic composites of several individual focal planes, using HeliconFocus. The figures were composed with Adobe Illustrator CC 2019 and Adobe Photoshop CS19 software. All specimens are housed in the Palaeontological collection of the Muséum National d'Histoire Naturelle in Paris (MNHN.F).

We follow the open nomenclature framework (Matthews 1973) to express uncertainty in fossil classification. This framework uses question marks after the genus name to denote uncertain genus affiliation and expressions like “incertae familiae”, “incertae sedis” and so on for higher-level classification. An uncertain subfamily placement would thus be indicated by “incertae subfamiliae” (e.g., Spasojevic et al. 2018a, 2018b). This can be very useful if subfamily affiliation is indeed mostly unknown or if only a handful of subfamilies exist within a family. However, as Ichneumonidae consists of 42 extant and six extinct subfamilies, we deem it important to also be able to express an uncertain placement within one particular subfamily, for instance in cases when all characters seen in a fossil are consistent with such a placement, but the unique synapomorphies of the group are not visible. We simply extend the framework by adding a question mark after the subfamily name in such cases.

Morphological terminology follows Broad et al. (2018), except for the wing terminology, which follows Spasojevic et al. (2018a). Tergites and sternites are often numbered in the text and abbreviated as “T1”, “T2”, etc. and “S1”, “S2” etc., respectively. Measurements were either taken directly from the fossils using an eyepiece with a scale or measured in ImageJ (Schneider et al. 2012) from photographs made without stacking. Unless stated otherwise, measurements correspond to lengths of the

respective structures. In those cases where photographs were deemed insufficient to illustrate our analyses of the fossils, interpretative drawings were made as overlaid layers in Adobe Photoshop (v. 21.2.3).

## Results

We examined more than 1,000 pieces of amber from Oise in search of Ichneumonidae, but only found two nearly complete specimens. In contrast, there were more than 60 amber pieces with Braconidae recovered, several dozen Aculeata (mostly Crabronidae), many Formicidae, and numerous Chalcidoidea and other small-bodied Hymenoptera. In Braconidae, a large proportion of the specimens could be identified as belonging to Cheloninae, a subfamily with representatives with a body size of about 4–6 mm, which is rather large for a braconid and comparable to many ichneumonids.

Along with the newly found specimens, we examined and redescribed the holotype of *Palaeometopius eocenicus*, which until now was the only ichneumonid found in Oise amber. The other two represent new species and will be described below.

## Systematic palaeontology

**Hymenoptera Linnaeus, 1758**

**Ichneumonidae Latreille, 1802**

**Tryphoninae? Förster, 1869**

***Palaeometopius eocenicus* Menier et al., 2004**

Figs 1, 2

**Systematic placement.** Menier et al. (2004) placed their monotypic genus in Metopiinae, stating that it “shares the main diagnostic characters of the Metopiinae, as defined by Townes (1971)”. Examining the holotype at MNHN.F, we found the evidence for such a placement unconvincing. This has already been indicated by the list of characters mentioned by the original authors as differing between the fossil and all other Metopiinae. In fact, this subfamily is one of the very few among Ichneumonidae that has a unique character to define it: the upper margin of the face is extended as a triangular process between the antennal sockets. While Menier et al. (2004) mentioned that his process was shorter in the fossil than in the extant species of the subfamily, we could not find any trace of it. Several other characters disagree with a placement in Metopiinae, including the long notauli that meet medially on the mesoscutum in the fossil; the strongly inclivous vein 2m-cu in the forewing with two widely separated bullae; and finally, the rather long ovipositor.

In contrast, all the characters visible in the fossil are in accordance with a placement in Tryphoninae, especially the strong and complete propodeal carination, the broad first tergite, the strongly convergent notauli, and the stout ovipositor, lacking a distinct

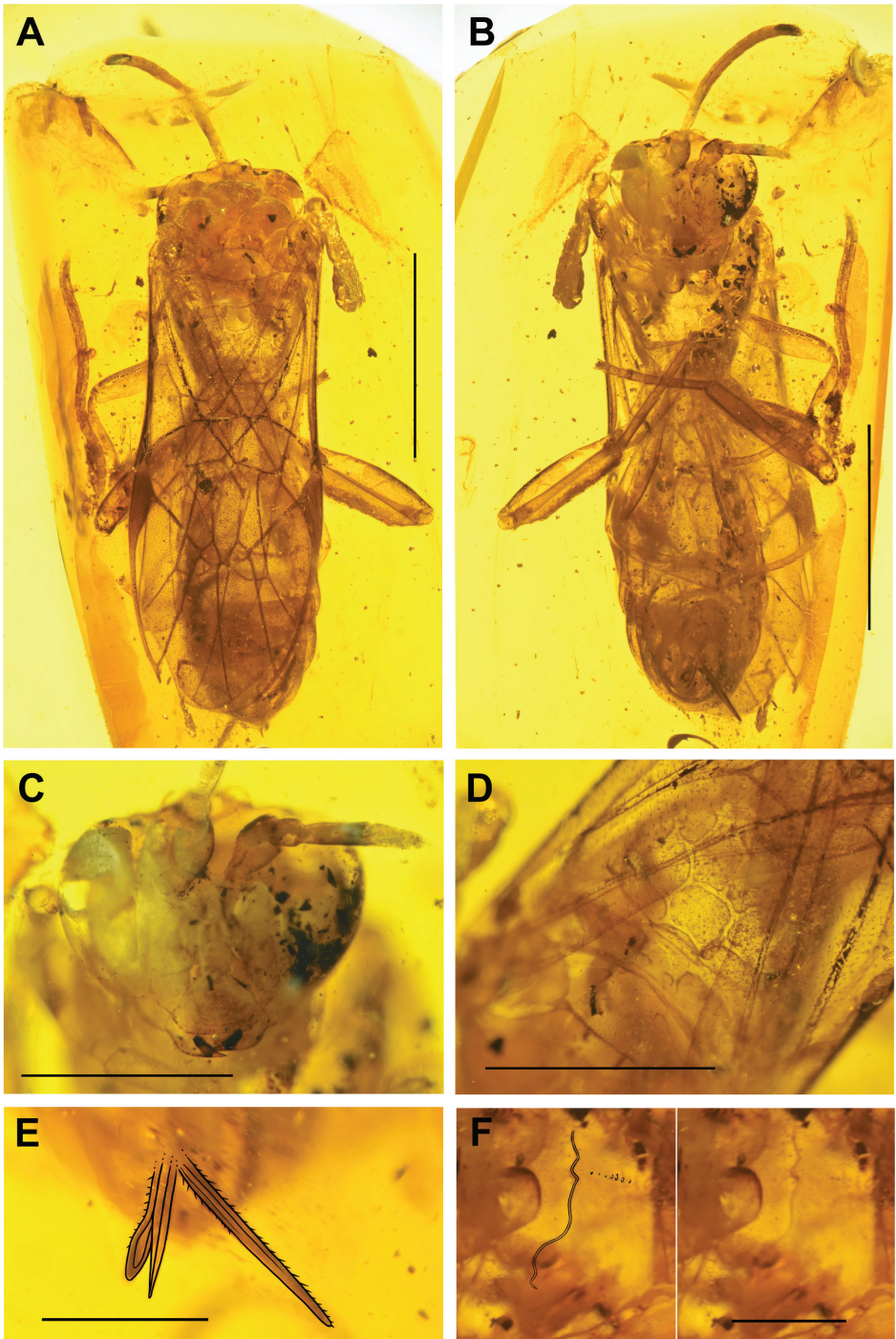


**Figure 1.** Holotype of *Palaeometopius eocenicus* Menier et al., 2004 **A** dorsal view of whole specimen **B** ventral view of whole specimen **C** front view of face **D** dorsal view of propodeum **E** ovipositor and ovipositor sheaths **F** epinematic carina on ventral side. Scale bars: 2 mm (**A,B**); 1 mm (**C,D**); 0.5 mm (**E,F**).

nodus or dorsal subapical notch. Also, none of the characters in the fossil are entirely absent from extant Tryphoninae, although some, such as the twisted mandibles and the clearly protruding ovipositor, are rather rare (other than in *Netelia* Gray, 1860). However, the combination of characters shown in the fossil is not in accordance with any of the extant tribes (Bennett 2015). There are two apomorphic characters uniting extant Tryphoninae, the stalked egg, which is often carried exposed on the ovipositor, and a fringe of long, parallel setae on the clypeus. Neither are visible in the fossil, either due to absence or just preservation or poor visibility. We thus label our placement of this fossil in Tryphoninae as tentative.

**Material examined.** FRANCE • *Holotype* female; Oise department, region of Creil, Chevière, Le Quesnoy; 49°20'06.0"N, 2°40'28.9"E; G. De Ploëg leg.; in amber mounted in Canada balsam; MNHN.FA30079 (PA2439).

**Type condition.** Nearly complete specimen; apical part of right and median part of left antenna, right foreleg from tibia and apex of left fore tibia missing; wings folded over metasoma, obscuring view on tergites; milky substance present ventrally from metasoma, thus in part obscuring view on sternites. Cuticula translucent in most places, interior partly hollow, organs partly preserved.

**Description.** Body 5.6 mm. Colour or colour pattern not visible.

**Head.** Mandibles long and overlapping, curved along main axis and strongly twisted; bidentate, with lower tooth about half as long as upper one. Labrum concealed below clypeus. Clypeus somewhat convex in profile, probably weakly separated from face; apical margin truncate medially, curved upwards laterally. Malar space clearly longer than mandibular width at base. Anterior tentorial pits distinct. Shape of face difficult to discern, but probably rather flat with weak median swelling. Eyes in profile about 0.8× height of head. Upper margin of face without process, without modification between antennal sockets. Frons without strong impressions for scape. Ocelli of normal size. Maxillary palp with five segments, labial palp not entirely visible. Scape slightly longer than wide; truncation strongly oblique, forming an angle of about 45° with the main axis. Pedicel much shorter and smaller than scape. Antenna 4.2 mm, with 25 flagellomeres, evenly thick throughout entire length; first flagellomere 3.2×, subapical flagellomere 1.1× as long as wide.

**Mesosoma.** Pronotum rather short, well visible around front half of mesoscutum when viewed from above; without modification at base of notaulus; with at least dorsal part of epomia present. Mesosternum with deep scrobe with cross-carinulae; posterior transverse carina absent. Sternaulus deeply impressed anteriorly, seemingly reaching only to about 0.4× length of mesopleuron. Epicnemial carina complete ventrally, dipped in mesosternal scrobe; laterally forming two widely spaced, strong curves; upper end not discernible. Mesopleuron only visible at angle, rather short; with short impression at around mid-height in front, where epicnemial carina shows a second curve above the one accommodating the sternaulus; mesopleural furrow not discernible. Notauli deeply impressed, with some cross-carinulae in the impression; strongly converging, meeting in an impressed area medially on mesoscutum. Scutellum short and wide, without lateral carinae; metanotum of normal length and convex. Submetapleural



+ Cu and 1M or nearly so. Pterostigma 4.0×, cell 2R1 2.5× as long as wide. 5M entirely tubular. 2Cu 0.8× of 1M + 1Rs, 0.85× of r-rs. 1m-cu & 2Rs + M angled. 3Cu clearly longer than 2cu-a. Hind wing with M + Cu complete, slightly curved on entire length. 1Cu about 0.6× cu-a. 1Rs about 1.5× rs-m, although upper end hardly discernible.

**Metasoma.** Sternites poorly visible, weakly sclerotized; hypopygium short, transverse, appears weakly sclerotized. T1–T4 depressed, apex of metasoma about circular. T1 poorly visible, appears subquadrate, evenly tapering anteriorly in dorsal view; spiracle seems around middle; latero-median carina seems present, widely parallel. T2 transverse, appears normally separated from T3. T4 and T5 well developed; T6 and following tergites very short and hidden below anterior tergites. T8 short, not elongated in horn or boss. Ovipositor sheaths about 0.7 mm, evenly setose, parallel, then tapering from about mid length. Ovipositor tip region rather long, evenly tapering, without discernible teeth.

### Tryphoninae? Förster, 1869

#### *Pappous* gen. nov. (masculine)

<http://zoobank.org/ED549916-A111-4353-A55D-3DEAD7A0A980>

**Etymology.** Derived from the Greek word (*pappous*) for grandfather, which highlights the age of the genus.

**Type species.** *Pappous trichomatius* sp. nov.

**Systematic placement.** The most conspicuous character of this fossil is probably the dense pilosity on the compound eyes, which is rather rare in Ichneumonidae. However, there are a few genera or species with setose eyes in a large portion of the subfamilies (*Schizopyga* Gravenhorst, 1829 and *Dreisbachia* Townes, 1962 in Pimplinae; *Trichomma* Wesmael, 1849 and *Ophionellus* Westwood, 1874 in Anomaloninae, *Cymodusa* Holmgren, 1859 in Campopleginae, *Collyria trichophthalma* Thomson, 1877 in Collyriinae, etc.) (Townes 1969, 1970b, 1971).

The fossil shares some similarities with taxa in the subfamily Orthocentrinae. First, the face of the fossil reminds of taxa in the *Helictes* genus-group, with a strongly convex clypeus both in front and profile view, a rather long malar space and tentorial pits that are placed much behind the clypeal plane (Townes 1971). Second, the converging but almost box-like first tergite with the spiracle around the middle, and strong and parallel latero-median carinae also occur in Orthocentrinae. Third, there are also some *Eusterinx*, in the subgenus *Trestis*, that share the setose eyes. All Orthocentrinae possess a conspicuous fringe of setae along the inner side of the hind tibia, but this body part is unfortunately not visible. However, the relatively short and fully carinated propodeum speak against most Orthocentrinae, except *Eusterinx*, and the mentioned characteristics also appear in some Tryphoninae taxa, and since many characters in Orthocentrinae are very variable and seem plesiomorphic in the fossil, a placement in Orthocentrinae seems ill-advised.

Although the setose eyes are a highly homoplastic character, it might give an important hint, as eyes with conspicuous setae occur rather often in Tryphoninae (e.g., *Thymaris* Förstner, 1869, *Oedemopsis* Tschek, 1869, *Zagryphus* Cushman, 1919), in the tribe Oedemopsini (Bennett 2015). Indeed, the combination of characteristics in this fossil are all consistent with a placement in Tryphoninae. The setose eyes and strongly tapered mandibles, the deeply impressed notauli, together with the full carination on the propodeum, lead to some genera in the tryphonine tribe Oedemopsini (Bennet 2015; Broad et al. 2018). The mesosoma, the very strong juxtacoxal carina, the posterior transverse carina of the mesosternum, which forms a lobe with the lateral part and is medially expanded into two lobes, as well as the shape of the first tergite are rather similar to *Acaenitellus* Morley, 1913. The setose eyes and mandible shape on the other hand would point to a close resemblance to *Thymaris* and *Neliopisthus* Thomson, 1883. The latter also shares similarities in the first tergite, which is in some species tapered gradually with more or less parallel latero-median carina. But although the fossil shares many characteristics that are consistent within Oedemopsini, it also features differences, which are rare in this tribe: a strongly bowed 2m-cu, a rather stout and box-like first tergite, and a closed areolet. The latter is only present in *Leptixys* Townes, 1969 from Chile and Argentina, *Debophanes* Gauld, 1984 from Australia and the fossil species *Thymariodes areolaris* Kasparyan, 1988 from Baltic amber (Bennet 2015). Although we have good arguments for placing *P. trichomatius* in Oedemopsini, important characteristics, like an antenna with a median light-coloured band, simple tarsal claws and an ovipositor with a weakly sclerotized ventral valve (Bennet 2015), which would distinguish this tribe from other Tryphoninae, are not visible. Therefore, we do not place the fossil in this tribe or any Tryphoninae tribe. Since the previously mentioned apomorphic characters in extant Tryphoninae, the stalked egg and the fringe of setae on the clypeus, are not visible in this fossil, we also label our placement of this fossil in Tryphoninae as tentative.

**Diagnosis.** *Pappous* gen. nov. differs from the only known fossil genus of Oedemopsini, *Thymariodes* Kasparyan, 1988, described from Baltic amber, in having unidentate or strongly twisted mandibles, a convex clypeus in profile, a longer malar space, as well as a long and slender pterostigma, an outwards bowed 2m-cu and with vein 1Rs + M present. It also differs from *Palaeometopius* by the shape and dimension of the mandibles, the presence of conspicuous setae on the eyes, and a quadrate-oblique areolet shape. In addition, *Pappous* gen. nov. differs from extant genera in Oedemopsini by its closed quadrate-oblique areolet, a strongly carinated propodeum, and subquadrate and non-petiolate T1. Since *Pappous* does have a different character combination than extant Oedemopsini or other Tryphoninae genera, we propose a new genus.

The genus combines dense and conspicuous setae on the eyes, a convex clypeus with simple margin, the malar space about as long as base width of mandibles or a little longer, a weak oblique truncation of the scape, a strongly areolated propodeum with rather simple surface sculpture and complete juxtacoxal carinae, fore wing with closed quadrate-oblique areolet and a box-like first tergite.

***Pappous trichomatius* sp. nov.**

<http://zoobank.org/A6ACD113-6520-40E8-91EF-3FD2678B05FD>

Figs 3, 4

**Etymology.** A combination of the two Greek words trichotos (hairy) and matius (matia for eyes), describing the short but regularly spaced setae on the fossil's eyes.

**Material examined.** FRANCE • *Holotype* male?; Oise department, region of Creil, Chevière, Le Quesnoy; 49°20'06.0"N, 2°40'28.9"E; 1998–2000; G. De Ploëg and A. Nel leg.; in amber; MNHN.FA71346 (PA-349).

**Type condition.** Fossil not complete and partially hidden by an insect inclusion, probably a Trichoptera. Head complete, but partially hidden behind other inclusion. Pronotum and metapleuron partially hidden by wings. Mesoscutum, scutellum and metanotum broken off. Propodeum and T1 well preserved. Legs mostly hidden. Dorsally broken after T2, ventrally after S6, but otherwise well preserved. Lateral view of T1–T4 partially visible on one side.

**Diagnosis.** See genus diagnosis.

**Description.** Body at least 5.6 mm (measured from head to T1, added length of T2–T5 in segments), estimated length about 6.1 mm. Colour and colour patterns not interpretable, because of dark orange colour of amber.

**Head.** Mandibles rather long and overlapping; seem unidentate or second tooth twisted and mandibles bidentate; outer surface sparsely pubescent. Malar space about 0.9–1.2× mandibular width. Labrum concealed below clypeus. Clypeus convex, weakly separated from face; apical margin simple. Anterior tentorial pits distinct. Face rather flat with weak median swelling. Eyes in profile about 0.8× height of head, with short but dense setae. Modifications between antennal sockets unclear. Frons without impressions. Ocelli of normal size, separated from eyes by more than their diameter. Vertex seems moderately long and rather flat. Occipital carina seems complete. Palps not visible. Scape longer than wide; truncation rather straight, forming an angle of 10°; without extended membranous area. Pedicel smaller than scape. Flagellum 4 mm long, with 23 segments, evenly thick throughout whole length; most flagellomeres about 1.5× as long as wide; first flagellomere 2.9× as long as wide; tip of last flagellomere unmodified.

**Mesosoma.** Propleuron not visible. Pronotum about 0.6–0.7× as long as high; epomia indiscernible; without modification at base of notaulus. Mesosternum with epicnemial carina partially visible ventrally, seems simple behind fore coxae; posterior transverse carina of mesosternum not discernible. Small lobe in lower hind corner of mesopleuron with two short extensions; mesopleuron rather short and flat, with sternaulus anteriorly visible, appears weak. Mesoscutum mostly broken off, difficult to interpret, with notauli deeply impressed. Scutellum not visible and metanotum rather short and flat. Metapleuron seems slightly higher than long or just about as long as high. Submetapleural carina complete with a small lobe on anterior part. Juxtacoxal carina very strong. Pleural carina distinct on whole length. Propodeum in profile seems evenly rounded and slightly shorter than high or similar in length as in height; sculpture seems smooth with very weak rugae occasionally; carination complete, with

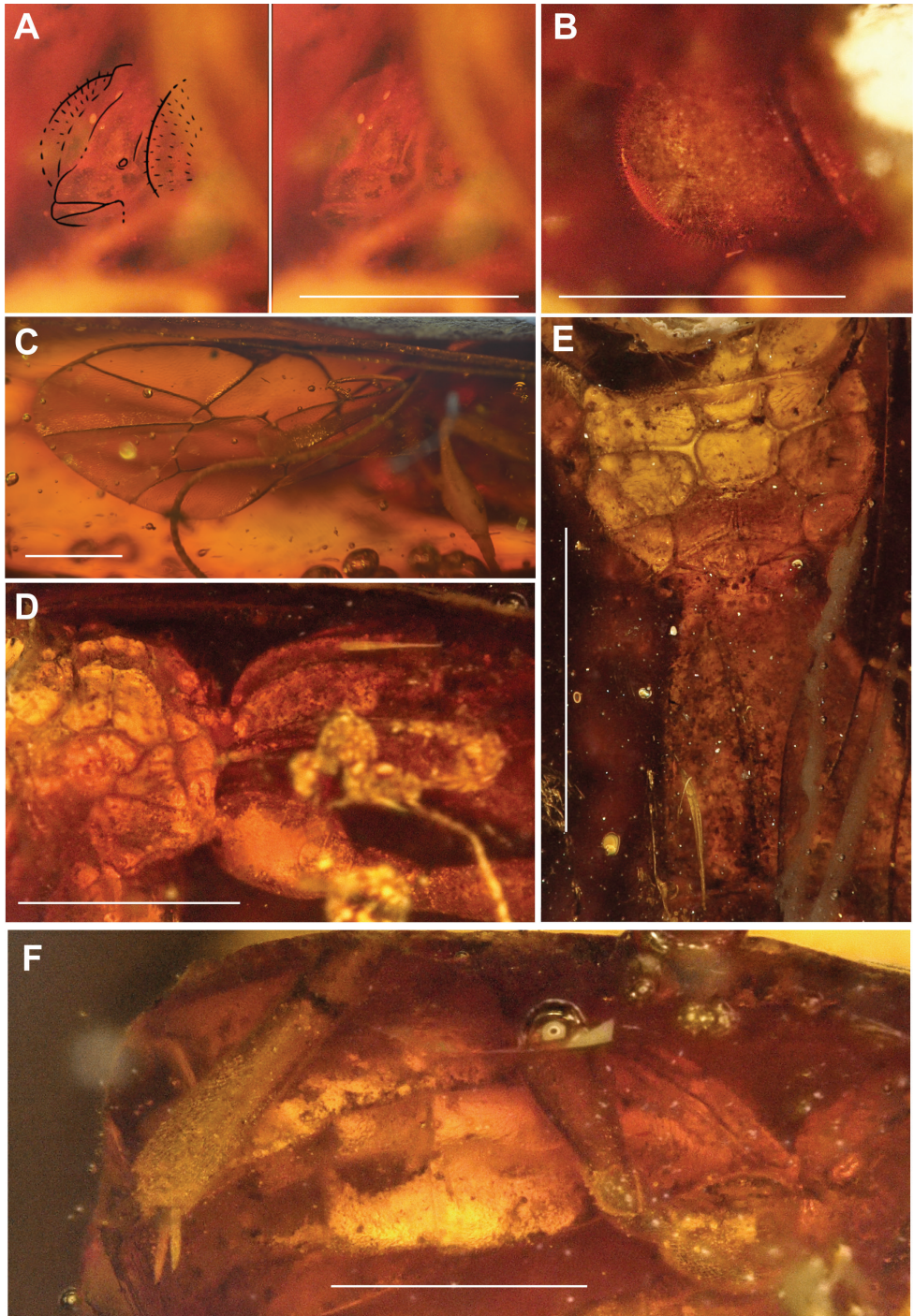


**Figure 3.** Holotype of *Pappous trichomatus* sp. nov. **A** latero-ventral view of face with and without interpretative drawing **B** lateral view of eye with short and dense setae **C** fore wing **D** lateral view on propodeum and first tergite **E** dorsal view on propodeum and first tergite. Scale bars: 1 mm.



**Figure 4.** Interpretative line drawing of *Pappous trichomatus* sp. nov. Dotted lines indicate uncertain interpretations. Photographs from different angles were used as templates to create a drawing of the whole specimen. Scale bar: 2 mm.

latero-median and lateral longitudinal, anterior and posterior transverse carinae present, latter two carinae angled; area superomedia wider than long, area petiolaris with an additional median longitudinal carina. Posterolateral angle evenly rounded. No modifications on junctions of propodeal carinae or surface. Spiracle subcircular. Hind margin of propodeum simple. Metacoxal cavity seems to begin slightly above ventral end of metasomal foramen magnum. Legs simple, fore tibia seems simple to slightly enlarged, with two spurs. Mid coxa simply convex, mid tibia with two spurs. Hind coxa evenly rounded, seems as long as wide. Hind femur and tibia simple, tibia evenly tapered. Inner side of hind tibia not visible. Claws indiscernible.

**Wings.** Fore wing 5.4 mm. Areolet closed, quadrate-oblique, 3rs-m with one bulla and same length as 2 + 3M, 4M extremely short. 2m-cu more or less evenly bowed outwards with two small bullae that cover together ~25% of total 2m-cu length. 4Cu about twice as long as 5Cu. 4Rs almost straight. Vein 1Rs + M about 1.5–2× longer than with of surrounding veins. 1cu-a posterior to junction of M + Cu and 1M, with 1Cu as long as width of surrounding veins. Pterostigma 3.0× as long as wide. Cell 2R1 2.9× as long as wide. 5M tubular through whole length. 2Cu 0.7× 1M + 1Rs and 0.8× r-rs. 1m-cu & 2Rs + M angled. 3Cu slightly longer than 2cu-a. Hind wing with M + Cu complete, slightly curved on entire length. 1Cu about 0.6× cu-a. 1Rs about 1.4× rs-m.

**Metasoma.** Appears depressed, after T4 unclear. S1 seems either not ornamented or with a low rounded swelling and hind margin transverse to shallowly V-shaped. Apical fusion of S1 to T1 is unclear. Laterotergite 1 short and triangular, at least partly sclerotized. Glymma seems absent or weakly impressed. T1 subquadrate, evenly

tapering to front in dorsal view; rather flat with weak median curve in profile; dorsal sculpture seems either smooth and impunctate or finely punctate. Dorso-lateral carina of T1 complete, above spiracle. Spiracle at around  $0.6\times$  of T1. Latero-median carina of T1 parallel, reaching beyond middle of total length. T2 is transverse without latero-median carinae, appears simple, with shallow impression close to base; thyridium present but not sunken in gastrocoelus, seems either ovoid or transverse. Laterotergite 2 moderately broad, sclerotized, and between  $0.25\text{--}0.4\times$  as wide as long, seems to have a shallow groove from base to spiracle. T2 and T3 separate. Laterotergites 3 and 4 appear separated by a crease.

### Phygadeuontinae Förster, 1869

#### *Madma* gen. nov. (feminine)

<http://zoobank.org/C7D5C3FD-1E5C-4D8A-859A-A232EB122A1C>

**Etymology.** The genus name comes from the French word “Mademoiselle”, which means “Miss”. “Madma” is also a Filipino word for “Madam”. The word is chosen to create a wordplay together with the name of the type species (see below).

**Type species.** *Madma oisella* sp. nov.

**Systematic placement.** The presence of a sternaulus, a pentagonal areolet, and the outwards bowed 2m-cu with two bullae, reminds of Claseinae at first. But in Claseinae the sternaulus is not reaching to the posterior end of the mesopleuron, the carination on the propodeum is largely reduced, the areolet smaller and the ovipositor is rather long, which makes this subfamily unlikely. Several characters associate this fossil with crown Phygadeuontinae: the petiolate T1 with the spiracle behind the middle; the long sternaulus that reaches the posterior margin of the mesopleuron above mid-height of the mid coxa; the short ovipositor with a nodus on the dorsal and oblique teeth on the ventral valve; and the two bullae in fore wing vein 2m-cu (Townes 1970a; Santos 2017). However, the wide and unevenly pentagonal areolet with 4M significantly shorter than  $2 + 3M$ , and the presence of a tooth on the apical margin of the fore tibia, do not occur in extant phygadeuontines. The tooth on the fore tibia is a homoplastic character occurring in multiple subfamilies across the ichneumonid tree, including Tryphoninae, Ctenopelmatinae, Tersilochinae, Metopiinae, Anomaloninae, Campopleginae and the more distantly related Eucerotinae and Labeninae (Townes 1969, 1970a, 1970b, 1971); it is thus not informative for the subfamily placement. The wide, pentagonal areolet is a rather plesiomorphic character which only occurs in the Cretaceous Labenopimplinae (Kopylov 2010b) and in extant and fossil Labeninae (Townes 1969; McKellar et al. 2013; Spasojevic et al. 2018b), including a tentative labenine from Cretaceous Canadian amber (McKellar et al. 2013), *Albertocryptus dossenus*. *Madma* clearly differs from Labenopimplinae and Labeninae based on the shape and position of T1 relative to the metacoxal cavities, but resembles *A. dossenus* in both areolet shape, two bullae in 2m-cu and the petiolate T1; it differs from it in the number of flagellomeres (17 in *A. dossenus*) and the much stouter scape, T1 and hind coxae. The wide pentagonal areolet, together with other plesiomorphic characters,

such as two bullae in 2m-cu and a long, strong carinae on T1 and long ovipositor, suggest *Madma* being a stem lineage of Phygadeuontinae or, less likely, its position further down the Ichneumoniformes tree. Given that Phygadeuontinae are currently polyphyletic (Santos 2017), we in fact also cover the latter scenario when placing the fossil in Phygadeuontinae; once Phygadeuontinae are revised in the light of further phylogenetic evidence, this placement will have to be reviewed.

**Diagnosis.** *Madma* gen. nov. differs from all other Phygadeuontinae genera in having a bilobed posterior transverse carina on the mesosternum, a tooth on the apical margin of the fore tibia and an unevenly pentagonal areolet with 4M shorter than  $2 + 3M$ . In addition, the genus is characterised by the following characters: 2m-cu curved outwards, with two bullae; mesopleuron with complete sternaulus curved around middle, reaching posterior margin of mesopleuron above mid-height of mid coxa; T1 petiolate with parallel and long latero-median carinae almost reaching its posterior margin; ovipositor slightly longer than height of metasoma at apex, straight and its apex with a nodus on upper valve and oblique teeth on lower valve.

***Madma oisella* sp. nov.**

<http://zoobank.org/83D47279-D75A-4BEB-80E9-9F3BA89F0A30>

Figs 5, 6

**Etymology.** Derived from the locality name: Oise. The word is transformed to resemble the ending of the French word for Miss “Madmoiselle” and latinised.

**Material examined.** FRANCE • *Holotype* female; Oise department, region of Creil, Chevière, Le Quesnoy; 49°20'06.0"N, 2°40'28.9"E; 1998–2000; G. De Ploëg and A. Nel leg.; in amber; MNHN.FA71347 (PA2189).

**Type condition.** Lateral aspects clearly visible through amber; dorsal and ventral aspects partly visible through irregular surface of amber. Complete, except few apical flagellomeres at surface of amber with their ventral side missing. Body translucent, thus parts of body from opposite side often visible below cuticle, as well as some inner structures. Body surface sculpture and carinae weakly visible; outer surface partly covered with dark material, which probably represents remains of organic matter.

**Diagnosis.** See genus diagnosis.

**Description.** Body around 4.9 mm. Color difficult to interpret, except tip of mandibles darker, hind tibiae clearly darker at base and apex (dark-light-dark), antennae uniformly colored and T1 dark.

**Head.** Mandibles moderately large, weakly tapered from base to apex, not twisted, with two oblique and subequal teeth; outer surface without strong sculpture, smooth or sparsely pubescent. Malar space moderately long, 0.9× mandibular width at base, smooth, seemingly without subocular sulcus. Labrum not clearly exposed below clypeus. Clypeus in frontal view subquadrate, transversely undivided and separated from face with weak clypeal groove, in lateral view clearly convex; apical margin simple, truncate, without tooth or tubercles. Face weakly convex with weak median swelling, without upper process. Eyes large, in lateral view 0.85× head height; inner margin of eyes

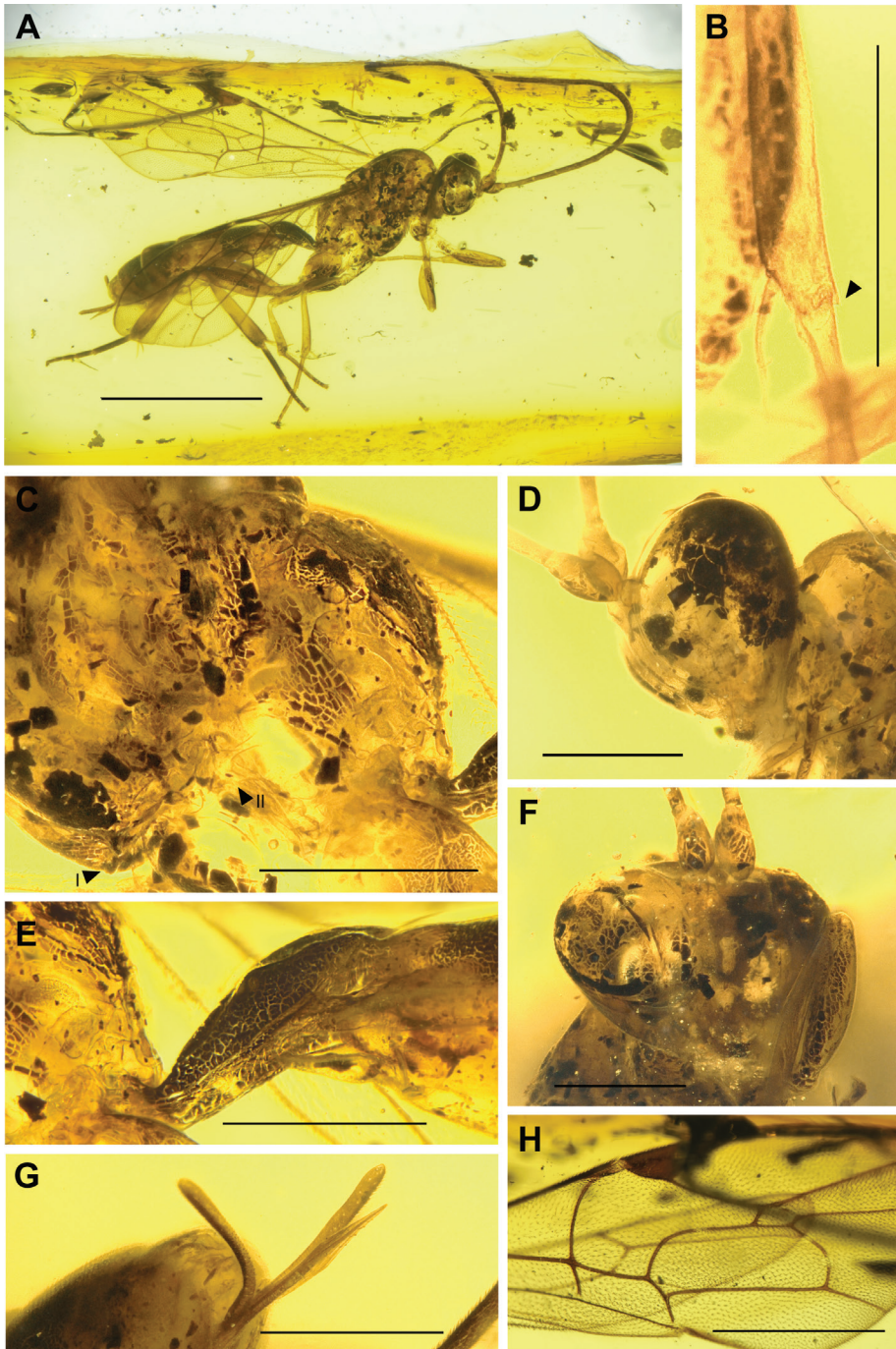


**Figure 5.** Holotype of *Madma oisella* sp. nov. **A** lateral view of whole specimen **B** fore tibia, black triangle points to tooth on apical margin **C** latero-ventral view showing propodeum and bilobed posterior transverse carina on mesosternum (I) and extended small lobe on metapleuron (II) **D** lateral view of head **E** first tergite and sternite **F** frontal view of face **G** ovipositor **H** Detailed photo of fore wing. Scale bar: 2 mm (**A**); 0.5 mm (**B, D–G**); 1 mm (**H**).

straight opposite antennal sockets, in frontal view parallel to each other. Modification between antennal sockets absent. Frons without strong impressions for scape. Ocelli of normal size, separated from eyes by more than their diameter. Vertex steeply declivous behind ocelli with straight surface to occipital carina. Occipital carina complete and dorsally evenly convex, high on head, in lateral view almost reaching height of dorsal eye margin. Maxillary palps with five segments, labial palps not visible. Scape about as long as wide, without extended membranous area; pedicel clearly smaller than scape. Flagellum 3.9 mm with 27 segments; first flagellomere  $6.25\times$  as long as wide; median and apical flagellomeres longer than wide; tip of apical flagellomere unmodified.

**Mesosoma.** Pronotum in profile on left side higher than long, on right side about as high as long (specimen clearly viewed only in slight diagonal position), without lateroventral posteriorly projecting lobe; pronotal collar not visible; anterior vertical part clearly extended dorsally. Epomia weakly visible, present ventrally, extending laterally but unclear how far. Modifications near base of notauli absent. Mesosternum with epicnemial carina extending laterally on mesopleuron at least to mid-height of pronotum, possibly longer, but dorsal part not visible clearly through amber; not modified behind fore coxae. Posterior transverse carina absent laterally, present in front of mid coxae as a raised flange and in between as a low carina. Mesopleuron evenly convex with sternaulus weakly visible, extending from ventrolateral anterior margin of mesopleuron to posterior margin of mesopleuron clearly above mid-height of mid coxa, bowed upwards around mid-height. Mesopleural furrow with horizontal impression extending from around mid-height to episternal scrobe. Mesoscutum evenly shagreened and matt. Notauli deeply impressed anteriorly, extending posteriorly past centre of mesoscutum but unclear how far. Carina along lateral margin of mesoscutum evenly raised and extending to anterior margin of scutellum. Scutellum in profile flat, smooth, without carinae. Postscutellum evenly convex in profile. Propodeum about as long as high; structure difficult to assess but either smooth or punctured. Metapleuron as long as high, with anteroventral corner extended to a small lobe, without juxtacoxal carina and at most with few rugae lateroventrally. Submetapleural carina difficult to interpret, present only in anterior half or completely absent. Propodeal carination complete, although presence of medial portion of anterior transverse carina uncertain; area basalis shorter than area superomedia; the latter similar in size to area petiolaris. Spiracle subcircular, separated from pleural carina by its own diameter, touching dorsal half of pleural portion of lateral longitudinal carina. Dorsal margin of metacoxal cavities above ventral margin of metasomal cavity. Legs simple, not unusually stout or slender. Fore tibia with small apical tooth. Mid and hind tibia with two long slender spurs. Hind tibia with fringe of parallel setae on inner apex; 1<sup>st</sup> tarsomere  $1.1\times$  as long as wide; 4<sup>th</sup> tarsomere apically more or less evenly truncated. Tarsal claws without modification.

**Wings.** Fore wing 3.8 mm. Areolet oblique pentagonal,  $1.5\text{--}2.2\times$  as wide as long, with 3Rs  $0.8\times$  2Rs, 2 + 3M  $2.1\times$  2Rs, 4M  $0.3\times$  2 + 3M; 3rs-m with two bullae. 2m-cu clearly curved outwards, with two bullae. 1Rs + M absent. 1m-cu at level of 1M + 1Rs. Pterostigma  $4.3\times$  as long as wide. Cell 2R1  $2.1\times$  as long as pterostigma,  $3.4\times$  as long as wide. 2Cu  $0.8\times$  1M + 1Rs,  $0.8\times$  r-rs. 3Cu about same length as 2cu-a. Hind wing with M + Cu curved distally. 1Cu around same length as cu-a. 1Rs  $1.2\times$  as long as rs-m.

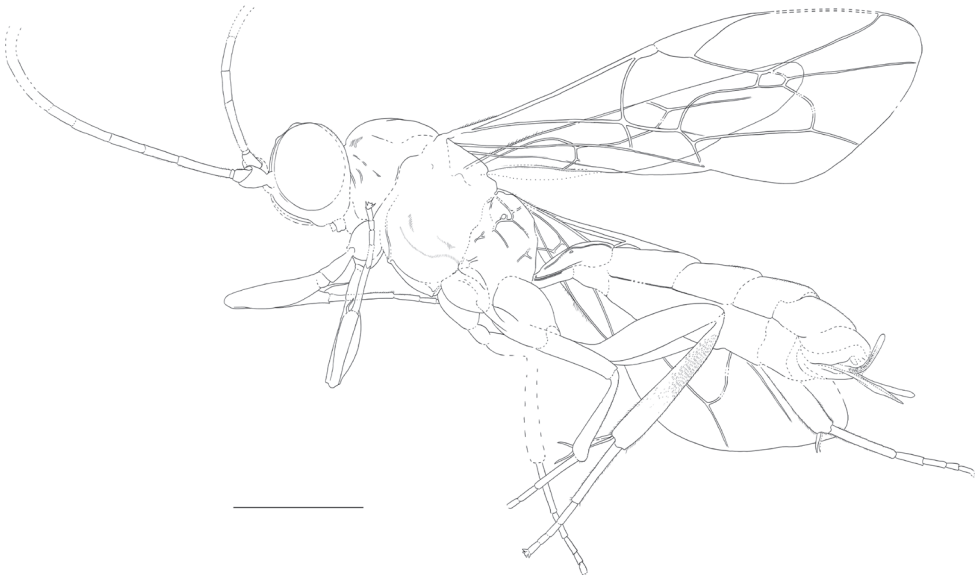


**Figure 6.** Interpretative line drawing of *Madma oisella* sp. nov. Dotted lines indicate uncertain interpretations. Different detailed photographs were used as templates to create this drawing. Scale bar: 1 mm.

**Metasoma.** Depressed to cylindrical. S1 reaches around middle of T1, anteriorly with a median keel, centrally with a weak median swelling. Presence of laterotergite 1 unclear; if present then membranous on entire length. T1 in dorsal view about 2–2.5× as long as wide, petiolate, but sides evenly tapering from apex to base as tergite relatively short, in lateral view continuously expanding in profile; spiracle at around 0.6× T1 length in profile; dorso-lateral carina complete, above spiracle; latero-median carinae long, almost reaching posterior margin, parallel to each other; sculpture shagreened or punctured, but could be an artefact. T2 in dorsal view transverse; sculpture if present not strong and even on entire tergite length; latero-median carinae absent; impressions in anterior half either absent or shallow; thyridium present and shape unclear. Dorsal surface of T3 and remaining tergites evenly convex. T3 and T4 with posterolateral corners rounded. S6 unclear, seems transverse with simple apical margin. T7 conspicuously shorter than T6. T8 short, not elongated in horn or boss. Ovipositor sheaths 0.2× metasoma length, parallel-sided, with dense short setae. Ovipositor straight and compressed, parallel sided until tip where dorsal valve expanding into nodus; tip of lower valve with at least four distinct oblique teeth.

## Discussion

### Why are there so few Oise amber ichneumonids?

In our examined material, we found many more Braconidae than Ichneumonidae. And while ichneumonids seem rare in Oise amber, they are, together with Braconidae, abundant in Baltic amber. For comparison, the Baltic amber collection in Copenhagen

contains about 145 Braconidae and 69 Ichneumonidae, so a ratio of about 2:1 (L. Vilhelmsen, pers. comm.), compared to nearly 20:1 in Oise amber. Although most Ichneumonidae in Baltic amber belong to only six subfamilies, more and more specimens are being described (Manukyan 2019; Manukyan and Zhindarev 2021). Even in the Cretaceous Taimyr amber, braconids and ichneumonids are found in very similar proportions (D. Kopylov, pers. comm.). Therefore, it is surprising that we found so few Ichneumonidae in Oise amber, while Braconidae are rather abundant.

There are many reasons why some organisms could get stuck more easily in one amber than in another. Entrapment in different ambers could differ because of resin viscosity, behaviour of the insect, habitat requirements, or how fast the tree produces resin (Martinez-Delclos et al. 2004). The major difference that may partially explain these different ratios is the size of the amber pieces which are, in general, much smaller for Oise amber. Indeed, it is rare to find Oise amber pieces exceeding a few centimetres while most of the Baltic amber ones are several centimetres long. Additionally, the most fossiliferous Oise amber pieces are, for the most part, the result of relatively thin vertical flows in which the insects are trapped between successive flows. As a result, large Ichneumonidae exceeding 10 mm in length are unlikely to be trapped in this type of resin flow. This directly results in a bias with larger specimens able to free themselves from the fresh resin.

While small ichneumonids may be trapped inside a small fresh resin flow, the big ones need more than just one flow of resin to be entirely covered and are exposed to predation during that time (Martinez-Delclos et al. 2004). A similar bias regarding size is also recorded in other Hymenoptera or insect lineages found in Oise amber (Brasero et al. 2009). In fact, the lineages with relatively large representatives are rarely found (e.g., Odonata) or only partially preserved since one amber fragment is not sufficient to preserve the entire specimen. However, the size bias does not explain the difference compared to Taimyr amber, which also is preserved only in very small pieces. And since Cheloninae (Braconidae) are similar in size to many Ichneumonidae and were found more frequently in our studied material, body size does not seem to be the main cause, or for sure not the only one, for our observed braconid/ichneumonid ratio.

A different behaviour between Eocene ichneumonids and braconids could explain the different ratio between the two families. However, this is clearly difficult to examine. Habitat, as another possible reason, seems less probable, since both groups mostly share habitats and have today similar distributions and hosts. However, there is still a lot of unstudied Oise amber in the collection of the MNHN, and the ratio between the two families could still change with further examination.

## Advantages of preservation in amber

While compression fossil localities are on average older than amber deposits, amber fossils often give us a more complete picture of the morphology of specimens and thus allow us to place them more accurately. Although the earliest ichneumonids were described from compression fossils, a lot of information about the past ichneumonid subfamily diversity comes from amber (Kasparyan 1988; Manukyan and Zhindarev 2021).

From 31 amber species described, many belong to extinct subfamilies, which were newly described and often uniquely present in amber. Although preferential preservation of small ichneumonids in amber partly explains its unique subfamily composition, the more complete preservation compared to the compression fossils might play a role, too. In the recently published morphological matrix with 222 characters, up to 64% of characters could be scored in amber fossils, compared to only 38% in compression fossils (Spasojevic et al. 2021). We estimate that an even higher percentage of those characters (around 70%) could be scored for our fossils from Oise amber. In contrast, the amount of missing data in compression fossils is often so big that the fossils must be labelled as *incertae subfamiliae* (Spasojevic et al. 2018a, b; Klopstein and Spasojevic 2019), which suggests that characters for identifying new subfamilies might be rarely preserved.

Not only the amount of missing data is different in amber compared to compression fossils, but also the type of the preserved characters varies (Grimaldi et al. 1994). Due to the chitinous exoskeleton, we usually do not see any inner structures in ichneumonid compression fossils. However, in amber, the remains of insects can become translucent, revealing inner structures. As this is often happening in Oise amber we were, for example, able to see inside the head of *P. eocenicus*, which was occupied by large vessels below each antenna, which might be tracheal air sacs, and a solid structure behind the clypeus, which could correspond to the muscles of the sucking pump. Further examination of Oise amber fossils, both by light microscopy and micro-CT scanning, will certainly reveal many more internal structures in Oise insects (Kehlmaier et al. 2014).

## Difficulties in placing fossil ichneumonids

All three species discussed in this paper exhibit several plesiomorphic characters in combination with more derived characters, making it difficult to decide on stem versus crown group placements. They share the complete propodeal carination, which is characteristic of all Cretaceous subfamilies (Kopylov 2009; 2010a, b; 2012), and possibly also of the earliest representatives of many extant subfamilies, which have subsequently lost some of the carinae (for a discussion on Pimplinae, see Kopylov et al. 2018). In addition, *M. oisella* has a wide, oblique and pentagonal areolet, which is rare among extant ichneumonids (present only in Labeninae), but occurs in many Cretaceous fossils and *Albertocryptus dossenus* that, although placed in Labeninae, was recovered within Ichneumoniformes in a total-evidence analysis (Santos et al. in press). *Pappous trichomatus* and *Palaeometopius eocenicus* both have a broad, subquadrate T1 with long latero-median carinae, which is present in the oldest ichneumonids, Palaeoichneumoninae, and in Labenopimplinae. Therefore, the derived characters, such as the petiolate T1 and bilobed posterior transverse carina on the mesosternum in *M. oisella*, and the setose eyes in *P. trichomatus*, are not enough to clearly place them in crown Phygadeuontinae and crown Tryphoninae, respectively. Finally, the crown group placement of *P. eocenicus* is also questionable, as the most similar extant Tryphoninae do not have a long ovipositor, another plesiomorphic character.

One of the reasons why it is so difficult to distinguish stem from crown groups in ichneumonids is the high prevalence of homoplastic characters (Gauld and Mound 1982) which do not reflect a common ancestry, but rather ecological similarities between groups. However, the problem is not unique to ichneumonids and not only a consequence of a wrong interpretation of homologies, but also of characters in fossil and taphonomic processes (Donoghue and Purnell 2009). The “stem versus crown” distinction became especially important with the advent of node dating, where a wrong interpretation of fossil position leads to erroneous divergence time estimates (Parham et al. 2012; Warnock et al. 2015). A stem group fossil wrongly interpreted as crown group, and thus used to constrain the minimum age of its most recent common ancestor, will directly lead to age estimates which are too old. Sometimes even correctly identified stem fossils are erroneously used to calibrate the age of crown groups. One solution to the problem is a more careful naming of newly described fossils, by expressing the uncertainty in their placement in a prominent place, for instance using the open nomenclature framework (Matthews 1973). Furthermore, palaeontologists should avoid naming fossils after extant genera when the subfamily placement is unclear, in order to avoid future confusion when a placement is revised, as in *Palaeometopius* now removed from Metopiinae. In addition, one can make use of total-evidence dating methods which do not require prior placement of fossils, but rather use morphological information to infer them (Ronquist et al. 2012).

### Lessons for morphological phylogenetics

Our analyses of three Oise amber fossils have demonstrated the difficulties associated with integrating fossils into the modern classification. In the end, only a phylogenetic view on fossil placement can deliver the full picture, as higher classification always somewhat blurs the true relationships, especially where stem lineages are concerned. However, morphological phylogenetic analyses suffer from issues concerning assumptions about character evolution and might thus find erroneous relationships, although Bayesian methods apparently show improvements over parsimony-based techniques (O’Reilly et al. 2016). Importantly, model-based approaches allow testing of scenarios for character evolution and even methods for character coding against one another and thus facilitate their critical evaluation (e.g., Wright et al. 2016; Klopstein and Spasojevic 2019).

The high prevalence of plesiomorphic character states found in this study, most of which are already present in the Cretaceous subfamilies, indicates that the commonly used stationary models of character evolution (Lewis 2001) might be misleading in Ichneumonidae morphology. Such models assume that evolution had reached its steady state already at the root of the tree of the taxa analysed; at least for areolet shape and propodeal carination, the Oise fossils indicate that this might not be the case. Although sample size is of course rather small, it counts several times when fossils are included alongside extant taxa to learn about character evolution (e.g., Coiro et al. 2018). In Hymenoptera, it was demonstrated that inclusion of fossils strongly enhances the signal of directional evolution of wing venation and sclerite fusion, and that

a non-stationary model of morphological evolution can capture this signal (Klopfstein et al. 2015). The use of such models should be evaluated in the future for ichneumonid phylogenetics, at least for the aforementioned character systems.

## Outlook

By describing two new ichneumonid specimens belonging to two new genera, and redescribing *Palaeometopius eocenicus* from Oise amber, we added crucial information and detailed morphological insights to the ichneumonid fossil record in amber. Fossils from the subfamilies Tryphoninae and Phygadeuontinae have been found before, but mostly as compression fossils and from the Late Eocene or younger. This makes *Madma oisella*, *Pappous trichomatius* and *Palaeometopius eocenicus* some of the oldest representatives of those subfamilies.

In this study we highlight the general difficulty of placing fossil species, mainly because they are much older and belong to stem lineages or even extinct side branches. Only a phylogenetic analysis can potentially resolve this issue and lead to a more adequate classification. The newly described fossil species, which are important representatives of early Tryphoninae and Phygadeuontinae, with their highly detailed preservation, will be added to the already existing morphological matrix of Spasojevic et al. (2021). Thus, their high number of coded characters will most certainly add useful information for future phylogenetic analyses integrating fossil and extant taxa.

By describing and carefully classifying new fossil ichneumonid species, we can improve the understanding of the diversity and species composition of this very species-rich group of parasitoids through time. Many inclusions in Oise amber remain unchecked and more ichneumonid specimens, probably including some from extant subfamilies, could be discovered. It remains unclear why there are only extinct subfamilies in the Cretaceous and only extant subfamilies in the Paleogene. It is therefore crucial to continue describing fossils and investigate deposits (e.g., Menat in France) from the time around the K-Pg boundary, to help us understand how the subfamilies evolved and what happened with them during the mass extinction event 66 million years ago.

## Acknowledgements

We thank André Nel (MNHN) for providing access to the collection of unidentified Oise amber pieces and Olivier Bethoux (MNHN) for allowing us to study the type of *Palaeometopius eocenicus*. Lars Vilhelmsen (Natural History Museum of Denmark) provided information about the taxonomic composition of their Ichneumonoidea in Baltic amber, and Istvan Miko (University of New Hampshire) helped interpret some visible internal structures. We thank Gavin Broad (Natural History Museum London) for his valuable opinion about the systematic placement of *Pappous trichomatius* and Andrew Bennett (Canadian National Collection of Insects, Arachnids and Nematods) for his elaborate comments on the systematic placement

of *Pappous trichomatus* and *Madma oisella*. A great thanks also to Dmitri Kopylov and Davide Dal Pos for their constructive comments and feedback in their review, which greatly improved our manuscript.

This study was supported by the Swiss National Science Foundation (grant 310030\_192544 to SK).

## References

- Antropov AV, Belokobylskij SA, Compton SG, Dlusskz GM, Khalaim AI, Kolyada VA, Kozlov MA, Perfilieva KS, Rasnitsyn AP (2014) The wasps, bees and ants (Insecta: Vespida=Hymenoptera) from the insect limestone (Late Eocene) of the Isle of Wight, UK. *Earth and Environmental Science Transactions of the Royal Society of Edinburgh* 104: 335–446. <https://doi.org/10.1017/S1755691014000103>
- Belokobylskij SA, Nel A, Waller A, De Plöeg G (2010) New fossil non-cyclostome braconid wasps from the lowermost Eocene amber of Paris Basin. *Acta Palaeontologica Polonica* 55: 519–527. <https://doi.org/10.4202/app.2009.1114>
- Benner AMR (2015) Revision of the world genera of Tryphoninae (Hymenoptera: Ichneumonidae). *Memoirs of the American Entomological Institute* 86: 1–387.
- Brasero N, Nel A, Michez D (2009) Insects from the Early Eocene amber of Oise (France): diversity and palaeontological significance. *Denisia* 26: 41–52.
- Broad GR, Shaw MR, Fitton MG (2018) Ichneumonid wasps (Hymenoptera: Ichneumonidae): their classification and biology. *Handbooks for the identification of British insects* 7: 1–418.
- Brues CT (1910) The parasitic Hymenoptera of the Tertiary of Florissant, Colorado. *Bulletin of the Museum of Comparative Zoology at Harvard University* 54: 1–125.
- Cockerell TDA (1921) Some Eocene insects from Colorado and Wyoming. *Proceedings of the United States National Museum* 59: 29–39. <https://doi.org/10.5479/si.00963801.59-2358.29>
- Coiro M, Chomicki G, Doyle JA (2018) Experimental signal dissection and method sensitivity analyses reaffirm the potential of fossils and morphology in the resolution of the relationship of angiosperms and Gnetales. *Paleobiology* 44: 1–21. <https://doi.org/10.1017/pab.2018.23>
- De Franceschi D, De Plöeg G (2003) Origine de l'ambre des faciès sparnaciens (Éocène inférieur) du Bassin de Paris: le bois de l'arbre producteur. *Geodiversitas* 25: 633–647.
- Donoghue PCJ, Purnell MA (2009) Distinguishing heat from light in debate over controversial fossils. *BioEssays* 31: 178–189. <https://doi.org/10.1002/bies.200800128>
- Gauld ID, Mound LA (1982) Homoplasy and the delineation of holophyletic genera in some insect groups. *Systematic Entomology* 7: 73–86. <https://doi.org/10.1111/j.1365-3113.1982.tb00127.x>
- Grimaldi DA, Bonwich E, Delannoy M, Doberstein S (1994) Electron microscopic studies of mummified tissues in amber fossils. *American Museum Novitates*, 31 pp.
- Kasparyan DR (1988) A new subfamily and two new genera of ichneumonids (Hymenoptera, Ichneumonidae) from Baltic amber. *Proceedings of the Zoological Institute Leningrad* 175: 38–42. [In Russian]

- Kasparyan DR (1994) A review of the ichneumon flies of Townesitinae Subfam. Nov. (Hymenoptera, Ichneumonidae) from the Baltic amber. *Paleontological Journal* 28: 114–126.
- Kehlmaier C, Dierick M, Skevington JH (2014) Micro-CT studies of amber inclusions reveal internal genitalic features of big-headed flies, enabling a systematic placement of *Metanephrocerus* Aczél, 1948 (Insecta: Diptera: Pipunculidae). *Arthropod Systematics and Phylogeny* 72: 23–36.
- Khalaim AI (2011) First record of the subfamilies Banchinae and Stilbopinae (Hymenoptera: Ichneumonidae) from the Late Eocene Rovno amber (Ukraine). *Russian Entomological Journal* 20(3): 295–298. <https://doi.org/10.15298/rusentj.20.3.13>
- Klopfstein S, Spasojevic T (2019) Illustrating phylogenetic placement of fossils using RoguePlots: An example from ichneumonid parasitoid wasps (Hymenoptera, Ichneumonidae) and an extensive morphological matrix. *PLoS ONE* 14: e0212942. <https://doi.org/10.1371/journal.pone.0212942>
- Klopfstein S, Vilhelmsen L, Ronquist F (2015) A nonstationary Markov model detects directional evolution in hymenopteran morphology. *Systematic Biology* 64: 1089–1103. <https://doi.org/10.1093/sysbio/syv052>
- Klopfstein S, Santos B, Shaw MR, Alvarado M, Bennett AMR, Dal Pos D, Giannotta M, Herrera Florez AF, Karlsson D, Khalaim AI, Lima AR, Mikó I, Sääksjärvi IE, Shimizu S, Spasojevic T, Van Noort S, Vilhelmsen L, Broad GR (2019) Darwin wasps: a new name heralds renewed efforts to unravel the evolutionary history of Ichneumonidae. *Entomological Communications* 1: ec01006. <https://doi.org/10.37486/2675-1305.ec01006>
- Klopfstein (2021) High diversity of pimpline parasitoid wasps (Hymenoptera, Ichneumonidae, Pimplinae) from the lowermost Eocene Fur Formation. *BioRxiv*, 1–30. <https://doi.org/10.1101/2021.11.18.468631>
- Kopylov DS (2009) A new subfamily of ichneumonids from the Lower Cretaceous of Transbaikalia and Mongolia (Insecta: Hymenoptera: Ichneumonidae). *Paleontological Journal* 43: 83–93. <https://doi.org/10.1134/s0031030109010092>
- Kopylov DS (2010a) Ichneumonids of the subfamily Tanychorinae (Insecta: Hymenoptera: Ichneumonidae) from the Lower Cretaceous of Transbaikalia and Mongolia. *Paleontological Journal* 44: 180–187. <https://doi.org/10.1134/s0031030110020097>
- Kopylov DS (2010b) A new subfamily of ichneumon wasps (Insecta: Hymenoptera: Ichneumonidae) from the Upper Cretaceous of the Russian Far East. *Paleontological Journal* 44: 422–433. <https://doi.org/10.1134/s003103011004009x>
- Kopylov DS (2012) New Ichneumonidae (Hymenoptera) from the Upper Cretaceous ambers of the Taimyr Peninsula. *Paleontological Journal* 46: 383–391. <https://doi.org/10.1134/S0031030112040041>
- Kopylov DS, Brothers DJ, Rasnitsyn AP (2010) Two New Labenopimpline Ichneumonids (Hymenoptera: Ichneumonidae) from the Upper Cretaceous of Southern Africa. *African Invertebrates* 51: 423–430. <https://doi.org/10.5733/afin.051.0211>
- Kopylov DS, Spasojevic T, Klopfstein S (2018) New ichneumonids (Hymenoptera, Ichneumonidae) from the Eocene Tadushi Formation, Russian Far East. *Zootaxa* 4442: 319–330. <https://doi.org/10.11646/zootaxa.4442.2.8>

- Lewis PO (2001) A likelihood approach to estimating phylogeny from discrete morphological character data. *Systematic Biology* 50: 913–925. <https://doi.org/10.1080/106351501753462876>
- Li L, Kopylov DS, Shih C, Ren D (2017) The first record of Ichneumonidae from the Upper Cretaceous of Myanmar. *Cretaceous Research* 70: 152–162. <https://doi.org/10.1016/j.cretres.2016.11.001>
- Manukyan AR (2019) New data on ichneumon wasps of the subfamily Pherhombinae (Hymenoptera, Ichneumonidae) from Baltic amber, with descriptions of three new species. *Entomological Review* 99: 1324–1338. <https://doi.org/10.1134/S0013873819090112>
- Manukyan AR, Zhindarev LA (2021) Fossil Darwin wasps (Hymenoptera: Ichneumonidae) from Baltic amber. *Palaeoentomology* 4: 637–647. <https://doi.org/10.11646/palaeoentomology.4.6.13>
- Martínez-Delclòs X, Briggs DEG, Peñalver E (2004) Taphonomy of insects in carbonates and amber. *Palaeogeography, Palaeoclimatology, Palaeoecology* 203: 19–64. [https://doi.org/10.1016/S0031-0182\(03\)00643-6](https://doi.org/10.1016/S0031-0182(03)00643-6)
- Matthews SC (1973) Notes on open nomenclature and synonymy lists. *Palaeontology* 16: 713–719.
- McKellar RC, Kopylov DS, Engel MS (2013) Ichneumonidae (Insecta: Hymenoptera) in Canadian Late Cretaceous amber. *Fossil Record* 16: 217–227. <https://doi.org/10.5194/fr-16-217-2013>
- Meier N, Wacker A, Klopstein S (2022) New fossil wasp species from the earliest Eocene Fur Formation has its closest relatives in late Eocene ambers (Hymenoptera, Ichneumonidae, Pherhombinae). *Bulletin of the Society of Systematic Biologists* 1. <https://doi.org/10.18061/bssb.v1i1.8427>
- Menier J-J, Nel A, Waller A, de Ploëg G (2004) A new fossil ichneumon wasp from the Lowermost Eocene amber of Paris Basin (France), with a checklist of fossil Ichneumonoidea s.l. (Insecta: Hymenoptera: Ichneumonidae: Metopiinae). *Geologica Acta* 2: 83–94.
- Nel A, de Ploëg G, Millet J, Menier J-J, Waller A (2004) The French ambers: a general conspectus and the Lowermost Eocene amber deposit of Le Quesnoy in the Paris Basin. *Geologica Acta* 2: 3–8.
- Nel A, Prokop J, De Ploëg G, Millet J (2005) New Psocoptera (Insecta) from the lowermost Eocene amber of Oise, France. *Journal of Systematic Palaeontology* 3: 371–391. <https://doi.org/10.1017/S1477201905001598>
- O'Reilly JE, Puttick MN, Parry L, Tanner AR, Tarver JE, Fleming J, Pisani D, Donoghue PCJ (2016) Bayesian methods outperform parsimony but at the expense of precision in the estimation of phylogeny from discrete morphological data. *Biology Letters* 12: e20160081. <https://doi.org/10.1098/rsbl.2016.0081>
- PaleoBioDB (2021) The Paleobiology Database. <https://paleobiodb.org/#/> [December 22, 2021]
- Parham JF, Donoghue PCJ, Bell CJ, Calway TD, Head JJ, Holroyd PA, Inoue JG, Irmis RB, Joyce WG, Ksepka DT, Patané JSL, Smith ND, Tarver JE, van Tuinen M, Yang Z, Angielczyk KD, Greenwood JM, Hipsley CA, Jacobs L, Makovicky PJ, Müller J, Smith

- KT, Theodor JM, Warnock RCM, Benton MJ (2012) Best practices for justifying fossil calibrations. *Systematic Biology* 61: 346–359. <https://doi.org/10.1093/sysbio/syr107>
- Piton L (1940) Paléontologie du gisement éocène de Menat (Puy-de-Dôme) (Flore et Faune). Thèse de doctorat, Clermont-Ferrand: Université de Clermont, 303 pp.
- Rasnitsyn AP (1978) Predislovie. In: Vostochnopalearkticheskie pereponchatokrylye nasekomye podsemeistva Ichneumoninae. Nauka Press, Leningradskoe otdelenie (Leningrad), 3–5.
- Ronquist F, Klopfstein S, Vilhelmsen L, Schulmeister S, Murray DL, Rasnitsyn AP (2012) A total-evidence approach to dating with fossils, applied to the early radiation of the Hymenoptera. *Systematic Biology* 61: 973–999. <https://doi.org/10.1093/sysbio/sys058>
- Rust J (1988) Biostratonomie von Insekten aus der Fur-Formation von Dänemark (Moler, oberes Paleozän/unteres Eozän). *Paläontologische Zeitschrift* 72: 41–58. <https://doi.org/10.1007/BF02987814>
- Sadowski EM, Schmidt AR, Seyfullah LJ, Kunzmann L (2017) Conifers of the ‘Baltic amber forest’ and their palaeoecological significance. *Stapfia* 106: 1–73.
- Sadowski E-M, Schmidt AR, Seyfullah LJ, Solórzano-Kraemer M, Neumann C, Perrichot V, Hamann C, Milke R, Nascimbene PC (2021) Conservation, preparation and imaging of diverse ambers and their inclusions. *Earth-Science Reviews* 220: e103653. <https://doi.org/10.1016/j.earscirev.2021.103653>
- Santos BF (2017) Phylogeny and reclassification of Cryptini (Hymenoptera, Ichneumonidae, Cryptinae), with implications for ichneumonid higher-level classification. *Systematic Entomology* 42: 650–676. <https://doi.org/10.1111/syen.12238>
- Santos BF, Sandoval M, Spasojevic T, Giannotta M, Brady SG (in press) A parasitoid puzzle: phylogenomics, total-evidence dating and the role of Gondwanan vicariance in the diversification of Labeninae (Hymenoptera, Ichneumonidae). *Insect Systematics and Diversity*.
- Schneider CA, Rasband WS, Eliceiri KW (2012) NIH Image to ImageJ: 25 years of image analysis. *Nature Methods* 9(7): 671–675. <https://doi.org/10.1038/nmeth.2089>
- Selden PA, Penney D (2017) Imaging techniques in the study of fossil spiders. *Earth-Science Reviews* 166: 111–131. <https://doi.org/10.1016/j.earscirev.2017.01.007>
- Sharkey MJ, Wahl DB (1992) Cladistics of the Ichneumonoidea (Hymenoptera). *Journal of Hymenoptera Research* 1: 15–24. <https://doi.org/10.5962/bhl.part.29715>
- Spasojevic T, Broad GR, Bennett AMR, Klopfstein S (2018a) Ichneumonid parasitoid wasps from the Early Eocene Green River Formation: five new species and a revision of the known fauna (Hymenoptera, Ichneumonidae). *Paläontologische Zeitschrift* 92: 35–63. <https://doi.org/10.1007/s12542-017-0365-5>
- Spasojevic T, Wedmann S, Klopfstein S (2018b) Seven remarkable new fossil species of parasitoid wasps (Hymenoptera, Ichneumonidae) from the Eocene Messel Pit. *PLoS ONE* 13: e0197477. <https://doi.org/10.1371/journal.pone.0197477>
- Spasojevic T, Broad GR, Sääksjärvi IE, Schwarz M, Ito M, Korenko S, Klopfstein S (2021) Mind the Outgroup and Bare Branches in Total-Evidence Dating: a Case Study of Pimpliform Darwin Wasps (Hymenoptera, Ichneumonidae). *Systematic Biology* 70: 322–339. <https://doi.org/10.1093/sysbio/syaa079>
- Statz G (1936) Ueber alte und neue fossile Hymenopterenfunde aus den Tertiären Ablagerungen von Rott am Siebengebirge. *Decheniana* 93: 256–312.

- Theobald N (1937) Les insectes fossiles des terrains Oligocenes de France. In: Theobald N (Ed.) *Insectes fossiles des Terrains Oligocene*. Imprimeria Georges Thomas, Nancy, 473 pp.
- Townes HK (1969) The genera of Ichneumonidae, Part 1. *Memoirs of the American Entomological Institute* 11: 1–300. <https://doi.org/10.1007/BF02027741>
- Townes HK (1970a) The genera of Ichneumonidae, Part 2. *Memoirs of the American Entomological Institute* 12: 1–543.
- Townes HK (1970b) The genera of Ichneumonidae, Part 3. *Memoirs of the American Entomological Institute* 13: 1–310.
- Townes HK (1971) The genera of Ichneumonidae, Part 4. *Memoirs of the American Entomological Institute* 17: 1–372.
- Van de Kamp T, dos Santos Rolo T, Baumbach T, Krogmann L (2014) Scanning the Past – Synchrotron X-ray microtomography of fossil wasps in amber. *Entomologie heute* 26: 151–160.
- Warnock RCM, Parham JF, Joyce WG, Lyson TR, Donoghue PCJ (2015) Calibration uncertainty in molecular dating analyses: there is no substitute for the prior evaluation of time priors. *Proceedings of the Royal Society B* 282: e20141013. <https://doi.org/10.1098/rspb.2014.1013>
- Wright AM, Lloyd GT, Hillis DM (2016) Modeling character change heterogeneity in phylogenetic analyses of morphology through the use of priors. *Systematic Biology* 65: 602–611. <https://doi.org/10.1093/sysbio/syv122>
- Yu DS, Van Achtenberg C, Horstmann K (2016) Taxapad 2016. Ichneumonoidea 2015 (Biological and taxonomical information), Taxapad Interactive Catalogue Database on flash-drive. Nepean, Ottawa. [www.taxapad.com](http://www.taxapad.com)



# Two new genera of Encyrtidae (Hymenoptera, Chalcidoidea) with reduced ovipositor sheaths

Serguei A. Simutnik<sup>1</sup>, Evgeny E. Perkovsky<sup>1</sup>,  
Mykola R. Khomych<sup>2</sup>, Dmitry V. Vasilenko<sup>3,4</sup>

**1** I.I. Schmalhausen Institute of Zoology, National Academy of Sciences of Ukraine, Kiev, 01601 Ukraine  
**2** Vil. Voronky, Varash Distr., Rovno Region, Rovno, 34330 Ukraine **3** Borissiak Paleontological Institute, Russian Academy of Sciences, Moscow, 117647 Russia **4** Cherepovets State University, Cherepovets, Vologda Region, 162600 Russia

Corresponding author: Serguei A. Simutnik ([simutnik@gmail.com](mailto:simutnik@gmail.com))

---

Academic editor: Petr Janšta | Received 10 December 2021 | Accepted 14 February 2022 | Published 28 February 2022

---

<http://zoobank.org/B7481032-36C1-4517-830D-9CDC3DB7C5DA>

---

**Citation:** Simutnik SA, Perkovsky EE, Khomych MR, Vasilenko DV (2022) Two new genera of Encyrtidae (Hymenoptera, Chalcidoidea) with reduced ovipositor sheaths. *Journal of Hymenoptera Research* 89: 47–60. <https://doi.org/10.3897/jhr.89.79180>

---

## Abstract

*Archaeocercoides puchkovi* Simutnik, **gen. et sp.nov.**, and *Rovnopositor voblenkoi* Simutnik, **gen. et sp.nov.**, are described and illustrated based on female specimens from late Eocene Rovno amber. Like most previously described Eocene Encyrtidae, the new taxa differ from the majority of extant encyrtids by the apical or nearly apical position of the cerci, the short radicle, and the long marginal vein of the forewing. Both new genera are characterized by a strongly reduced ovipositor sheaths but long and upwardly bent ovipositor stylets (in the “ovipositing position”), a stigmal vein with a long uncus, and the absence of a filum spinosum. The new genera differ from each other in the width of frontovertex, the location of the cerci, and the lengths of funicular segments and marginal vein. *A. puchkovi* was fossilized near a Coccoidea crawler.

## Keywords

Cerci, Coccoidea, radicle, Rovno amber, syninclusion, valvulae of ovipositor

## Introduction

An extremely apical or near apical position of the cerci is very rare among extant encyrtids, but is seen in most extinct ones (Simutnik and Perkovsky 2006, 2018a; Simutnik 2021; Simutnik et al. 2021a, 2021b). Two new fossil encyrtid genera with this character state are described below.

This brings the number of Rovno amber hymenopteran genera unknown in Baltic amber to 28 of 90, i.e., 31% (our unpublished data). This includes 22 of 52 (42.3%) non-ant hymenopterans genera and 46 of 69 of non-ant species (66.7%) (Perkovsky 2018; Manukyan 2019; Martynova et al. 2019; Perkovsky et al. 2020; Simutnik and Perkovsky 2020; Simutnik et al. 2020, 2021b; Belokobylskij et al. 2021; Colombo et al. 2021a, b, c; Manukyan and Zhindarev 2021). Baltic amber species from large arthropod orders and suborders reported from Rovno amber vary from 32.4% for Trichoptera (Perkovsky 2017; Melnitsky et al. 2021a, 2021b, 2021c), 24% for Nematocera (Gilka et al. 2021) and 15% for Coleoptera (Telnov et al. 2021; Kirichenko-Babko et al. 2022; Perkovsky et al. 2022); 33% of non-ant hymenopterans common for Baltic and Rovno amber is close to the ratio for caddisflies (Trichoptera), which have been extensively studied (e.g., Melnitsky et al. 2021c and references therein). As more than 300 insect species have been described from Rovno amber (Martynov et al. 2021), this supports an independent origin of its fauna.

## Material and methods

The studied specimens are housed in the collection of the Schmalhausen Institute of Zoology of the National Academy of Sciences of Ukraine, Kiev (SIZK). The amber pieces containing the holotypes were found in the Varash District of Rovno Region (UA-28099) (Yamamoto et al. 2022 and references therein), and in Pugach quarry (Klesov) (fauna of the deposit reviewed in Mitov et al. 2021), Sarny District, Rovno Region (K-9948). The Varash specimen was cut from the big piece, the Klesov specimen is part of an unbiased sample (Perkovsky et al. 2012), bought from the Ukramber factory (Rovno); the raw weight of clear piece 2-1410 was 7.3 g, size 45×25×15 mm.

Photographs were taken using a Leica Z16 APO stereomicroscope equipped with a Leica DFC 450 camera and processed with LAS Core and Adobe Photoshop software (brightness and contrast only). To improve imaging, we applied sucrose syrup of approximately the same refractive index as the amber itself and then placed a glass cover slip on top. To photograph some of the structures, the cover slip was placed at different angles to the surface of the amber (Fig. 1A). Afterwards, the syrup was removed by warm water.

Terminology and abbreviations follow Sharkov (1985), Gibson (1997), and Heraty et al. (2013). The following abbreviations are used in the text: **F1**, **F2**, **etc.** = funicular segments 1, 2, etc.; **LOL** = minimum distance between the anterior ocellus and a

posterior ocellus; **Mt1, Mt2, etc.** = metasomal terga, numbering starts from petiole (Mt1); **OOL** = minimum distance between an eye margin and the adjacent posterior ocellus; **OCL** = minimum distance between a posterior ocellus and the occipital margin; **POL** = minimum distance between the posterior ocelli.

## Results

### Systematic paleontology

**Chalcidoidea Latreille, 1817**

**Encyrtidae Walker, 1837**

**Genus *Archaeocercoides* Simutnik, gen. nov.**

<http://zoobank.org/DAE286E2-09CB-438D-A5B7-F467697167DB>

**Type species.** *Archaeocercoides puchkovi* Simutnik, sp. nov.

**Species composition.** Type species only.

**Etymology.** The new genus resembles the extinct genus *Archaeocercus* Simutnik, 2018 by its extremely apical position of the cerci (Fig. 3B–D, and figs 5, 6 in Simutnik and Perkovsky 2018a). The genus name is a masculine noun.

**Diagnosis.** Habitus not ‘encyrtiform’, body not compact, slightly elongated and flattened; minimum distance between eyes almost 0.5× head width; frontovertex broader than long, ocelli in strongly obtuse triangle, posterior ocelli elliptical in dorsal view; all 6 funicular segments transverse, first funicular segment ring-like; clava only slightly shorter than funicle, about 2.2× as long as broad; mesoscutum and scutellum flat, notaular lines absent; scutellum as long as broad, flat, and as long as mesoscutum; marginal vein more than three times as long as broad, shorter than postmarginal one; covering setae (sensu Sharkov 1985) along basal margin of linea calva present, poorly-developed, but much longer than in *Archaeocercus* (Fig. 3A: cs and fig. 6 in Simutnik and Perkovsky 2018a); filum spinosum absent; parastigma not widened, only slightly wider than previous part of submarginal vein; strigil poorly developed; cerci located extremely close to gastral apex (Fig. 3B–D); apex of hypopygium reaching way past apex of gaster (Fig. 3B–D), lateral margins of hypopygium with row of short setae (Fig. 3C); ovipositor sheaths very small (supposedly, their rudiments are visible in Fig. 3C, D: v3?); protruding part of ovipositor stylet upwardly bent, approximately as long as mesotarsus (Fig. 3B–D). However, the ovipositor, partly, is in the “laying or ovipositing position”. Therefore, when it was not in the ovipositing position, it would be mostly retracted and enclosed within the hypopygium and not really truly exerted. The hypopygium may also slightly not reach to the apex of the gaster.

**Remarks.** The new genus is very similar to *Archaeocercus* Simutnik, 2018, but differs by the OOL being equal to the posterior ocellar diameter, the posterior ocelli are relatively larger and elliptical in dorsal view; the clava is more narrow and elongated;

the parastigma is not expanded (*Archaeocercus* with distinct parastigma, see figs 1, 2, 6 in Simutnik and Perkovsky 2018a); notauli are absent; the scutellum is longer, as broad as long, not shorter than the mesoscutum; the inner angles of the axillae are wider; the covering setae along linea calva are short but distinctly present; and by its long ovipositor stylet (in the “ovipositing position”) (see figs 1–6 in Simutnik and Perkovsky 2018a). *Trjapitzion* Simutnik, 2018 clearly differs from the new genus in a high interantennal prominence, strongly expanded parastigma, strongly widened scape and mandible, and in very short legs, especially tarsi (figs 2, 3, 6 in Simutnik and Perkovsky 2018b).

***Archaeocercoides puchkovi* Simutnik, sp. nov.**

<http://zoobank.org/50A0A5E5-EFD7-4C7C-AD5B-2B095282C5A9>

Figs 1A, B, D, 2, 3

**Material.** *Holotype*, SIZK, no. UA-28099, 1♀, Varash District, Rovno Region, Ukraine; Rovno amber; late Eocene. The inclusion is in a yellow and clear piece of amber in a shape of parallelepiped (ca. 40 × 10 × 9 mm), one side of which contains a layer of organic residues. All body parts are preserved.

**Syninclusion.** Crawler of Coccoidea (Fig. 1C, D).

**Etymology.** The species is named in memory of our colleague coleopterist Prof. Aleksandr Vasilievich Puchkov.

**Description. Female.** Habitus as in Figs 1B, 2C. Body not compact, slightly elongated and flattened. Body length 1.2 mm.

**Coloration.** Body, antenna, tegula, gaster dorsally and ventrally black; surface of frontovertex, mesoscutum, scutellum and axillae smooth, shiny, but without metallic shine, monotonously shallow reticulate with sparse punctures, evenly clothed in short setae (Figs 1B, 2A); coxae, and legs black, meso- and metatibia with lighter apices; protarsus dark; mesotibial spur, meso- and metatarsus light brown to yellowish.

**Head.** Hypognathous, slightly wider than thorax (8:7) in dorsal view, twice as broad as long, with rounded occipital margin; eyes bare, with inner orbits parallel; minimum distance between eyes almost 0.5× head width; OOL about equal to posterior ocellar diameter (Fig. 2A); OCL about equal to half of posterior ocellar diameter; OOL:POL:LOL:OCL about 1:9:5.5:1.5; eye reaching occipital margin; facial cavity and interantennal prominence present but without distinct antennal scrobes (Fig. 2A); toruli located above of mouth margin, about at level of lower margin of eyes (Fig. 2B); malar sulcus complete; mandibles, probably two-toothed, with powerful teeth (Fig. 2B).

**Antenna.** Genuiculate, 11-segmented (1:1:6:3); radicle short, about 2–2.5× as long as broad; scape wide, flattened (Fig. 2A); pedicel conical, slightly shorter than F1–F4 combined, longer than any segment of funicle; funicle cylindrical, all segments broader than long, width of flagellomeres increases toward apex; F4–F6 and all segments of clava with mps (Fig. 2A, B); clava large, only slightly shorter than funicle, about 2.2×

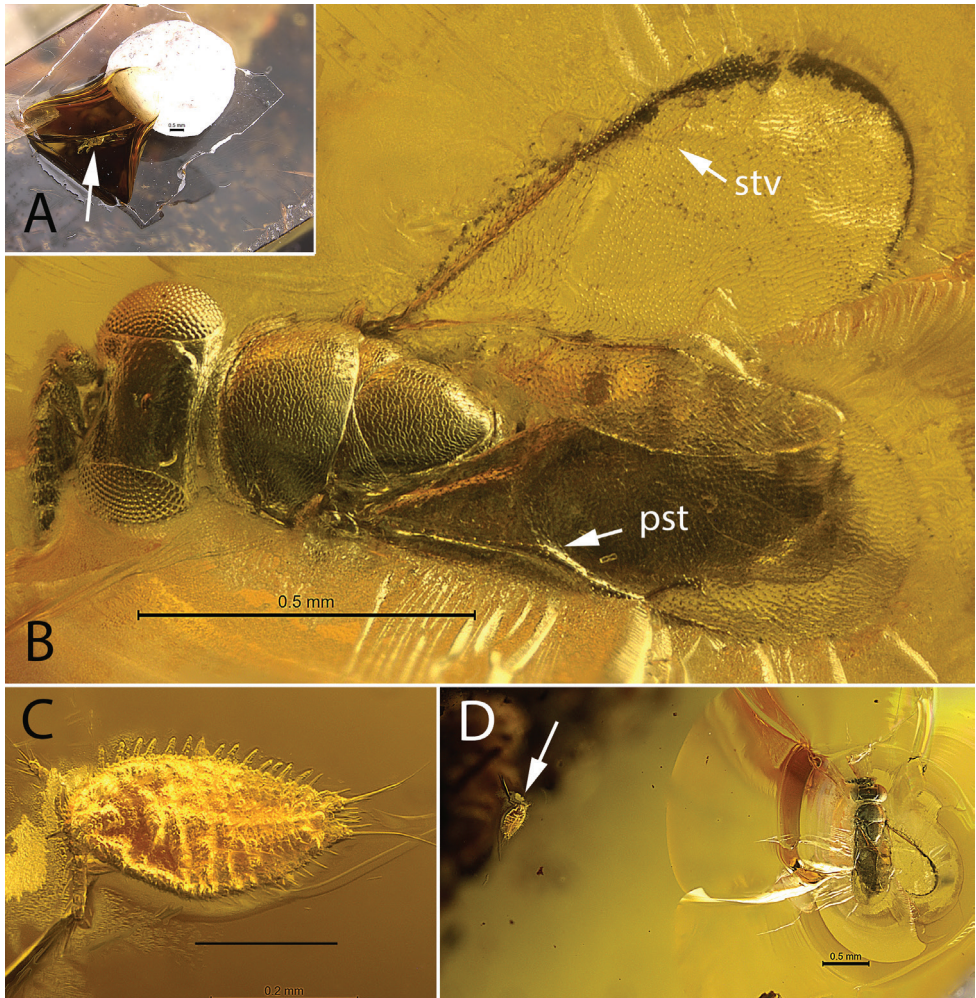


**Figure 1.** **A** cover slip at some angle to the surface of the amber, the inclusion is shown by an arrow **B** *Archaeocercoides puchkovi*, gen. et sp. nov., holotype female, body, dorsal (pst – parastigma, stv – stigmal vein) **C** syninclusion, crawler of Coccoidea **D** *A. puchkovi*, gen. et sp. nov., fossilized near the crawler of Coccoidea (arrow). Scale bars: 0.5 mm (**A**, **B**, **D**); 0.2 mm (**C**).

as long as broad, with small oblique truncation on non-acute apical segment (Fig. 2B: ot), slightly wider than F6; flagellum and clava clothed in short setae.

**Mesosoma.** Pronotum short, almost vertical, in dorsal view without transverse dorsal surface (Fig. 2A); mesoscutum broader than long, flat; axillae transverse-triangular with anteromedial angles contiguous (Fig. 2A); prepectus large, bare, polygonally reticulate, posterior margin extended to base of tegula; acropleuron convex, bare, with shallow longitudinal reticulate sculpture, long, in lateral view twice as long as height (Fig. 2C: ac), with distinct acropleural sulcus; subtegular region (Fig. 2D: str) of acropleuron large, convex, delineated by distinct sulcus; metapleuron narrow, without visible setation (Fig. 2C).

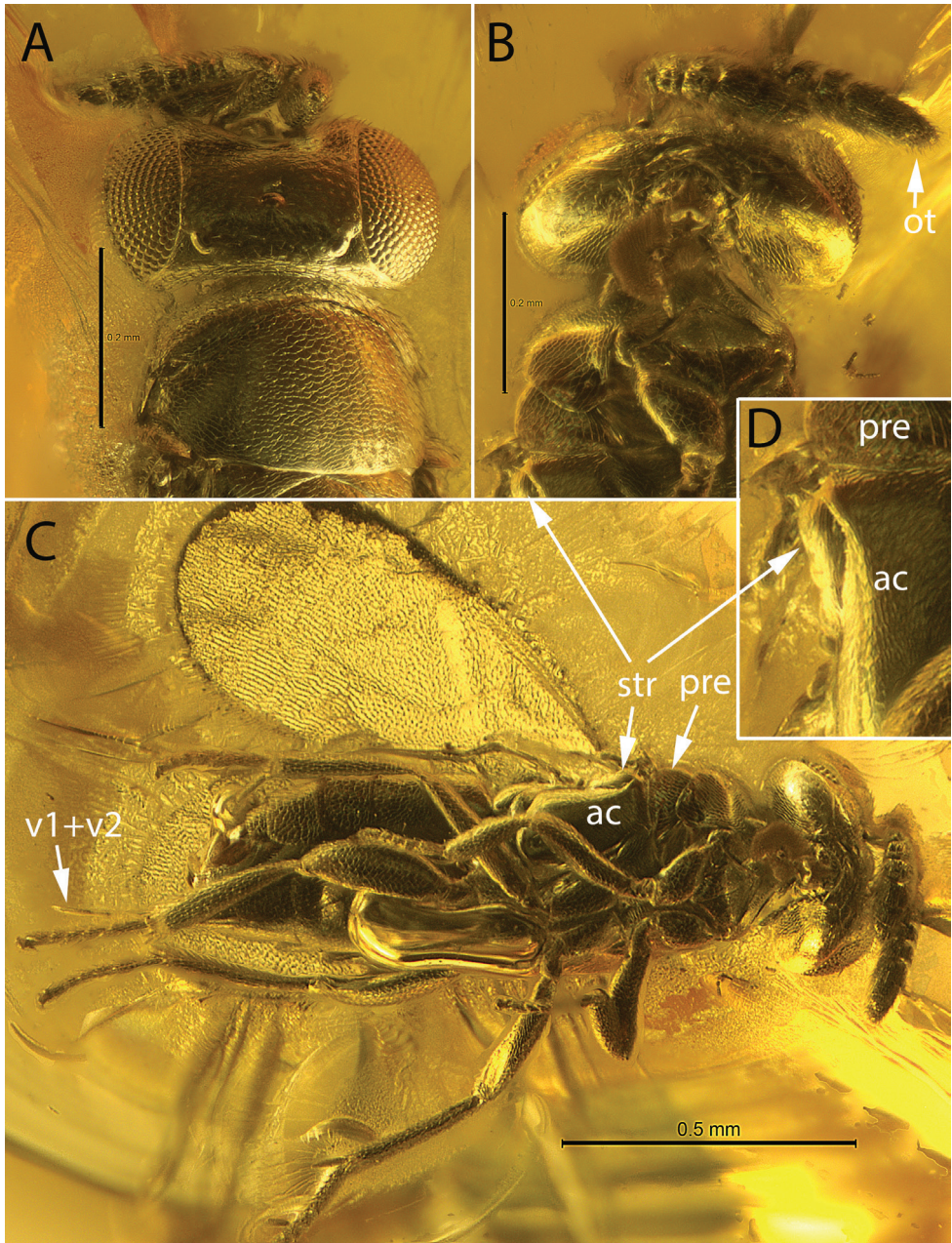


**Figure 2.** *A. puchkovi*, gen. et sp.nov., holotype female **A** head, mesoscutum, dorsal **B** head, anterior part of the mesosoma, ventral (ot – oblique truncation) **C** body, ventrolateral (ac – acropleuron, pre – prepectus, str – subtegular region, v1 + v2 – ovipositor stylet) **D** subtegular region, ventrolateral. Scale bars: 0.2 mm (**A**, **B**); 0.5 mm (**C**).

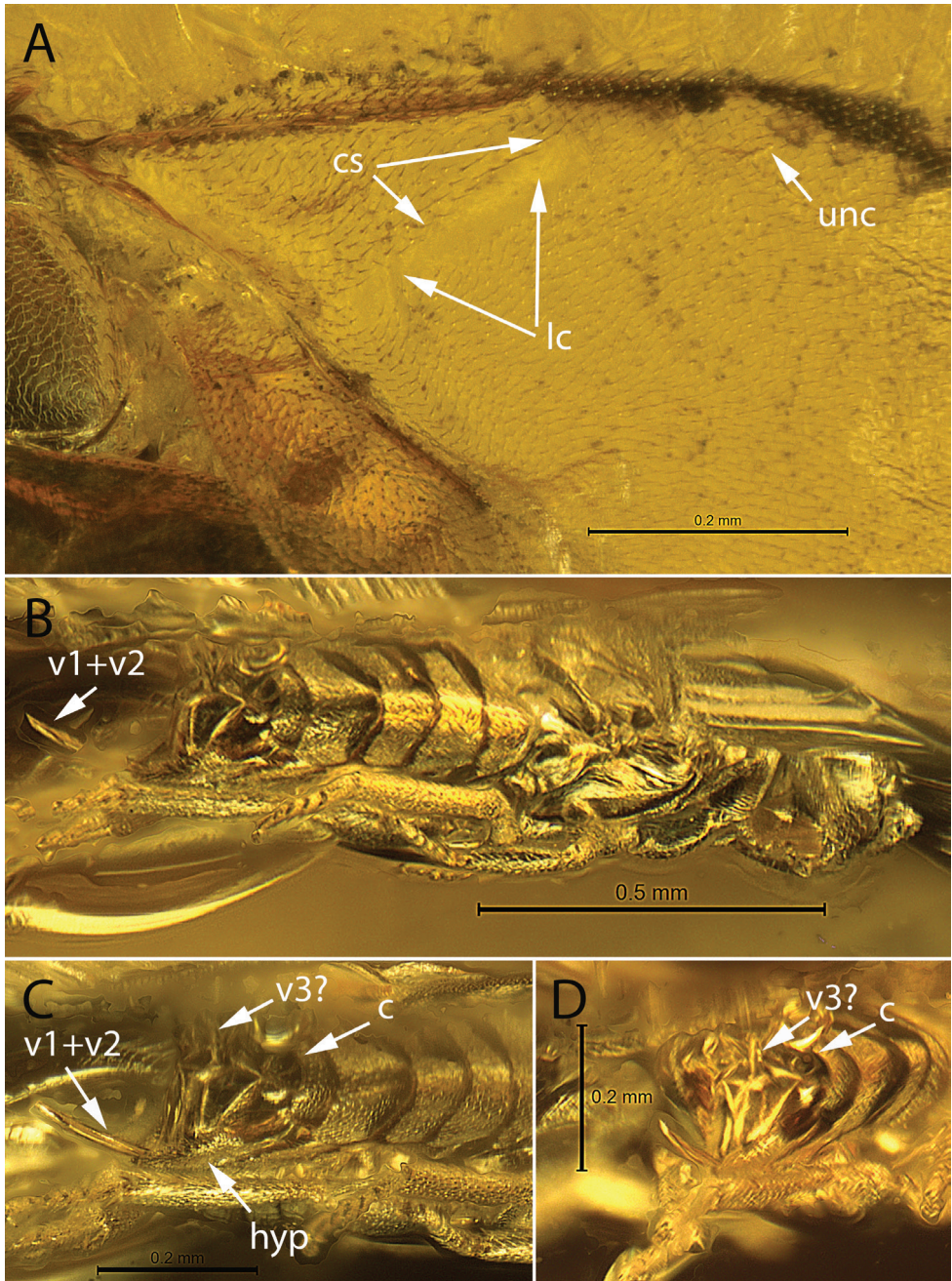


**Figure 3.** *A. puchkovi*, gen. et sp. nov., holotype female **A** wings (cs – covering setae, lc– linea calva, unc – uncus) **B** body, lateral (v1 + v2 – ovipositor stylet) **C** apex of gaster, lateral (c – cercus, hyp– hypopygium, v3? – supposedly, ovipositor sheath) **D** apex of gaster, posterolateral. Scale bars: 0.2 mm (**A**, **C**, **D**); 0.5 mm (**B**).

**Wings.** Fully developed. Fore wing with basal cell uniformly setose; costal cell narrow; submarginal vein without distinct extension (Fig. 3A), although, when lighting from above, parastigma appears to be somewhat swollen (Fig. 1B: pst); hyaline break (unpigmented area) present; marginal vein long, but slightly shorter than stigmal and postmarginal veins (Fig. 1B, left wing); proportions of forewing venation as in Figs 1B, 2C, 3A; stigmal vein with long narrow uncus, consisting row of uncal sensillae (Fig. 3A: unc); enlarged seta marking apex of postmarginal vein of fore wing rather absent (Fig. 3A); setae of marginal fringe short.

**Legs.** Normal in size, alike polygonally reticulate; protibia with long, curved calcar; basitarsal comb poorly developed; tarsi 5-segmented; mesotibial spur slightly shorter than mesobasitarsus; metatibia with two spurs.

**Gaster.** As long as mesosoma, polygonal reticulate equal dorsally and ventrally, apical margins of metasomal terga straight, parallel; paratergites and cercal setae not visible; ovipositor stylet combined from 1<sup>st</sup> and 2<sup>nd</sup> valvulae (stylet suture presumably visible in Fig. 3C); hypopygium in Fig. 3B–D: hyp.

**Male.** Unknown.

### **Genus *Rovnopositor* Simutnik, gen. nov.**

<http://zoobank.org/45722928-C925-48E9-930F-D5BD9759E370>

**Type species.** *Rovnopositor voblenkoi* Simutnik, sp. nov.

**Species composition.** Type species only.

**Etymology.** The name of the genus is a combination of the words “Rovno” and “ovipositor”. The new genus is distinguished by an unusual ovipositor structure. Gender masculine.

**Diagnosis.** Habitus not ‘encyrtiform’, body not compact, not flattened; ocelli in almost right angled triangle (Fig. 5B), posterior ocelli elliptical in dorsal view; frontovertex about as long as broad; flagellum long, first funicular segment 1.5× as long as broad, funicle without transverse segments; clava slightly longer than F4–F6 combined, 2.5× as long as broad; mesoscutum and scutellum convex, notauli absent; scutellum as broad as long, and as long as mesoscutum; marginal vein relatively short, twice as long as broad, and one-third as long as postmarginal vein; setae along basal margin of linea calva short; filum spinosum absent; parastigma almost not widened; strigil present, well-developed; cerci slightly advanced toward gastral base, with long cercal setae (Fig. 5D: cers); apex of hypopygium reaching way past apex of gaster (in ovipositing position, Fig. 5A,D: hyp), lateral margins of hypopygium bare, without row of setae; protruding part of ovipositor stylet stout, upwardly bent (in ovipositing position); ovipositor sheaths strongly reduced, not visible in lateral view.

**Remarks.** The new genus differs from *Archaeocercoides* in the right angled ocellar angle; the frontovertex is about as long as broad; its long flagellum, the first funicular segment being longer than broad, the funicle without transverse segments; the clava slightly longer than F4–F6 combined, 2.5× as long as broad; the relatively short marginal vein, twice as long as broad and one-third length of postmarginal vein; the

convex mesoscutum and scutellum; the well-developed strigil; the cerci are noticeably advanced toward the gastral base; the lateral margins of hypopygium are bare; and in its stouter and longer protruding part of the ovipositor stylet (in ovipositing position).

***Rovnpositor voblenkoi* Simutnik, sp. nov.**

<http://zoobank.org/1940BF44-3174-40EE-8DD7-305A9013317C>

Figs 4, 5

**Material. Holotype.** SIZK, no. K-9948, 1 ♀, Klesov, Sarny District, Rovno Region, Ukraine; Rovno amber; late Eocene. The inclusion is in a reddish and not very transparent piece of amber in a shape of irregular triangular prism (ca. 10 × 10 × 15 × 7 mm) (Fig. 4B). All body parts are preserved.

**Syninclusions.** SIZK, no. K-9949, 2 Dolichopodidae, Aranei, stellate hairs.

**Etymology.** The species is named in memory of our colleague Aleksandr Sergeevich Voblenko, an entomologist, zoologist, naturalist, and teacher.

**Description. Female.** Habitus as in Fig. 4C. Body not compact, not flattened. Body length 1.25 mm.

**Coloration.** Body, antennae, gaster dorsally and ventrally dark, without metallic shine, monotonously shallow reticulate; pronotum, mesoscutum, and scutellum clothed in more long setae.

**Head.** Hypognathous, wider than its length, slightly wider than thorax, with rounded occipital margin (Fig. 5B); eyes bare, with inner orbits rather slightly divergent (Fig. 4D); OOL equal to posterior ocellar diameter; OCL about twice as long as posterior ocellar diameter; eye reaching occipital margin; interantennal projection small but visible in lateral view (Fig. 4A); toruli located at level of lower margin of eyes (Fig. 4A); malar sulcus complete; height of eye about twice larger than malar space; mandibles narrow, probably two-toothed (Figs 4A, C; 5A).

**Antenna.** 11-segmented (1:1:6:3); radicle short, twice as long as broad; scape long, about 5× as long as broad (Fig. 4A); pedicel conical, as long as F1 and F2 combined, longer than any segment of funicle; funicle not flattened, width of flagellomeres slightly increases toward apex; all segments of funicle and clava with mps (Fig. 4A); clava with small oblique truncation on rounded apical segment (Fig. 4A), slightly wider than F6; flagellum and clava clothed in short setae.

**Mesosoma.** Pronotum short, almost vertical, in dorsal view without transverse dorsal surface (Fig. 5B); mesoscutum about as broad as long; axillae transverse-triangular with anteromedial angles contiguous; prepectus large, bare, polygonally reticulate (Fig. 5B); acropleuron convex, bare, with shallow longitudinal reticulate sculpture, long; subtegular region of acropleuron large, convex, delineated by distinct sulcus; metapleuron and propodeum without visible setation (Fig. 4C).

**Wings.** Fully developed. Fore wing with costal cell narrow; submarginal vein without extension; hyaline break present; setation of linea calva in holotype poorly visible (Fig. 5C); marginal vein 0.5× as long as stigmal one; proportions of forewing venation as in Fig. 5C; stigmal vein with long narrow uncus, consisting row of uncal

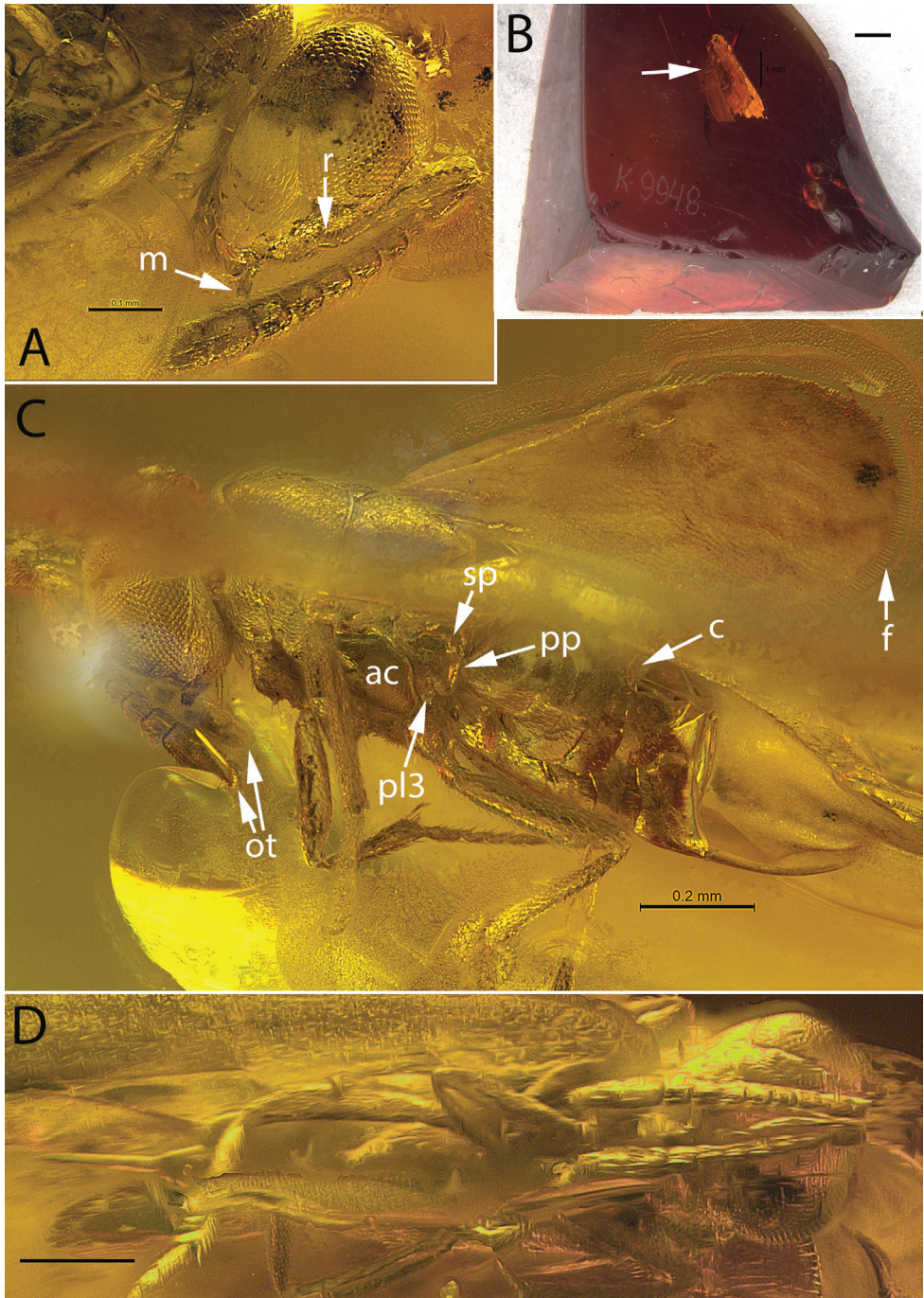


**Figure 4.** *Rovnopositor voblenkoi* gen. et sp. nov., holotype female **A** head, antenna, lateral (m – mandible, r – radicle) **B** piece of amber with holotype (arrow) **C** body, dorsolateral (ac – acropleuron, c – cercus, f – marginal fringe, ot – oblique truncation, pl3 – metapleuron, pp – prepectus, sp – spiracle) **D** body, ventral. Scale bars: 0.1 mm (**A**); 1 mm (**B**); 0.2 mm (**C, D**).

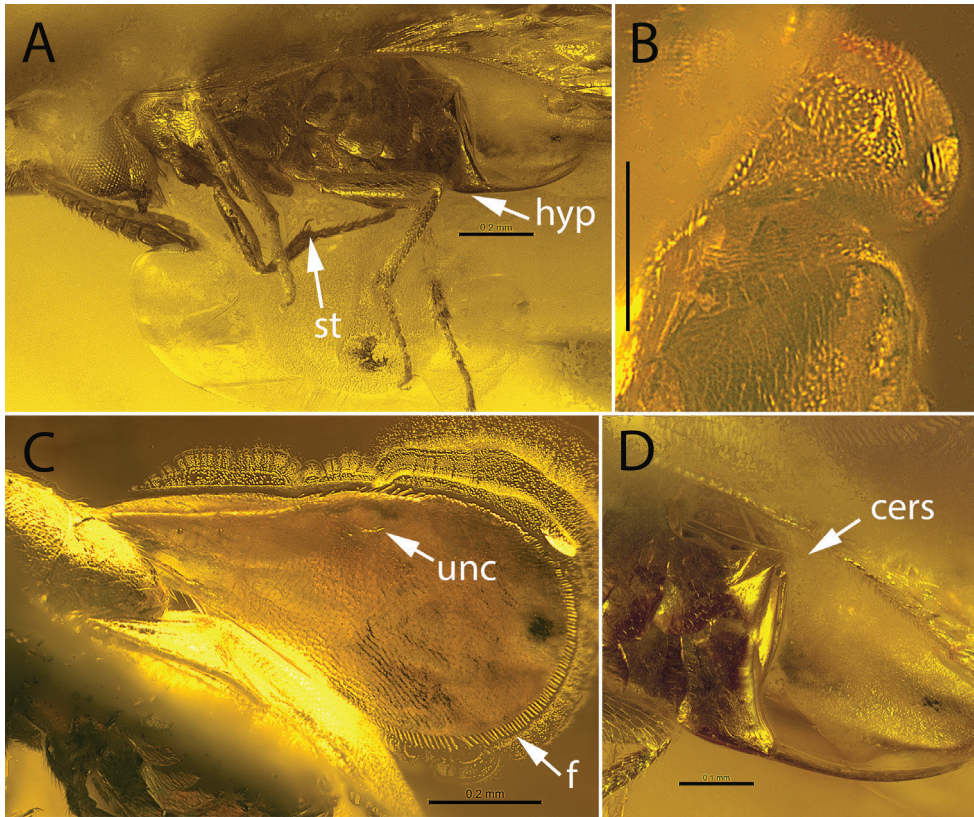


**Figure 5.** *R. voblenkoi*, gen. et sp. nov., holotype female **A** body, lateral (hyp – hypopygium, st – strigil) **B** head, anterior part of the mesosoma, dorsolateral **C** forewing (f – marginal fringe, unc – uncus) **D** apex of gaster, lateral (cers – cercal setae). Scale bars: 0.2 mm (**A–C**); 0.1 mm (**D**).

sensillae; postmarginal vein with row of long setae; setae of marginal fringe present (Fig. 5C).

**Legs.** Normal in size, alike polygonal reticulate; protibia with long, curved, bifurcate calcar; strigil well-developed but distinct basitarsal comb absent (Figs 4C, 5A: st); tarsi 5-segmented; mesotibial spur slightly shorter than mesobasitarsus; metatibia with two spurs.

**Gaster.** As long as mesosoma, polygonal reticulate equal dorsally and ventrally; protruding part of ovipositor stylet approximately as long as metatarsus (in ovipositing position); suture between 1<sup>st</sup> and 2<sup>nd</sup> valvulae clearly visible at base and at apex of stylet (Fig. 5D).

**Male.** Unknown.

## Discussion

The new genera differ from most extant members of the family by their short radicle, long veins of the forewing, and by the apical position of the cerci. A more detailed

comparison with extant genera with apical or nearly apical position of the cerci is provided by Simutnik 2021; Simutnik et al. 2021a, 2021b. In particular, extant *Eucoccidophagus* Hoffer, 1963; *Aphycoides* Mercet, 1921; and *Prionomastix* Mayr, 1876 are well distinguished from the all known extinct genera by having a very short marginal vein. *Archaeocercoides*, *Rovnopositor*, and *Archaeocercus* also differ from *Aphycoides* and *Prionomastix* in the absence of a filum spinosum and the shape of Mt8 (fig. 12C in Simutnik 2021 and fig. 9 in Simutnik et al. 2021b).

The venation of the forewings and the very small ovipositor sheaths in the newly described taxa most closely resemble those of *Moraviella* Hoffer, 1954; *Monodiscodes* Hoffer, 1954; *Savzdargia* Trjapitzin, 1979; possible, some species of *Ercydnus* Walker, 1837; and some other extant Tetracneminae. *Savzdargia* may be the “most primitive” extant Tetracnemine (Trjapitzin 1989; Noyes and Hayat 1994; J. S. Noyes pers. comm., 2022). At the same time, the paratergites (the presence of which is one of the main features of Tetracneminae) has not yet been found in fossil encyrtids, including the taxa described here. Tetracneminae is probably a more derived group – it always comes out as a derived group in DNA based phylogenetic analyses (J. S. Noyes pers. comm., 2022). Therefore, it would be premature to classify *Archaeocercus*, *Archaeocercoides*, *Rovnopositor* and other known fossil Encyrtidae without the filum spinosum as members of the Tetracneminae within the current concept of this subfamily. Their taxonomic placement within the family remains uncertain.

## Acknowledgements

We are grateful to John S. Noyes, Alexandr P. Rasnitsyn, S. Bruce Archibald for their help, valuable comments, and discussion, and to A.P. Vlaskin (SIZK) for cutting and polishing the sample. The authors are thankful to the editor Petr Janšta. This work was supported by grants NRFU No. 2020/02/0369 (to S.A. Simutnik).

## References

- Belokobylskij SA, Pankowski MG, Pankowski MV, Zaldívar-Riverón A (2021) A new genus and three new species of fossil braconid wasps (Hymenoptera, Ichneumonoidea) from Eocene Baltic and Rovno ambers. *Journal of Paleontology* 95(6): 1259–1272. <https://doi.org/10.1017/jpa.2021.47>
- Colombo WD, Gobbi FT, Perkovsky EE, Azevedo CO (2021a) Synopsis of the fossil Pristocerinae (Hymenoptera, Bethyridae), with description of two new genera and six species from Burmese, Taimyr, Baltic and Rovno ambers. *Historical Biology* 33(9): 1736–1752. <https://doi.org/10.1080/08912963.2020.1733551>
- Colombo WD, Perkovsky EE, Vasilenko DV (2021b) The first sclerodermine flat wasp (Hymenoptera: Bethyridae) from upper Eocene Rovno amber, Ukraine. *Alcheringa* 45(4): 429–434. <https://doi.org/10.1080/03115518.2021.2006311>
- Colombo WD, Perkovsky EE, Waichert C, Azevedo CO (2021c) Synopsis of the fossil flat wasps Epyrinae (Hymenoptera, Bethyridae), with description of three new genera and 10

- new species, *Journal of Systematic Palaeontology* 19(1): 39–89. <https://doi.org/10.1080/14772019.2021.1882593>
- Gibson GAP (1997) Chapter 2. Morphology and terminology. In: Gibson GAP, Huber JT, Woolley JB (Eds) *Annotated keys to the genera of Nearctic Chalcidoidea (Hymenoptera)*. NRC Research Press, Ottawa, 16–45. [794 pp.]
- Giřka W, Harbach RE, Perkovsky EE (2021) Mosquitoes (Diptera: Culicidae) in Eocene amber from the Rovno region, Ukraine. *Zootaxa* 5016 (2): 257–270. <https://doi.org/10.11646/zootaxa.5016.2.6>
- Heraty JM, Burks RA, Cruaud A, Gibson GA, Liljeblad J, Munro J, Rasplus JY, Delvare G, Janřta P, Gumovsky A, Huber JT, Woolley JB, Krogmann L, Heydon S, Polaszek A, Schmidt S, Darling DC, Gates MW, Mottern J, Murray E, Dal Molin A, Triapitsyn S, Baur H, Pinto JD, van Noort S, George J, Yoder M (2013) A phylogenetic analysis of the megadiverse Chalcidoidea (Hymenoptera). *Cladistics* 29: 466–542. <https://doi.org/10.1111/cla.12006>
- Kirichenko-Babko M, Perkovsky EE, Vasilenko DV (2022) †*Antephilorhizus zerovae* sp. nov. (Carabidae: Lebiini), the second ground beetle species from Rovno amber. *Historical Biology*. <https://doi.org/10.1080/08912963.2021.2018686>
- Manukyan AR (2019) New data on ichneumon wasps of the subfamily Pherhombinae (Hymenoptera, Ichneumonidae) in Baltic amber with descriptions of three new species. *Entomological Review* 99(9): 1324–1338. <https://doi.org/10.1134/S0013873819090112>
- Manukyan AR, Zhindarev LA (2021) Fossil Darwin wasps (Hymenoptera: Ichneumonidae) from Baltic amber. *Palaeoentomology* 4(6): 637–647. <https://doi.org/10.11646/palaeoentomology.4.6.13>
- Martynov AV, Vasilenko DV, Perkovsky EE (2021) First Odonata from Upper Eocene Rovno amber (Ukraine). *Historical Biology*. <https://doi.org/10.1080/08912963.2021.2005040>
- Martynova KV, Perkovsky EE, Olmi M, Vasilenko DV (2019) New records of Upper Eocene chrysidoid wasps (Hymenoptera: Chryridoidea) from basins of Styr and Stokhod rivers (Rovno amber). *Paleontological Journal* 53(10): 998–1023. <https://doi.org/10.1134/S0031030119100125>
- Melnitsky SI, Ivanov VD, Perkovsky EE (2021a) A new species of *Plectrocnemia* (Trichoptera: Polycentropodidae) from Rovno amber. *Zootaxa* 5006(1): 106–109. <https://doi.org/10.11646/zootaxa.5006.1.14>
- Melnitsky SI, Ivanov VD, Perkovsky EE (2021b) A new species the fossil genus *Electrotrichia* (Insecta: Trichoptera: Hydroptilidae) from Rovno amber (Zhytomyr region, Olevsk amber locality). *Palaeoentomology* 4(5): 421–424. <https://doi.org/10.11646/palaeoentomology.4.5.4>
- Melnitsky SI, Ivanov VD, Perkovsky EE (2021c) A new species of the genus *Holocentropus* (Trichoptera: Polycentropodidae) from Rovno amber. *Zoosystematica Rossica* 30: 298–302. <https://doi.org/10.31610/zsr/2021.30.2.298>
- Mitov PG, Perkovsky EE, Dunlop JA (2021) Harvestmen (Arachnida: Opiliones) in Eocene Rovno amber (Ukraine). *Zootaxa* 4984(1): 43–72. <https://doi.org/10.11646/zootaxa.4984.1.6>
- Noyes JS, Hayat M (1994) *Oriental mealybug parasitoids of the Anagyrini (Hymenoptera: Encyrtidae)*. Wallingford, Oxon: CAB International, [viii +] 554 pp.
- Perkovsky EE (2017) Rovno amber caddisflies (Insecta, Trichoptera) from different localities, with information about three new sites. *Vestnik zoologii* 51(1): 15–22. <https://doi.org/10.1515/vzoo-2017-0003>

- Perkovsky EE (2018) Only a half of species of Hymenoptera in Rovno amber is common with Baltic amber. *Vestnik zoologii* 52(5): 353–360. <https://doi.org/10.2478/vzoo-2018-0037>
- Perkovsky EE, Odnosum VK, Nazarenko VY, Vasilenko DV (2022) First record of the genus *Cyrtanaspis* Emery (Insecta: Coleoptera: Scaptiidae) from Baltic amber. *Paleontological Journal* 56(2). In press. <https://doi.org/10.1134/S0031030122020101>
- Perkovsky EE, Rasnitsyn AP, Vlaskin AP, Rasnitsyn SP (2012) Contribution to the study of the structure of amber forest communities based on analysis of syninclusions in the Rovno Amber (Late Eocene of Ukraine). *Paleontological Journal* 46(3): 293–301. <https://doi.org/10.1134/S0031030112030136>
- Sharkov AV (1985) Encyrtids (Hymenoptera, Chalcidoidea, Encyrtidae) of the southern Far East of the USSR [dissertation]. Extended Abstract of Cand. Sci. (Biol.). Leningrad. [in Russian]
- Simutnik SA (2021) The earliest Encyrtidae (Hymenoptera, Chalcidoidea). *Historical Biology* 33(11): 2931–2950. <https://doi.org/10.1080/08912963.2020.1835887>
- Simutnik SA, Perkovsky EE (2006) A description of the encyrtoid male with archaic structure of metasoma (Hymenoptera, Chalcidoidea, Encyrtidae) from Rovno amber. *Vestnik Zoologii* 40(6): 283–286. <http://www.v-zool.kiev.ua/pdfs/2006/3/12>
- Simutnik SA, Perkovsky EE (2018a) *Archaeocercus* gen. nov. (Hymenoptera, Chalcidoidea, Encyrtidae) from late Eocene Rovno amber. *Zootaxa* 4441(3): 543–548. <https://doi.org/10.1080/08912963.2020.1835887>
- Simutnik SA, Perkovsky EE (2018b) *Trjapitzion* Simutnik, gen. n. (Hymenoptera, Chalcidoidea: Encyrtidae), a new genus of encyrtid wasps from the late Eocene Rovno amber. *Entomological Review* 98(8): 1152–1156. <https://doi.org/10.1134/S0013873818080225>
- Simutnik SA, Perkovsky EE (2020) *Ektopicercus* Simutnik gen. nov. (Hymenoptera, Chalcidoidea, Encyrtidae) from late Eocene Rovno amber. *Palaeoentomology* 3(4): 342–346. <https://doi.org/10.11646/palaeoentomology.3.4.3>
- Simutnik SA, Perkovsky EE, Vasilenko DV (2020) First record of *Leptoemus janzeni* Gibson (Hymenoptera, Chalcidoidea) from Rovno amber. *Journal of Hymenoptera Research* 80: 137–145. <https://doi.org/10.3897/jhr.80.58882>
- Simutnik SA, Perkovsky EE, Vasilenko DV (2021a) *Sakhalinencyrtus leleji* Simutnik gen. et sp. nov. of earliest Encyrtidae (Hymenoptera, Chalcidoidea) from Sakhalinian amber. *Journal of Hymenoptera Research* 84: 361–372. <https://doi.org/10.3897/jhr.84.66367>
- Simutnik SA, Perkovsky EE, Khomych MR, Vasilenko DV (2021b) First record of the *Sulia glaesaria* Simutnik, 2015 (Hymenoptera, Chalcidoidea, Encyrtidae) from Rovno amber. *Journal of Hymenoptera Research* 88: 85–102. <https://doi.org/10.3897/jhr.88.75941>
- Telnov D, Perkovsky EE, Vasilenko DV, Yamamoto S (2021) The first fossil Coleoptera record from the Volyn Region, Ukraine, with description of a new *Glesoconomorphus* (Coleoptera, Mycteridae) in syninclusion with Winterschmidtidae (Acari) and a key to species. *ZooKeys* 1068: 189–201. <https://doi.org/10.3897/zookeys.1068.75391>
- Trjapitzin VA (1989) Parasitic Hymenoptera of the fam. Encyrtidae of Palearctics. *Opredeliteli po faune SSSR izdavavaemiye Zoologicheskim institutom AN SSSR* 158: 1–489. [in Russian]
- Yamamoto S, Nazarenko VY, Vasilenko DV, Perkovsky EE (2022) First fossil species of ship-timber beetles (Coleoptera: Lymexylidae) from Eocene Rovno amber (Ukraine). *Fossil Record* 25(1): 65–74. <https://doi.org/10.3897/fr.25.81054>

# A new species of *Gilpinia* Benson (Hymenoptera, Diprionidae) from Lishui, China

Ze-Jian Li<sup>1</sup>, Han-Nan Wang<sup>2</sup>, Meng-Meng Liu<sup>3</sup>, Mei-Cai Wei<sup>4</sup>

**1** Provincial postdoctoral Research Station, Scientific Research and Management Center of East China Medicinal Botanical Garden, Lishui Ecological Forestry Development Center, Lishui, Zhejiang 323000, China **2** Lab of Insect Systematics and Evolutionary Biology, Central South University of Forestry and Technology, Changsha, Hunan 410004, China **3** College of Ecology, Lishui University, Lishui, Zhejiang 323000, China **4** College of Life Science, Jiangxi Normal University, Nanchang, Jiangxi 330022, China

Corresponding author: Mei-Cai Wei ([weimc@126.com](mailto:weimc@126.com))

Academic editor: Marko Prous | Received 11 December 2021 | Accepted 31 January 2022 | Published 28 February 2022

<http://zoobank.org/8662CCCC-9A34-419F-BFEB-DA7972A24889>

**Citation:** Li Z-J, Wang H-N, Liu M-M, Wei M-C (2022) A new species of *Gilpinia* Benson (Hymenoptera, Diprionidae) from Lishui, China. Journal of Hymenoptera Research 89: 61–71. <https://doi.org/10.3897/jhr.89.79200>

## Abstract

*Gilpinia* was established by Benson (1939). In this paper, a new species of *Gilpinia lishui* Li, Wang & Wei, **sp. nov.** (Hymenoptera: Diprionidae) from Lishui, Zhejiang Province, China is described. A key to Chinese species of *Gilpinia* is provided.

## Keywords

China, Diprioninae, key, sawflies, Symphyta, taxonomy

## Introduction

*Gilpinia* Benson, 1939 is the second largest genus in Diprionidae including 38 world species and 15 Chinese species (Taeger et al. 2010; Hara and Nakamura 2015; Hara and Shinohara 2015; Wang et al. 2019). The previously known Chinese species were listed and keyed by Wang et al. (2019).

The village Dayuan, the type locality of the new species described below, is located in the town of Dayuan in Jinyun County of Lishui City, Zhejiang Province in East China. Five females were collected there and identified as new to science. A diagnosis and description of the new species as well as a revised key to the Chinese species of *Gilpinia* are reported herein.

## Materials and methods

Specimens studied in this work were collected near the village Dayuan by a light trap. The specimens were examined with a Motic-SMZ-171 stereomicroscope. Images of adults were taken with a Nikon D700 digital camera and a Leica Z16APO microscope. The genitalia were examined with a Motic BA410E microscope and photographed with a Motic Moticom Pro 285A. Images were focus-stacked using Helicon Focus (HeliconSoft, Kharkiv, Ukraine) and further processed with Adobe Photoshop CS 11.0. The terminology of genitalia follows Ross (1945) and that of general morphology follows Viitasaari (2002). For a few terms (e.g., middle fovea and lateral fovea), we follow Takeuchi (1952).

The holotype and a paratype are deposited in the Asian Sawfly Museum, Nanchang, China (ASMN). The remaining paratypes are deposited in the Scientific Research and Management Center of East China Pharmaceutical Botanical Garden, Lishui, Zhejiang, China (formerly Lishui Academy of Forestry, LSAF). Specimens of other species examined in this research are deposited in the National Museum of Natural History, Smithsonian Institution, Washington, D.C., USA (USNM), and National Museum of Nature and Science, Ibaraki, Japan (NSMT). We have examined examples of the following species: *G. baiyinaobaoa* G. Xiao and X. Huang (NSMT), *G. fennica* (Forsius) (USNM), *G. hebedentata* Xu (ASMN), *G. infuscalae* Wang and Wei (ASMN, USMN), *G. jingxii* Xiao and Huang (USNM), *G. lishui* Li, Wang and Wei (ASMN, LSAF), *G. lipuensis* Xiao and Huang (ASMN, USNM), *G. marshalli* (Forsius) (USNM), *G. masoniana* Xiao (USNM), *G. tabulaeformis* Xiao (ASMN, USNM), *G. yongrenica* Xiao and Huang (USNM), *G. virens* (Klug) (ASMN, USNM).

Abbreviations used in the text and illustrations are as follows:

- OCL** The distance between a lateral ocellus and the occipital carina, or the hind margin of the head where this carina would be if it was developed (Benson 1954);  
**OOL** The distance between an eye and a lateral ocellus;  
**POL** The distance between the mesal margins of the 2 lateral ocelli.

## Results

### Taxonomy

#### Genus *Gilpinia* Benson, 1939

*Gilpinia* Benson, 1939: 341.

**Type species.** *Lophyrus polytomus* Hartig, by original designation.

**Diagnosis.** See Wang et al. (2019) for the diagnosis and character assessment of the genus.

***Gilpinia lishui* Li, Wang & Wei, sp. nov.**

<http://zoobank.org/CE900234-517E-4901-A99E-B168EC874921>

Figs 1–12

**Type locality.** China, Zhejiang, Lishui City, Jinyun County, Dayuan Town, Dayuan Village.

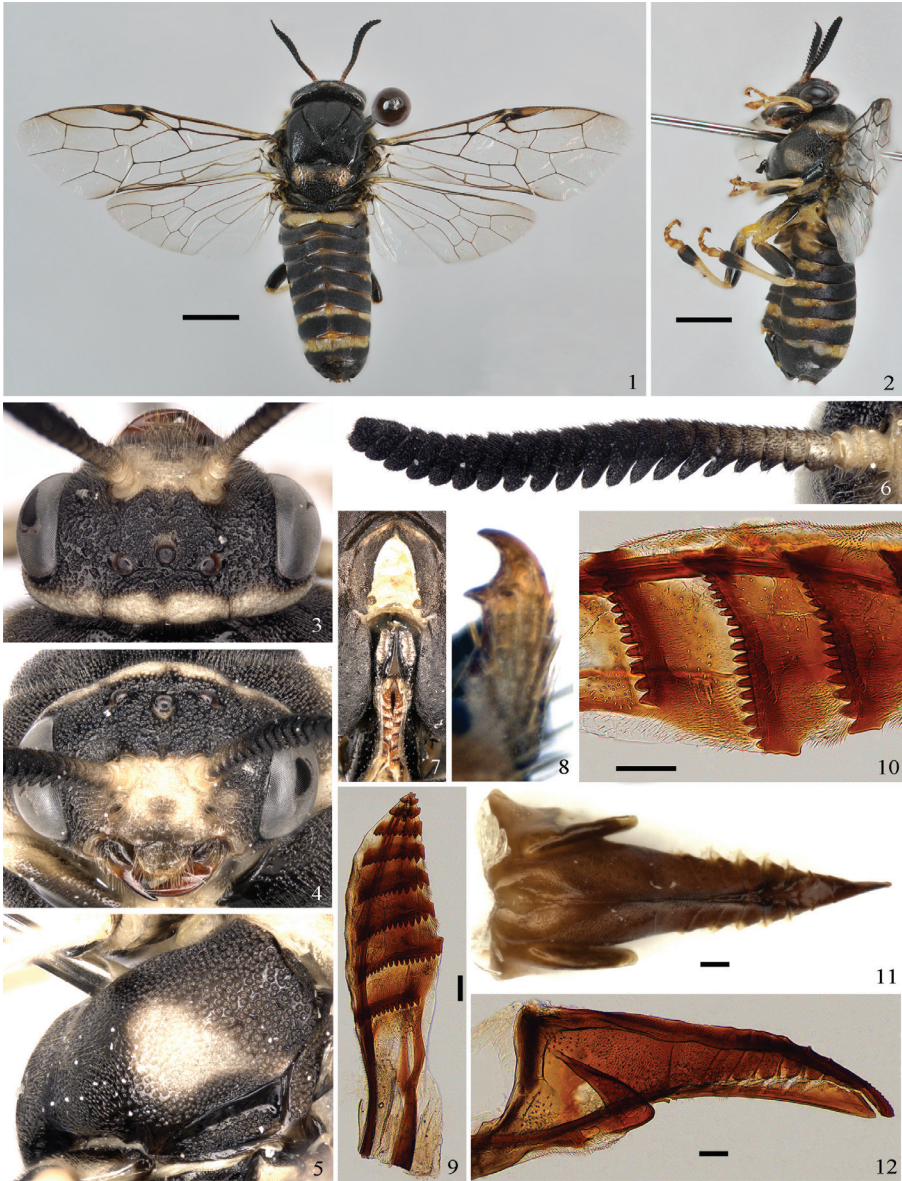
**Type material examined.** *Holotype*, female, CHINA: Zhejiang Province, Lishui City, Jinyun County, Dayuan Town, Dayuan Village, 28.612°N, 120.309°E, alt. 273 m, 10 August 2021, leg. Ze-Jian Li, alcohol (LSAF21043). *Paratypes*, 4 females, same data as holotype.

**Diagnosis.** The genus *Gilpinia* is similar to *Macrodiiprion* in most external morphology characters, but there are clear differences in lancet structures. This new species resembles *G. tohi* Takeuchi, 1940 in external morphology and lancet characters together, but differs from the latter by the following characters: Lancet with 9 annuli (Fig. 9), annulus 1 about 1.2–1.3× the length of annulus 2 at middle, the first annulus weakly curved and distinctly oblique (Fig. 10), distance between the lower end of the second annulus and apex of lancet about 1.6× the height of the second annulus as measure perpendicular to the longitudinal axis of the lancet (Fig. 9), the serrulae 2–6 flat (Fig. 9); posterior margin of head and supraclypeal area white (Fig. 3), labrum yellow brown, clypeus black except for lateral corners white (Fig. 4); abdomen black, the first tergum largely white, the following 4 terga black with small lateral white maculae (Figs 1–2). *G. lishui* sp. nov. differs from *Macrodiiprion wui* Xu, 1997, possibly a species of *Gilpinia*, by the posterior margin of head and supraclypeal area white; the apical half of pterostigma pale brown; the basal 7 flagellomeres yellow brown; the lancet with 9 annuli, the distance between the lower end of the second annulus and the apex of lancet 1.6 times the height of second annulus.

**Description.** Holotype, female. Body length 10–10.5 mm, wingspan 19–20 mm (Figs 1–2).

**Color.** Body largely black, following parts yellowish white: supraclypeal area and toruli (Fig. 4), scape and pedicel (Fig. 6), apical 3/5 of postocellar area, posterior half of temple and of hind orbit (Fig. 3), a large triangular macula on mesepisternum (Fig. 5) and two large lateral maculae on mesoscutellum (Fig. 1), abdominal tergum 1 largely, antero-lateral stripe on recurved portions of terga 2–4, narrow anterior band wider laterally on terga 5–8, posterior margin of tergum 10, anterior 4/7 of sterna 3–7; mandibles reddish brown with black base; palp and labrum brown; narrow base of clypeus and dorsum of flagellomeres 1–7 pale brown; legs yellowish white, following parts black: fore coxa except for apex, middle and hind coxae except for apex and lateral macula, most of fore coxa, each femur except for dorsal stripe, apical 1/3 of hind tibia; apex of fore and middle tibiae and of each tarsomere brown. Wings hyaline, apex of cell R1 and posterior margin of fore wing infuscate, basal 2/5 and narrow margins of stigma black, apical 2/3 of stigma, veins R1 and most of vein A whitish, vein C pale brown, other veins blackish brown. (Figs 1–2)

**Punctuation.** Head and thorax densely punctured, microsculpture smooth, shiny, except as follows: labrum, temple, anterior part of clypeus and of supraclypeal area



**Figures 1–12.** *Gilpinia lishui* sp. nov., female, holotype **1** female adult, dorsal view **2** female adult, lateral view **3** head of female, dorsal view **4** head of female, anterior view **5** mesopleuron and metapleuron of female **6** antenna of female, lateral view **7** ovipositor sheath, ventral view **8** claw of hind leg, lateral view **9** lancet **10** the 1–3 annuli of lancet **11** lance, dorsal view **12** lance, lateral view. Scale bars: 2 mm (**1, 2**); 100  $\mu$ m (**9–12**).

sparsely punctured, anterior part of parapsis, lower posterior corner of mesepisternum, anterior third and narrow posterior margin of mesepimeron smooth and strongly shiny; metapleuron and bottom of parapsis weakly striate microsculptured; abdomen strongly and densely striate microsculptured, almost matte, ovipositor sheath largely smooth and shiny.

**Head.** Hairs on dorsum of head slightly shorter than diameter of median ocellus, curved at apex; hairs on mesonotum very short and erect, and on mesopleuron very short. Anterior margin of clypeus shallowly and broadly incised, malar space as long as diameter of median ocellus, middle fovea distinct, distance between eye and torulus approximately 1.3× distance between toruli (Fig. 4), postocellar area elevated with a shallow median furrow, approximately 2.5× as broad as long, postocellar furrow clear, POL : OOL : OCL = 61 : 48 : 40 (Fig. 3). Antenna serrate with 22 distinct antennomeres, apex of terminal flagellomere obtuse and truncate, scape approximately 1.3× as broad as long, pedicel approximately 0.5× as broad as long, antennomere 1 slightly broader than long, other antennomeres distinctly broader than long, ventral teeth of middle antennomeres clearly shorter than apical breadth of each antennomere (Fig. 6).

**Thorax.** Anterior margin of mesoscutellum almost truncate, slightly convex at middle, anterior margin of mesoscutellum approximately 1.5× as broad as long; distance between cenchri equal to length of a cenchrus.

**Abdomen.** Ovipositor sheath in ventral view shown in Fig. 7; middle lobe of sternum 7 narrowly and deeply incised at middle, posterior margin of sternum 7 deeply incised submedially. Inner apical spur of hind tibia simple and approximately 0.8× length of tarsomere 1; subapical tooth of claw short and remote from apical tooth (Fig. 8). Lancet with 9 distinct annuli, weakly narrowing from annulus 2 to 5 and then abruptly narrowed toward apex (Fig. 9); annulus 1 without serrula, about 1.2–1.3× length of annulus 2 at middle, weakly curved and oblique, subparallel with annulus 2, distance between lower end of annulus 2 and apex of lancet about 1.6× height of annulus 2 (Fig. 9); basal 1–3 annuli as shown in Fig. 10, serrulae of annuli 2–6 flat, width of annulus 2 approximately 1.15× width of annulus 3; lance in dorsal view as shown in Fig. 11, auricular process large and triangular; lance in lateral view as shown in Fig. 12.

**Male.** Unknown.

**Variety.** In one specimen, the mesoscutellum has a uniformly white band with two lateral yellowish white maculae connected.

**Host plants.** Unknown.

**Distribution.** China (Zhejiang).

**Etymology.** The specific epithet “*lishui*” is derived from the type locality, Lishui City, Zhejiang Province of East China.

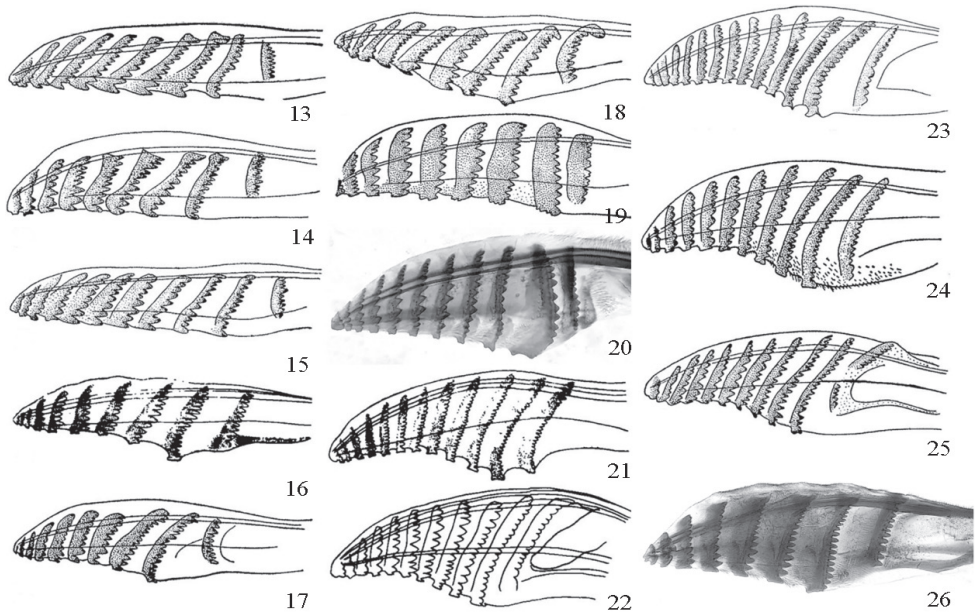
**Key to the Chinese species of *Gilpinia* Benson (females; not examined species are marked with\*)**

- 1 Inner spur of hind tibia scale like ..... 2
- Inner spur of hind tibia simple..... 4
- 2 Annuli 2 and 3 divergent downwards (Fig. 14); pronotum entirely yellow; only posterior margin of mesoscutellum black. China (Heilongjiang), Finland .....  
..... *G. fennica* (Forsius, 1911)
- Annuli 2 and 3 parallel (Figs 13, 15); pronotum yellow with black marks; both anterior and posterior margins of mesoscutellum black..... 3

- 3 Serrulae 3–5 broader than their respective ctenidia (Fig. 13); head with a transverse dark band on ocellar area, not reaching inner margins of eyes; apical margin of clypeus straight; ocellar area with 3 small brownish marks; pronotum pale with anterior margin black. China (Inner Mongolia) .....  
 ..... ***G. baiyinaobaoa* G. Xiao & X. Huang, 1985**
- Serrulae 3–5 equal in breadth to their respective ctenidia (Fig. 15); head with a transverse dark band on ocellar area, reaching inner margins of eyes; apical margin of clypeus slightly incised; ocellar area without brownish marks; pronotum black with lateral corners pale. China (Heilongjiang, Jilin), Siberia, Europe.....  
 ..... ***G. virens* (Klug, 1812)**
- 4 Wings strongly smoky; body entirely black in both sexes without pale markings; basal two ctenidia inclined apically, second annulus more than 2× as broad as first annulus, lamnium triangular, widest near second annulus and strongly tapering toward apex (Fig. 20). China (Jiangxi).....  
 ..... ***G. infuscalae* Wang & Wei, 2019**
- Wings hyaline; body at least partly pale; second ctenidium usually inclined basally, if perpendicular then lamnium not enlarged at middle; second annulus about as long as and at most slightly longer than first annulus ..... **5**
- 5 Head largely black at least between ocellar area and toruli; lancet weakly broadened at middle, and weakly narrowed toward both ends, ventral margin of lamnium straight or nearly so; distance between lower end of second annulus and apex of lancet 1.6–2.5 times the height of second annulus as measure perpendicular to the longitudinal axis of the lancet..... **6**
- Head pale with a small black macula at most on ocellar area; lancet strongly narrowed from 2<sup>nd</sup> annulus both to base and apex, ventral margin of lamnium distinctly concave, distance between lower end of second annulus and apex of lancet 1.3–1.6× the height of second annulus as measure perpendicular to the longitudinal axis of the lancet ..... **11**
- 6 First ctenidium strongly curved and strongly divergent downwards from second ctenidium ..... **7**
- First ctenidium straight or slightly curved and subparallel or even convergent downwards towards second ctenidium ..... **8**
- 7 OOL slightly longer than POL (OOL : POL = 12 : 11); scape, pedicel and flagellomere 1 black and each basally pale; lateral mesoscutal lobe black with anterior and lateral margins pale; mesoscutellum pale with a central longitudinal black line; mesopleuron black with upper half of mesepisternum pale; annuli 4 and 5 parallel (Fig. 17). China (Sichuan, Yunnan) .....  
 ..... ***G. yongrenica* G. Xiao & X. Huang, 1984**
- OOL much shorter than POL; scape pale, flagellomere 1 black; lateral mesoscutal lobe black with lateral margins pale; mesoscutellum pale with posterior margin black, mesopleuron entirely yellow; annuli 4 and 5 distinctly divergent

- downwards (Fig. 18). China (Heilongjiang) .....  
 ..... \**G. pinicola* G. Xiao & X. Huang, 1985
- 8 Black macula on frons laterally not touching eye; first ctenidium weakly apically curved at middle; distance between lower end of second annulus and apex of lancet 2× the height of second annulus. China (Fujian), Thailand.....  
 ..... *G. marshalli* (Forsius, 1931)
- Black macula on frons laterally touching eye or head almost entirely black; first ctenidium straight or weakly basally curved at middle; distance between lower end of second annulus and apex of lancet 1.6–2.5× the height of second annulus..... **9**
- 9 Mesoscutal median and lateral lobes entirely black; second trochanters white; lancet with 9 annuli ..... **10**
- Mesoscutal median lobe with distinct pale lateral maculae; head black with labrum, clypeus, supraclypeal area and dorsal margin of head pale, trochanters black; lancet narrow with 10 annuli, annulus 1 about 1.0–1.1× length of annulus 2 and both oblique, annuli 2 and 3 parallel, distance between lower end of annulus 2 and apex of lancet about 2× the height of second annulus. China (Anhui) ..... *G. massoniana* G. Xiao, 1992
- 10 Lancet with annulus 1 about 0.7× length of annulus 2 and both perpendicular, distance between lower end of second annulus and apex of lancet about 2.3× height of second annulus as measure perpendicular to the longitudinal axis of the lancet, serrulae 2–5 with distinct teeth (Fig. 19); head black with labrum and ventral margin of clypeus yellow; abdomen yellowish brown, basal 5 terga dark brown; China (Heilongjiang), Japan (Hokkaido)\**G. tobi* Takeuchi, 1940
- Lancet with annulus 1 about 1.2–1.3× length of annulus 2 at middle, first annulus weakly curved and distinctly oblique, distance between lower end of second annulus and apex of lancet about 1.6× the height of second annulus as measure perpendicular to the longitudinal axis of the lancet, serrulae 2–6 flat (Fig. 26); posterior margin of head and supraclypeal area white, labrum yellow brown, clypeus black except for lateral corners; abdomen black, first tergum largely white, following 4 terga black with small lateral white maculae. Zhejiang.....  
 ..... *G. lishui* Li, Wang & Wei, sp. nov.
- 11 Annulus 1 with a distinct serrula (Fig. 21) ..... **12**
- Annulus 1 without serrula (Figs 22–25)..... **13**
- 12 Body reddish brown; ocellar area with a short dark transverse band; mesoscutellum, central part of pronotum and most of lateral mesoscutal lobe black (median mesoscutal lobe sometimes with black triangular mark); tergum 1 black. Lancet in Fig. 21. China (Gansu)..... *G. tabulaeformis* G. Xiao, 1992
- Body yellowish brown; ocellar area pale without black marks; pronotum, median mesoscutal lobe, lateral mesoscutal lobe and tergum 1 pale; mesoscutellum black. China (Hebei)..... \**G. funingensis* Wen, Sun & Li, 1991

- 13 Ctenidium 1 broken at middle (Fig. 25); lateral mesoscutal lobe entirely pale. China (Anhui, Guangxi) ..... ***G. lipuensis* G. Xiao & X. Huang, 1985**
- Ctenidium 1 entire; lateral mesoscutal lobe pale with dark marks or entirely black ..... **14**
- 14 Annuli 1 and 2 straight and parallel (Fig. 22); body yellow; mesoscutellum entirely pale; sheath with slender scopae close to each other. China (Yunnan).....  
..... ***G. hebedentata* Xu, 1997**
- Annuli 1 and 2 curved and divergent downwards (Figs 23, 24); body reddish brown, mesoscutellum entirely black or pale with posterior margin black; sheath with broad scopae not close to each other ..... **15**
- 15 Annuli 1 and 2 distinctly divergent ventrally, basal serrulae acute (Fig. 23); labrum black; flagellomeres dorsally reddish brown, ventrally black; dorsal mesonotum mostly pale, median mesoscutal lobe pale, lateral mesoscutal lobe with central longitudinal dark stripe; mesoscutellum with posterior margin black. China (Yunnan) ..... **\**G. jinghongensis* G. Xiao & X. Huang, 1984**
- Annuli 1 and 2 weakly divergent ventrally, basal serrulae truncate (Fig. 24); labrum reddish brown; flagellomeres black; dorsal mesonotum mostly black; median mesoscutal lobe with posterior dark mark; lateral mesoscutal lobe and mesoscutellum entirely black. China (Yunnan, Guizhou).....  
..... ***G. jingxii* G. Xiao & X. Huang, 1984**



**Figures 13–26.** Lancets **13** *Gilpinia baiyinaobaoa* **14** *G. femica* **15** *G. virens* **16** *G. masoniana* **17** *G. yongrenica* **18** *G. pinicola* **19** *G. tobi* **20** *G. infuscalae* **21** *G. tabulaeformis* **22** *G. hebedentata* **23** *G. jinghongensis* **24** *G. jingxii* **25** *G. lipuensis* **26** *G. lishui* **13–19, 21–25** drawings of lancet by Xiao (1992), Xiao et al. (1992) and Xu (1997) **20** Photo by HNW (2019) **26** Photo by ZJL.

## Discussion

Sixteen species of *Gilpinia*, including the new species have been recorded in China. We believe that more undescribed species of the genus have yet to be found from Central and Southern China. *G. lishui* is unusual among species of the genus in that its antennae are distinctly broadened at the middle and blunt at the apex. The antennae the new species are similar in this regard to species of *Macrodiprion*. However, we place the new species in *Gilpinia* due to the cenchri being close together and longer than the middle length of the metascutellum, and because the lancet is typical in structure for *Gilpinia*. *Macrodiprion wui* Xu (1997) is probably also a species of *Gilpinia* as the antennae, cenchri and lancet are all similar to those of *G. lishui*. *Gilpinia wui* Wang & Wei, 2019 has a possible problem with the homonym. A new name may need to be proposed in the subsequent study.

Collection of the new species by light trap was photographed by Zejian Li (Fig. 27) and a live specimen was photographed by Junfeng Wang (Fig. 28). The Village Dayuan

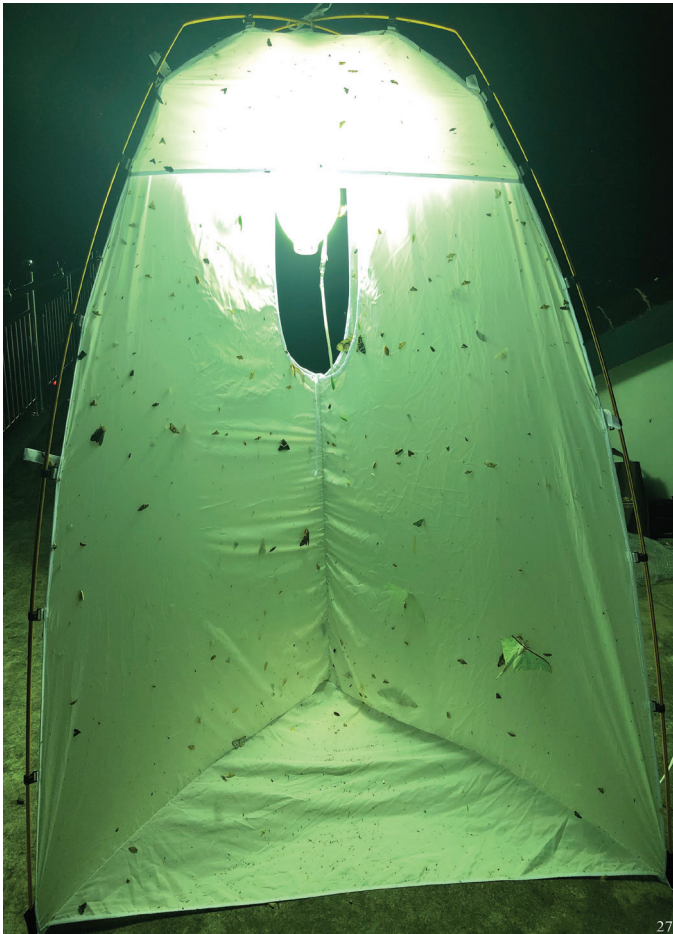


**Figure 27.** Photograph of light trap used to collect the new species, by Ze-Jian Li (10 August 2021).



**Figure 28.** Habitus photograph of the new species by Jun-Feng Wang (10 August 2021).

is apparently a suitable habitat for collecting sawflies, with an elevation of about 300 m above sea level. At present, we are not sure that Dayuan represents a unique habitat in Lishui City to species of Diprionidae.

## Acknowledgements

The authors are deeply grateful to Mr. Spencer Monckton and Dr. Marko Prous referees for valuable comments and suggestions. This research was partly supported by the scientific research project of Baishanzu National Park (No. 2021KFLY08), Background investigation of insect biodiversity in Jinyun County (No. WHT-HX-2021-0123-22), the National Natural Science Foundation of China (grant No. 31970447), starting fund for doctoral research of Lishui University (No. 6004LMM01Z) and special fund for scientific research of postdoctoral work station assessment in Zhejiang Province, China (No. 2021).

## Reference

- Benson RB (1939) On the genera of the Diprionidae (Hymenoptera Symphyta). *Bulletin of Entomological Research* 30: 339–342. <https://doi.org/10.1017/S0007485300004673>
- Benson RB (1954) Some sawflies of the European Alps and the Mediterranean region (Hymenoptera: Symphyta). *Bulletin of the British Museum (Natural History), Entomology* 3(7): 267–295. <https://doi.org/10.5962/bhl.part.1054>

- Hara H, Shinohara A (2015) The *Gilpinia abieticola* species group (Hymenoptera, Diprionidae). Bulletin of the National Museum of Nature and Science, Tokyo, Series A, 41: 21–41.
- Hara H, Nakamura H (2015) Pine sawfly *Gilpinia albiclavata* sp. nov. (Hymenoptera: Diprionidae) infesting *Pinus pumila* in the Japanese Alps. Entomological Science 2015(18): 31–40. <https://doi.org/10.1111/ens.12088>
- Ross HH (1945) Sawfly genitalia: terminology and study techniques. Entomological News 61(10): 261–268.
- Taeger A, Blank SM, Liston AD (2010) World catalog of Symphyta (Hymenoptera). Zootaxa 2580: 1–1064. <https://doi.org/10.11646/zootaxa.2580.1.1>
- Takeuchi K (1952) A Generic Classification of the Japanese Tenthredinidae (Hymenoptera: Symphyta). Kyoto, 90 pp.
- Viitasaari M (2002) The Suborder Symphyta of the Hymenoptera. In: Viitasaari M (Ed.) Sawflies (Hymenoptera, Symphyta) I. A Review of the Suborder, the Western Palaearctic Taxa of Xyeloidea and Pamphilioidea. Tremex, Helsinki, 11–174.
- Wang HN, David RS, Xiao W, Niu GY, Wei MC (2019) *Gilpinia infuscalae* Wang & Wei, sp. nov. and a key to the Chinese *Gilpinia* species (Hymenoptera: Diprionidae). Zootaxa 4571(4): 589–596. <https://doi.org/10.11646/zootaxa.4571.4.11>
- Xiao GR (1992) Two new sawflies of the genus *Gilpinia* in China (Hymenoptera, Symphyta, Diprionidae). Forest Research 5(2): 193–195.
- Xiao GR, Huang XY, Zhou SZ, Wu J, Zhang PY (1992) Economic Sawfly Fauna of China. Tianze Eldonejo, Beijing, 221 pp.
- Xu ZH (1997) Two new species and one new combination of the conifer sawfly family Diprionidae (Hymenoptera: Symphyta) from Yunnan, China. Zoological Research 18(2): 171–176.



# A new *Mymaromma* sp. (Mymarommatoidea, Mymarommatidae) in Hawai'i and first host record for the superfamily

David N. Honsberger<sup>1</sup>, John T. Huber<sup>2</sup>, Mark G. Wright<sup>1</sup>

**1** Department of Plant and Environmental Protection Sciences, University of Hawai'i at Mānoa, 3050 Maile Way #310, Honolulu, HI, 96822, USA **2** Natural Resources Canada c/o Canadian National Collection of Insects, K.W. Neatby Building, 960 Carling Ave., Ottawa, ON, K1A 0C6, Canada

Corresponding author: David N. Honsberger ([dnh8@hawaii.edu](mailto:dnh8@hawaii.edu))

Academic editor: Petr Janšta | Received 8 December 2021 | Accepted 18 January 2022 | Published 28 February 2022

<http://zoobank.org/DD914715-4804-4F7E-A4FF-196047B83756>

**Citation:** Honsberger DN, Huber JT, Wright MG (2022) A new *Mymaromma* sp. (Mymarommatoidea, Mymarommatidae) in Hawai'i and first host record for the superfamily. Journal of Hymenoptera Research 89: 73–87. <https://doi.org/10.3897/jhr.89.77931>

## Abstract

A new species of *Mymaromma*, *M. menebune* sp. nov., is described from the Hawaiian Islands. It was found emerging as a solitary endoparasitoid from eggs of a *Lepidopsocus* sp. (Psocodea: Lepidopsocidae) on branches of *Ficus microcarpa* (Moraceae) on the island of O'ahu. This the first host record for the superfamily Mymarommatoidea, coming almost exactly 100 years after the first extant species of Mymarommatidae was described.

## Keywords

barklice, egg parasitoid, *Lepidopsocus* sp., Psocoptera

## Introduction

Mymarommatoidea are a superfamily of beautiful but minuscule wasps with a two segmented petiole, a bellows-like expandable structure forming the back of the head, exodont mandibles, fore wings with long fringe setae and a reticulate pattern on the membrane, and hind wings reduced to a bifurcated haltere-like structure with no wing

membrane (Gibson et al. 2007). Vilhelmsen and Krogmann (2006) described them as “arguably the most enigmatic wasp taxon.” Very little is known about the life histories of any members of this superfamily as all collection records have come from traps, sifting through leaf litter, sweep netting, or amber fossils, and one species found emerging from a bracket fungus (Gibson et al. 2007; Huber et al. 2008; Hatten et al. 2011; Mohanraj and Kamalanathan 2011; Machado Benassi et al. 2014; Ayyamperumal and Manickavasagam 2017). The superfamily currently contains three families Mymarommatidae, Gallorommatidae, and Alvarommatidae; Gallorommatidae and Alvarommatidae are only known from fossils, and Mymarommatidae contains both fossil and extant species (Ortega-Blanco et al. 2011). The oldest known fossil mymarommatoids date back to the Cenomanian and Albian ages in the Cretaceous approximately 100 million years ago (Schlüter 1978; Engel and Grimaldi 2007; Gibson et al. 2007; Ortega-Blanco et al. 2011), and members of this superfamily have been found on all continents other than Antarctica (Gibson et al. 2007). Huber et al. (2008) speculated that mymarommatoids might be parasitoids of insect eggs based on their minute size, less than 1 mm in length, and short ovipositors, and that they are most likely parasitoids in eggs of bark lice (Psocoptera), based on a good correlation of both taxa in terms of their wide biogeographical distribution, presence mainly in forest habitats, local abundance, phenology, and palaeontology. The combination of exodont mandibles and expandable head may be used to break out through the flexible chorion of psocopteran eggs, and the exodont mandibles may also be useful for penetrating the silk that many species produce to cover their eggs.

Here we confirm, through rearing of psocopteran eggs taken from wood from which a species of mymarommatoid has been observed to emerge, that this suspicion was accurate for at least one species and we describe it. It is the same undescribed species previously reported by Beardsley et al. (2000), collected on sticky cards suspended from trees in Hālawā Valley and the central, coastal area of the Kona moku on the island of Molokaʻi, and also reported from the Puʻuloa area and Waimea Valley on Oʻahu. It is currently the only species of Mymarommatidae known from the Hawaiian Islands.

## Methods

In a separate study (D. Honsberger, unpublished), specimens of the mymarommatid were observed to emerge from branches of a large *Ficus microcarpa* L.f. tree (Fig. 1A) in an unmaintained area of the campus of the University of Hawaiʻi at Mānoa 21.2954°N, 157.8145°W, 15 m, on the island of Oʻahu. Live branches had been cut from the tree and suspended from it approximately 8 m off the ground for six weeks to allow colonization by bark-dwelling insects, and subsequently placed in an emergence container. Among the large variety of arthropods found to be associated with this wood over the course of approximately one year, four species of psocopterans were found to develop on the branches.

In the present study, approximately 8 branches 2–8 cm in diameter and 30–60 cm long were cut from the same tree and suspended from it in the same position as in the previous study. After 5 weeks, the branches were taken to a laboratory and their surface

inspected under a Leica MZ16 stereomicroscope. All arthropod eggs found on the surface of the wood were either picked off the bark or carefully cut from the bark together with a small piece of the surrounding wood and placed individually in gelatin capsules. The branches were then placed again in the tree. Inspection of the branches and collection of eggs was repeated approximately once per week, and new branches were added after the previous branches had been exposed for 6 weeks. Branches were removed after they had been exposed for 12 weeks. The capsules were periodically inspected under the microscope for emergence of parasitoids from the eggs. After mymaromatoids had been observed to emerge from eggs in the capsules, morphologically identical eggs were collected from the surface of the branches and reared to adulthood for host identification. Eggs putatively belonging to other species of psocopterans found on the branches were also reared to associate the adult stage of the psocopterans known to occur on that tree with their egg morphology, and thereby determine whether any of their eggs could be confused with eggs of the species reared for host identification. Photographs and videos of psocopterans, their eggs, and parasitoids were also opportunistically recorded during inspection of the wood.

Wasps that emerged from host eggs were point mounted, with the egg from which the individual emerged also glued to the point, and both were photographed using a Macropod Pro imaging system. Other specimens were slide mounted and photographed under an Olympus CX31 compound microscope, or point mounted and examined under a stereomicroscope. Morphological terms follow Gibson et al. (2007). Abbreviations used are: **fl** = flagellar segment (in males), **fu** = funicular segment (in females), **P<sub>1</sub>** = anterior petiole segment, **P<sub>2</sub>** = posterior petiole segment. Morphometric measurements of the antenna, petiole segments, wings, and mesosoma were obtained from slide mounted specimens as follows. Antennal segments were measured as they appeared in the plane of the slide, any component in the perpendicular direction unaccounted for. Fore wing length was measured from the junction of the humeral plate with the base of venation to the apex of the wing membrane; fore wing width was measured across the widest point of the wing membrane; the longest seta of the marginal fringe was measured from the edge of the wing membrane (i.e., excludes the base, which is inserted between the dorsal and ventral membranes). **P<sub>1</sub>** was measured from the flange at the anterior of the segment to its junction with **P<sub>2</sub>**; **P<sub>2</sub>** was measured from its junction with **P<sub>1</sub>** to where it abruptly tapers at its junction with the gaster (Fig. 1B). The anterior apex of **P<sub>2</sub>** narrows and extends more or less into the posterior apex of **P<sub>1</sub>**, so it is best to exclude that narrow apex from the **P<sub>2</sub>** measurement. Propodeum length was measured from the dorsal apex of the propodeal flange to the anterior flange of the spiracular peritreme (Fig. 1B). Mesosoma length was measured medially from the dorsal apex of the propodeal flange to the anterior margin of the mesonotum where it meets the pronotum. Measurements are in micrometers except entire specimen length is in millimeters. Most structures are illustrated either from males, females, or both, e.g., colour. Although not technically correct, a male figure may also be referred to in the female description to avoid repetition, as no significant differences occur between the sexes except in the antenna and genitalia. The specimen depositories are:

**UHIM** University of Hawai‘i Insect Museum, Honolulu, Hawai‘i, USA

**BPBM** Bernice Pauahi Bishop Museum, Honolulu, Hawai‘i, USA

**CNC** Canadian National Collection of Insects, Arachnids, and Nematodes, Ottawa, Ontario, Canada

## Results

### *Mymaromma menehune* Honsberger & Huber, sp. nov.

<http://zoobank.org/09DE5C66-46AC-4769-A296-E1A12C4F0C66>

Figs 1B–D, 2, 4, 7

**Material examined. Holotype:** female (Fig. 2A,B) (UHIM) uncleared in Hoyer’s medium sealed with epoxy, on slide with two labels as follows: “Hawaiian Islands, O‘ahu I., Mānoa, 21.2954°N, 157.8145°W, 15 m, 28.vi.2019, ex *Ficus microcarpa* branches, D. Honsberger”. “*Mymaromma menehune* Honsberger & Huber Holotype ♀”. **Allotype:** male (Fig. 2C,D) (UHIM) with same locality data as holotype. **Paratypes:** 12 females, 6 males, all except the two Moloka‘i island specimens with same locality data as holotype except as indicated. **Moloka‘i** • Mapulehu Valley near Ili‘ili‘opae heiau, 10–40’, 8–22.xii.1995 and 12–26.iv.1996, W.D. Perreira, yellow sticky board traps (1♀ & 1♂ slide mounted, CNC). **O‘ahu** • 19.vi.2021, walking on *Ficus microcarpa* branches (1♀ slide mounted, UHIM) • 18.vi.2021, emerged from *Lepidopsocus* sp. eggs on *Ficus microcarpa* branches (1♂, UHIM, 1♀, BPBM, 1♂, CNC, all point mounted, each with host egg from which it emerged also glued to point) • 28.vi.2019 (1♀ & 1♂, BPBM, 1♀, CNC all slide mounted, 2♀ point mounted, CNC) • 17.v.2019 (1♀ slide mounted, BPBM, 1♀ point mounted, UHIM) • 27.vii.2018 (1♀, slide mounted, UHIM, 1♀ & 1♂ both slide mounted, CNC, 1♀ point mounted, 1♂ slide mounted, BPBM).

**Other material examined.** 1 female, 5 males, all slide mounted. **Moloka‘i** • Mapulehu Valley near Ili‘ili‘opae heiau, 10–40’, viii.1995, 29.ix–13.x.1995, 1–15.iii.1996, W.D. Perreira, yellow sticky board traps (3♂, BPBM) • Hālawa Valley, 200’, 29.ix–13.x.1995 and 27.x–10.xi.1995, J.W. Beardsley, W.D. Perreira, yellow sticky board traps (2♂, BPBM) • near Honomuni Str., 24.xi–8.xii.1995, W.D. Perreira, yellow sticky board traps (1♀, BPBM).

**Diagnosis.** *Mymaromma menehune* is most similar to *M. goethei* Girault, 1920 and *M. longipterus* Ayyamperrumal & Manickavasagam, 2017. All are distinguished from other described species of *Mymaromma* by the sculpture of the propodeum: obliquely striate in anterior half and transversely striate in posterior half (Figs 2F, 4B,E,J and as in fig. 79 – M. sp. 6 in Gibson et al. 2007) (propodeum with more or less isodiametric reticulations in most other described *Mymaromma* species).

Beardsley et al. (2000) and Gibson et al. (2007) had already noted that the Hawaiian specimens (not named at the time) were similar to *M. goethei*. *Mymaromma menehune* females differ slightly from *M. goethei* as follows:  $fu_1$  longer than  $fu_2$  and  $fu_3$  in *M. menehune* (Fig. 2B) ( $fu_1$  and  $fu_3$  subequal in *M. goethei*); clava 3.5× as long as wide in *M. menehune* (Fig. 2B) (clava 5.4× as long as wide in *M. goethei* (CNC

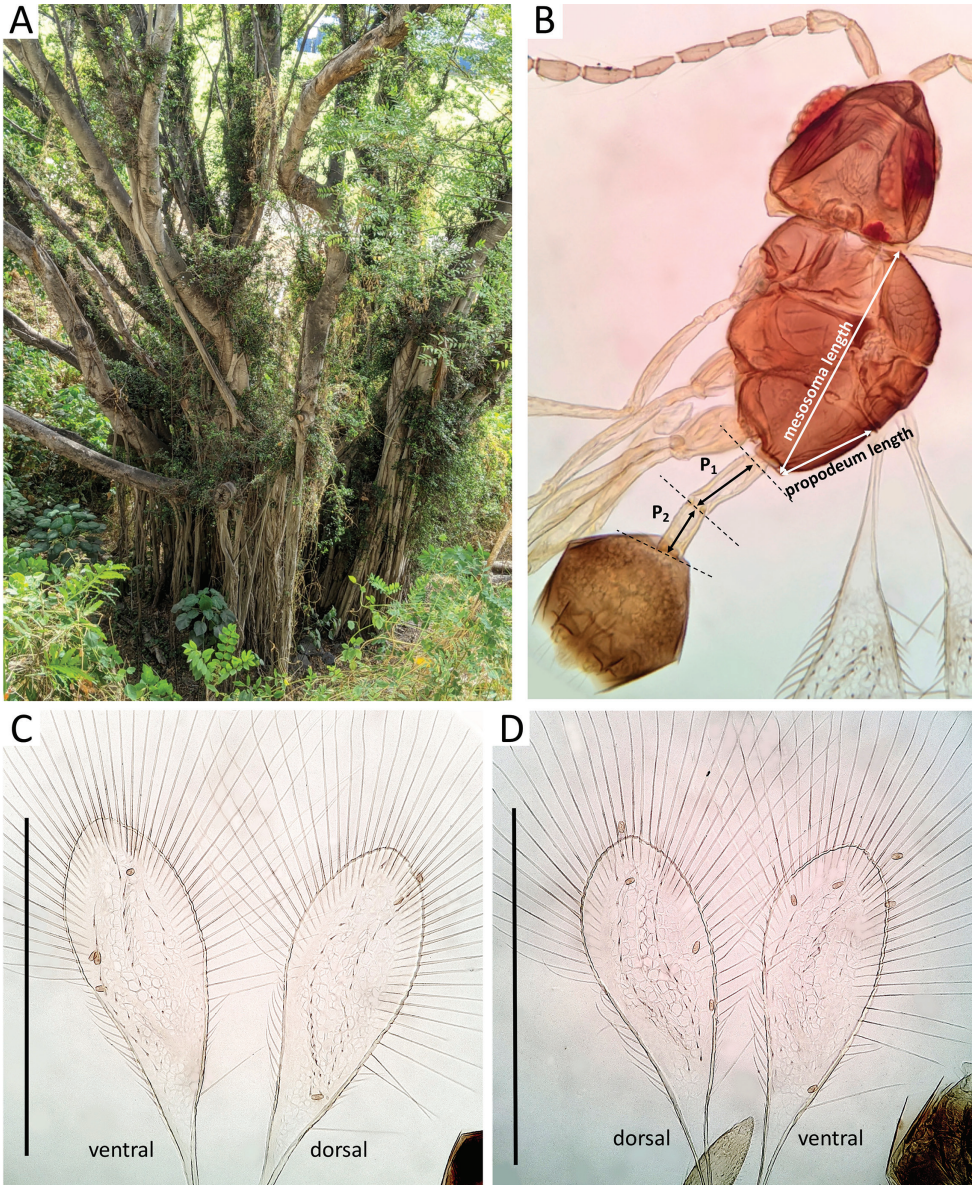


**Figure 1.** **A** *Ficus microcarpa* tree on which the *Mymaromma* sp. was found and from which branches were obtained for collection of potential host eggs **B** the lengths of structures measured as shown. See text for more explanation **C, D** *Mymaromma menehune* sp. nov. wings **C** allotype wing on left showing ventral microtrichia only, wing on right showing dorsal microtrichia only **D** holotype wing on left showing dorsal microtrichia only, wing on right showing ventral microtrichia only. Scale bars: 250  $\mu$ m (**C, D**).

specimen)); mandible dorsal tooth rounded and subcircular, abruptly meeting at an approximate right angle the straight section that extends to the apex of the mandible in *M. menehune* (Fig. 2E,G) (dorsal tooth sharp and after its apex continues in a concave curve toward the base of the mandible in *M. goethei* (see Gibson et al. 2007, fig.

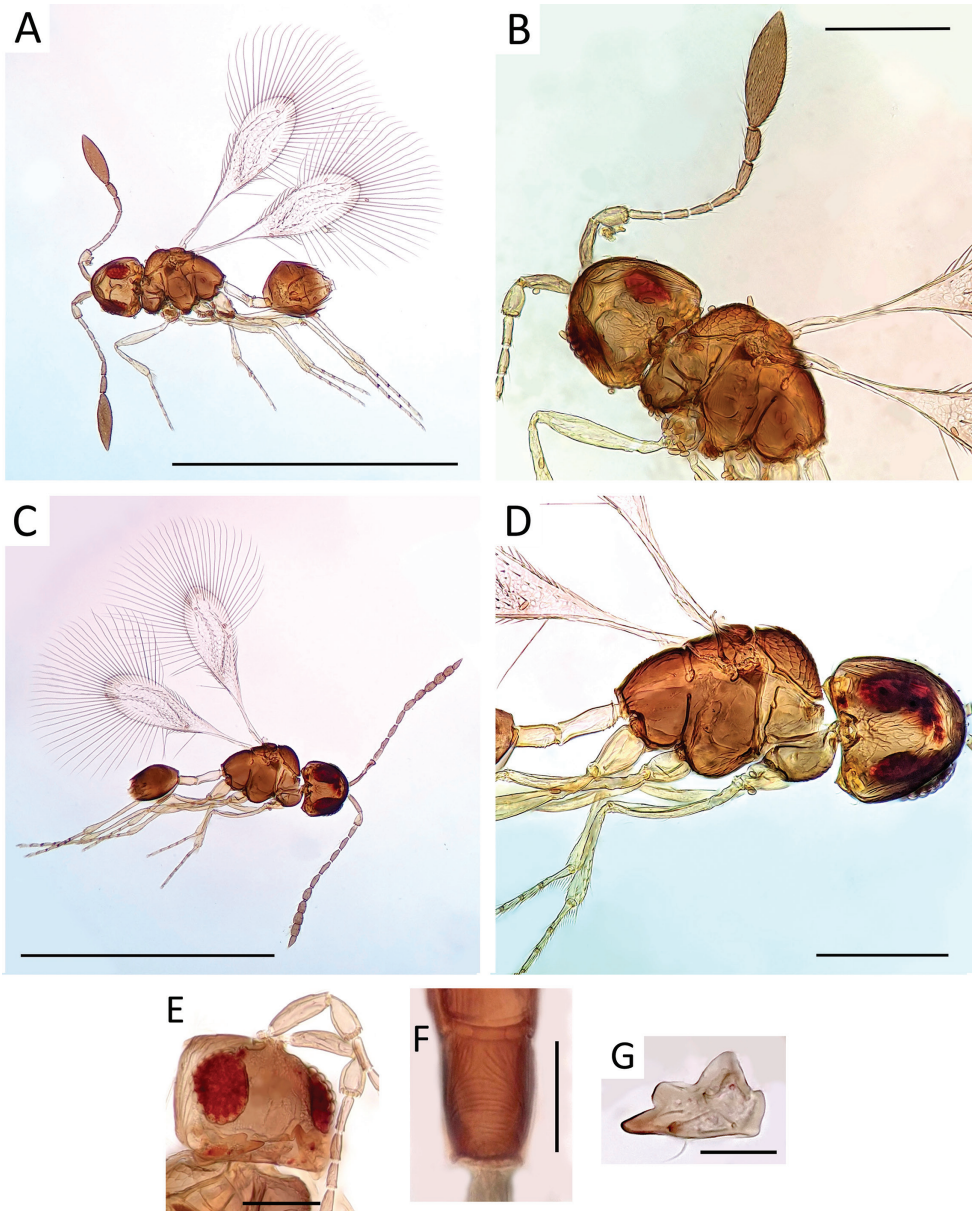


**Figure 2.** *Mymaromma menehune* sp. nov. **A, B** holotype ♀ **C, D** allotype ♂ **E** head showing mandible (non type, ♀) **F** dorsal view of propodeum (non type, ♀) **G** close up of mandible (non type, ♀). Scale bars: 500  $\mu\text{m}$  (**A, C**); 100  $\mu\text{m}$  (**B, D**); 50  $\mu\text{m}$  (**E, F**); 25  $\mu\text{m}$  (**G**).

29)); meso/metapleural suture ventral to metapleural pit consistently deep throughout (Figs 1B, 2D) (suture shallow ventrally below the metapleural pit in *M. goethei*). *Mymaromma menehune* females are distinguished from *M. longipterus* by having: 6 funicular segments (Fig. 2B) (7 segments in *M. longipterus*), with  $\text{fu}_1$  subequal to pedicel,  $\text{fu}_5$  and  $\text{fu}_6$ , and longer than  $\text{fu}_2$  or  $\text{fu}_3$  ( $\text{fu}_1$  distinctly shorter than pedicel,  $\text{fu}_2$ ,  $\text{fu}_3$ ,  $\text{fl}_5$  and  $\text{fl}_6$

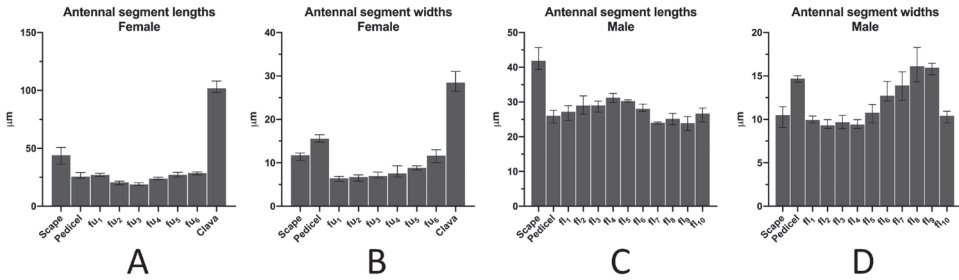


**Figure 3.** Relative lengths and widths for 5 females and 4 males of antennal segments of *M. menehune* sp. nov. **A, B** female **C, D** male. Bar heights are means, error bars are ranges.

in *M. longipterus*). *Mymaromma menehune* males have 10 flagellomeres with the apical 4 flagellomeres more widely joined together. Males are unknown for *M. goethei* and *M. longipterus*. A male from Thailand and two males from Taiwan that have the same propodeal sculpture as *M. menehune* and *M. longipterus* but differ in other features also have a 10-segmented flagellum. Males of *M. goethei* and *M. longipterus* must be discovered and correctly associated with conspecific females before any differences among males of the three species can be determined.

**Description. Female** (Figs 1D, 2A,B,E–G, 3A,B, 4E–G, 7). Body length of point mounted specimens 0.39–0.43 mm ( $n = 6$ ), body length of slide mounted specimens 0.43–0.46 mm ( $n = 5$ ), holotype 0.43 mm. **Colour:** Uniformly brown except for head ventral to eye yellow and small triangular patch ventral to tegula almost black; legs and petiole translucent yellow (Figs 2A–D, 4A,B,E,F,I,J); tarsal segments 1–3 with apex dorsally dark brown, and segments 4 and 5 with apex dorsally light brown (Figs 2A,C,D, 4A,B,E,F,I,J).

**Head.** Eye with about 35 ommatidia. Ocelli absent. Vertex, temple and gena faintly and finely transversely striate, with a few scattered white setae (Fig. 4). Malar space short, about the length of one ommatidium. **Antennae:** Funicle 6-segmented (Fig. 2A,B). Length range/width range (ratio range) ( $n = 5$ ) (Fig. 3A,B) of all segments: scape 36–51/11–12 (3.2–4.2), pedicel 24–29/15–16 (1.5–1.9), fu<sub>1</sub> 26–28/6–7 (4.0–4.8), fu<sub>2</sub> 19–22/6–7 (2.8–3.8), fu<sub>3</sub> 18–20/6–8 (2.4–3.1), fu<sub>4</sub> 23–25/7–9 (2.7–3.3), fu<sub>5</sub> 25–29/8–9 (3.0–3.2), fu<sub>6</sub> 27–30/10–13 (2.3–2.7), clava 98–108/26–31 (3.3–3.8). **Mouthparts:** Mandible tridentate (Fig. 2G); dorsal tooth rounded, its margin subcircular and abruptly meeting at an approximate right angle the straight projection forming the (mainly brown) apical tooth.

**Mesosoma.** Mesosoma length 2.22–2.42× propodeum length ( $n = 5$ ). Mesoscutum with raised isodiametric reticulate sculpture and four thick setae in a transverse line near posterior margin (Fig. 4B,F,J). Scutellum (Fig. 4B,F,J) with sculpture longitudinally striate anteriorly and laterally but isodiametric posteromedially and 1 lateral seta extending to anterior margin of frenum; frenum (Figs 2F, 4B,F,J) with longitudinally striate sculpture. Pronotum laterally, propleuron and mesopleuron apparently with faint, fine, longitudinally striate sculpture at least in ventral half (Fig. 4A,E,I). Mesopleuron mostly smooth and shiny. Mesopleuron and metapleuron partially fused,

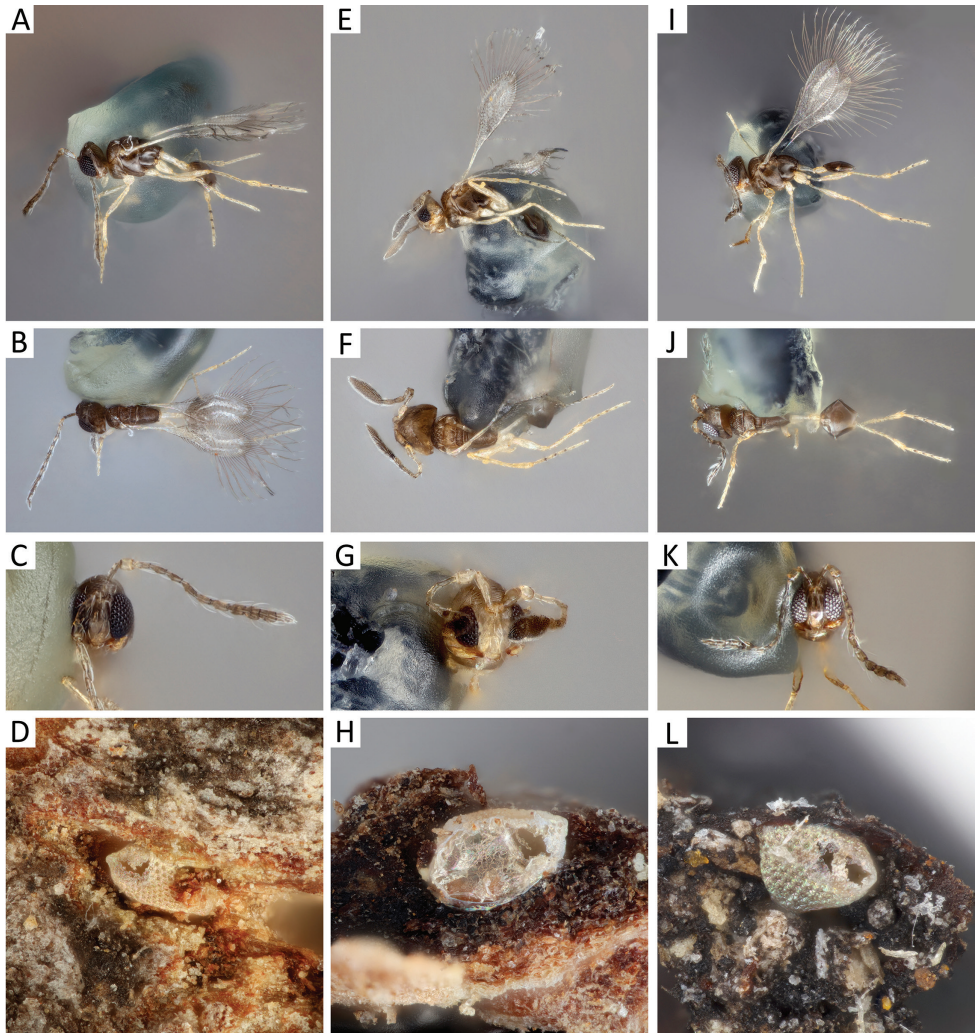


**Figure 4.** *Mymaromma menehune* sp. nov., ex *Lepidopsocus* sp. eggs on *F. microcarpa* branches. **A–C** *M. menehune* ♂ (paratype) and **D** egg from which it emerged **E–G** *M. menehune* ♀ (paratype) and **H** egg from which it emerged **I–K** *M. menehune* ♂ (paratype) and **L** egg from which it emerged.

in lateral view with suture between them consistently deep along its length and extending to metapleural pit at 0.74–0.76× distance between sternum and propodeal spiracle ( $n = 5$ ) (Figs 2B,D, 4A,E,I). Metanotum in dorsal view as a narrow band about 10× as wide as long, smooth (Figs 2F, 4B,F,J) and apparently fused laterally with metapleuron. Propodeum (Figs 2F, 4B,F,J) in dorsal view with  $\Lambda$ -shaped striations in about anterior third, these usually well-defined laterally (in some individuals becoming smooth near midline) and in posterior two thirds with transverse striations medially but curving posteriorly towards lateral margin, and in lateral view smooth; propodeum separated dorsally and laterally from metanotum by groove-like spiracular peritreme

forming, in lateral view, acute angle with posterior margin of metanotum (Figs 2B,D, 4A,E,I). Propodeal spiracle round to apostrophe shaped, somewhat like outline of a garden snail shell, with a single seta posterior to spiracle; propodeal flange  $\cap$  shaped and evenly projecting, extending to bottom of petiolar insertion. **Legs:** Protarsal segments 3–5 subequal, with segment 1 slightly the longest and segment 2 very slightly the shortest. Meso- and metatarsal segments 2–5 subequal, with segment 1 slightly the longest. **Wings:** Fore wing with isodiametric reticulations, subhyaline and without infuscations (Figs 1C,D, 2A,B,C,D, 4B,E,I); fore wing length range/width range (ratio range) 354–385/85–96 (3.83–4.21); longest marginal (fringe) setae (1.74–1.88)  $\times$  wing width. From basal seta on the posterior margin around the wing to anterior basal setae, the fringe setae as follows: 1 long basal seta inserted at wing margin; 6 or 7 shorter setae generally increasing in length distally and inserted at wing margin; about 38–41 ( $n = 5$ ) long setae, the proximal 2 or 3 on both anterior and posterior margins inserted at wing margin, the remainder inserted well inside wing margin; about 11 short setae projecting from wing margin, the medial setae longer than the basal and apical setae, and 1 or 2 very short basal setae. Fore wing membrane with 2 long rows of microtrichia dorsally (Fig. 1C–right wing, 1D–left wing) and 2 long rows and an additional, posterior short row of about 3 setae ventrally (Figs 1C–left wing, 1D–right wing), generally as in Figs 1C,D, 2A,C but with exact placement varying slightly among individuals. Hind wing apically bifurcate, diverging into two rounded hooks with sharp ends smoothly bending back toward each other, leaving a subcircular opening between them.

**Metasoma.** Length range of  $P_1$ /length range of  $P_2$  (ratio range) = 49–55/31–37 (1.42–1.58);  $P_1$  with small spicules ventrobasally, otherwise smooth; segment  $P_2$  slightly rougher especially ventrobasally. Cercus with four long setae. Ovipositor length 0.55–0.59  $\times$  metatibia length ( $n = 5$ ).

**Male** (Figs 1B,C, 2C,D, 3C,D, 4A–C,I–K). Body length of point mounted specimens 0.39–0.40 mm ( $n = 2$ ), body length of slide mounted specimens 0.43–0.46 mm ( $n = 4$ ), allotype 0.43 mm. Similar to female except as follows: profemur and protibia sometimes brown (Fig. 4K); antenna with 10 flagellar segments, forming a loose, indistinct clava with  $fl_6$ – $fl_9$  more widely united to each other, and wider and more globular than the consistently narrow (except  $fl_6$ ) basal segments and the smaller apical segment. Each segment with a whorl of long white setae (Fig. 4K) among other shorter ones. Antennal length range/width range (ratio range) ( $n = 4$ ) (Fig. 3C,D): scape 39–46/9–11 (3.4–4.6), pedicel 24–28/14–15 (1.6–1.9),  $fl_1$  25–29/10 (2.6–3.0),  $fl_2$  27–32/9–10 (2.9–3.5),  $fl_3$  27–30/9–10 (2.9–3.1),  $fl_4$  30–32/9–10 (3.0–3.6),  $fl_5$  30–31/10–12 (2.6–3.2),  $fl_6$  27–29/12–14 (1.9–2.4),  $fl_7$  24/12–15 (1.6–1.9),  $fl_8$  23–27/14–18 (1.3–1.8),  $fl_9$  22–26/15–16 (1.4–1.6),  $fl_{10}$  24–28/10–11 (2.3–2.7). Mesosoma length 2.28–2.43  $\times$  propodeum length ( $n = 4$ ). Fore wing length range/width range (ratio range) 342–395/89–97 (3.83–4.08); longest marginal (fringe) setae 1.83–1.98  $\times$  wing width ( $n = 4$ ). Length range of  $P_1$ /length range of  $P_2$  (ratio range) = 45–49/33–34 (1.36–1.46) ( $n = 4$ ).

**Etymology.** Because of its size and elusivity, this species is named after the Menehune, in Hawaiian legend a people who were small and not often seen, that live in the

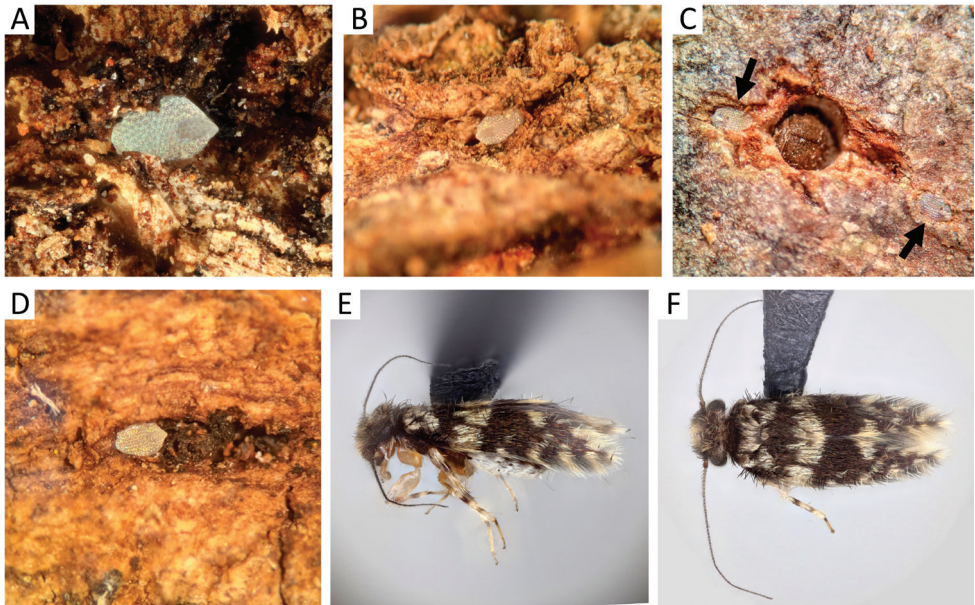


**Figure 5.** *Lepidopsocus* sp., host of *Mymaromma menehune* sp. nov. **A–D** *Lepidopsocus* sp. eggs, found on *F. microcarpa* branches, in **C** two eggs visible, oviposited into a fissure in the wood presumably chewed by an ovipositing cerambycid, and secondarily inhabited by *Cryphalus brasiliensis* (Coleoptera: Scolytinae) **E, F** *Lepidopsocus* sp. adult reared from morphologically identical eggs.

forests and are known for being industrious craftspeople who emerge during the night and build structures.

**Host record and parasitoid behavior.** Three *M. menehune* individuals emerged from the eggs in the capsules, all from morphologically identical eggs, and each *M. menehune* individual from a single egg in a single capsule (Fig. 4). These eggs were confirmed through rearing of additional identical eggs to be of a *Lepidopsocus* sp. (Psocodea: Lepidopsocidae) (Fig. 5). Eggs of this species on the branches inspected were observed to be placed singly, typically in the trough of a shallow topographical feature on the wood surface, such as a small fissure or recess in the bark, the crevice chewed for egg placement by an ovipositing cerambycid, or the crevice created by bark separating from the xylem on a broken branch (Fig. 5). We are confident that the eggs reared for identification and the eggs from which *M. menehune* emerged belong to the same species. A previous study of arthropods emerging from similar branches taken from the same tree over the course of approximately one year (D. Honsberger, unpublished) yielded four species of bark lice from the wood: *Lepidopsocus* sp., *Ectopsocus* ?*pilotus* and *Ectopsocus* ?*pilosus*, and a Psocidae sp. There is great variation in egg morphology within Psocodea. *Ectopsocus* ?*pilosus* and the Psocidae sp. were found through rearing of other eggs collected on the wood to have morphologically dissimilar eggs to those of the *Lepidopsocus* sp. (Fig. 6), and eggs of *E. ?pilotus* could be assumed to be similar to those of the congeneric *E. ?pilosus* and dissimilar to *Lepidopsocus* sp. eggs (New 1987). The host-parasitoid association was thus confirmed.

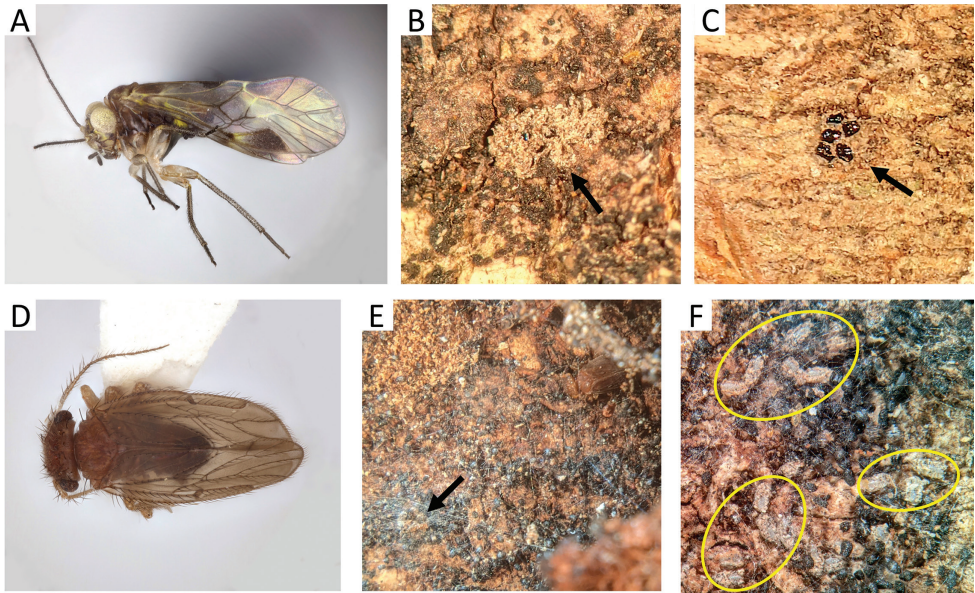


**Figure 6.** Eggs and adults of two other species of bark lice found to emerge from *F. microcarpa* branches from the same tree **A** Psocidae sp. adult **B–C** eggs of Psocidae sp. (**B** unhatched **C** hatched) **D** *Ectopsocus* ?*pilosus* adult **E–F** eggs, frass, and web of *E. ?pilosus* (**E** a patch of eggs visible near bottom left **F** the eggs are the white ovoids).

Three mymarommatoids were observed on the surface of the branches inspected under the microscope (Fig. 7; Video 1 <https://vimeo.com/666102893>). They were subsequently identified as the same species that emerged from the eggs and is described above. The wasps were observed to walk rapidly over the bark surface and groom themselves frequently. No encounter with host eggs was observed. The position of the bellows on the head while the wasps were exploring the wood may be of note, as it has not previously been reported in living individuals. The occiput was flush with the vertex, and expansion or movement of the bellows was not observed. This lack of utilization of the bellows while searching on wood is consistent with its possible function proposed by Huber et al. (2008) where, in combination with the exodont mandibles, the bellows is expanded to assist in bursting out of a host egg with a flexible chorion.

## Discussion

We provide the first host record for the superfamily Mymarommatoidae, thus confirming the hypothesis by Huber et al. (2008) that these wasps are solitary parasitoids in the eggs of Psocoptera, as demonstrated for at least one species. The host range of *M. menehune* is unknown. It was not observed to emerge from eggs of the other species of bark lice collected in this study though not enough eggs were collected to determine with

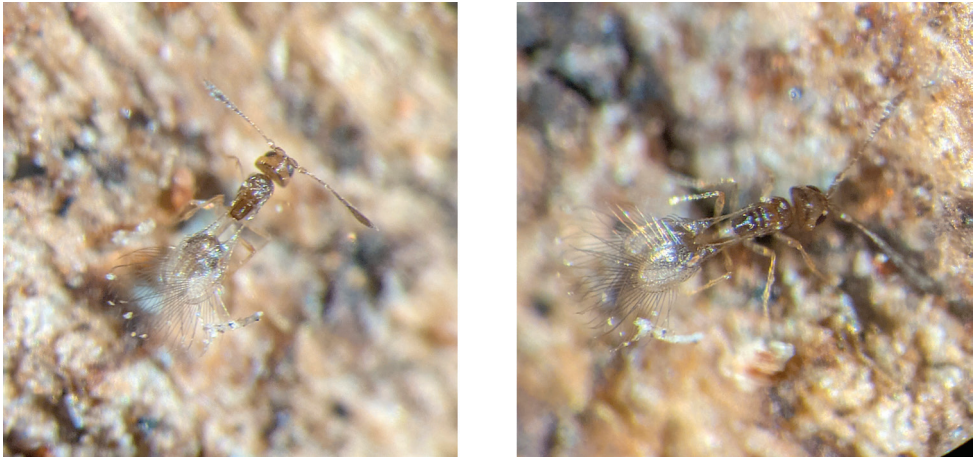


**Figure 7.** *Mymaromma menehune* sp. nov. (♀) exploring wood, found and photographed during inspection of *F. microcarpa* branches.

confidence that it does not also parasitize them. In Hawai‘i, there is an endemic radiation of *Kilauella* (Elipsocidae; 7 known species), *Palistrepus* (Elipsocidae; 20 known species), and *Prycta* (Psocidae; 63 known species) (Nishida 2002). Parasitism of these endemic species by *M. menehune* is not expected, but any relationship it may have with them is unknown. Among described species of *Lepidopsocus*, the known host appears to be closest to *L. pretiosus* (Banks, 1942) and *L. marmoratus* (Banks, 1931), though its exact identity is unclear. Both these species, and the genus *Lepidopsocus* as a whole, appear to be fairly widespread over islands of the tropical western Pacific (Thornton et al. 1972; Thornton 1981a; Thornton 1981b; Thornton 1989); *L. marmoratus* but not *L. pretiosus* is also recorded from Hawai‘i (Banks 1931; Banks 1942; Thornton 1981c). Both are also known from Indonesia (Thornton 1988), and *L. pretiosus* has also been recorded in Zanzibar (Georgiev 2021) and Gorgona Island, Colombia (Sarria-S et al. 2014; García Aldrete et al. 2018). If Mymaromatidae occur on other Pacific islands (none recorded so far) they may well belong to *M. menehune*. *M. menehune* is likely not native to Hawai‘i, like much of the fauna at lower elevations on these islands. The host tree itself was introduced to Hawai‘i; its native range is tropical Asia. Similarly, its host is likely to be among the species of Lepidopsocidae widely distributed over islands of the western Pacific, and thus may not be native to the Pacific Islands but rather, possibly, to southeast Asia.

Only one described species of Mymaromatidae, *M. longipterus*, has a striated propodeum exactly as in *M. menehune* but it differs in number of funicle segments. Most *Mymaromma* females appear to have a 7-segmented funicle but a few, e.g., *M. goethei*, have a 6-segmented funicle. Two slide-mounted females and 1 male from Thailand, and 2 males from Taiwan (CNC) with a striate propodeum were examined. One of the Thailand females had one antenna with 7 funicle segments and the other with 6, the segments 3 and 4 clearly having fused with only a slight break visible between them.

The other Thailand female was missing one antenna but the remaining antenna had 7 funicle segments. These two females had  $P_1$  1.58 $\times$  and 1.96 $\times$  as long as  $P_2$ , fairly different from the 1.4 ratio reported for *M. longipterus*. The male petiole ratio was similar to one of the females, however, with  $P_1$  1.59 $\times$  as long as  $P_2$ . To what extent the petiole segments vary in relative lengths is unknown for *M. longipterus* as it was described from a single specimen. Although the wing proportions and relative lengths of the two petiole segments are fairly similar, with some variation among the specimens from all three populations, we suspect that *M. menehune* is not the same as the Thailand and Taiwan specimens but cannot determine this with confidence. We also cannot be certain that they are *M. longipterus*, though the Thailand females likely are.

## Acknowledgements

We thank Maya Honsberger for her observations, support, and help examining branches for eggs. We also thank Keith Arakaki, Lisha Jasper, and Neil Evenhuis of the Bernice Pauahi Bishop Museum for supporting visits to the museum, and their help locating and imaging specimens; and Whit Farnum, Crystal Maier, and Brian Farrell of the Museum of Comparative Zoology for locating and imaging specimens. We are very grateful to Hawai'i Department of Agriculture, USDA-APHIS, USDA-ARS, and NIFA Hatch project HAW09041-H, administered by CTAHR, for their funding.

## References

- Ayyamperumal M, Manickavasagam S (2017) Four new species of *Mymaromma* Girault (Hymenoptera: Mymarommatidae) from India with a key to Indian species. *Transactions of the American Entomological Society* 143: 589–599. <https://doi.org/10.3157/061.143.0304>
- Banks N (1931) On some Psocidae from the Hawaiian Islands. *Proceedings of the Hawaiian Entomological Society* 7(3): 437–444. <http://hdl.handle.net/10125/15807>
- Banks N (1942) Neuropteroid insects from Guam. *Bishop Museum Bulletin* 172: 25–30. <http://hbs.bishopmuseum.org/pubs-online/pdf/b172p25-30.pdf>
- Beardsley JW, Huber JT, Perreira WD (2000) Mymarommatoidea, a superfamily of Hymenoptera new for the Hawaiian Islands. *Proceedings of the Hawaiian Entomological Society* 34: 61–63. <http://hdl.handle.net/10125/8410>
- Engel MS, Grimaldi DA (2007) New false fairy wasps in Cretaceous amber from New Jersey and Myanmar (Hymenoptera: Mymarommatoidea). *Transactions of the Kansas Academy of Science* 110(3/4): 159–168. [https://doi.org/10.1660/0022-8443\(2007\)110\[159:NFFWIC\]2.0.CO;2](https://doi.org/10.1660/0022-8443(2007)110[159:NFFWIC]2.0.CO;2)
- García Aldrete AN, Carrejo NS, Mendivil J, Calderón N, Saenz O, Panche J, Román C, González Obando R (2018) Checklist of 'Psocoptera' (Psocodea) of Colombia and identification key to the families. *Dugesiana* 25(2): 77–103. <https://doi.org/10.32870/dugesiana.v25i2.7031>

- Georgiev D (2021) On the fauna of Psocoptera of Unguja (Zanzibar) Island (Tanzania, East Africa). *Historia Naturalis Bulgarica* 42: 35–42. <https://doi.org/10.48027/hnb.42.061>
- Gibson GAP, Read J, Huber JT (2007) Diversity, classification and higher relationships of Mymarommatoidea (Hymenoptera). *Journal of Hymenoptera Research* 16(1): 51–146.
- Hatten TD, Merz N, Johnson JBD, Looney C, Ulrich T, Soultis S, Capilo R, Bergeron D, Anders P, Tanimoto P, Shafi B (2010) Note on occurrence of *Mymarommella pala* Huber and Gibson (Hymenoptera: Mymarommatidae) in Montana: a new state record. *Western North American Naturalist* 70(4): 567–569. <https://doi.org/10.3398/064.070.0417>
- Huber JT, Gibson GAP, Bauer LS, Liu H, Gates M (2008) The genus *Mymarommella* (Hymenoptera: Mymarommatidae) in North America, with a key to described extant species. *Journal of Hymenoptera Research* 17(2): 175–194.
- Machado Benassi VLR, Iglesias Valente F, Cristina Lenzi J, Carvalho S (2014) Survey of Mymarommatidae and their occurrence in agricultural systems in Brasil. *Journal of Insect Science* 14(1): e15. <https://doi.org/10.1093/jis/14.1.15>
- Mohanraj P, Kamalanathan V (2015) A new species of *Mymaromma* Girault (Hymenoptera: Mymarommatoidea: Mymarommatidae) from India. *Entomological News* 124(5): 325–330. <https://doi.org/10.3157/021.124.0504>
- New TR (1987) Biology of the Psocoptera. *Oriental Insects* 21: 1–109. <https://doi.org/10.1080/00305316.1987.11835472>
- Nishida GM (2002) Hawaiian terrestrial arthropod checklist, fourth edition. Bishop Museum Technical Report 22: 1–313. <http://hbs.bishopmuseum.org/hbsdb.html>
- Ortega-Blanco J, Peñalver E, Delclós, Engel MS (2011) False fairy wasps in early Cretaceous amber from Spain (Hymenoptera: Mymarommatoidea). *Palaeontology* 54(3): 511–523. <https://doi.org/10.1111/j.1475-4983.2011.01049.x>
- Sarria-S FA, González Obando R, García Aldrete AN (2014) Psocoptera (Insecta: Psocodea) from the National Natural Park Gorgona, Cauca, Colombia. *Revista de Biología Tropical* 62(1): 243–256. <https://doi.org/10.15517/rbt.v62i0.16337>
- Schlüter T (1978) Zur Systematic und Palökologie harzkonservierter Arthropoda einer Raphozönose aus dem Cenomanium von NW-Frankreich. *Berliner Geowissenschaftliche Abhandlungen (A)*:9, 150 pp. <http://doi.org/10.17169/refubium-29434>
- Thornton IWB (1981a) Psocoptera of the Fiji islands. *Pacific Insects Monograph* 37: 1–105. <http://hbs.bishopmuseum.org/pim/pdf/pim37-1.pdf>
- Thornton IWB (1981b) Psocoptera of the Tongan archipelago. *Pacific Islands Monograph* 37: 106–135. <http://hbs.bishopmuseum.org/pim/pdf/pim37-106.pdf>
- Thornton IWB (1981c) The Psocoptera of the Hawaiian Islands: Parts I and II. Introduction and the nonendemic fauna. *Pacific Insects* 23(1–2): 1–49. [http://hbs.bishopmuseum.org/pi/pdf/23\(1-2\)-1-49.pdf](http://hbs.bishopmuseum.org/pi/pdf/23(1-2)-1-49.pdf)
- Thornton IWB (1989) Psocoptera (Insecta) of the island of Moorea, French Polynesia, and comparisons with other Pacific island faunas. *Bulletin du Museum national d'Histoire naturelle* 11(4): 783–828. <http://bionames.org/bionames-archive/issn/0181-0626/11/783.pdf>
- Thornton IWB, Lee SS, Chui WD (1972) Psocoptera. *Insects of Micronesia* 8(4): 45–144. <http://hbs.bishopmuseum.org/pubs-online/pdf/iom8-4pso.pdf>

- Thornton IWB, New TR, Vaughan PJ (1988) Colonization of the Krakatau Islands by Psocoptera (Insecta). *Philosophical Transactions of the Royal Society of London B* 322: 427–443. <https://doi.org/10.1098/rstb.1988.0136>
- Vilhelmsen L, Krogmann L (2006) Skeletal anatomy of the mesosoma of *Palaeomymar anomalum* (Blood & Kryger, 1922) (Hymenoptera: Mymarommatidae). *Journal of Hymenoptera Research* 15(2): 290–306.

## Supplementary material I

### Video 1. *Mymaromma menehune* sp. nov. ♀ exploring a *F. microcarpa* branch and grooming

Authors: David N. Honsberger, John T. Huber, Mark G. Wright

Data type: Mp4 file.

Explanation note: <https://vimeo.com/666102893>

Copyright notice: This dataset is made available under the Open Database License (<http://opendatacommons.org/licenses/odbl/1.0/>). The Open Database License (ODbL) is a license agreement intended to allow users to freely share, modify, and use this Dataset while maintaining this same freedom for others, provided that the original source and author(s) are credited.

Link: <https://doi.org/10.3897/jhr.89.77931.suppl1>



# Integrated taxonomy unveils three new species of *Foenobethylus* (Hymenoptera, Bethylidae) from China

Yang Li<sup>1\*</sup>, Zheng Wang<sup>2\*</sup>, Hua-Yan Chen<sup>3</sup>, Shi-Xiao Luo<sup>3</sup>

**1** Sichuan Provincial Key Laboratory for Development and Utilization of Characteristic Horticultural Biological Resources, College of Chemistry and Life Sciences, Chengdu Normal University, Chengdu 611130, China

**2** Key Laboratory of Genetic Improvement and Quality Regulation for Tropical Spice and Beverage Crops of Hainan Province, Research Institute of Spice and Beverage, Chinese Academy of Tropical Agricultural Sciences, Wanning 571533, China

**3** Key Laboratory of Plant Resources Conservation and Sustainable Utilization, South China Botanical Garden, Chinese Academy of Sciences, Guangzhou 510650, China

Corresponding author: Hua-Yan Chen ([huayanc@scbg.ac.cn](mailto:huayanc@scbg.ac.cn))

Academic editor: Michael Ohl | Received 4 December 2021 | Accepted 16 January 2022 | Published 28 February 2022

<http://zoobank.org/74E70C08-3253-4CA6-BFCF-BDAAEF80D5BD>

**Citation:** Li Y, Wang Z, Chen H-Y, Luo S-X (2022) Integrated taxonomy unveils three new species of *Foenobethylus* (Hymenoptera, Bethylidae) from China. *Journal of Hymenoptera Research* 89: 89–108. <https://doi.org/10.3897/jhr.89.78856>

## Abstract

Species of the genus *Foenobethylus* Kieffer, 1913 are parasitoids wasps rarely collected and are only found in the Oriental region. In this study, based on both morphological and molecular evidence, we describe three new species from China: *F. robusta* Li & Chen, **sp. nov.**, *F. xinglongsensis* Wang & Chen, **sp. nov.**, and *F. yunkaishanensis* Chen & Luo, **sp. nov.** An updated key to species of the genus is provided. Additionally, the phylogenetic relationships between *Foenobethylus* and other three morphologically similar genera are discussed based on the analyses of *COI* and *28S* genes.

## Keywords

Flat wasps, key, new species, parasitoid wasp, phylogeny, Pristocerinae

\* These two authors contributed equally to this work.

## Introduction

*Foenobethylus* Kieffer is a rare genus of Pristocerinae in the flat wasp family Bethyridae, with only 11 described species Oriental (Várkonyi and Polaszek 2007; Liu et al. 2011; Saverognini and Azevedo 2013; Chen and Azevedo 2020). Of the 11 described species, 10 species were described based on only males. Until recently, the first female of the genus was discovered by Chen and Azevedo (2020). The new finding suggested that *Foenobethylus* might be a synonym under *Parascleroderma*. Although the morphological differences between *Foenobethylus* and *Parascleroderma* were intensely discussed (Azevedo and Lanés 2007; Várkonyi and Polaszek 2007; Chen and Azevedo 2020), Chen and Azevedo (2020) concluded that the precise taxonomic delimitation of both genera only could be solved under phylogenetic analyses. Interestingly, before the discovery of the female of *Foenobethylus*, considering the extreme sexual dimorphism in Pristocerinae, Várkonyi and Polaszek (2007) also suspected that the females of *Foenobethylus* might be already known to science under a different generic name and the exact phylogenetic status of *Foenobethylus* could be resolved by preferably molecular evidence.

Recently, we have accumulated some fresh specimens of several *Foenobethylus* species collected by Malaise traps in South China. In this study, we aim to identify this new material to species using an integrated taxonomic approach that combines both morphology and molecular data and to conduct a preliminary phylogenetic analysis between *Foenobethylus* and morphologically similar genera based on DNA sequences.

## Materials and methods

### Collection and identification

This work is based on specimens of *Foenobethylus* collected by Malaise traps (MT) set up across southern China. Specimens were identified using the keys of Chen and Azevedo (2020). All studied specimens are deposited in the Insect Collection of South China Botanical Garden, Chinese Academy of Sciences, Guangzhou, China (**SCBG, curator:** Huayan Chen). The morphological terms generally follow Lanés et al. (2020) and Brito et al. (2021), and the sculptural and texture of integument nomenclature follows Harris (1979).

### Abbreviations and morphological terms used in text are:

**WH** width of the head;

**LH** length of the head;

**WF** width of the frons;

**HE** height of the eye;

**OOL** ocello-ocular line;

**WOT** width of the ocellar triangle.

The genitalia and subgenital plate of a male paratype were removed and cleared using 10% potassium hydroxide solution, and mounted in glycerol on slides, when examined and photographed. Images and measurements were made using Nikon SMZ25 microscope with a Nikon DS-Ri 2 digital camera system. Images were post-processed with Adobe Photoshop 2022.

## DNA extraction, amplification, and sequencing

In total, 7 specimens of 4 morphospecies were used for DNA acquisition (see Table 1). Collecting information of the studied specimens are available in the material examined section by the associated codes. Genomic DNA was extracted from entire specimens using a DNeasy Blood & Tissue Kit (QIAGEN, Inc.), following a nondestructive DNA extraction protocol as described in Taekul et al. (2014). Following DNA extraction, the “barcode” region of the mitochondrial cytochrome oxidase subunit 1 (*COI*) and nuclear 28S rRNA D1–2 (*28S*) were amplified using the LCO1490/HCO2198 (Folmer et al. 1994) and D2–3551F/D2–4057R (Gillespie et al. 2005) primer pairs, respectively. Polymerase chain reactions (PCRs) were performed using Tks Gflex DNA Polymerase (Takara), and conducted in a T100 Thermal Cycler (Bio-Rad). Thermo-cycling conditions were: an initial denaturing step at 94 °C for 5 min, followed by 35 cycles of 94 °C for 30 s, 50 °C for 30 s, 72 °C for 30s and an additional extension at

**Table 1.** List of analyzed taxa and accession numbers.

Species	Code	GenBank accession No.	
		28S	COI
Ingroup			
<i>Apenesia</i> sp.1	–	MG760810	MG760759
<i>Apenesia</i> sp.2	–	MG760811	MG760760
<i>Cleistepyris</i> sp.1	–	MG760830	MG760774
<i>Cleistepyris</i> sp.2	–	MG760832	MG760776
<i>Dissomphalus</i> sp.1	–	MG760834	MG760778
<i>Dissomphalus</i> sp.2	–	MG760821	MG760768
<i>Parascleroderma</i> sp.1	–	MG760813	MG760762
<i>Parascleroderma</i> sp.2	–	MG760816	MG760763
<i>Foenobethylus emiliacasellae</i>	–	–	MG760815
<i>Foenobethylus robusta</i> sp. nov.	SCAU 3042641	–	OL678509
<i>Foenobethylus syndesis</i>	SCAU 3042642	OL678115	OL678510
<i>Foenobethylus syndesis</i>	SCAU 3042643	OL678116	OL678511
<i>Foenobethylus xinglongensis</i> sp. nov.	SCAU 3042638	OL678117	OL678512
<i>Foenobethylus xinglongensis</i> sp. nov.	SCAU 3042656	OL678118	OL678513
<i>Foenobethylus yunkaishanensis</i> sp. nov.	SCAU 3042639	OL678119	OL678514
<i>Foenobethylus yunkaishanensis</i> sp. nov.	SCAU 3042658	OL678120	OL678515
Outgroup			
<i>Prorops nasuta</i>	–	MG760840	MG760784
<i>Sierola gracilis</i>	–	MG760837	MG760781

Note: accession numbers begin with OL are sequences generated in this study.

72 °C for 5 min. Amplicons were directly sequenced in both directions with forward and reverse primers on an Applied Biosystems (ABI) 3730XL by Guangzhou Tianyi Huiyuan Gene Technology Co., Ltd. (Guangzhou, China). Chromatograms were assembled with Geneious 11.0.3. All sequences generated from this study are deposited in GenBank (accession numbers see Table 1). All residual DNAs are archived (–30 °C) in the molecular laboratory of SCBG, Guangzhou, China, and are available for further study upon request.

## Molecular species delimitation and phylogenetic analysis

All sequences were blasted in BOLD (Barcode of Life Database, [http://www.barcodinglife.org/index.php/IDS\\_OpenIdEngine](http://www.barcodinglife.org/index.php/IDS_OpenIdEngine), only for *COI*) and GenBank. Sequences were aligned using MAFFT v7.470 by the G-INS-I strategy for 28S and G-INS-I strategy for *COI* (Kato and Standley 2013). Genetic Kimura-2 parameter (K2P) distances of *COI* sequences within and between species were calculated in MEGA 7 with pairwise deletion for gaps (Kumar et al. 2016). For phylogenetic analysis, sequences of specimens of three morphologically similar or phylogenetically close genera, *Apenesia* Westwood, *Cleistopyris* Kiefer, *Dissomphalus* Ashmead and *Parascleroderma* Kieffer, as suggested by previous studies (Alencar et al. 2018; Chen and Azevedo 2020), were extracted from Alencar et al. (2018) (Table 1). The 28S sequence of *Foenobethylus emiliacasellae* Várkonyi and Polaszek was downloaded from Genbank. *Prorops nasuta* (Waterston, 1923) and *Sierola gracilis* Fullaway, 1920 (Hymenoptera, Bethyridae) selected as outgroups as used by Alencar et al. (2018). The concatenated sequences of 28S and *COI* were then analyzed using RAxML as implemented in Geneious 11.0.3 under the GTRGAMMA evolutionary model to generate a maximum likelihood (ML) tree.

## Results

This study generated seven sequences of *COI* and six sequences of 28S for seven specimens. These seven voucher specimens were subjected to further morphological examination and four species were recognized, of which three are described as new. The *COI* sequences do not show a high match with sequences in both BOLD and GenBank databases. The closest match is an undetermined species of *Parascleroderma*, with 86.4% identical base pairs. Genetic distances of *COI* sequences among *Foenobethylus* species and representative species of four other morphologically similar or purported phylogenetically close genera and outgroups are in Table 2. Intraspecific distances of the *COI* sequences of *Foenobethylus* are identical. Interspecific distances among *Foenobethylus* species range between 10.3% and 13.6%. Intergeneric distances between *Foenobethylus* and the four potential close genera and the outgroups range between 14.3% and 28.6%, with *Parascleroderma* is the most close genus, which shows 14.8–

18.6% divergence. The morphology-based delimitations of species are congruent with the molecular species identification based on *COI* sequences. Phylogenetic relationships between *Foebethylus* and the studied genera are shown in Fig. 1. *Foebethylus* was recovered as a monophyletic clade, with *Parascleroderma* as a sister group.

**Table 2.** Genetic distances of *COI* sequences among studied taxa (%).

Taxon	1	2	3	4	5	6	7	8	9	10	11	12	13	14
1 <i>Apenesia</i> sp1	-	-	-	-	-	-	-	-	-	-	-	-	-	-
2 <i>Apenesia</i> sp2	1.4	-	-	-	-	-	-	-	-	-	-	-	-	-
3 <i>Cleistopyris</i> sp1	20.3	19.4	-	-	-	-	-	-	-	-	-	-	-	-
4 <i>Cleistopyris</i> sp2	19.8	19.4	15	-	-	-	-	-	-	-	-	-	-	-
5 <i>Dissomphalus</i> sp1	27.3	26.9	26.5	25.4	-	-	-	-	-	-	-	-	-	-
6 <i>Dissomphalus</i> sp2	23.4	23.5	27.2	22.6	26.4	-	-	-	-	-	-	-	-	-
7 <i>Parascleroderma</i> sp1	19.8	19.2	19.4	17.4	24.9	21	-	-	-	-	-	-	-	-
8 <i>Parascleroderma</i> sp2	17	16.4	21.1	20.8	26.2	23.4	17.3	-	-	-	-	-	-	-
9 <i>Foebethylus robusta</i> sp. nov.	18.7	18.7	20.9	18.6	25	23.5	14.3	18.6	-	-	-	-	-	-
10 <i>Foebethylus syndesis</i>	21.4	21.2	22.5	19.9	25.2	24.6	15.4	17.4	11.3	-	-	-	-	-
11 <i>Foebethylus xinglongensis</i> sp. nov.	20.1	19.6	20.9	17.7	24.8	24.7	14.6	16.4	13.1	13.6	-	-	-	-
12 <i>Foebethylus yunkaishanensis</i> sp. nov.	19.8	19.6	21.2	19.4	31.5	23.9	14.8	16.7	10.8	10.3	12.3	-	-	-
13 <i>Sierola gracilis</i>	25.2	24.7	27.1	27	28.6	27.4	24.7	25.5	27	28.6	27.8	27.5	-	-
14 <i>Prorops nasuta</i>	25	24.7	26.2	25.5	25.5	27	23.7	25.5	25.3	27.5	26.4	25.2	27.2	-

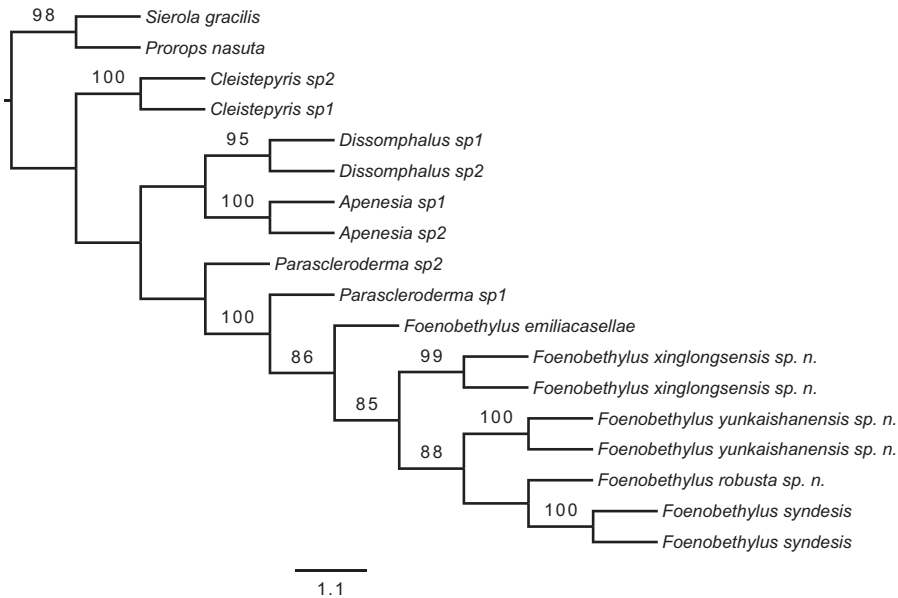


**Figure 1.** Maximum likelihood tree demonstrating the clustering of *Foebethylus* and related genera based on concatenated sequences (*COI* and *28S*).

## Species treatment

### *Foenobethylus robusta* Li & Chen, sp. nov.

<http://zoobank.org/B2F138C5-2376-458B-9488-D2E965C42744>

Figures 2, 3

**Diagnosis. Male.** Head rectangular and elongate (Fig. 2B). Clypeus with median lobe truncate, median carina incomplete, not reaching anterior clypeal margin, and straight in dorsal profile. Eye glabrous (Fig. 2B). Notaulus very weakly converging posteriorly, complete and deep (Fig. 2C). Propodeum polished (Fig. 2C). Pterostigma broad, about 0.4× as wide as long (Fig. 2F). Metatrochanter without spine (Fig. 3G). Metafemur with only one acute spine in ventral midline, 0.26× as long as metafemoral width, touching apical margin of metatrochanter, and with one small, broad and dentate protuberance ventrally, 0.04× metafemoral width, located on second quarter of metafemur (Fig. 3G). Posterior hypopygeal margin strongly incurved, lateral lobe without conical protuberance (Fig. 3E). Basivolsella large, 0.6× as long as gonostipe, basal half about as wide as apical half, basal margin incurved (Fig. 3C, D).

**Description. Male holotype.** Body length 4.52 mm. Forewing length 3.10 mm.

**Colors.** Head, mesosoma, metasoma, antenna and apex of mandible dark castaneous; palpi, base of mandible, all tibiae and tarsi castaneous; wings subhyaline, fore wing somewhat infusate medially.

**Head.** Head (Figs 2B, 3A) rectangular and elongate, 1.2× as long as wide. Mandible with five apical sharpened teeth, posterior tooth largest, middle three teeth smaller, anterior tooth smallest. Clypeus with median lobe truncate, median carina incomplete, not reaching anterior clypeal margin, and straight in dorsal profile. Eye glabrous, almost touching mandible base at anterior corner. Malar space reduced. Frons weakly coriaceous, almost polished, punctures very sparse and small. WH 0.84× LH. WF 0.66× WH. WF 1.63× HE. OOL 1.44× WOT. Frontal angle of ocellar triangle obtuse. Anterior ocellus far posterior to supra-ocular line. Temple divergent anterad, corner rounded. Vertex badly outcurved. First four antennomeres in ratio of about 25:12:11:11 (Fig. 2E). All flagellomeres distinctly longer than wide, pubescence erect, about 0.48× as long as flagellomeral width. Maxillary palpus with five palpomeres (Fig. 3A). Labial palpus with two palpomeres (Fig. 3A). Occipital carina complete. Medioccipito-genal carina complete. Hypostomal carina thick, almost straight, angled medially.

**Mesosoma** (Figs 2C, D, 3B). Mostly polished and weakly coriaceous. Pronotal flange short, exposing propleuron dorsally. Dorsal pronotal area short, without anterior carina strongly progressively narrowing anterad, lateral surface concave. Notaulus very weakly converging posteriorly, complete, deep, and progressively more evident posteriorly. Parapsidal signum sinuous, absent anteriorly. Mesoscutellum shorter than anteromesoscutum. Mesoscutum-mesoscutellar sulcus deep, arched, sides wider than middle. Metanotum conspicuous, metascutellum wide and short, metanotal trough not trabeculate, metanotal fovea outlined. Metapectal-propodeal disc polished, metapostnotal median carina complete, although weak posteriorly,

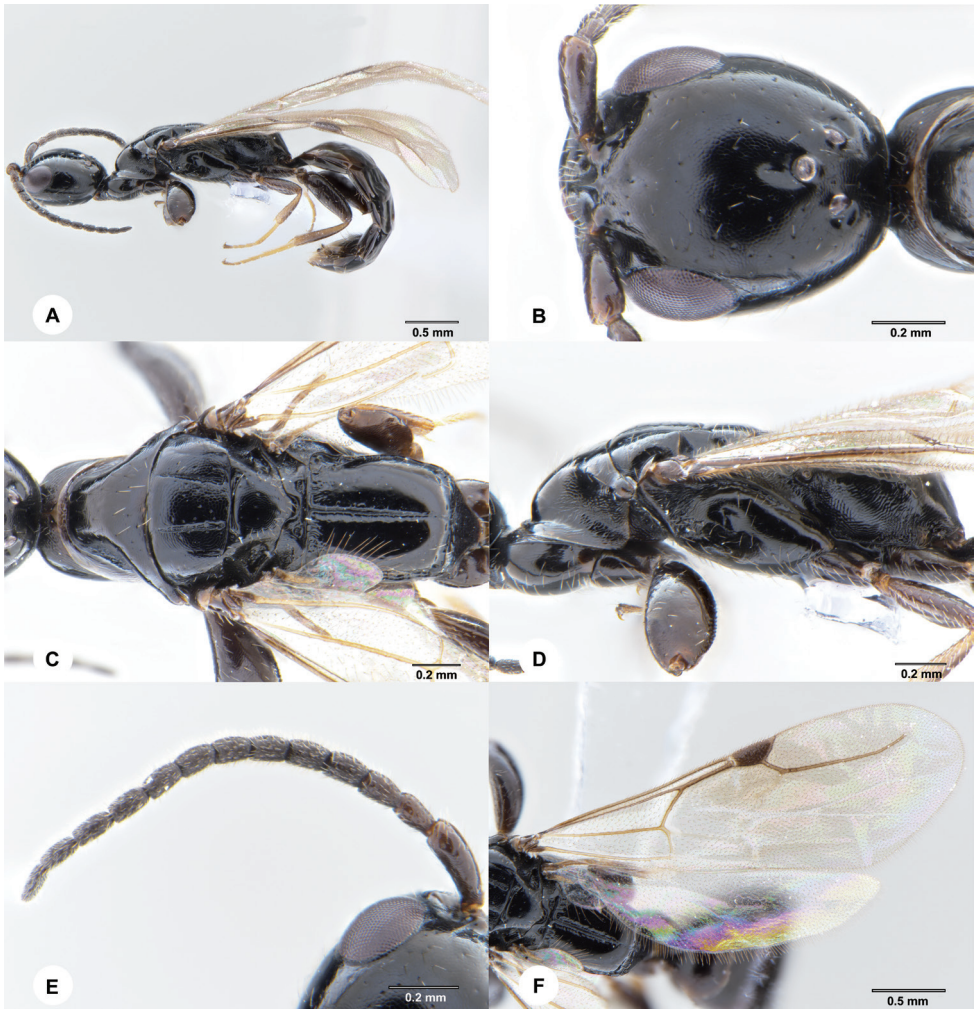


**Figure 2.** *Foenobethylus robusta* Li & Chen, sp. nov., male, holotype (SCAU 3042645) **A** lateral habitus **B** head, dorsal view **C** mesosoma, dorsal view **D** mesosoma, lateral view **E** antenna **F** wings.

lateral and transverse posterior carinae complete; propodeal spiracle circular, located on lateral surface of propodeum, ventral to lateral carina. Propodeal declivity transverse sculptured, without median carina. Mesopleuron with mesopleural pit large and well defined. Pleurosternum small, triangular, with vertex directed posterad. Prepectus with epicnemial medial projection complete, posterior prepectal flange thick. **Wings** (Fig. 2F). Forewing with three closed cells (Costal, Radial and First Cubital); pterostigma about 0.4× as wide as long, anterior board outcurved; 2r-rs&Rs sector vein long; Rs&M reaching Sc+R far from pterostigma. Hind wing with one straight hamulus, and four distal hamuli equally distant, and strongly curved. **Legs.** Profemur swollen, 2.7× as long as wide, apical half of ventral margin serrulate. Metatrochanter



**Figure 3.** *Foenobethylus robusta* Li & Chen, sp. nov., male, **A, B, G** holotype (SCAU 3042645) **C–F** paratype (SCAU 3042641) **A** head, ventral view **B** mesosoma, ventral view **C** genitalia, dorsal view **D** genitalia, ventral view **E** subgenital plate **F** 7<sup>th</sup> sternite **G** metaleg, lateral view.

(Fig. 3G) without spine. Metafemur (Fig. 3G) with one acute spine in ventral midline,  $0.26\times$  as long as metafemoral width, touching apical margin of metatrochanter, and with one small, broad and dentate protuberance ventrally,  $0.04\times$  metafemoral width, located on second quarter of metafemur.

**Metasoma.** Weakly longer than mesosoma. Seventh sternite (Fig. 3F) with posterior margin incurved at about middle third. Hypopygium (Fig. 3E) with spiculum longer than median length of hypopygium, and  $1.3\times$  longer than anteromedial apodeme, latter strongly curved mesad apically; posterior margin strongly incurved, lateral lobe

obtuse rounded. **Genitalia** (Fig. 3C, D). Harpe shorter than gonostipe; aedeagus slightly wide, 2.32× as long as wide, apex aedeagus posterior to posterior margin of gonostipe, 0.6× as long as gonostipe; basivolsella large, 0.6× as long as gonostipe, basal half about as wide as apical half, basal margin incurved.

**Variation.** Mesosoma more polished, especially pronotum and propodeum.

**Etymology.** The specific epithet derived from the Latin word for robust, and refers to the robust body of this species.

**Material examined.** *Holotype*, male, CHINA: Yunnan, Dali, Yunlong County, 2608 m, 25°50'57.94"N, 99°14'30.58"E, 27.xiii–12.ix.2020, MT, SCAU 3042645 (SCBG). *Paratypes*: 2 males. 1 male, same collecting data as holotype, SCAU 3042641 (SCBG); 1 male, CHINA: Yunnan, Dali, Yunlong County, 2537 m, 25°50'49.91"N, 99°14'22.95"E, 28.v–14.vi.2020, MT, SCAU 3042657 (SCBG).

**Distribution.** Oriental region, China, Yunnan Province.

**Remarks.** This new species is very similar to *F. syndesis* Chen & Azevedo [Yunnan and Hainan, China], but can be separated from the latter by the following characters: median carina of clypeus incomplete (complete in *F. syndesis*); notaulus complete and deep (incomplete and shallow in *F. syndesis*); declivity of propodeum without median carina (with median carina in *F. syndesis*); metafemur with only one acute spine in ventral midline (with two acute spines in *F. syndesis*); lateral lobe of hypopygium without conical protuberance (with conical protuberance in *F. syndesis*).

### *Foenobethylus syndesis* Chen & Azevedo, 2020

*Foenobethylus syndesis* Chen & Azevedo, 2020: 1241–1246 (diagnosis, description, distribution, key).

**Material examined.** Other material. 1 male, CHINA: Hainan, Mt. Diaoluoshan, 18°40'2.4"N, 109°54'32.09"E, 31.x–30.xi.2020, MT, Long-long Chen, SCAU 3042642 (SCBG); 1 male, CHINA: Hainan, Mt. Jianfengling, 18°41'42.37"N, 108°51'36.11"E, 688.01m, 30.iv–10.v.2020, MT, Chun-yang Xu, SCAU 3042643 (SCBG).

**Distribution.** Oriental region, China, Yunnan and Hainan Provinces.

### *Foenobethylus xinglongensis* Wang & Chen, sp. nov.

<http://zoobank.org/ABD5BAD9-35DB-4466-B782-94B367020F84>

Figures 4, 5

**Diagnosis. Male.** Head rectangular and elongate (Fig. 4B). Clypeus with median lobe obtuse rounded, median carina complete, reaching anterior clypeal margin, high, straight in lateral profile. Eye glabrous (Fig. 4B). Frons almost polished (Fig. 4B). Notaulus converging posteriorly, incomplete and shallow (Fig. 4C). Metapostnotal median carina incomplete, posterior third absent. Declivity of propodeum transversely

rugulose (Fig. 4D). Metatrochanter without spine (Fig. 5F). Metafemur with only one proximal acute spine in ventral midline,  $0.19\times$  as long as metafemoral width, touching apical margin of metatrochanter (Fig. 5F). Posterior hypopygeal margin strongly incurved, lateral lobe with conical protuberance (Fig. 5B). Basivolsella large,  $0.6\times$  as long as gonostipe, basal half about as wide as apical half, basal margin incurved (Fig. 5C, D).

**Description. Male holotype.** Body length 2.32 mm. Forewing length 1.67 mm.

**Colors.** Head, mesosoma (but pronotum and propleura castaneous), metasoma castaneous; base of scape, flagellomeres, apex of mandible, all coxae, all trochanter, all femora, basal half of all tibiae and claws pale castaneous; apex of scape, pedicel, base of mandible, palpi, protibia, apical half of all tibiae and tarsi yellow; wings subhyaline.

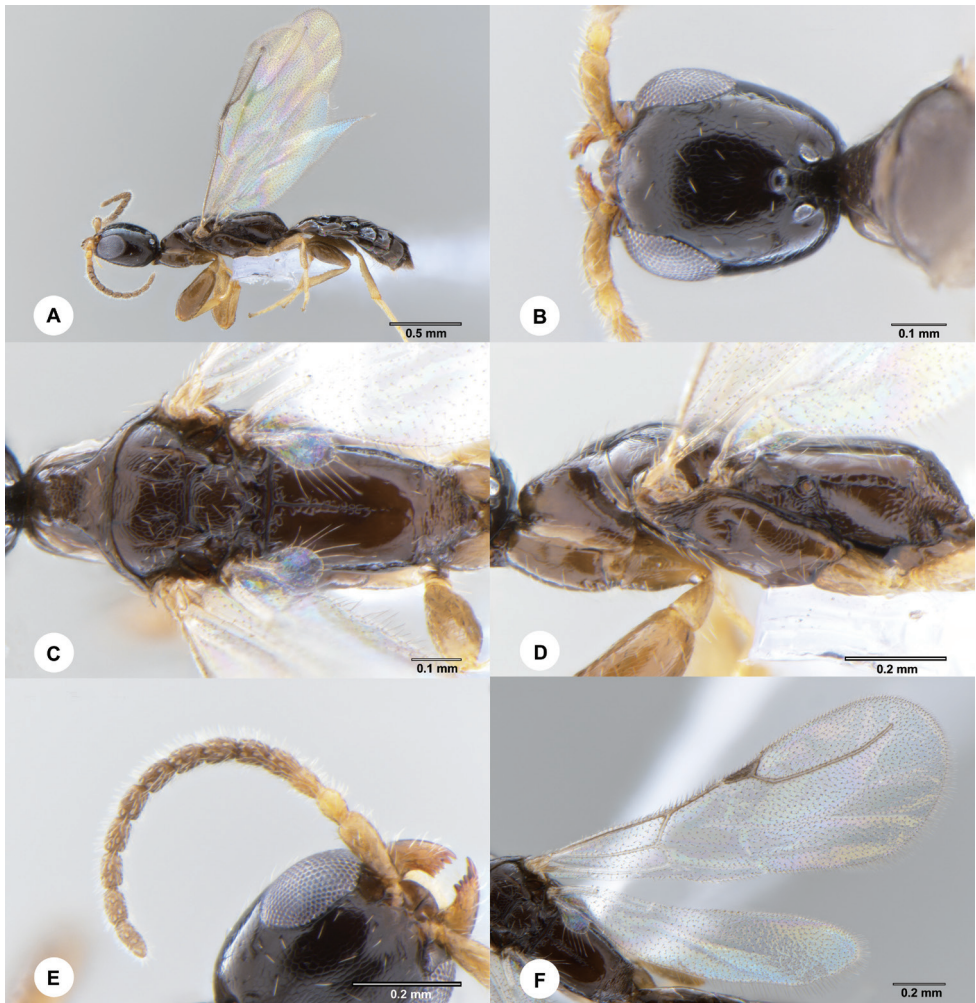


**Figure 4.** *Foenobethylus xinglongensis* Wang & Chen, sp. nov., male, holotype (SCAU 3042798) **A** lateral habitus **B** head, dorsal view **C** mesosoma, dorsal view **D** mesosoma, lateral view **E** antenna **F** wings.

**Head.** Head (Figs 4B, 5A) rectangular and elongate,  $1.2\times$  as long as wide. Mandible with five apical sharpened teeth, posterior tooth largest, middle three teeth smaller, anterior tooth smallest. Clypeus with median lobe obtuse rounded, median carina complete, reaching anterior clypeal margin, high, straight in lateral profile. Eye glabrous, almost touching mandible base at anterior corner. Malar space reduced. Frons very weakly coriaceous, almost polished, punctures very sparse and small. WH  $0.86\times$  LH. WF  $0.62\times$  WH. WF  $1.35\times$  HE. OOL  $1.19\times$  WOT. Frontal angle of ocellar triangle obtuse. Anterior ocellus far posterior to supra-ocular line. Temple divergent anterad, corner rounded. Vertex badly outcurved. First four antennomeres in ratio of about 35:15:14:13 (Fig. 4E). All flagellomeres distinctly longer than wide, pubescence erect, about  $0.63\times$  as long as flagellomeral width. Maxillary palpus with five palpomeres (Fig. 5A). Labial palpus with two palpomeres (Fig. 5A). Occipital carina complete. Medioccipito-genal carina complete. Hypostomal carina thick, almost straight, angled medially.

**Mesosoma** (Figs 4C, D, 5A). Mostly polished and weakly coriaceous. Pronotal flange short, exposing propleuron dorsally. Dorsal pronotal area short, without anterior carina strongly progressively narrowing anterad, lateral surface concave. Notaulus converging posteriorly, incomplete, shallow, faint, but progressively more evident posteriorly. Parapsidal signum almost straight, absent anteriorly, but wide and deep posteriorly. Mesoscutellum slightly shorter than anteromesoscutum. Mesoscutum-mesoscutellar sulcus deep, arched, sides wider than middle. Metanotum conspicuous, metascutellum wide and short, metanotal trough trabeculate, metanotal fovea outlined. Metapectal-propodeal disc polished, metapostnotal median carina incomplete, absent posteriorly, lateral and transverse posterior carinae complete; propodeal spiracle circular, located on lateral surface of propodeum, ventral to lateral carina. Propodeal declivity transversely rugulose, without median carina. Mesopleuron with mesopleural pit large and well defined. Pleurosternum small, triangular, with vertex directed posterad. Prepectus with epicnemial medial projection complete, posterior prepectal flange thick. **Wings** (Fig. 4F). Forewing with three closed cells (Costal, Radial and First Cubital); pterostigma about  $0.24\times$  as wide as long, anterior board outcurved; 2r-rs&Rs sector vein long; Rs&M reaching Sc+R far from pterostigma. Hind wing with one straight hamulus, and four distal hamuli equally distant, and strongly curved. **Legs.** Profemur swollen,  $2.4\times$  as long as wide, apical half of ventral margin serrulate. Metatrochanter (Fig. 5F) without spine. Metafemur (Fig. 5F) with only one proximal acute spine in ventral midline,  $0.19\times$  as long as metafemoral width, touching apical margin of metatrochanter.

**Metasoma.** Weakly longer than mesosoma. Seventh sternite (Fig. 5E) with posterior margin incurved at middle two fifths. Hypopygium (Fig. 5B) with spiculum about as long as median length of hypopygium, and  $1.5\times$  longer than anteromedial apodeme, latter slightly curved mesad apically; posterior margin strongly incurved, lateral lobe with conical protuberance. **Genitalia** (Fig. 5C, D). Harpe shorter than gonostipe; aedeagus wide,  $2.26\times$  as long as wide, apex aedeagus posterior to posterior margin of gonostipe,  $0.6\times$  as long as gonostipe; basivolsella large,  $0.6\times$  as long as gonostipe, basal half about as wide as apical half, basal margin incurved.



**Figure 5.** *Foenobethylus xinglongensis* Wang & Chen, sp. nov., male, **A, F** holotype (SCAU 3042798), **B–E** paratype (SCAU 3042638). **A** head and mesosoma, ventral view **B** subgenital plate **C** genitalia, dorsal view **D** genitalia, ventral view **E** 7<sup>th</sup> sternite **F** metaleg, lateral view.

**Variation.** Notauli are more well impressed; metapostnotal median carina slightly longer.

**Etymology.** The specific epithet refers to the locality (Xinglong Tropical Botanical Garden) where the type specimens were collected.

**Material examined.** *Holotype*, male, CHINA: Hainan, Wangning, Xinglong Tropical Botanical Garden, 18°44'24"N, 110°11'38"E, 30.i–30.ii.2021, MT, Zheng Wang, SCAU 3042798 (deposited in SCBG). *Paratypes*: 2 males. 1 male, CHINA:

Hainan, Wangning, Xinglong Tropical Botanical Garden, 18°43'52"N, 110°11'30"E, 18.vii–25.viii.2020, MT, Zheng Wang, SCAU 3042638 (SCBG); same data as holotype, but 9.vi–18.vii.2020, SCAU 3042656 (SCBG).

**Distribution.** Oriental region, China, Hainan Province.

**Remarks.** This new species is very similar to *F. sharkeyi* Savergnini & Azevedo [Thailand], but can be separated from the latter by the following characters: frons almost polished (coriaceous in *F. sharkeyi*); metapostnotal median carina incomplete, posterior third absent (complete in *F. sharkeyi*); declivity of propodeum transversely rugulose (areolate-rugose in *F. sharkeyi*); profemur 2.4× as long as wide (1.2–1.3× in *F. sharkeyi*).

***Foenobethylus yunkaishanensis* Chen & Luo, sp. nov.**

<http://zoobank.org/F57CCCF3-51B8-4137-82A4-55325A4C10B7>

Figures 6, 7

**Diagnosis. Male.** Head rectangular and elongate (Fig. 6B). Clypeus with median lobe truncate, median carina incomplete, not reaching anterior clypeal margin, but high and straight in lateral profile. Eye glabrous (Fig. 6B). Distance between posterior margin of compound eye and occipital carina longer than length of compound eye in dorsal view. Notaulus converging posteriorly, almost complete except the apex (Fig. 6C). Metatrochanter without spine (Fig. 7G). Metafemur with acute spine in ventral midline, proximal one 0.35× as long as metafemoral width, touching apical margin of metatrochanter, distal one 0.14× metafemoral width, located on basal two fifth of metafemur (Fig. 7G). Posterior hypopygeal margin strongly incurved, lateral lobe with conical protuberance (Fig. 7E). Basivolsella large, 0.6× as long as gonostipe, basal half distinctly wider than apical half, basal margin incurved (Fig. 7C, D).

**Description. Male holotype.** Body length 3.14 mm. Forewing length 2.08 mm.

**Colors.** Head, mesosoma, metasoma, base of scape, all flagellomeres, apical half of mesotibia and metatibia, all trochanter, and claws dark castaneous; apex of scape, pedicel, palpi, protibia, basal half of mesotibia and metatibia, and tarsi castaneous; wings subhyaline.

**Head.** Head (Figs 6B, 7A) rectangular and elongate, 1.2× as long as wide. Mandible with five apical sharpened teeth, posterior tooth largest, middle three teeth smaller, anterior tooth smallest. Clypeus with median lobe truncate, median carina incomplete, not reaching anterior clypeal margin, but high and straight in lateral profile. Eye glabrous, almost touching mandible base at anterior corner. Malar space reduced. Frons very weakly coriaceous, almost polished, punctures very sparse and small. WH 0.86× LH. WF 0.61× WH. WF 1.19× HE. OOL 1.20× WOT. Frontal angle of ocellar triangle obtuse. Anterior ocellus far posterior to supra-ocular line. Temple divergent anterad, corner rounded. Vertex badly outcurved. First four antennomeres in ratio of about 21:8:8:7 (Fig. 6E). All flagellomeres distinctly longer than wide, pubescence erect, about 0.67× as long as flagellomeral width. Maxillary palpus with five palpomeres (Fig. 7A). Labial palpus with two palpomeres (Fig. 7A). Occipital carina complete. Medioccipitogena carina complete. Hypostomal carina thick, almost straight, not angled medially.

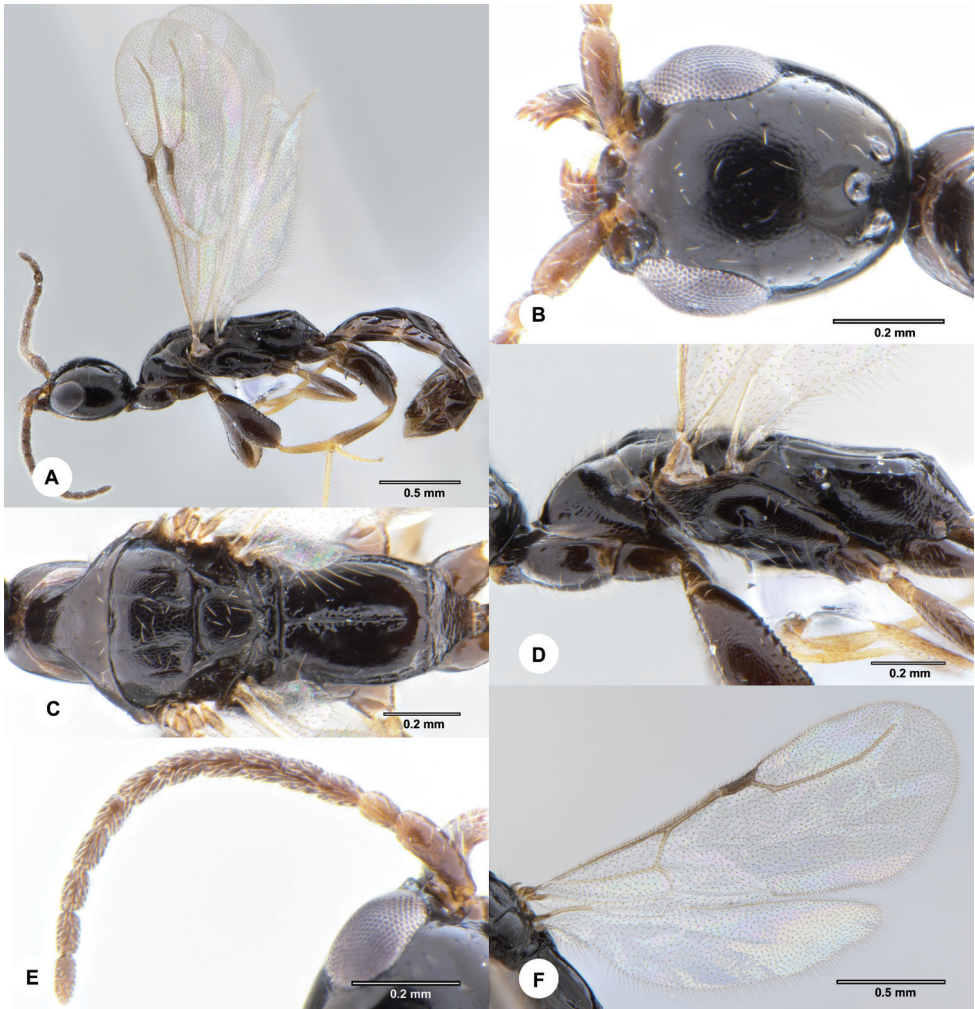


**Figure 6.** *Foenobethylus yunkaishanensis* Chen & Luo, sp. nov., male, holotype (SCAU 3048315) **A** lateral habitus **B** head, dorsal view **C** mesosoma, dorsal view **D** mesosoma, lateral view **E** antenna **F** wings.

*Mesosoma* (Figs 6C, D, 7B). Mostly polished and weakly coriaceous. Pronotal flange short, exposing propleuron dorsally. Dorsal pronotal area short, without anterior carina strongly progressively narrowing anterad, lateral surface concave. Notaulus converging posteriorly, almost complete except the apex, deep, distinct, and progressively more evident posteriorly. Parapsidal signum sinuous, absent anteriorly. Mesoscutellum shorter than anteromesoscutum. Mesoscutum-mesoscutellar sulcus deep, arched, sides wider than middle. Metanotum conspicuous, metascutellum wide and short, metanotal trough trabeculate, metanotal fovea outlined. Metapectal-propodeal disc polished, metapostnotal median carina incomplete, absent posteriorly, lateral and transverse posterior carinae complete; propodeal spiracle circular, located



**Figure 7.** *Foenobethylus yunkaishanensis* Chen & Luo, sp. nov., male **A, B, G** holotype (SCAU 3048315), **C–F** paratype (SCAU 3042639) **A** head, ventral view **B** mesosoma, ventral view **C** genitalia, dorsal view **D** genitalia, ventral view **E** subgenital plate **F** 7<sup>th</sup> sternite **G** metaleg, lateral view.

on lateral surface of propodeum, ventral to lateral carina. Propodeal declivity transverse sculptured, and without median carina. Mesopleuron with mesopleural pit large and well defined. Pleurosternum small, triangular, with vertex directed posterad. Prepectus with epicnemial medial projection complete, posterior prepectal flange thick. **Wings** (Fig. 6F). Forewing with three closed cells (Costal, Radial and First Cubital); pterostigma about 0.3× as wide as long, anterior board outcurved; 2r-rs&Rs sector vein long; Rs&M reaching Sc+R far from pterostigma. Hind wing with one straight hamulus, and four distal hamuli equally distant, and strongly curved. **Legs**. Profemur swollen, 2.6× as long as wide, apical half of ventral margin serrulate. Metatrochanter (Fig. 7G)

without spine. Metafemur (Fig. 7G) with acute spine in ventral midline, proximal one  $0.35\times$  as long as metafemoral width, touching apical margin of metatrochanter, distal one  $0.14\times$  metafemoral width, located on basal two fifth of metafemur.

**Metasoma.** Much longer than mesosoma. Seventh sternite (Fig. 7F) with posterior margin incurved at middle third. Hypopygium (Fig. 7E) with spiculum much longer than median length of hypopygium, and  $1.2\times$  longer than anteromedial apodeme, latter distinctly curved mesad apically; posterior margin strongly incurved, lateral lobe with conical protuberance. **Genitalia** (Fig. 7C, D). Harpe shorter than gonostipe; aedeagus wide,  $1.93\times$  as long as wide, apex aedeagus posterior to posterior margin of gonostipe,  $0.65\times$  as long as gonostipe; basivolsella large,  $0.6\times$  as long as gonostipe, basal half distinctly wider than apical half, basal margin incurved.

**Variation.** Body size maller and color lighter.

**Etymology.** The specific epithet refers to the locality (Mt. Yunkaishan) where the type specimens were collected.

**Material examined.** *Holotype*, male, CHINA: Guangdong Yunkaishan National Nature Reserve, 1480 m,  $22^{\circ}17'40.72''\text{N}$ ,  $111^{\circ}12'37.97''\text{E}$ , 29.v–4.vii.2020, MT, Long-long Chen, SCAU 3048315 (deposited in SCBG). *Paratypes*: 2 males. 1 male, CHINA: Guangdong Yunkaishan National Nature Reserve,  $22^{\circ}16'22.67''\text{N}$ ,  $111^{\circ}11'38.7''\text{E}$ , 30.vi–23.vii.2020, MT, Long-long Chen, SCAU 3042639 (SCBG); 1 male, CHINA: Guangdong Yunkaishan National Nature Reserve,  $22^{\circ}17'40''\text{N}$ ,  $111^{\circ}12'37.97''\text{E}$ , 1480 m, 9.v–4.vii.2020, MT, Long-long Chen, SCAU 3042658 (SCBG).

**Distribution.** Oriental region, China, Guangdong Province.

**Remarks.** This new species is very similar to *F. bidentatus* Várkonyi & Polaszek [Brunei, Thailand], but can be separated from the latter by the following characters: distance between posterior margin of compound eye and occipital carina longer length of compound eye in dorsal view (as long as in *F. bidentatus*); seventh sternum with distal margin strongly emarginated (narrowly emarginated in *F. bidentatus*); posterior margin of hypopygium strongly incurved (broadly and almost evenly emarginate in *F. bidentatus*).

### Key to males of *Foenobethylus*

- 1 Metatrochanter with one ventral spine or tooth ..... 2
- Metatrochanter without ventral spine or tooth..... 5
- 2 Metafemur with one long proximal spine,  $0.5\times$  as long as metafemur width .... 3
- Metafemur with one short proximal spine,  $0.6\times$  as long as metafemur width... 4
- 3 Pronotum with anterior horizontal flange medially very narrow; metatrochanter with one needle-like long spine ventrally; metafemur with a ventral oblique furrow ..... *F. emiliacasellae* Várkonyi & Polaszek
- Pronotum with anterior horizontal flange medially as broad as laterally; metatrochanter with one tooth or broad spine; metafemur ventrally flattened, without oblique furrow ..... *F. elongatus* Várkonyi & Polaszek

- 4 Hypopygium with posterior margin strongly concave, base of paramere with triangular protuberance on dorsal margin ..... *F. pyramidis* Savergnini & Azevedo
- Hypopygium with posterior margin weakly concave, base of paramere without triangular protuberance on dorsal margin ..... *F. thomascokeri* Várkonyi & Polaszek
- 5 Metafemur with one spine ..... 6
- Metafemur with two spines ..... 8
- 6 Middle of metafemur with one small, broad and dentate protuberance ventrally ..... *F. gracilis* Kieffer
- Middle of metafemur without protuberance ventrally ..... 7
- 7 Frons almost polished; metapostnotal median carina incomplete, posterior third absent; declivity of propodeum transversely rugulose ..... *F. xinglongensis* Wang & Chen, sp. nov.
- Frons coriaceous; metapostnotal median carina complete; declivity of propodeum areolate-rugose ..... *F. sharkeyi* Savergnini & Azevedo
- 8 Proximal spine locates at basal 1/3 of metafemora and close to distal spine, and tips of two spines slightly convergent ..... 9
- Proximal spine locates on very base of metafemora and distantly separated from distal spine, and tips of two spines almost parallel ..... 10
- 9 Aedeagus wide, 2.0× as long as wide ..... *F. hainanensis* Liu, Chen & Xu
- Aedeagus narrower, 1.2× as long as wide ..... *F. thaianus* (Terayama)
- 10 Distal spine locates before midpoint of metafemora and close to proximal spine ..... 11
- Distal spine locates at or after midpoint of metafemora and distantly separated from proximal spine ..... 12
- 11 Distance between posterior margin of compound eye and occipital carina as long as length of compound eye in dorsal view; seventh sternum with distal margin narrowly emarginated; posterior margin of hypopygium broadly and almost evenly emarginate ..... *F. bidentatus* Várkonyi & Polaszek
- Distance between posterior margin of compound eye and occipital carina longer than length of compound eye in dorsal view; seventh sternum with distal margin strongly emarginated; posterior margin of hypopygium strongly incurved ..... *F. yunkaishanensis* Chen & Luo, sp. nov.
- 12 Distal spine obtuse ..... 13
- Distal spine acute ..... *F. syndesis* Chen & Azevedo
- 13 Lateral lobe of hypopygium without conical protuberance; propodeum polished; pterostigma broad, about 0.4× as wide as long ..... *F. robusta* Li & Chen, sp. nov.
- Lateral lobe of hypopygium with conical protuberance; propodeum coriaceous, areas along metapostnotal median carina rugose; pterostigma relatively slender, about 0.3× as wide as long ..... *F. zhejiangensis* Liu, Chen & Xu

## Discussion

Based on a preliminary phylogenetic analysis using morphological data, Várkonyi and Polaszek (2007) first assigned *Foenobethylus* to the subfamily Pristocerinae. However, the phylogenetic position of *Foenobethylus* within Pristocerinae was still unclear in their study. According to Azevedo and Lanes (2007), *Afgoiogfa*, *Foenobethylus* and *Parascleroderma* are closely related genera. However, currently no molecular sequences of *Afgoiogfa* are available for phylogenetic analysis. From the results of Alencar et al. (2018), the clade of *Foenobethylus* + *Parascleroderma* + *Cleistopyris* was recovered as the sister-group of *Apenesia*. In the light of the first discovery of *Foenobethylus* female, Chen and Azevedo (2020) suggested that *Foenobethylus* might be a synonym under *Parascleroderma* due the extreme similarity they share in females. *Foenobethylus* also shares some similar characters with *Apenesia* and *Dissomphalus* (Chen and Azevedo 2020), although *Dissomphalus* was never found close to *Foenobethylus* in any phylogenetic analyses (Alencar et al. 2018). The molecular data seem to support the relatedness between *Foenobethylus* and *Parascleroderma*, as suggested by their similar morphology. In the present study, all of the five studied *Foenobethylus* species form a monophyletic clade, with *Parascleroderma* as a sister group (Fig. 1). This result is congruent with that of Alencar et al. (2018), in which *Parascleroderma* is sister to *Foenobethylus*. The intergeneric distances between *Foenobethylus* and *Parascleroderma* ranged between 14.8–18.6%, generally higher than interspecific distances within *Foenobethylus*. This high genetic distance suggests that *Foenobethylus* is likely a distinct genus, as similar intergeneric distances have been found in Epyrinae of Bethylinidae (Colombo et al. 2020). However, given that the two *Parascleroderma* species together with all the *Foenobethylus* also form a monophyletic group in this study, the possibility that these two genera are synonymous cannot be ruled out. The precise taxonomic delimitation of both genera could be resolved by accumulating molecular data of more *Parascleroderma* taxa for phylogenetic analyses.

The relatively high interspecific genetic distances (10.3%–13.6%) indicate that the use of DNA barcoding for delimitating morphologically similar species of *Foenobethylus* may be promising. For example, *F. robusta* is very similar to *F. syndesis*, but the genetic distance between them is up to 11.3% and they are well supported as different species. Future comprehensive taxon sampling and molecular analyses should be able to test the power of DNA barcoding in delimitating morphologically similar species.

With the three newly described species, the total number of *Foenobethylus* is raised from 11 to 14 (Table 3). Species of *Foenobethylus* mainly occur in tropical forests (Savergnini and Azevedo 2013). All of the three new species described in this study were also collected in tropical or subtropical forests, indicating that species diversity of *Foenobethylus* from tropical and subtropical forests of Southeast Asia is still undersampled and intensive study is required. The wingless feature of the females allows these parasitoids to adapt to the restricted environments such as tunnels under the tree bark, where the females look for preys (Chen and Azevedo 2020). However, the host of *Foenobethylus* species is still unknown. As other members of Pristocerinae,

**Table 3.** List of the world species of *Foenobethylus* (updated from Chen and Azevedo 2020).

Species	Distribution	
	Country	Region
<i>F. bidentatus</i> Várkonyi & Polaszek, 2007	Brunei, Thailand	Oriental
<i>F. elongatus</i> Várkonyi & Polaszek, 2007	Malaysia, Indonesia	Oriental
<i>F. emiliacasellae</i> Várkonyi & Polaszek, 2007	Thailand	Oriental
<i>F. gracilis</i> Kieffer, 1913	Philippines, Thailand	Oriental
<i>F. hainanensis</i> Liu, Chen & Xu, 2011	China	Oriental
<i>F. pyramidis</i> Savernini & Azevedo, 2013	Thailand	Oriental
<i>F. robusta</i> Li & Chen, sp. nov.	China	Oriental
<i>F. sharkeyi</i> Savernini & Azevedo, 2013	Thailand	Oriental
<i>F. syndesis</i> Chen & Azevedo, 2020	China	Oriental
<i>F. thaianus</i> (Terayama, 1998)	Thailand	Oriental
<i>F. thomascokeri</i> Várkonyi & Polaszek, 2007	Malaysia, Thailand	Oriental
<i>F. xinglongensis</i> Wang & Chen, sp. nov.	China	Oriental
<i>F. yunkaishanensis</i> Chen & Luo, sp. nov.	China	Oriental
<i>F. zhejiangensis</i> Liu, Chen & Xu, 2011	China	Oriental

species of *Foenobethylus* are likely ectoparasitoids of beetle larvae in concealed habitat (Terayama 2006). Searching for wood boring beetle larvae in tropical and subtropical forests should be a promising direction in finding the hosts of these parasitoids.

## Acknowledgements

Thanks to Dr. Yan-Qiong Peng (Xishuangbanna Tropical Botanical Garden, Chinese Academy of Sciences) for providing some of the fresh specimens. We thank the subject editor Dr. Michael Ohl and the two reviewers, Dr. Colombo and Dr. Azevedo for their valuable suggestions. This material is based upon work supported in part by the Program of Ministry of Science and Technology of China (2018FY100406), the Foundation of Chengdu Normal University Talent Introduction Research Funding (YJRC202009, No. 111/111158701), and the Agricultural Ecology and Green Food Development Project (CSCXTD2020B11).

## References

- Alencar IDCC, Waichert C, Azevedo CO (2018) Opening Pandora's box of *Pristocerinae*: molecular and morphological phylogenies of *Apenesia* (Hymenoptera, Bethyridae) reveal several hidden genera. *Systematic Entomology* 43: 481–509. <https://doi.org/10.1111/syen.12295>
- Azevedo CO, Lanes GO (2007) Rediscovery of Oriental *Foenobethylus* Kieffer, 1913 with discussion of allied genus (Hymenoptera, Bethyridae). *Mittelugen des Internationalen Entomologischen Vereins* 32: 133–141.
- Brito CD, Lanes GO, Azevedo CO (2021) Anatomic glossary of mesopleural structures in Bethyridae (Hymenoptera: Chrysidoidea). *Papéis Avulsos de Zoologia* v.61: e20216152. <http://doi.org/10.11606/1807-0205/2021.61.52>

- Chen HY, Azevedo CO (2020) Discovery of a couple of *Foenobethylus* (Hymenoptera, Bethylidae) in copulation suggests a synonym under *Parascleroderma*. *Journal of Asia-Pacific Entomology* 23: 1241–1247. <https://doi.org/10.1016/j.aspen.2020.10.001>
- Colombo WD, Waichert C, Azevedo CO (2020) Molecular and morphological species delimitation of Epyrinae (Hymenoptera: Bethylidae) from Papua New Guinea. In: Robillard T, Legendre F, Villemant C, Leponce M (Eds) *Insects of Mount Wilhelm, Papua New Guinea – volume 2*. Muséum national d'Histoire naturelle, Paris, 209–319.
- Folmer O, Black M, Hoch W, Lutz R, Vrijenoek R (1994) DNA primers for amplification of mitochondrial cytochrome c oxidase subunit I from diverse metazoan invertebrates. *Molecular Marine Biology and Biotechnology* 3: 294–299.
- Gillespie JJ, Munro JB, Heraty JM, Yoder MJ, Owen AK, Carmichael AE (2005) A Secondary Structural Model of the 28S rRNA Expansion Segments D2 and D3 for Chalcidoid Wasps (Hymenoptera: Chalcidoidea). *Molecular Biology and Evolution* 22: 1593–1608. <https://doi.org/10.1093/molbev/msi152>
- Harris RA (1979) A glossary of surface sculpturing. *Occasional Papers in Entomology* 28: 1–31. <https://doi.org/10.1371/journal.pone.0140051>
- Katoh K, Standley DM (2013) MAFFT multiple sequence alignment software version 7: Improvements in performance and usability. *Molecular Biology and Evolution* 30: 772–780. <https://doi.org/10.1093/molbev/mst010>
- Kumar S, Stecher G, Tamura K (2016) MEGA7: Molecular evolutionary genetics analysis version 7.0 for bigger datasets. *Molecular Biology and Evolution* 33: 1870–1874. <https://doi.org/10.1093/molbev/msw054>
- Lanes GO, Kawada R, Azevedo CO, Brothers D (2020) Revisited morphology applied for Systematic of flat wasps (Hymenoptera, Bethylidae). *Zootaxa* 4752(1): 1–127. <https://doi.org/10.11646/zootaxa.4752.1.1>
- Liu J, Chen H, Xu Z (2011) Two new species of genus *Foenobethylus* Kieffer, 1913 (Hymenoptera, Bethylidae) from China with a key to the known species. *Zootaxa* 2806: 53–59. <https://doi.org/10.11646/zootaxa.2806.1.4>
- Savergnini JR, Azevedo CO (2013) Taxonomy of *Foenobethylus* Kieffer (Hymenoptera, Bethylidae) with description of two new species. *Journal of Asia-Pacific Entomology* 16: 433–441. <https://doi.org/10.1016/j.aspen.2013.06.004>
- Taekul C, Valerio AA, Austin AD, Klompen H, Johnson NF (2014) Molecular phylogeny of telenomine egg parasitoids (Hymenoptera: Platygasteridae s.l.: Telenominae): evolution of host shifts and implications for classification. *Systematic Entomology* 39: 24–35. <https://doi.org/10.1111/syen.12032>
- Terayama M (2006) *The Insects of Japan. Vol. I, Bethylidae* (Hymenoptera). Fukuoka, (Japan): Entomological Society of Japan, 319 pp.
- Várkonyi G, Polaszek A (2007) Rediscovery and revision of *Foenobethylus* Kieffer, 1913 (Hymenoptera, Bethylidae). *Zootaxa* 1546: 1–14. <https://doi.org/10.11646/zootaxa.1546.1.1>

# Contribution to the taxonomy, bionomics and distribution of the Palaearctic *Celonites cyprius*-group (Hymenoptera, Vespidae, Masarinae) with the description of two new species from the North Caucasus and East Anatolia

Volker Mauss<sup>1</sup>, Alexander V. Fateryga<sup>2</sup>, Erol Yildirim<sup>3</sup>, James M. Carpenter<sup>4</sup>

**1** Stuttgart State Museum of Natural History, Entomology Department, Rosenstein 1, D-70191 Stuttgart, Germany **2** T.I. Vjazemsky Karadag Scientific Station, Nature Reserve of RAS, Branch of A.O. Kovalevsky Institute of Biology of the Southern Seas of RAS, Nauki Str. 24, Kurortnoye, 298188 Feodosiya, Russia **3** Atatürk University, Faculty of Agriculture, Department of Plant Protection, TK 25240 Erzurum, Turkey **4** Division of Invertebrate Zoology, American Museum of Natural History, Central Park West at 79<sup>th</sup> street, New York, NY 10024, USA

Corresponding author: Volker Mauss ([volker.mauss@gmx.de](mailto:volker.mauss@gmx.de))

Academic editor: Michael Ohl | Received 27 December 2021 | Accepted 24 January 2022 | Published 28 February 2022

<http://zoobank.org/6FA46014-BC04-4A27-9F49-B4437925DE4E>

**Citation:** Mauss V, Fateryga AV, Yildirim E, Carpenter JM (2022) Contribution to the taxonomy, bionomics and distribution of the Palaearctic *Celonites cyprius*-group (Hymenoptera, Vespidae, Masarinae) with the description of two new species from the North Caucasus and East Anatolia. Journal of Hymenoptera Research 89: 109–155. <https://doi.org/10.3897/jhr.89.79832>

## Abstract

*Celonites ivanovi* sp. nov. is described as a new species from Dagestan where it has been recorded from dry habitats in a small area on the northern side of the Greater Caucasus. *Celonites cagrii* sp. nov. is described from Erzurum Province in east Turkey. As in other members of the *C. cyprius*-group, the females of both species were observed to visit flowers of *Heliotropium* (Boraginaceae). A morphological examination including the male genitalia of all species of the *C. cyprius*-group revealed that *C. ivanovi* sp. nov. and *C. cagrii* sp. nov. share the apomorphic characters of this group and are closely related to *Celonites osseus* Morawitz, 1888. Mean genetic distance between *C. ivanovi* sp. nov. and *C. cagrii* sp. nov. based on COI-5 sequences is 7.40%. The geographical distribution of all members of the *C. cyprius*-group is summarized and an illustrated key is provided for the identification of males and females of the species. A lectotype is designated for *C. osseus*.

## Keywords

Boraginaceae, distribution, flower visiting behaviour, *Heliotropium*, key to species, male genitalia, Palaearctic region, taxonomy, trophic relationships

## Introduction

The pollen wasp genus *Celonites* Latreille, 1802 forms a well defined monophylum (Carpenter 1993; Krenn et al. 2002) whose members share a number of distinctive characters such as the wide horizontal lamellae on the propodeum, the acute sides of the metasoma and the ability to roll up (Richards 1962; Gess and Gess 2010). The biogeographical distribution of *Celonites* is disjunct with 21 species occurring in the semi-arid to arid areas in the southwest of the Afrotropical region (Gess and Gess 2010) and approximately 42 species in the Palaearctic and adjacent dry areas in the north of the Afrotropical and Oriental region (according to the list of Carpenter 2001, combined with newly described or synonymized species by Gusenleitner 2002, 2007, 2012, 2018; Mauss 2013; Mauss et al. 2016; Mauss and Prosi 2018). Among the Palaearctic taxa of *Celonites* the subgenus *Eucelonites* Richards, 1962 is characterised by a small laterally directed process of the axilla which lies on the tegula or even fits into a slight emargination of the tegula opposite to the projection (Richards 1962). This unique apomorphy defines *Eucelonites* as a monophyletic group (Carpenter 2001; note that the nominate subgenus is evidently paraphyletic). Up till now 26 species and nine additional subspecies were assigned to this monophylum indicating high diversity. However, many of these taxa were described from small type series often containing only one sex and the last summarizing key provided by Richards (1962) left out several rarely collected species from the Middle East and Central Asia. Therefore, the identity and status of some described *Eucelonites* taxa is still uncertain and species identification can be difficult. Within *Eucelonites*, *Celonites cyprius* Saussure, 1854 and its closer relatives form a distinct group which is characterized by male genitalia with distally tapering more or less spatula-like harpides, the medial and lateral margin of which are partly raised ventrally in addition (Figs 12, 13). We suggest naming this group the *Celonites cyprius*-group.

The purpose of the present paper is to describe two new species of *Celonites* belonging to the *C. cyprius*-group from the Republic of Dagestan, Russia, and Erzurum Province in East Anatolia, Turkey, as well as to summarize taxonomic and chorological data on the related taxa and to provide a key for their identification.

## Materials and methods

Field investigations of the hitherto unknown *Celonites ivanovi* sp. nov. were made by A. Fateryga on 23 June 2018 in the vicinity of Maydanskoye in the Untsukul'skiy district of the Republic of Dagestan, Russia [locality 1: 42°37'36"N, 46°56'48"E], where 3 females were observed and 2 females were collected, and on 11 June 2019, 15 and 16 June 2021 at a second site in the vicinity of Maydanskoye, 3 km to the southeast of the first locality [locality 2: 42°36'07"N, 46°58'13"E], where numerous females and males were observed and 17 females and 10 males were collected. Wasp activity and

flower visiting behaviour were observed with the naked eye for approximately one hour in the morning of 11 June 2019 and documented with a Canon PowerShot SX160 IS camera. The pictures were compared to single frames of video sequences of *C. cyprius* and *C. rugiceps* Bischoff, 1928 visiting *Heliotropium* flowers in Rhodes (taken with a Canon EOS 80D, 50 frames per second, scale up to 1:1, Mauss et al. in prep.). Flower preferences of the wasps were studied by counting the number of sightings (= first observations) of flower visiting individuals while walking randomly across the locality. A single female was recorded on 22 June 2021 in the vicinity of Turtsi in the Lakskiy district [locality 3: 42°11'34"N, 47°09'33"E]. Field observations of *Celonites cagrii* sp. nov. were made by E. Yildirim at Şenkaya-Akşar in the Erzurum province of Turkey on 12 July, 14 July and 1 August 2020. For identification of the collected *Heliotropium* plants the keys provided by Grossheim (1967) and Dönmez (2008) were used.

For the morphological and chorological investigations in total 479 dry specimens of the *Celonites cyprius*-group were examined from the following collections: Museum of Zoology Lausanne, Switzerland (**MCZL**), Museum of Natural History Mainz, Germany (**NHM**), Natural History Museum of Venice, Italy (**MSNVE**), Upper Austrian State Museum – Biology Centre, Linz, Austria (**OLML**), State Museum of Natural History Karlsruhe, Germany (**SMNK**), Stuttgart State Museum of Natural History, Germany (**SMNS**), Zoological Institute of the Russian Academy of Sciences, Saint Petersburg, Russia (**ZISP**), Zoological Museum of the M.V. Lomonosov Moscow State University, Russia (**ZMMU**), as well as the private collections of A.V. Fateryga stored in the T.I. Vyazemsky Karadag Scientific Station – Nature Reserve of RAS – Branch of A.O. Kovalevsky Institute of Biology of the Southern Seas of RAS, Feodosia, Russia (**AF**), J. Gusenleitner, Linz, Austria (**JG**), V. Mauss, Michelfeld, Germany (**VM**), M. Schindler, Bonn, Germany (**MS**), C. Schmid-Egger, Berlin, Germany (**CSE**) and E. Yildirim, Erzurum, Turkey (**EY**) (Suppl. material 1: Table S1). Every specimen examined by V. Mauss was labelled with an individual, serial database number (**dbM** = database Mauss) printed on the determination label. The holotypes were deposited in OLML, paratypes in American Museum of Natural History (**AMNH**), OLML, ZISP, AF, VM and EY.

Specimens were investigated under a WILD M3 stereo microscope (maximum magnification 80 times). Numbers of terga and sterna apply to metasomal segments. Antennal articles are termed A1–A12 counted from the proximal to the distal end. Nomenclature of male genitalia follows that of Birket-Smith (1981). Measurements of the exoskeleton were made using an ocular micrometer (highest resolution 0.011 mm; microscope in monaxial position). Distances between the ocelli, the compound eyes and the mesonotum width were measured according to Eck (1978). Proportion of head width to head length in the key was calculated from measurements of the maximum distance between the lateral margins of the compound eyes and the distance in the median axis between the bottom of the ventral emargination of the clypeus and the dorsal end of the median ocellus, while the head was aligned with dorsal and median part of ventral margin of the clypeus in focus plane and the lateral margins of

the compound eyes in symmetrical distance to the median axis. Drawings were made with a drawing tube (WILD Type 308700) in monaxial position. For drawings of the postero-lateral part of the propodeum the metasoma was removed from the specimens. The postero-lateral part of the propodeum was viewed from dorso-posterior with the dorso-anterior border of the pronotum becoming just visible anteriorly, so that the dorsal area of the pronotum was visible at a flat angle, while the apical ends of the postero-lateral processes were orientated exactly transversal. Male genitalia were removed after resoftening of the specimens and studied in 80% ethanol or glycerine. Macrophotos of whole specimens were taken with a Canon EOS 80D camera with a 100 mm macro-lens and extension tube (scale more than 1:1, resolution 24 mega pixel) and macro flash-lights. Microphotos were taken with a Keyence VHX-5000 Digital Microscope (combined stacking and stitching). Photographs of the lectotype of *C. osseus* Morawitz, 1888 were taken in ZISP with a Canon EOS 70D camera mounted on an Olympus SZX10 stereomicroscope. Multifocus-pictures were generated with Helicon Focus 6 Pro software. Final illustrations were post-processed for sharpness, contrast, and brightness using Adobe Photoshop CS2 software.

DNA barcoding was accomplished by AIM Advanced Identification Methods GmbH Leipzig following standard methods of DNA extraction from a single leg of dry specimens or specimens collected and stored in 96% pure ethanol, PCR for Cytochrome Oxidase subunit 1 (COI-5P), cycle sequencing of forward and reverse strand and sequence editing. Nucleotide sequences of ten individuals from four taxa of the *C. cyprius*-group were obtained uploaded and compared to the BOLD database ([www.BOLDsystem.org](http://www.BOLDsystem.org)). Another eight COI-5P sequences of three taxa of the *C. cyprius*-group were obtained from the BCHYM- and GBACU-project by courtesy of Christian Schmid-Egger and Stefan Schmidt and added to the data set. Finally genetic distances (Kimura 2 Parameter) and a neighbour joining BOLD TaxonID Tree were computed including 18 COI-5P sequences of morphologically identified specimens of *C. cagrii* sp. nov., *C. cyprius*, *C. ivanovi* sp. nov., *C. rugiceps* and *C. yemenensis* Giordani Soika, 1957 using the following parameters: distance model Kimura 2 Parameter; pairwise deletion of positions containing gaps and missing data; minimum complete overlap 100 bp; alignment with BOLD Aligner (Amino Acid based HMM); individual nucleotide sequence length 557–699 bp.

For the investigation of the geographic distribution label information of 479 specimens of the *C. cyprius*-group coming from 114 localities was entered into the database Mauss (Suppl. material 1: Table S1). Additionally, 55 published records were taken from Bischoff (1928), Blüthgen (1952), Bytinsky-Salz and Gusenleitner (1971), Carpenter (2001), Ebrahimi and Carpenter (2008), Giordani Soika (1957), Gusenleitner (1966, 1973, 1997, 2005, 2010), Richards (1962, 1984) and Schmid-Egger (2017) (Suppl. material 1: Table S1). If not given on the label or in the publication, WGS 84 coordinates were reconstructed mainly with the aid of Google Maps ([www.google.de/maps](http://www.google.de/maps)). The distribution map was created with Natural Earth ([www.naturalearthdata.com](http://www.naturalearthdata.com)) using the open-source geographic information system QGIS, version 3.4 ([www.qgis.org](http://www.qgis.org)).

## Systematics

### *Celonites osseus* Morawitz, 1888

*Celonites osseus* Morawitz, 1888: 268–269, ♀, type locality: “territorio transcaspico (Tschikischljar) [Turkmenistan]”, **lectotype (designated here)**: ♀, <golden disc>, “Tschikischljar. Pom.[eranzev]”, “*Celonites osseus* ♀. F. Moraw.”, “к. Ф Моравица [coll. F Morawitz]”, “Lectotypus ♀ *Celonites osseus* Morawitz des. Fateryga, 2018 <red label>” ZISP (Fig. 3a–c); Kostylev, 1935: 114, Turkestan, Transcaspian sands, Armenia; Richards, 1962: 216 (key), 226–227, Turkmenistan (Repetek), misidentification of *Celonites crenulatus* Morawitz, 1888 not *C. osseus*; Carpenter, 2001: 11, Armenia, Turkmenistan.

**Additional material studied.** **Armenia:** Zanga [currently Hrazdan] River, near Yerevan, 19.07.1935 1♀ (dbM 5855) leg. G. Kostylev ZMMU; Yerevan, Nork [=Nor Nork], 23.06.1930 1♀ leg. A. Shelkovnikov ZISP. **Turkmenistan, Balkan region:** Krasnovodsk [currently Türkmenbaşy], 13.06.1928 1♀ leg. V. Gussakovskij ZISP, 16.06.1928 1♂ leg. V. Gussakovskij ZISP; Jebel, 25 km NW Balkanabat, 22.05.1993 1♂ (dbM 5521) leg. M. Halada OLML. **Iran:** Elburz, 30 km S of Ab Ali, 09.07.1965 1♀ (dbM 5788) leg. Giordani Soika & Mavromoustakis MSNVE; Elburz, Vana 50 km N di Ab Ali, 12–13.07.1965 10♀♀ (dbM 5676, 5677, 5678, 5780, 5781, 5782, 5783, 5784, 5785, 5786) leg. Giordani Soika & Mavromoustakis MSNVE; Elburz (Mazandaran), Pulour [=Polour] 22 km N of Ab Ali, 13–14.07.1965 1♀ (dbM 5787) leg. Giordani Soika & Mavromoustakis MSNVE; Fars, Daria Namak, steppe presso lago salato 27 km E Shiraz, 07.07.1965 3♀♀ (dbM 5679, 5778, 5779) leg. Giordani Soika & Mavromoustakis MSNVE; Fars prov., 20 km E Kazarun, 29°33.034'N, 51°49.416'E, 1256 m, 14.06.2019 1♂ leg. V.M. Gnezdilov ZISP; Golestan prov., 70 km E Minudasht, 1050 m, 12.06.2010 1♀ (dbM 4617) leg. M. Halada OLML; Teheran, Steppa presso Chitgar, 18 km W di Teheran, 15.07.1965, 1♀ (dbM 5675) leg. Giordani Soika & Mavromoustakis MSNVE.

**Taxonomic remarks.** The identity of *C. osseus* was probably not clear to O.W. Richards, since in his key and in his description of the species he emphasizes that the dorsal area of the mesoscutum has smooth shining interstices at least as wide as the punctures, which is clearly inconsistent with the original description of Morawitz (1888: 269), and that the metasomal terga II–V are not at all crenulated (Richards 1962: 216, 227). Moreover, the measurements given by him for the length of body and fore-wing seem to be too large to represent *C. osseus*. His description was based on a single female from Repetek collected on 7 June 1937 by G. Kostylev placed in ZMMU and determined by Kostylev as *C. osseus* (Richards 1962: 227). However, this particular specimen is lacking in the ZMMU, but there is another female (dbM 5854) from Repetek collected on 9 June 1937 labelled by Kostylev as *C. osseus*, which is clearly misidentified and belongs to *Celonites crenulatus* Morawitz, 1888 or an undescribed taxon close to it. The description of *C. osseus* given by Richards (1962: 226–227) is

almost identical with the characters of this misidentified specimen. Moreover, there is a series of seven correctly identified males of *C. crenulatus* in the collection of the ZMMU collected on 1 and 9 June 1937 at Repetek by G. Kostylev, while genuine specimens of *C. osseus* are lacking from this locality. Obviously, Kostylev misinterpreted two females of his *C. crenulatus* series with weak crenulation on the metasomal terga as *C. osseus*. Almost certainly, Richards investigated one of these wrongly identified specimens (maybe it was given to him, because it was the only duplicate specimen identified as *C. osseus* in the collection of the ZMMU) and finally based his description on it. As a consequence, the key and the description provided by Richards (1962) cannot be used for the identification of *C. osseus*.

**Distribution.** Armenia, Turkmenistan, Iran (new record) (Fig. 17).

**Bionomics.** Unknown.



**Figure 1.** Imagines of the *C. cyprius*-group in lateral view, proboscis protruded (*C. rugiceps* female dbM 5447 male dbM 5450, *C. cyprius* female dbM 5428 male dbM 5434).

***Celonites cagrii* Mauss & Yildirim, sp. nov.**

<http://zoobank.org/36232674-C53A-462F-8FFA-B47D84ACC4DF>

**Holotype.** ♀ (dbM 5610) “[Turkey] TR-Erzurum Şenkaya-Akşar [40.648262°N, 42.342351°E] 14.VII.2020-1275 m Leg. E. Yildirim [on *Heliotropium ellipticum* Ledeb.]” OLML, BOLD process ID CECYP006-20.

**Paratypes.** “[Turkey] TR-Erzurum Şenkaya-Akşar [40.648262°N, 42.342351°E] 20.VIII.2011-1275 m Leg. E. Yildirim” 1♀ (dbM 4574) EY; “[Turkey] TR-Erzurum Şenkaya-Akşar [40.648262°N, 42.342351°E] 12.VII.2020-1275 m Leg. E. Yildirim [on *Heliotropium ellipticum* Ledeb.]” 3♀ (dbM 5607, 5608 (BOLD process ID CECYP005-20), 5609) VM; “[Turkey] TR-Erzurum Şenkaya-Akşar [40.648262°N, 42.342351°E] 01.VIII.2020-1275 m Leg. E. Yildirim [on *Heliotropium ellipticum* Ledeb.]” 1♀ (dbM 5616) AMNH, 1♂ (dbM 5619) 3♀ (dbM 5611, 5612, 5615) VM, 4♀ (dbM 5613, 5614, 5617, 5618) EY; “ARMENIA Erevan Monti desertici Aighepat 40 Km. SE 23-VII-63 [leg. Giordani Soika]” 2♂♂ (dbM 5789, 5790) MSNVE.

**Diagnosis.** See key.

**Description. Female.** Colour (Figs 2, 4f): Black. The following are light yellowish-white: rectangular spot dorso-medial on clypeus; large spot on each ocular sinus dorso-medially extending over lateral part of frons; medium-sized spot on antero-dorsal angle of pronotum (humeral spot); broad stripe along dorso-medial (inner) margin of pronotum, anteriorly somewhat angularly enlarged with little median dent; small irregular postero-medial spot on mesoscutum; large spot on dorsal mesepisternum; laterally directed process of axilla; medium-sized narrow transversal spot postero-medial on scutellum; dorsal and ventral side of propodeal lamella; antero-lateral one-fifth and posterior two-fifth of tegula, interrupted by brownish translucent area on bulge; posterior band on tergum I occupying whole of sides but less than half of middle part, somewhat widened anteriorly in median axis, anteriorly with small brownish tinge towards adjacent black area; laterally and medially widened posterior bands on terga II–V, anteriorly with small brownish tinge towards adjacent black area, interrupted on each side of middle by blackish area; two weak minute little spots [medial on tergum VI; outside of distal tips of fore-, mid- and hind-femora; outside of proximal third to half of fore-, mid- and hind-tibia and little marking on outside at distal end of mid-, and hind-tibia. Brown are: distal half of mandible; maxillary and labial palpi, protrudeable parts of proboscis; ventral margin of labrum; postero-lateral margin of scutellum; median third of metanotum; postero-lateral process of propodeum; humeral plate; posterior translucent margin of tergum VI; tarsi; sterna I–V, posterior margin of sterna II–V translucent. Antenna black except: yellowish white markings medial on A4–A7 and proximal part of A8; brown-suffused area ventral on A10–A11. Wings moderately infusate, pterostigma blackish-brown, veins blackish-brown becoming somewhat lighter at base.

Variation (number of differing specimens in brackets): Light yellowish-white markings: spot on each ocular sinus dorso-medially separated from spot on lateral part of frons (1); frons with two isolated little (4) or medium-sized (2) spots above antennal sockets, or both spots above antennal sockets large and dorso-laterally fused with

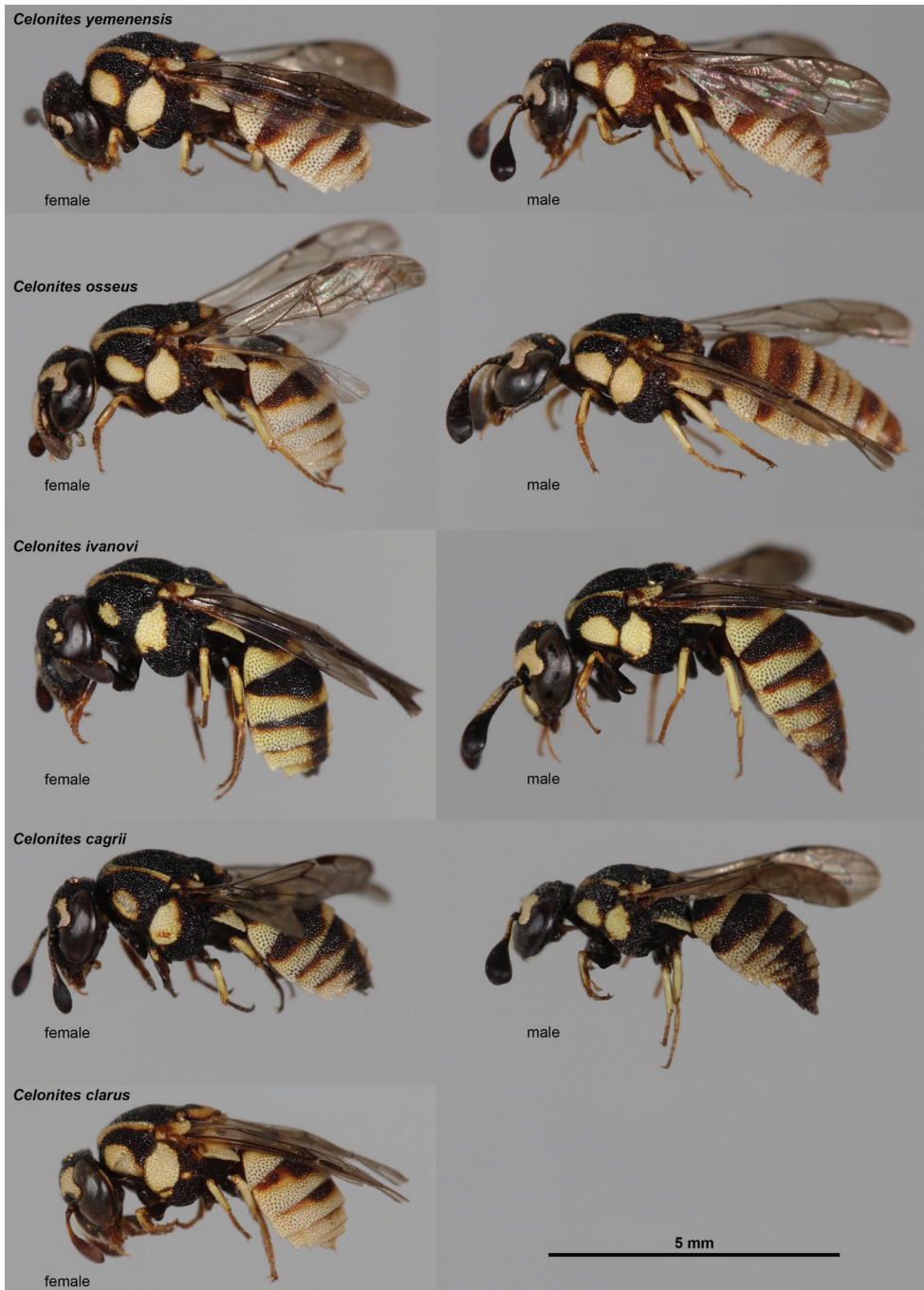


**Figure 2.** Imagines of the *C. cyprius*-group in lateral view, proboscis retracted (*C. yemenensis* female dbM 4944 male dbM 4945, *C. osseus* female dbM 4617 male dbM 5521, *C. ivanovi* sp. nov. female dbM 5493 male dbM 5498, *C. cagrii* sp. nov. female dbM 5607 male dbM 5619, *C. clarus* female dbM 5674).

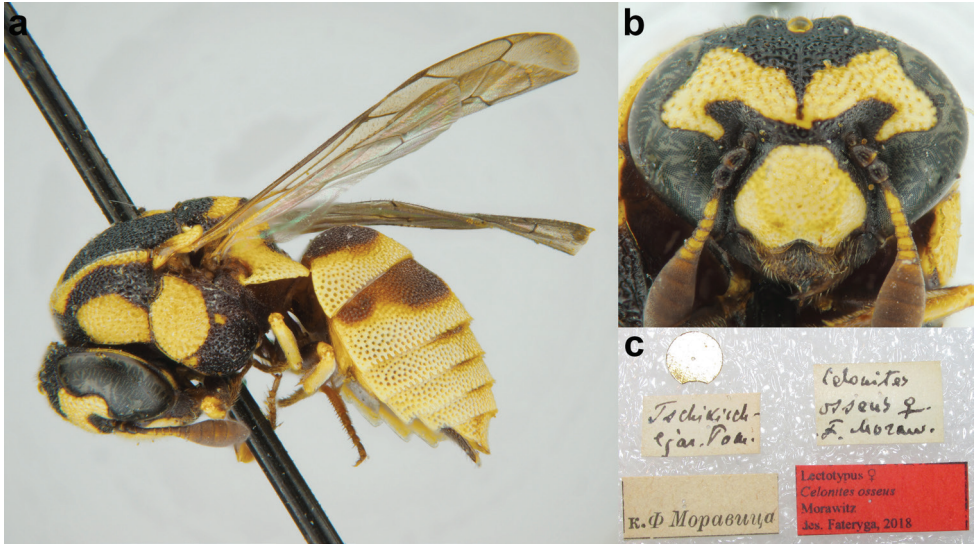


**Figure 3.** Lectotype of *Celonites osseus* **a** lateral view **b** head in frontal view **c** labels.

large marking extending from ocular sinus over lateral part of frons (1); continuous narrow stripe on gena and postgena along occipital carina from dorso-lateral corner of head to postero-ventral corner of compound eye (1), this stripe can be shortly interrupted (1) or reduced to short narrow spot on gena and postgena along occipital carina at dorso-lateral corner of head (3) and/or little spot on postgena adjacent to occipital carina level with postero-ventral corner of compound eye (7); minute spot on malar area above condylus (7); humeral spot small (2); little spot antero-dorsally on ventral mesepisternum (2); mesoscutum completely black (1) or with rectangular spot (2) or triangular spot with top directing posteriorly (1); transversal spot postero-medial on scutellum large (2); narrow transversal stripe on median third of metanotum (10); minute spot on pointed protuberance on posterior face of propodeum dorsally on each side of middle (1); tergum I with little (1) or medium sized (1) separated longitudinal antero-medial spot that can be posteriorly fused with posterior band in median axis in addition (1); posterior band on tergum II (4) or on terga II–III (2) not completely interrupted along posterior margin on each side of middle; tergum VI with large medial spot and little spot on each postero-lateral angle (2) or only with large (5) or small (2) medial spot that can be reduced to four weak minute little dots (1); continuous stripe on outside of mid-tibia only (1) or on outside of mid- and hind-tibia (7). Other markings: light yellowish-white marking on A7 darkened (1); medial on proximal part of A8 only light brownish suffused (3) or with same colour than distal part (1).

Structure: Head in frontal view 1.50 times as wide as long in median (min 1.45, max 1.54, n=5) (Fig. 4f). Mandible with two large blunt incisivi at distal end separated by acute-angled cleft and two smaller more acute subapical incisivi on antero-medial

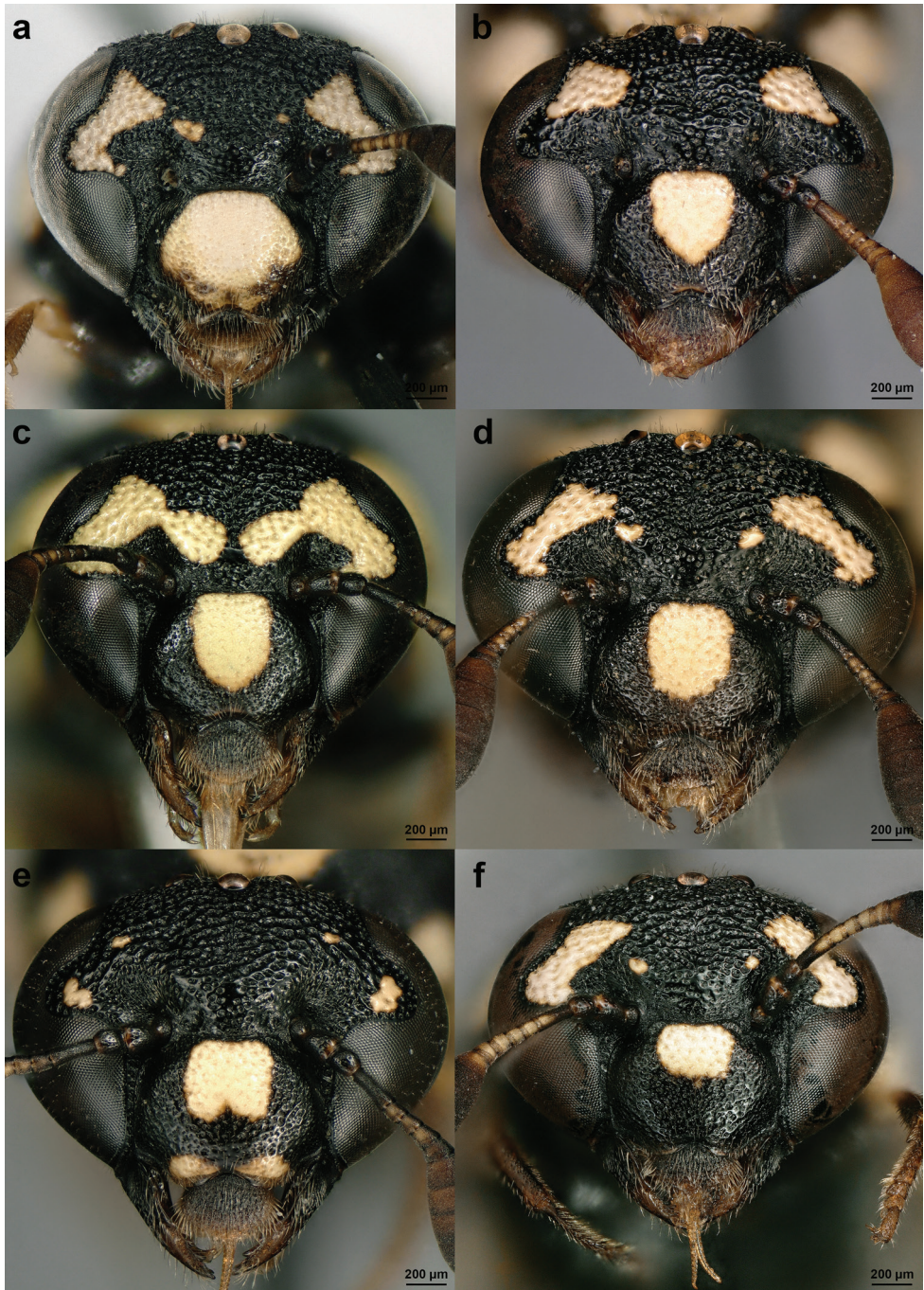


**Figure 4.** Female head in frontal view **a** *C. yemenensis* (dbM 5528) **b** *C. clarus* (dbM 4616) **c** *C. cyprius* (dbM 5431) **d** *C. osseus* (dbM 5678) **e** *C. ivanovi* sp. nov. (dbM 5490) **f** *C. cagrii* sp. nov. (dbM 5609).

margin. External side of mandible distally bearing longitudinal rows of long stiff setae; at base without distinct transverse depression; basal area with shagreened cuticula moderately covered with pubescence of tiny thin setae (longer than in *C. cyprius*); anterior to condylar ridge cuticula of basal area extends further apically becoming distinctly striated in longitudinal direction; this area contrasts to smooth shiny but somewhat longitudinally striated cuticula on condylar ridge and postero-apically adjoining surface; condylar ridge distinct at basal two-third of mandible continuing in more gentle curve into apical side (strongest bend approximately after basal third of mandible). Labrum matt shining, finely shagreened and longitudinally wrinkled; densely covered with pale stiff setae directing obliquely downwards; setae as long as A7 maximum wide, with distal end curved ventro-medially, laterally at apex of labrum thicker with larger diameter at base. Clypeus 1.4 times wider than long; translucent ventro-medial margin becoming much narrower medially resulting in distinct median emargination; cuticula shiny, ventro-medially above emargination smooth with sparse micropunctuation becoming moderately spaced dorsally and laterally on disc with larger irregular flat depressions and wrinkles in addition; dorso-lateral vertical parts of clypeus smooth with moderately spaced micropunctuation partly striated at base; covered with pale thin stiff setae arising from micropunctures; setae on disc about as long as A4, vertically erected with distal ends strongly curved in ventro-medial direction, on sides shorter lying more flatly. Frons very coarsely punctured, interstices shining, raised to  $\pm$ transversal little rounded ridges; protruding central part of supra-antennal area smooth, with moderately to sparsely spaced macropunctures and few micropunctures; semi-circular depression of antennal groove wrinkly shagreened; slight median depression dorsal to supra-antennal area, frontal line weak; sparsely covered with pale short setae arising from coarse punctures. Vertex with close macropunctuation, becoming more closely reticulate behind ocelli with smaller punctures and interstices more strongly raised forming short sharp-edged  $\pm$ transversal ridges; sparsely covered with pale short setae arising from punctures; cuticula of interstices shiny not shagreened (Fig. 5f). Median ocellus 1.2 times larger in diameter than lateral ocelli; median ocellus somewhat bilateral symmetric with anterior sector less strongly curved than posterior sector; lateral ocelli  $\pm$ circular (in dorso-lateral view). Compound eyes sparsely covered with tiny setae. Preoccipital carina sharp; medially straight, nearly transversal; laterally behind dorso-lateral end of each compound eye curved downwards for short distance becoming obsolete posterior to dorsal end of postocular carina. Gena narrow, less than half as wide as basal width of A3. Postocular carina sharp; extends dorsad from posterior mandibular articulation along posterior margin of gena; ends level with dorsal end of compound eye anterior to preoccipital carina that runs parallel for short distance. Antennal articles A8–A12 forming ventrally flattened club about 2.0–2.2 times as long as broad (in dorsal view).

Pronotum with anterior margin raised to carina; anterior pronotal carina (*sensu* Carpenter 1988) in antero-ventral area of pronotum weak, forming anterior sharp edge along ventral half of crenate groove dorsally continuing into sharply bent but



**Figure 5.** a, b Female clypeus in frontal view a *C. cyprius* (dbM 5431) b *C. ivanovi* sp. nov. (dbM 5490) c, d female mandible outside c *C. cyprius* (dbM 5431) d *C. ivanovi* sp. nov. (dbM 5490) e, f female ocelli and vertex in dorsal view e *C. ivanovi* sp. nov. (dbM 5492) f *C. cagrii* sp. nov. (dbM 5609).

rounded anterior border of crenate groove; crenate groove straight small trough-like, with nearly vertical anterior and posterior wall running parallel, bottom with sulcature of transverse ribs; running at very acute angle along posterior margin of pronotum slightly diverging from the posterior margin dorsally; cuticula between posterior margin of crenate groove and posterior margin of pronotum at same level as surrounding surface, shiny, with some micropunctures; on lateral quarter distinct posterior pronotal carina sharply separating semicircular antero-ventral area from dorsal area of pronotum; antero-medial front behind head nearly vertical; slight depression along dorso-medial margin especially anteriorly; posterior margin raised to short translucent carina dorsally in front of upper half of tegula; cuticula of antero-ventral area shiny, shagreened, with few small shallow punctures; cuticula of dorso-lateral area shiny, with close coarsely reticulate macropunctuation, smooth interstices raised to narrow edges postero-laterally forming lines; cuticula of pronotal lobe and dorsally continuing concavely curved depression in front of tegula smooth with a few distinct punctures but without reticulation, ventro-laterally more distinctly set off from adjacent parts of pronotum than dorsally. Mesoscutum with distinct median notal suture on anterior third; cuticula shiny, coarsely reticulate with close deep macropunctuation and narrow, distinctly raised interstices. Mesoscutellum with distinct transverse sulcature of longitudinal cuticula-ribs separated by intercostal spaces along antero-medial margin; laterally with distinct smooth carina along posterior margin, carina medially increasingly reduced so that cuticula of medial lobe continues evenly into crenulate margin; cuticula more coarsely reticulate than on mesoscutum. Metanotum laterally with distinct sulcature of longitudinal cuticula-ribs separated by intercostal spaces; carina along posterior margin medially with small irregular indentations continuing in vertical median keel. Axilla produced into curved tapering projection which fits into slight emargination of tegula. Tegula shiny, closely covered by macropunctures except completely smooth central convex area. Antero-ventral parts of pronotum, ventral corner of dorsal mesepisternum and ventral mesepisternum form continuous antero-ventral cavity delimited from lateral parts of mesosoma by posterior pronotal carina, carina along ventral margin of dorsal mesepisternum and epicnemial carina. Dorsal mesepisternum separated from ventral mesepisternum by weak mesepisternal groove; with distinct carina along ventral margin, which is in one line with epicnemial carina though separated from it by little notch. Ventral mesepisternum with pronounced epicnemial carina, posteriorly deflexed backwards running medially in a curve to front of mid-coxa. Mesepimeron feebly separated by weak scrobal groove; postero-ventrally bearing mesopleural process of moderate size, distally rounded, its posterior side shagreened matt shiny without punctures. Cuticula laterally on mesopleurum and dorsal metapleurum shiny, with closely reticulate macropunctuation; longitudinally striated by raised interstices in parts; ventral mesepisternum coarsely punctured with some interstices strongly raised to knife-like edges forming coarse rugose sculpture. Propodeum with horizontal propodeal triangles and dorso-lateral margins of posterior face of propodeum reduced to two pointed protuberances dorsally on each side of

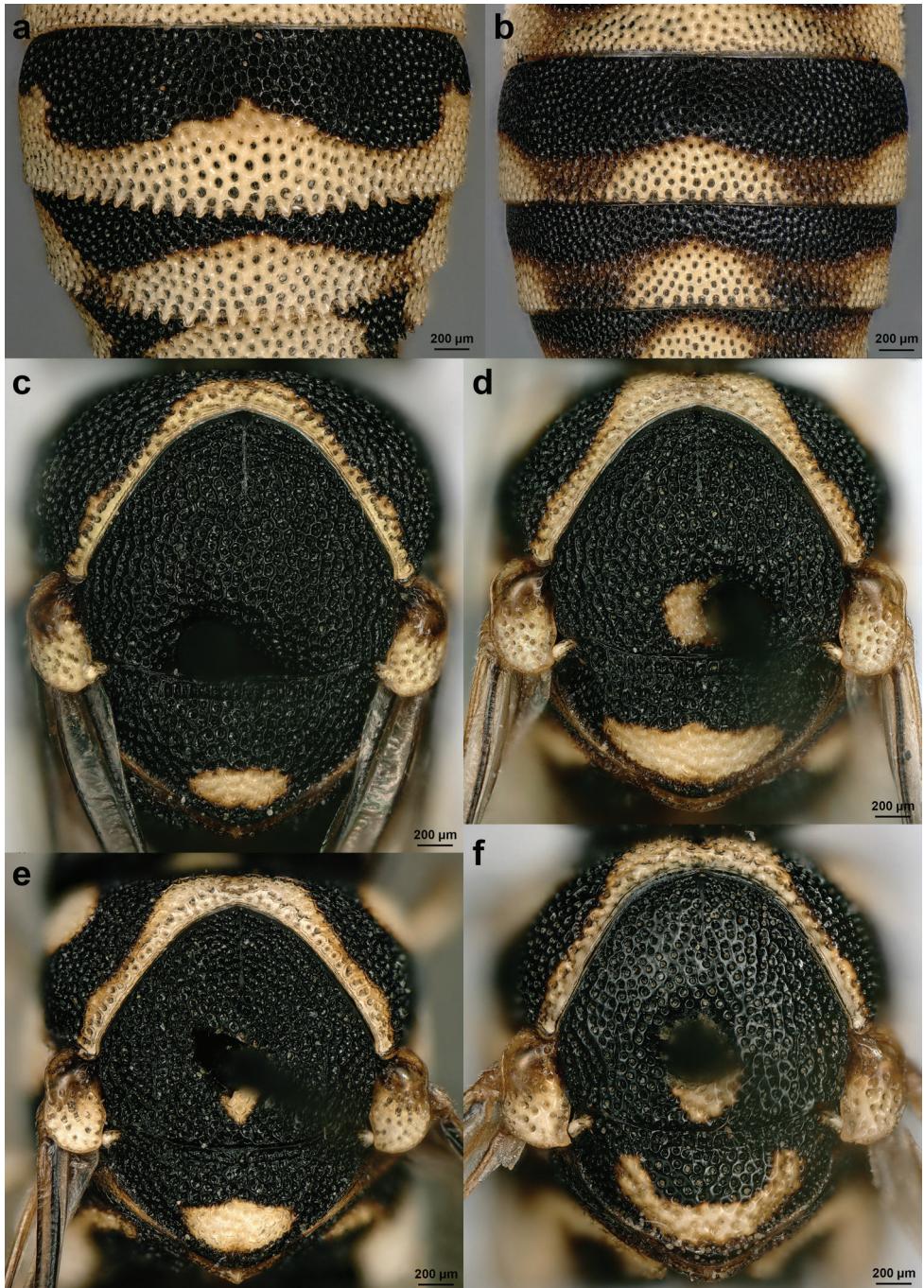


**Figure 6.** a,b Metasomal tergum II and III of female in dorsal view **a** *C. rugiceps* (dbM 5446) **b** *C. ivanovi* sp. nov. (dbM 5481) **c–f** mesonotum of female in dorsal view **c** *C. ivanovi* sp. nov. (dbM 5492) **d** *C. osseus* (dbM 4617) **e** *C. yemenensis* (dbM 5528) **f** *C. clarus* (dbM 4616).

middle, cuticula on protuberances rugose with interstices raised to knife-like edges; posteriorly with narrow medial cuticula-fold running from dorsal margin to postero-medial flange of propodeum; posterior surface ventrally striated by strong vertical cuticula-folds arising below anterior transversal carina of postero-medial flange of propodeum, with shallow macropunctures between folds, moderately covered with fine pale setae arising from macropunctures, laterally and dorsally continuing into coarsely reticulate macropunctuation with shorter setae. Cuticula below lateral lamella shiny, on metepisternum densely horizontally wrinkled, on side of propodeum shagreened with moderately spaced small shallow punctures. Lateral lamella moderate, slightly curved laterally downwards, its outer margin gently curved, its apex truncate, outer and posterior margins somewhat crenate; inner margin of lateral lamella and lateral apex of postero-lateral process of postero-medial flange of propodeum separated by small gap; anterior margin of postero-lateral process straight transverse, while posterior margin converges in weak curve towards lateral apex; outline of emargination being broad at its base with short narrow neck between lateral apex of postero-lateral process and inner margin of lateral lamella and small oval-rounded apical part (Fig. 7c); dorsal cuticula of lateral lamella and adjacent dorso-lateral part of propodeum shiny, with reticulate macropunctuation. On whole exoskeleton single thin seta arises from bottom of each macropuncture, seta short if not stated otherwise.

Fore-femur postero-ventrally produced in middle forming anteriorly curved lobe distally changing into tapering carina along ventral margin of femur; end of tibia when folded against femur coinciding with produced region; tarsomeres I–IV broad and flattened; underside of tibia and tarsomere I with strong obliquely distally directing setae forming stiff brush; underside of tarsomere I and II with comb-like row of particularly strong setae along distal margin. Claws ventrally with small tooth.

Metasomal terga with postero-lateral corners slightly produced; posterior margin of tergum I weakly crenulated, crenulation not produced into spines and not projecting over smooth translucent lower posterior margin of tergum; posterior margin of terga II–V weakly to moderately crenulated, crenulation in middle of terga II–IV produced into little slightly raised teeth projecting approximately to end of translucent lower posterior margin of terga; cuticula moderately shining, densely covered with reticulate macropunctuation, punctures distinct, smaller and more regular than on mesoscutum; interstices finely shagreened. Tergum VI with lateral margins converging in weakly convex, nearly straight or slightly concave curve, at transition to posterior median lobe strongly bend inwards forming distinct postero-lateral angle on each side; posterior margin of posterior median lobe running in convex oval curve formed by distinct translucent lamella; posterior median lobe set off from more strongly sloping median area of tergum VI by well-defined concave curvature at its base; cuticula covered with fine pubescence of thin pale setae arising from micropunctures on interstices of reticulate macropunctuation, slightly projecting beyond postero-median translucent lamella and lateral margins; on ventral side (viewed from ventral) posterior translucent lamella of median lobe continues on both sides into distinct carina running anteriorly

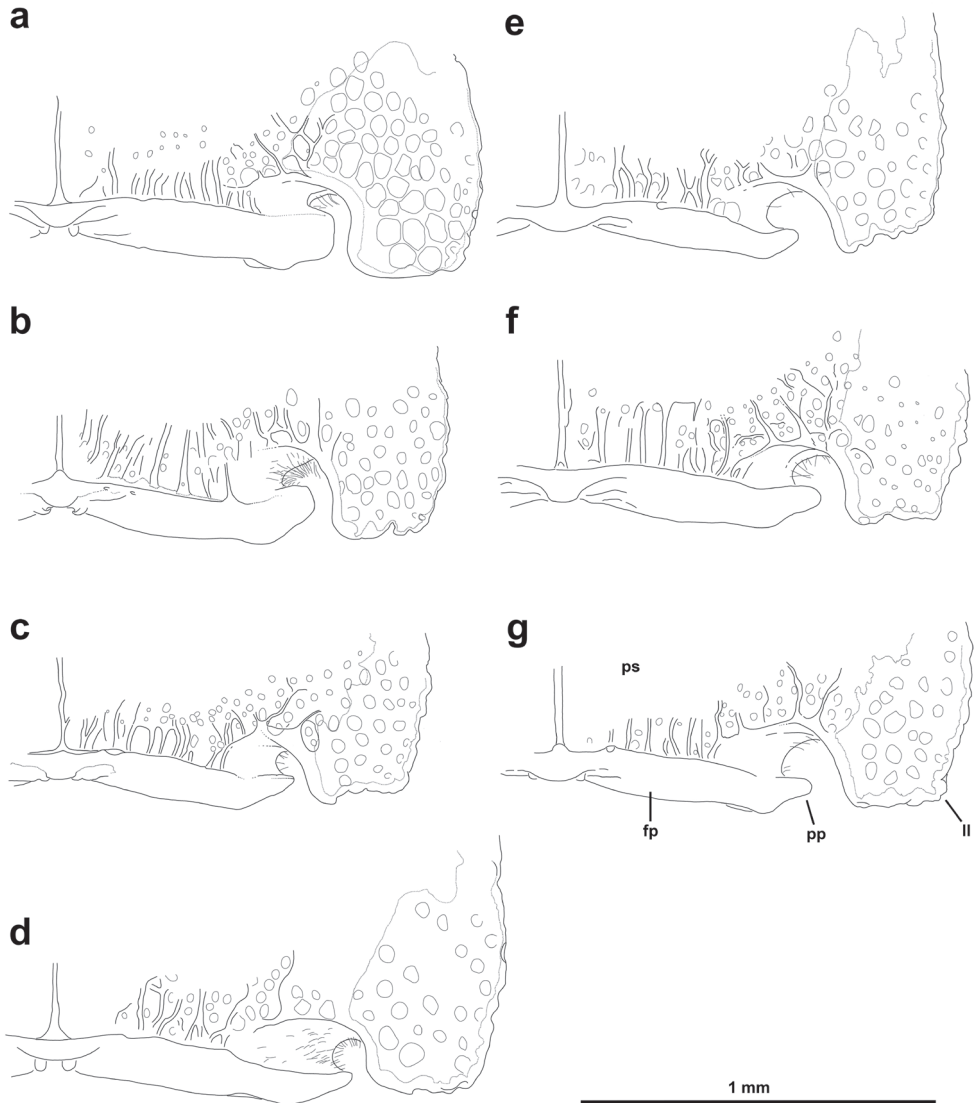


**Figure 7.** Right side of postero-lateral part of the propodeum of females in dorso-posterior view **a** *C. yemenensis* (dbM 4759) **b** *C. clarus* (dbM 4616) **c** *C. cagrii* sp. nov. (dbM 5611) **d** *C. rugiceps* (dbM 5446) **e** *C. cyprius* (dbM 5433) **f** *C. oseus* (dbM 5677) **g** *C. ivanovi* sp. nov. (dbM 5491) (**ps** = posterior surface of propodeum **fp** = postero-medial flange of propodeum **pp** = postero-lateral process **ll** = lateral lamella).

along medial margin adjoining sternum VI, thereby slightly but continuously diverging from lateral margin of tergum VI.

Metasomal sternum I shiny, finely shagreened, with tiny setae but without punctures. Sterna II–V posteriorly with broad stripe of asetose, translucent cuticula adjacent to posterior margin of more strongly sclerotized cuticula; small sparse row of setae along posterior sclerotized margin somewhat projecting over anterior part of translucent

stripe of cuticula; small outer area of postero-lateral corners distinctly depressed with some deep macropunctures; rest of sclerotized cuticula shiny, at least on anterior half of each sternum finely shagreened becoming weaker towards its posterior end; sternum II with median area moderately covered with small shallow macropunctures from which short pale setae arise, laterally sparsely covered with shallow macropunctures and micropunctures, micropunctation becoming fairly denser along posterior margin; sterna III–V anteriorly with moderate to dense shallow macropunctation, posteriorly changing into nearly unpunctured cuticula becoming moderately to densely covered by micropunctures further postero-laterally and along posterior margin. Posterior margin of sterna I–IV straight, posterior margin of sternum V medially concave running in a gentle curve. Sternum VI (Fig. 8c) tapering towards distal end; with outer margin forming bulged shiny rim, anteriorly raised to inwardly bent carina, postero-laterally strongly curved medially resulting in blunter appearance of distal end of sternum VI; rim at posterior end obtuse to nearly transverse, partly interrupted by depressions of macropunctures, postero-medially protruded into little median spine; cuticula with smooth median area tapering posteriorly, slightly raised to weak median keel at posterior end that continues into median spine, laterally with moderately spaced deep macropunctures becoming densely spaced and partly fused along lateral rim; stiff setae of moderate length arising obliquely backwards from macropunctures; posterior along distal end of rim densely covered with posteriorly directed stiff setae medially of same length as median spine becoming shorter anteriorly; at dorso-posterior margin dorsal (inner) cuticula protruded into irregularly serrated crystalline horizontal lamella situated immediately above the posteriorly directed stiff setae (Fig. 8h-i), dorso-medially fused with median spine, at postero-lateral edges somewhat more protruded.

**Male.** Colour (Fig. 2): Resembles female, except as follows. Light yellowish-white are: large M-shaped band on frons, laterally filling each ocular sinus (Fig. 9b); clypeus except dorso-lateral vertical sides and brownish translucent ventro-medial margin; little spot proximally on outside of mandible; complete longitudinal stripe on outside of fore-tibia; whole outside of mid- and hind-tibia; outside of hind-metatarsus. Labrum translucent brown with two yellowish-white antero-lateral spots medially fused. Terga II–VI with laterally and medially widened posterior band, anteriorly with small brownish tinge towards adjacent blackish-brown area, on terga III–VI interrupted on each side of middle by blackish-brown area. Tergum VII blackish-brown. Antenna black, with light yellowish-white stripe antero-medial on A3–A7 and proximal part of A8.

Structure: Resembles female, except as follows. Head in front view 1.49 times as wide as long (Fig. 9b, i). Mandible with single pointed tooth at distal end and two smaller acute teeth distally on antero-medial margin. Labrum with flat ventro-medial area, shiny with few thin short pale setae; dorsal and lateral area set off by tiny edge, strongly convex, weakly shagreened with rows of micropunctures from which short thin pale setae arise. Clypeus 1.36 times wider than long, strongly convex; shiny, ventro-medial area above emargination smooth, sparsely covered with micropunctures, dorsally and laterally changing into moderately spaced micro- and dense uneven shallow macropunctation; covered with short fine pale erected setae with distal end not



**Figure 8.** **a–c** Female sternum VI in ventral view **a** *C. yemenensis* (dbM 4759) **b** *C. ivanovi* sp. nov. (dbM 5491) **c** *C. cagrii* sp. nov. (dbM 5611) **d–f** female fore femur in posterior view **d** *C. cyprius* (dbM 5431) **e** *C. osseus* (dbM 5678) **f** *C. ivanovi* sp. nov. (dbM 5493) **g–i** female sternum VI posterior margin in dorso-posterior view **g** *C. ivanovi* sp. nov. (dbM 5493) **h** *C. cagrii* sp. nov. (dbM 5607) **i** *C. cagrii* sp. nov. (dbM 5618).

curved. Frons with distinct depression dorsal to protruding centre of supra-antennal area. Antennal club formed by A8–A12 in dorsal view about 1.68 times as long as broad; asymmetrical (Fig. 9g), with anterior margin evenly rounded, strongly curved

at distal end into straight-line transverse distal margin, and posterior margin nearly straight, bent into distal margin at postero-distal edge forming nearly right angle; with distinct longitudinal depression on posterior two-fifth of ventral side bearing three somewhat oval shaped tyloids, situated within A9, A10 and A11, tyloid of A9 smaller than others. Mid-coxa without small spine at distal end on anterior side close to anterior-medial angle.

Tergum VII at posterior end with narrow median lobe and well set off postero-lateral angle on each side (Fig. 9e); median lobe moderately produced, its posterior margin weakly concave in middle, with adjacent posterior translucent lamella fairly emarginated; translucent lamella continues on ventral side (in ventral view) at its base on both sides into distinct carina running anteriorly along medial margin adjoining sternum VII+VIII (fused); medial margin of postero-lateral angles running in semi-circular curve medially continuing into cuticula of median lobe slightly dorsal to base of translucent lamella; posterior median lobe and postero-lateral angles nearly horizontal distinctly set off at their base by sharp bend from anteriorly adjacent rising part of tergum; posteriorly with increasingly close and deep macropunctuation, strongest medially above sharp bend; interstices anteriorly distinctly shagreened, posteriorly smooth and more shiny, postero-medially moderately covered with tiny pale setae.

Sternum VIII (Fig. 14f) acutely produced running into two pointed lancet-like tips at posterior end with deep median incision between them, lancet-like tips and median incision between them narrower than in *C. ivanovi* sp. nov.; convex with large longitudinal depression in centre, lateral margins in proximal half bent horizontally; cuticula shiny, with shallow macropunctures; pale postero-medially directed setae arising from macropunctures, posteriorly increasing in length, forming little tuft projecting over posterior median incision. Sparse transverse fringe of tiny setae along distal end of sternum VII projecting over base of fused sternum VIII.

Male genital as in Figs 10f, 11f, 12f, 13f. Genital comparatively narrow and elongated; in lateral view broadest at base of stipites tapering into flat distal ends of harpides, in dorsal view basal opening narrow with stipites curved towards cupula without substantial lateral enlargement. Dorsal part of stipes distally continuing into harpide, with dorsal outline of harpide nearly straight in lateral view. Harpide in ventral view with tapering spatula-like distal end with distinctly concave latero-distal margin; medial margin strongly bent in ventral direction resulting in longitudinal vertical duplication, upper margin of which slightly curved towards longitudinal axis of harpide in addition; ventro-lateral margin continues proximally into curved sides of stipes; distally moderately covered with thin setae, with longest setae along apical margin. Volsella continues ventro-proximally into ventral plate of stipes; medially set off from ventral plate of stipes by deep emargination of medial margin; ventrally moderately covered with strong setae that are longer apically; apically on dorsal side with strongly sclerotized large, dark tubercles. Aedoeagus with broadly rounded distal end; thyrsos not distinctly separated from surrounding transparent soft cuticula, though clearly stronger sclerotized laterally along basal two-third of aedoeagus, only weakly converging towards distal end; each thyrsos ventrally with distinct ventro-anteriorly directed comparatively broad and blunt process (uncus thyrsos); apodema thyrsos

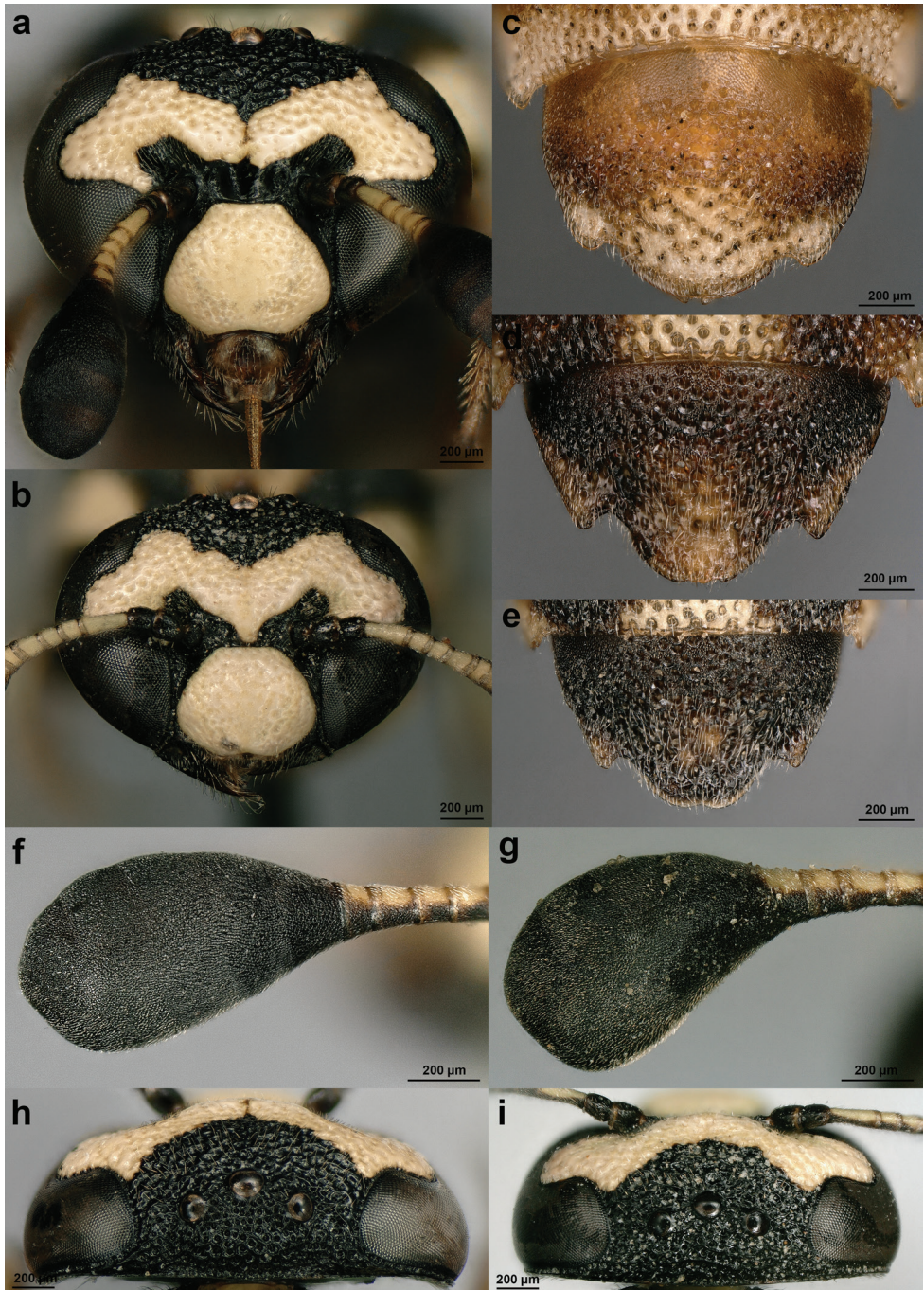


**Figure 9.** **a, b** Male head in frontal view **a** *C. ivanovi* sp. nov. (dbM 5498) **b** *C. cagrii* sp. nov. (dbM 5619) **c–e** male tergum VII in dorso-posterior view **c** *C. osseus* (dbM 5521) **d** *C. ivanovi* sp. nov. (dbM 5498) **e** *C. cagrii* sp. nov. (dbM 5619) **f, g** male antennal club in dorsal view **f** *C. ivanovi* sp. nov. (dbM 5499) **g** *C. cagrii* sp. nov. (dbM 5619) **h, i** male head in dorsal view **h** *C. ivanovi* sp. nov. (dbM 5498) **i** *C. cagrii* sp. nov. (dbM 5619).

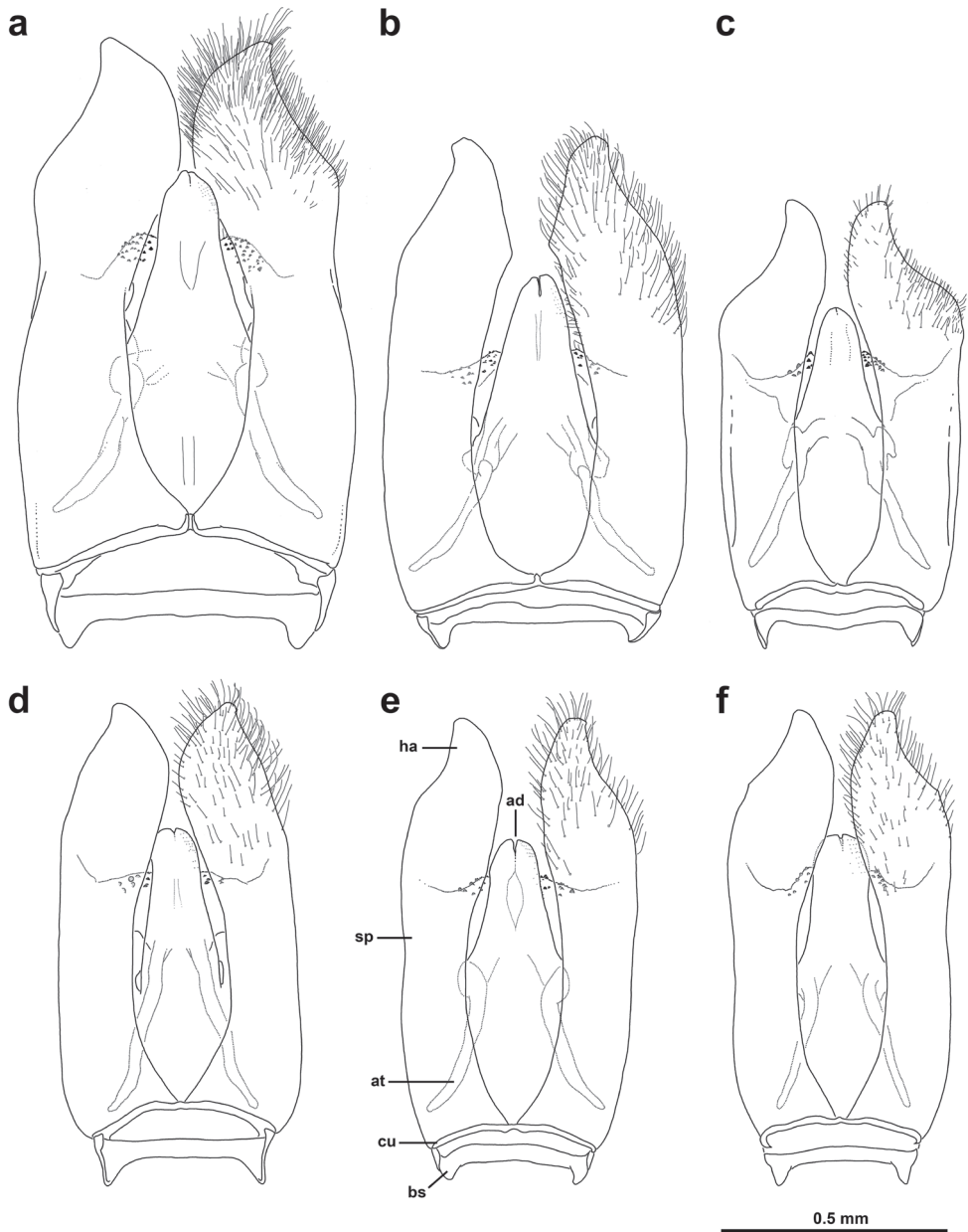


**Figure 10.** Male genitalia in dorsal view **a** *C. rugiceps* (dbM 2834) **b** *C. cyprius* (dbM 5452) **c** *C. yemenensis* (dbM 5531) **d** *C. osseus* (dbM 5521) **e** *C. ivanovi* sp. nov. (dbM 5497) **f** *C. cagrii* sp. nov. (dbM 5619) (ad = aedeagus at = apodema thyrsois bs = basal sclerite cu = cupula ha = harpide sp = stipes).

delicate, anteriorly running nearly straight. Basal region with cupula and basal sclerite; cupula fused with base of each stipes connecting both stipites dorsally, while ventro-medial ends of cupula are separated by wide gap from each other; basal sclerite forming

half ring on ventral side basal to cupula; medially slightly convex in ventral direction, laterally strongly curved upwards forming vertical sides, rounded at dorsal end.

**Measurements.** Measurements of the exoskeleton are listed in Table 1.

**DNA barcoding.** COI-5P gene sequences were obtained from two specimens and entered in BOLD database (CECYP005-20, CECYP006-20). The intraspecific sequence divergence of *C. cagrii* sp. nov. is 0.37%. The clade is clearly separated from the other investigated *Celonites* taxa (Fig. 16). The lowest interspecific genetic distance exists between *C. cagrii* sp. nov. and *C. ivanovi* sp. nov. with a minimum of 6.86% (mean 7.40%).

**Etymology.** The species is named after M. Çağrı Yildirim, the son of E. Yildirim.

**Distribution.** Turkey, Armenia (Fig. 17).

**Bionomics. Habitat.** The locus typicus of *C. cagrii* sp. nov. is situated in an arid mountainous area at an altitude of 1275 m a.s.l. in a valley near Akşar, which is a village in the Şenkaya district of Erzurum. Mean annual temperature is approximately 7.2 °C, annual precipitation is 456 mm (calculated by <https://de.climate-data.org>). The sides of the valley are formed by the steep slopes of adjacent dry mountains and a stream is running at its bottom. The upper part of the valley is covered with rocks, while the lower part is characterized by stony ruderal sites mainly used for grazing, and a few dry pastures and fields (Fig. 18i). General plant diversity is low, but plants of *Heliotropium ellipticum* Ledeb. (Boraginaceae) were growing solitarily or in patches on the sides of a little dirt road in an area that extended over 300 m, where the imagines of *C. cagrii* sp. nov. were observed.

**Flower association.** Twelve females and a single male of *C. cagrii* sp. nov. were collected while they were visiting flowers of *Heliotropium ellipticum*.

### *Celonites ivanovi* Mauss & Fateryga, sp. nov.

<http://zoobank.org/1AB3C8D3-A445-409F-8443-C3BC920350B8>

**Holotype.** ♀ (dbM 5492), “[Russia] Dagestan, Maydanskoye 42°36'16"N 46°58'10"E [corrected to 42°36'07"N, 46°58'13"E in 2021] 11.VI.2019 on *Heliotropium styligerum* leg. [A.V.] Fateryga” OLML (Figs 5e, 6c).

**Paratypes.** “[Russia] Dagestan, Untsukul'skiy distr. vicinity of Maydanskoye [42°37'36"N 46°56'48"E] on *Heliotropium styligerum* 23.06.2018 leg. [A.V.] Fateryga”, 1♀ AF, 1♀ (dbM 5287) VM; “[Russia] Dagestan Maydanskoye 42°36'16"N 46°58'10"E [corrected to 42°36'07"N, 46°58'13"E in 2021] 11.VI.2019 leg. [A.V.] Fateryga”, 1♂ (dbM 5497) AMNH, 1♂ (dbM 5498) OLML, 1♂ ZISP, 3♂ AF, 2♂ (dbM 5496, 5499) VM; “[Russia] Dagestan, Maydanskoye 42°36'16"N 46°58'10"E [corrected to 42°36'07"N, 46°58'13"E in 2021] 11.VI.2019 on *Heliotropium styligerum* leg. [A.V.] Fateryga”, 1♀ (dbM 5494) AMNH, 1♀ ZISP, 5♀ AF, 3♀ (dbM 5490, 5491, 5493) 1♂ (dbM 5495) VM; “[Russia] Dagestan, Maydanskoye 42°36'07"N, 46°58'13"E 15.VI.2021 on *Heliotropium styligerum* leg. [A.V.] Fateryga”, 4♀ (dbM 5856, 5857, 5858, 5995) VM; “[Russia] Dagestan, Maydanskoye 42°36'07"N, 46°58'13"E 16.VI.2021 on

**Table 1.** Measurements of the exoskeleton of females and males of *Celonites cagrii* sp. nov., *C. ivanovi* sp. nov., *C. osseus* and *C. clarus* (x = median; min = minimum, max = maximum, n = sample size; maximum accuracy 0.011 mm, all distances in mm).

Parameter	female												male																							
	<i>C. cagrii</i> sp. nov.				<i>C. ivanovi</i> sp. nov.				<i>C. osseus</i>				<i>C. clarus</i>				<i>C. cagrii</i> sp. nov.				<i>C. ivanovi</i> sp. nov.				<i>C. osseus</i>											
	x	min	max	n	x	min	max	n	x	min	max	n	x	min	max	n	x	min	max	n	x	min	max	n	x	min	max	n	x	min	max	n				
lateral ocelli distance	0.39	0.36	0.42	13	0.41	0.37	0.43	11	0.39	0.36	0.43	10	0.41	0.36	0.42	3	0.34	0.34	0.35	3	0.39	0.32	0.43	5	0.39	0.32	0.43	5	0.39	0.32	0.43	5	0.39	0.32	0.43	5
med./lat. ocellus distance	0.13	0.12	0.14	13	0.14	0.13	0.17	11	0.14	0.12	0.15	10	0.14	0.12	0.14	3	0.11	0.11	0.12	3	0.13	0.10	0.14	5	0.13	0.10	0.14	5	0.13	0.10	0.14	5	0.13	0.10	0.14	5
compound eyes distance	1.17	1.11	1.22	13	1.21	1.16	1.24	11	1.17	1.12	1.24	10	1.21	1.16	1.22	3	0.90	0.86	0.94	3	0.86	0.72	1.09	5	1.09	0.72	1.09	5	1.09	0.72	1.09	5	1.09	0.72	1.09	5
A1 length	0.17	0.15	0.18	13	0.19	0.18	0.20	11	0.17	0.15	0.18	10	0.15	0.14	0.17	3	0.17	0.15	0.19	3	0.19	0.17	0.20	5	0.17	0.15	0.20	5	0.17	0.15	0.20	5				
A3 length	0.23	0.22	0.24	13	0.24	0.23	0.25	11	0.23	0.21	0.24	10	0.18	0.18	0.19	3	0.23	0.23	0.26	3	0.24	0.23	0.26	5	0.22	0.23	0.26	5								
A3 width	0.09	0.08	0.10	13	0.10	0.09	0.11	11	0.09	0.09	0.10	10	0.09	0.09	0.10	3	0.10	0.10	0.10	3	0.11	0.09	0.11	5	0.11	0.09	0.11	5								
A4–A5 length	0.17	0.15	0.18	13	0.18	0.15	0.18	11	0.17	0.15	0.18	10	0.13	0.12	0.14	3	0.20	0.19	0.22	3	0.20	0.18	0.21	5	0.21	0.18	0.21	5								
A8–A12 length	0.65	0.63	0.67	13	0.70	0.66	0.74	11	0.69	0.65	0.72	10	0.64	0.62	0.70	3	0.85	0.81	0.88	3	0.85	0.78	0.95	5	0.99	0.78	0.95	5								
A8–A12 width	0.31	0.29	0.32	13	0.32	0.31	0.34	11	0.32	0.32	0.34	10	0.32	0.31	0.34	3	0.48	0.47	0.48	3	0.44	0.42	0.51	5	0.45	0.42	0.51	5								
antennal sockets distance	0.56	0.54	0.59	13	0.58	0.54	0.61	11	0.58	0.54	0.61	10	0.57	0.54	0.63	3	0.41	0.40	0.42	3	0.42	0.40	0.48	5	0.47	0.40	0.48	5								
clypeus max. width	0.87	0.85	0.90	13	0.94	0.87	0.97	11	0.90	0.88	0.95	10	0.88	0.86	0.92	3	0.70	0.68	0.73	3	0.70	0.67	0.84	5	0.77	0.67	0.84	5								
clypeus apical width	0.46	0.43	0.51	13	0.54	0.44	0.56	11	0.46	0.40	0.48	10	0.41	0.31	0.44	3	0.34	0.33	0.37	3	0.45	0.33	0.50	5	0.39	0.33	0.50	5								
clypeus length	0.62	0.59	0.65	13	0.68	0.65	0.70	11	0.65	0.62	0.69	10	0.58	0.56	0.61	3	0.53	0.52	0.55	3	0.56	0.50	0.64	5	0.58	0.50	0.64	5								
mesonotum width	2.10	1.99	2.18	13	2.30	2.13	2.38	11	2.21	2.10	2.27	10	2.04	1.93	2.13	3	1.90	1.88	2.02	3	2.24	1.85	3.77	5	2.18	1.85	3.77	5								
mesoscutum length	1.31	1.24	1.38	13	1.48	1.39	1.53	11	1.42	1.29	1.50	10	1.33	1.29	1.39	3	1.12	1.03	1.19	3	1.12	1.00	1.34	5	1.24	1.00	1.34	5								
wing length	4.14	4.00	4.32	13	4.69	4.46	4.90	11	4.53	4.23	4.65	10	4.09	4.00	4.32	3	3.96	3.77	4.09	3	4.14	3.77	4.62	5	4.37	3.77	4.62	5								
R+Sc length	2.21	2.18	2.32	13	2.49	2.41	2.58	11	2.44	2.24	2.55	10	2.16	2.13	2.35	3	2.13	2.04	2.21	3	2.16	2.04	2.60	5	2.32	2.04	2.60	5								
number of hamuli	7	6	8	13	7	6	8	11	7	7	9	10	7	7	9	3	8	7	9	3	7	7	8	5	8	7	8	5								
femur I length	1.01	0.97	1.06	13	1.11	1.08	1.14	10	1.04	0.94	1.10	10	0.97	0.95	0.99	3	0.90	0.84	0.95	3	1.00	0.87	1.07	4	0.95	0.87	1.07	4								
tibia I length	0.67	0.62	0.69	13	0.76	0.74	0.77	11	0.69	0.66	0.74	10	0.64	0.63	0.65	3	0.62	0.62	0.65	3	0.67	0.62	0.75	5	0.64	0.62	0.75	5								
tibia I width	0.36	0.34	0.40	13	0.42	0.40	0.45	11	0.20	0.19	0.20	10	0.36	0.36	0.40	3	0.17	0.17	0.17	3	0.33	0.29	0.36	5	0.34	0.29	0.36	5								
metatarsus I length	0.45	0.40	0.48	13	0.51	0.46	0.54	11	0.42	0.39	0.43	10	0.45	0.43	0.51	3	0.28	0.28	0.29	3	0.45	0.42	0.48	5	0.51	0.42	0.48	5								
metatarsus I width	0.19	0.18	0.20	13	0.20	0.19	0.21	11	0.13	0.13	0.14	10	0.18	0.18	0.20	3	0.10	0.10	0.10	3	0.17	0.14	0.19	5	0.19	0.14	0.19	5								
tarsus IT2–T5 length	0.14	0.13	0.14	13	0.15	0.13	0.15	11	0.50	0.47	0.54	10	0.12	0.12	0.13	3	0.42	0.40	0.45	3	0.11	0.10	0.12	5	0.11	0.10	0.12	5								
tergum I width	2.21	2.10	2.30	13	2.41	2.30	2.49	11	2.30	2.13	2.46	10	2.10	2.07	2.27	3	2.07	2.04	2.27	3	2.27	1.90	2.52	5	2.30	1.90	2.52	5								
tergum I length	0.88	0.73	0.94	13	1.02	0.95	1.04	11	0.94	0.87	1.04	10	0.87	0.78	0.90	3	0.88	0.80	0.96	3	0.97	0.80	1.12	5	1.00	0.80	1.12	5								
tergum II width	2.18	2.07	2.24	13	2.41	2.27	2.52	11	2.32	2.21	2.46	10	2.07	2.07	2.30	3	2.07	1.99	2.18	3	2.24	1.96	2.52	5	2.35	1.96	2.52	5								
total length	5.7	5.3	6.6	13	6.0	5.6	6.5	11	6.1	5.4	6.2	10	5.4	5.3	6.5	3	5.4	5.3	6.2	3	6.2	5.0	7.0	4	6.5	5.0	7.0	4								

*Heliotropium styligerum* leg. [A.V.] Fateryga”, 2♀ (dbM 5859, 5860) VM; “[Russia] Dagestan, Maydanskoye 42°36'07"N, 46°58'13"E 16.VI.2021 leg. [A.V.] Fateryga”, 1♂ (dbM 5996) VM; “[Russia] Dagestan, vicinity of Turtsi 42°11'34"N, 47°09'33"E on *Heliotropium styligerum* 22.VI.2021 leg. [A.V.] Fateryga”, 1♀ (dbM 5997) VM.

**Diagnosis.** See key.

**Description. Female.** Colour (Figs 2, 4e): Black. The following are yellowish-white: large rectangular spot dorso-medial on clypeus; two small spots adjoining ventral margin of clypeus to both sides of median emargination; small spot on each ocular sinus and two spots on frons; medium-sized spot on antero-dorsal angle of pronotum (humeral spot); broad stripe along dorso-medial (inner) margin of pronotum, anteriorly somewhat angularly enlarged with little median dent; large spot on dorsal mesepisternum; laterally directed process of axilla; medium-sized spot postero-medially on scutellum; dorsal and ventral side of propodeal lamella; antero-lateral one-fifth and posterior two-fifth of tegula, interrupted by brownish translucent area on bulge changing into black towards antero-medial margin of tegula; posterior band on tergum I occupying whole of sides but less than half of middle part, somewhat widened anteriorly in median axis, anteriorly with small brownish tinge towards adjacent black area; laterally and medially widened posterior bands on terga II–V, anteriorly with small brownish tinge towards adjacent black area, interrupted on each side of middle by brownish area (Fig. 6b); little longitudinal spot antero-medial on tergum VI; small spots on postero-lateral edges of sterna II–III; outside of distal tips of fore-, mid- and hind-femora; outside of proximal end of fore-tibia; outside of mid-tibia except small diagonal blackish-brown interruption in middle; outside of hind-tibia except blackish ring covering one-third below middle. Brown are: distal half of mandible; maxillary and labial palpi, protrudeable parts of proboscis; ventral margin of labrum; translucent ventro-medial margin of clypeus; postero-lateral margin of scutellum; median third of metanotum; postero-lateral process of propodeum; humeral plate (at base of wing underneath tegula); sides and posterior translucent margin of tergum VI; tarsi; sternum I; sterna II–V, lighter along posterior translucent margin. Antenna black except: weak yellowish markings medial on A4–A6; brown-suffused area ventral on A9–A11 and proximal part of A12. Wings moderately infuscate, pterostigma black, veins black becoming somewhat lighter at base.

Variation (number of specimens in brackets): Yellowish-white markings: clypeus with two additional lateral spots (1), only with two small separate spots dorso-medial on clypeus (1) or clypeus completely black (1); spot on ocular sinus and frons narrowly fused (1); spot on ocular sinus or frons asymmetrically reduced (4) or completely reduced (1); short narrow spot on gena along postocular carina at dorso-lateral corner of head (3); humeral spot small (4); little spot antero-ventrally on mesepimeron (1); little spot postero-medially on mesoscutum (5); bands on terga II–V interrupted on each side of middle by blackish-brown area (3); antero-medial spot on tergum VI absent (2); continuous stripe on outside of mid-tibia (5); continuous stripe on outside of hind-tibia (2) or marking on outside of mid- and hind-tibia reduced to small area at distal and proximal end (3); little spot disto-medially on A3 (1), weak yellowish markings medial on A7 (3).

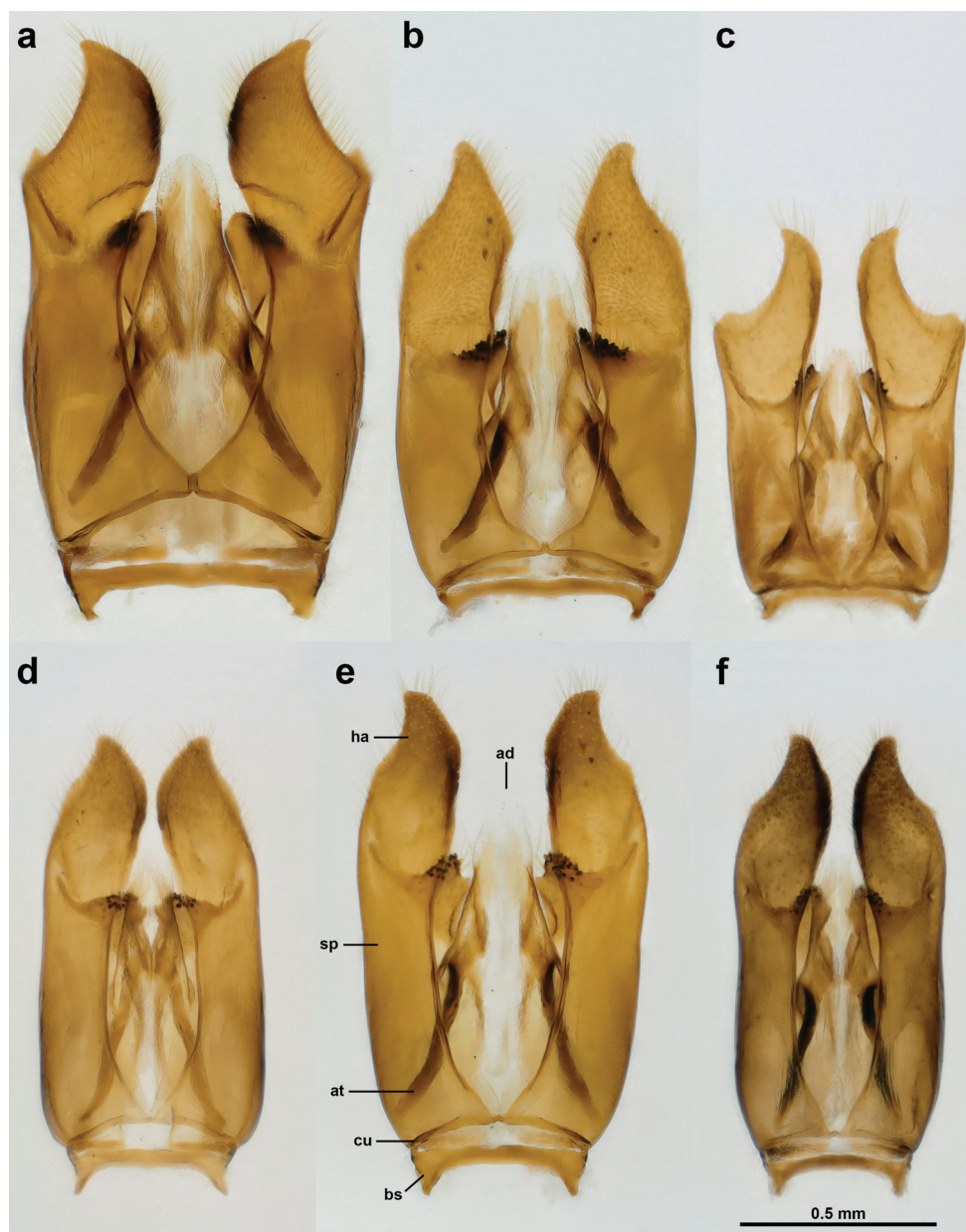


**Figure 11.** Microphotographs of male genitalia in dorsal view **a** *C. rugiceps* (dbM 5450) **b** *C. cyprius* (dbM 5439) **c** *C. yemenensis* (dbM 5532) **d** *C. osseus* (dbM 5521) **e** *C. ivanovi* sp. nov. (dbM 5498) **f** *C. cagrii* sp. nov. (dbM 5619) (**ad** = aedoeagus **at** = apodema thyrso **bs** = basal sclerite **cu** = cupula **ha** = harpide **sp** = stipes).

Structure: Head in front view 1.48 times as wide as long in median (min 1.45, max 1.53, n=5) (Fig. 4e). Mandible with two large blunt incisivi at distal end separated by acute-angled cleft and two smaller more acute subapical incisivi on antero-medial

margin. External side of mandible (Fig. 5d) distally bearing longitudinal rows of long stiff setae; at base without distinct transverse depression; basal area with shagreened cuticula moderately covered with pubescence of tiny thin setae (longer than in *C. cyprius*); anterior to condylar ridge cuticula of basal area extends further apically becoming distinctly striated in longitudinal direction; this area contrasts to smooth shiny cuticula on condylar ridge and postero-apically adjoining surface; condylar ridge distinct at basal two-third of mandible continuing in more angled curve into apical side (strongest bend approximately after basal third of mandible). Labrum matt shining, finely shagreened and longitudinally wrinkled; densely covered with pale stiff setae directing obliquely downwards; setae as long as A7 maximum wide, with distal end curved ventro-medially, laterally at apex of labrum thicker with larger diameter at base. Clypeus 1.4 times wider than long (Fig. 5b); translucent ventro-medial margin becoming much narrower medially resulting in distinct median emargination; cuticula shiny, ventro-medial above emargination with sparse micropunctuation becoming moderately spaced dorsally and laterally on disc with larger irregular flat depressions and wrinkles in addition; dorso-lateral vertical parts of clypeus smooth with moderately spaced micropunctuation partly striated at base; covered with pale thin stiff setae arising from micropunctures; setae on disc about as long as A4, vertically erected with distal ends strongly curved in ventro-medial direction, on sides shorter lying more flatly. Frons very coarsely punctured, interstices shining, raised to  $\pm$ transversal little rounded ridges; protruding central part of supra-antennal area smooth without punctures in middle; semi-circular depression of antennal groove wrinkly shagreened; slight median depression dorsal to supra-antennal area, frontal line weak; sparsely covered with pale short setae arising from coarse punctures, setae on supra-antennal area as on clypeus. Vertex with close macropunctuation, becoming more closely reticulate behind ocelli with smaller punctures and interstices more strongly raised forming short sharp-edged  $\pm$ transversal ridges; sparsely covered with pale short setae arising from punctures; cuticula of interstices shiny, weakly shagreened (Fig. 5e). Median ocellus 1.2 times larger in diameter than lateral ocelli; median ocellus somewhat bilateral symmetric with anterior sector less strongly curved than posterior sector; lateral ocelli  $\pm$ circular (in dorso-lateral view). Compound eyes sparsely covered with tiny setae. Preoccipital carina (*sensu* Snelling 1986) sharp; medially straight, nearly transversal; laterally behind dorso-lateral end of each compound eye curved downwards for short distance becoming obsolete posterior to dorsal end of postocular carina (*sensu* Snelling 1986). Gena narrow, less than half as wide as basal width of A3. Postocular carina sharp; extends dorsad from posterior mandibular articulation along posterior margin of gena; ends level with dorsal end of compound eye anterior to preoccipital carina that runs parallel for short distance. Antennal articles A8–A12 forming ventrally flattened club about 2.1–2.3 times as long as broad (in dorsal view).

Pronotum with anterior margin raised to carina; anterior pronotal carina (*sensu* Carpenter 1988) in antero-ventral area of pronotum starting close to posterior margin, running in a short parabolic curve antero-laterally and then parallel to posterior margin, preceding distinct crenate groove; fairly projecting in posterior direction over anterior border of crenate groove, especially along ventral parabolic curve; crenate

groove with anterior wall nearly vertical, bottom with sulcature of transverse ribs, posteriorly gradually inclined up to posterior margin of pronotum, cuticula in this area obliquely striated with some folds  $\pm$  continuing into bottom ribs; on lateral quarter distinct posterior pronotal carina sharply separating semicircular antero-ventral area

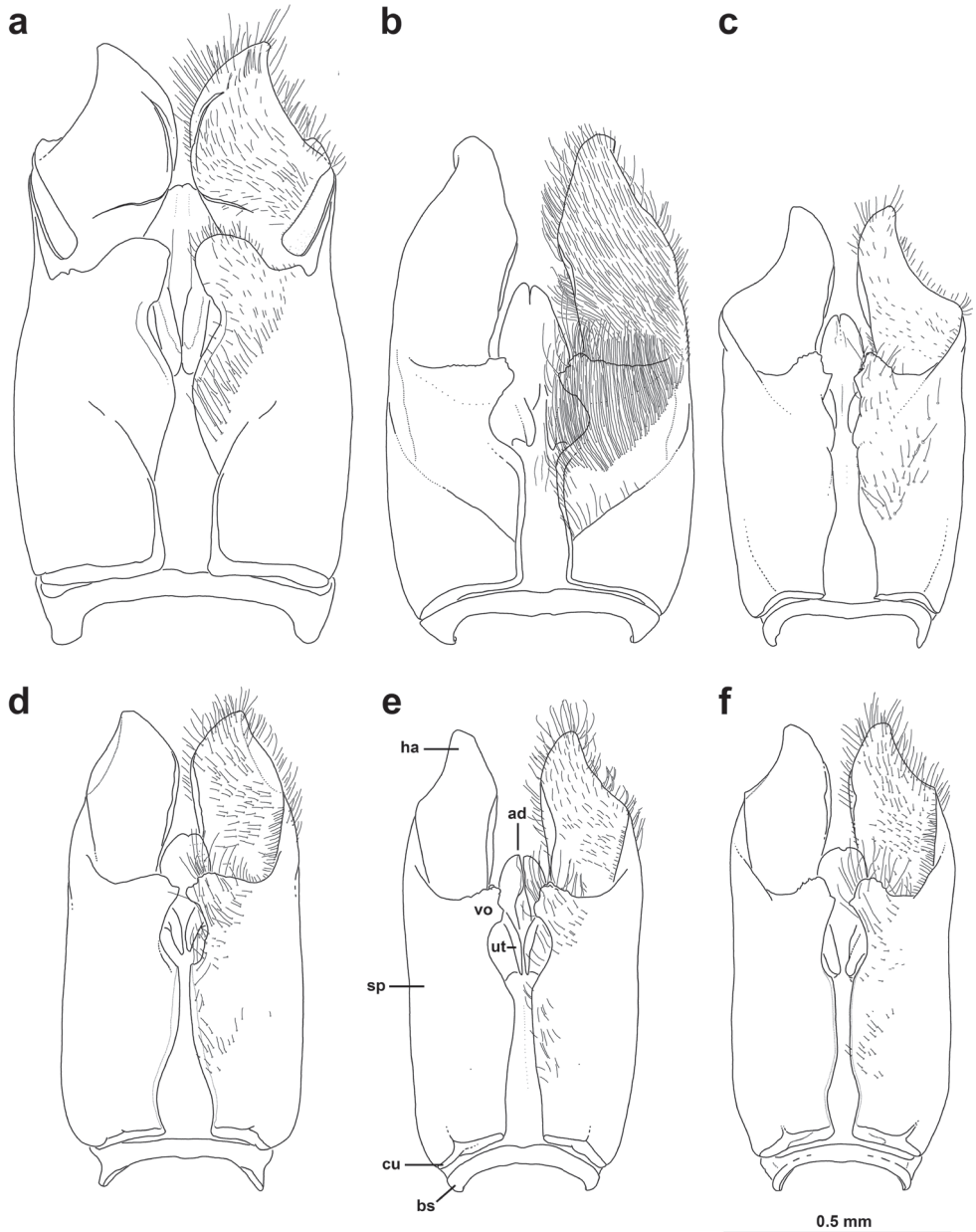


**Figure 12.** Male genitalia in ventral view **a** *C. rugiceps* (dbM 2834) **b** *C. cyprius* (dbM 5452) **c** *C. yemenensis* (dbM 5531) **d** *C. osseus* (dbM 5521) **e** *C. ivanovi* sp. nov. (dbM 5497) **f** *C. cagrii* sp. nov. (dbM 5619) (**ad** = aedoeagus **bs** = basal sclerite **cu** = cupula **ha** = harpide **sp** = stipes **vo** = volsella **ut** = uncus thyrsos).

from dorsal area of pronotum; antero-medial front behind head nearly vertical; slight depression along dorso-medial margin especially anteriorly; posterior margin raised to short translucent carina dorsally in front of upper half of tegula; cuticula of antero-ventral area shiny, shagreened, with moderately spaced small shallow punctures; cuticula of dorso-lateral area shiny, with close coarsely reticulate macropunctuation, smooth interstices raised to sharp edges postero-laterally forming lines; cuticula of pronotal lobe and dorsally continuing concavely curved depression in front of tegula smooth with a few distinct punctures but without reticulation, distinctly set off from adjacent parts of pronotum. Mesoscutum with distinct median notal suture on anterior third; cuticula shiny, coarsely reticulate with close deep macropunctuation and narrow distinctly raised interstices (Fig. 6c). Mesoscutellum with distinct transverse sulcature of longitudinal cuticula-ribs separated by intercostal spaces along antero-medial margin; laterally with distinct smooth carina along posterior margin, carina medially increasingly reduced so that cuticula of medial lobe continues evenly into crenulate margin; cuticula more coarsely reticulate than on mesoscutum. Metanotum laterally with distinct sulcature of longitudinal cuticula-ribs separated by intercostal spaces; carina along posterior margin medially with small irregular indentations continuing in vertical median keel. Axilla produced into curved tapering projection which fits into slight emargination of tegula. Tegula shiny, closely covered by macropunctures except completely smooth central convex area. Antero-ventral parts of pronotum, ventral corner of dorsal mesepisternum (= prepectus *sensu* Richards 1962) and ventral mesepisternum form continuous antero-ventral cavity delimited from lateral parts of mesosoma by posterior pronotal carina, carina along ventral margin of dorsal mesepisternum and epicnemial carina. Dorsal mesepisternum separated from ventral mesepisternum by weak mesepisternal groove; with distinct carina along ventral margin, which is in one line with epicnemial carina though separated from it by little notch. Ventral mesepisternum with pronounced epicnemial carina, posteriorly deflexed backwards running medially in a curve to front of mid-coxa. Mesepimeron feebly separated by weak scrobal groove; postero-ventrally bearing mesopleural process (= process at or below mesepisternal scrobe *sensu* Richards 1962) of moderate size, distally rounded, its posterior side shagreened matt shiny without punctures. Cuticula laterally on mesopleurum and dorsal metapleurum shiny, with closely reticulate macropunctuation; longitudinally striated by raised interstices in parts; ventral mesepisternum coarsely punctured with some interstices strongly raised to knife-like edges forming coarse rugose sculpture. Propodeum with horizontal propodeal triangles and dorso-lateral margins of posterior face of propodeum reduced to two pointed protuberances dorsally on each side of middle; posteriorly with narrow medial cuticula-fold running from dorsal margin to postero-medial flange of propodeum; posterior surface ventrally striated by strong vertical cuticula-folds arising below anterior transversal carina of postero-medial flange of propodeum, weakly coriaceous, with shallow macropunctures between folds, moderately covered with fine pale setae arising from macropunctures, laterally and dorsally continuing into coarsely reticulate macropunctuation with shorter setae. Cuticula below lateral lamella shiny, on metepisternum densely horizontally wrinkled, on side of propodeum shagreened with moderately spaced small shallow punctures. Lateral lamella moderate, slightly

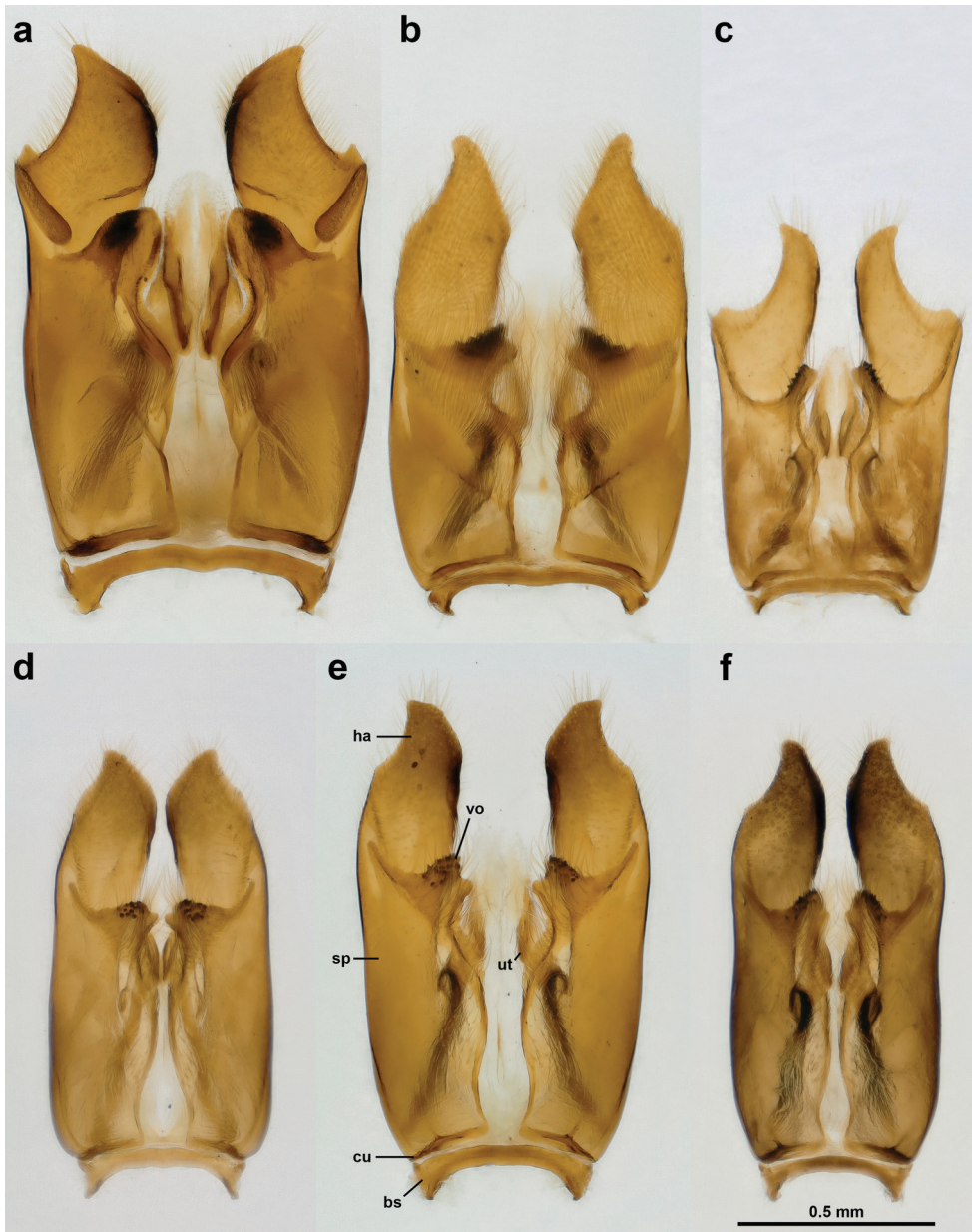


**Figure 13.** Microphotos of male genitalia in ventral view **a** *C. rugiceps* (dbM 5450) **b** *C. cyprius* (dbM 5439) **c** *C. yemenensis* (dbM 5532) **d** *C. osseus* (dbM 5521) **e** *C. ivanovi* sp. nov. (dbM 5498) **f** *C. cagrii* sp. nov. (dbM 5619) (**ad** = aedoeagus **bs** = basal sclerite **cu** = cupula **ha** = harpide **sp** = stipes **vo** = volsella **ut** = uncus thyrsos).

curved laterally downwards, its outer margin gently curved, its apex truncate, outer and posterior margins somewhat crenate; inner margin of lateral lamella and postero-lateral process of postero-medial flange of propodeum separated by moderate gap; anterior margin of postero-lateral process straight transverse, while posterior margin

converges in a gentle curve towards lateral apex; outline of emargination being broad at its base with short moderately wide neck between lateral apex of postero-lateral process and inner margin of lateral lamella and deep medially extended apical part (Fig. 7g); dorsal cuticula of lateral lamella and adjacent dorso-lateral part of propodeum shiny, with reticulate macropunctuation. On whole exoskeleton single thin seta arises from bottom of each macropuncture, seta short if not stated otherwise.

Fore-femur postero-ventrally produced in middle forming anteriorly curved lobe (Fig. 8f) distally changing into tapering carina along ventral margin of femur; end of tibia when folded against femur coinciding with produced region; tarsomeres I–IV broad and flattened; underside of tibia and tarsomere I with strong obliquely distally directing setae forming stiff brush; underside of tarsomere I and II with comb-like row of particularly strong setae along distal margin. Claws ventrally with small tooth.

Metasomal terga with postero-lateral corners slightly produced; posterior margin of tergum I weakly crenulated, crenulation not produced into spines and not projecting over smooth translucent lower posterior margin of tergum; posterior margin of terga II–V weakly to moderately crenulated, crenulation in middle of terga II–IV produced into little slightly raised teeth projecting approximately to end of translucent lower posterior margin of terga (Fig. 6b); cuticula moderately shining, densely covered with reticulate macropunctuation, punctures distinct, smaller and more regular than on mesoscutum; interstices finely shagreened. Tergum VI with lateral margins converging in weakly convex curve, at transition to posterior median lobe strongly bend inwards forming distinct postero-lateral angle on each side; posterior margin of posterior median lobe running in convex oval curve formed by distinct translucent lamella; posterior median lobe set off from more strongly sloping median area of tergum VI by slight concave curvature at its base; cuticula covered with fine pubescence of thin pale setae arising from micropunctures on interstices of reticulate macropunctuation, slightly projecting beyond postero-median translucent lamella and lateral margins; on ventral side (viewed from ventral) posterior translucent lamella of median lobe continues on both sides into distinct carina running anteriorly along medial margin adjoining sternum VI, thereby slightly but continuously diverging from lateral margin of tergum VI.

Metasomal sternum I shiny, finely shagreened, with tiny setae but without punctures. Sterna II–V posteriorly with broad stripe of asetose, translucent cuticula adjacent to posterior margin of more strongly sclerotized cuticula; small sparse row of setae along posterior sclerotized margin somewhat projecting over anterior part of translucent stripe of cuticula; outer area of postero-lateral corners distinctly depressed, densely covered with macropunctures; rest of sclerotized cuticula shiny, finely shagreened on sterna II–III, shagreening weaker or missing on sternum IV and absent on sternum V; sternum II antero-laterally with moderately spaced shallow macropunctuation and a few micropunctures becoming barely punctured towards posterior margin, whole medial area densely covered with small macropunctures from which short pale setae arise; sterna III–V anteriorly with moderate to dense shallow macropunctuation, posteriorly changing into nearly unpunctured area along posterior margin. Posterior margin of sterna I–IV straight, posterior margin of sternum V medially concave running in a gentle curve. Sternum VI tapering towards distal end; with outer margin

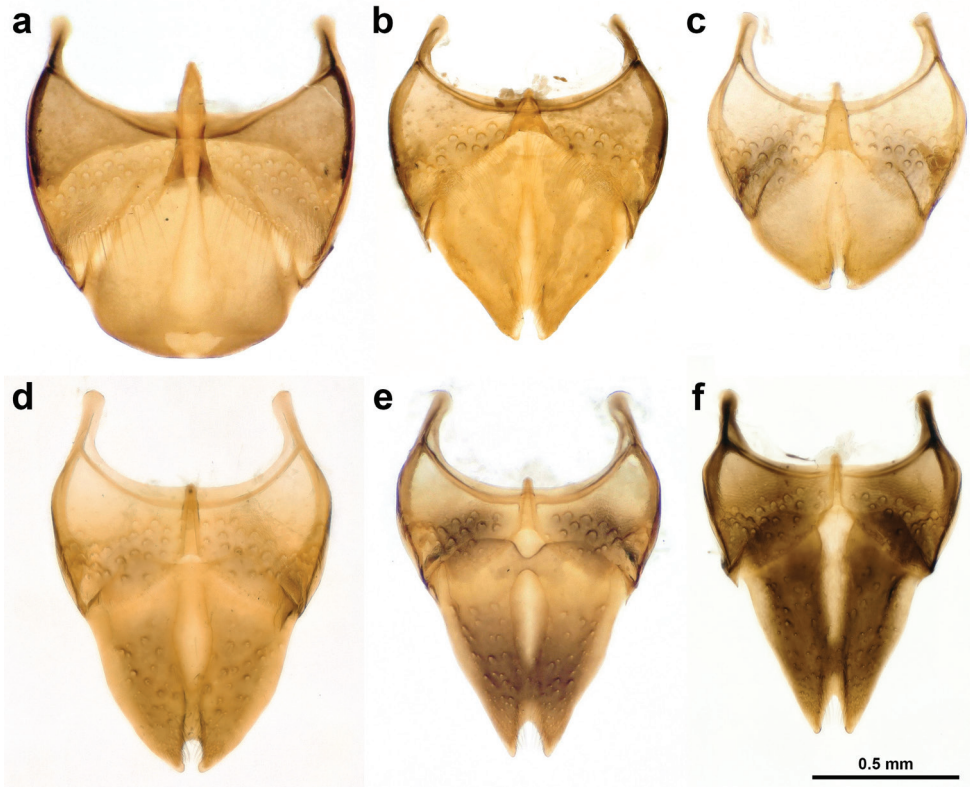


**Figure 14.** Male fused sterna VII+VIII in ventral view **a** *C. rugiceps* (dbM 5289) **b** *C. cyprius* (dbM 5439) **c** *C. yemenensis* (dbM 5532) **d** *C. osseus* (dbM 5521) **e** *C. ivanovi* sp. nov. (dbM 5498) **f** *C. cagrii* sp. nov. (dbM 5619).

forming bulged rim, anteriorly raised to inwardly bent carina, posteriorly running in regular curve postero-medially protruded into little median spine (Fig. 8b); cuticula with smooth median area tapering posteriorly, slightly raised to weak median keel at posterior end that continues into median spine, laterally with moderately spaced deep macropunctures becoming densely spaced and partly fused along lateral rim; stiff setae of moderate length arising obliquely backwards from macropunctures; posterior along distal end of rim densely covered with posteriorly directed stiff setae medially of same length as median spine becoming shorter anteriorly; at dorso-posterior margin dorsal (inner) cuticula weakly protruded into horizontal lamella, situated immediately above the posteriorly directed stiff setae, dorso-medially slightly raised and fused with median spine, becoming continuously smaller postero-laterally (Fig. 8g).

**Male.** Colour (Fig. 2): Resembles female, except as follows. Yellowish-white are: large M-shaped band on frons, laterally nearly filling each ocular sinus except small area along upper inner margin of eye, narrowly interrupted medially on supra-antennal area; clypeus except dorso-lateral vertical sides and brownish translucent ventro-medial margin; complete longitudinal stripe on outside of fore-tibia; whole outside

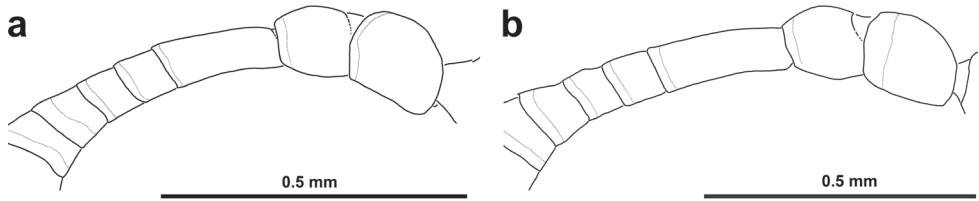


**Figure 15.** Female antennal articles A1–A6 in medial view (scaled to same size to show different proportions of A3) **a** *C. clarus* (dbM 5674) **b** *C. osseus* (dbM 5678).

of mid- and hind-tibia; outside of hind-metatarsus. Labrum translucent brown with two yellowish-white antero-lateral spots. Tergum VI as in terga II–V with laterally and medially widened posterior band, anteriorly with small brownish tinge towards adjacent black area, interrupted on each side of middle by brownish area. Tergum VII blackish-brown posteriorly changing into brown. Antenna black, with yellowish-white stripe antero-medial on A3–A7.

Variation (number of specimens in brackets): yellowish-white M-shaped band on frons filling ocular sinus completely (1), medially not completely interrupted (1); short narrow interrupted yellowish-white streak on gena along occipital carina at dorso-lateral corner of head (2); one or two little yellowish-white spots postero-medial on mesoscutum (2); humeral plate with yellowish-white marking (4); outside of mid-metatarsus yellowish-white (1).

Structure: Resembles female, except as follows. Head in front view 1.4–1.6 times as wide as long (Fig. 9a, h). Mandible with single pointed tooth at distal end and two smaller acute teeth distally on antero-medial margin. Labrum with flat ventro-medial area, shiny with few thin short pale setae; dorsal and lateral area set off by tiny edge, strongly convex, weakly shagreened with rows of micropunctures from which short thin pale setae arise. Clypeus 1.3 times wider than long, strongly convex; shiny, ventro-medial area above emargination smooth, sparsely covered with micropunctures, dorsally and laterally changing into moderately spaced micro- and dense uneven shallow macropunctuation; covered with fine pale erected setae, only very few with distally curved ends. Frons with distinct depression dorsal to protruding centre of supra-antennal area. Antennal club formed by A8–A12 about 1.8–1.9 times as long as broad (in dorsal view); asymmetrical (Fig. 9f), with anterior margin evenly rounded, strongly curved at distal end into weakly concave distal margin that is running obliquely upwards, and posterior margin weakly convex curved into distal margin at postero-distal edge forming blunt angle; with distinct longitudinal depression on posterior half of ventral side bearing three somewhat oval shaped tyloids, situated within A9, A10 and A11, tyloid of A9 smaller than others. Mid-coxa without small spine at distal end on anterior side close to anterior-medial angle.

Tergum VII at posterior end with characteristically narrow median lobe and well set off postero-lateral angle on each side (Fig. 9d); median lobe with translucent lamella, that continues on ventral side (in ventral view) at its base on both sides into distinct carina running anteriorly along medial margin adjoining sternum VII+VIII

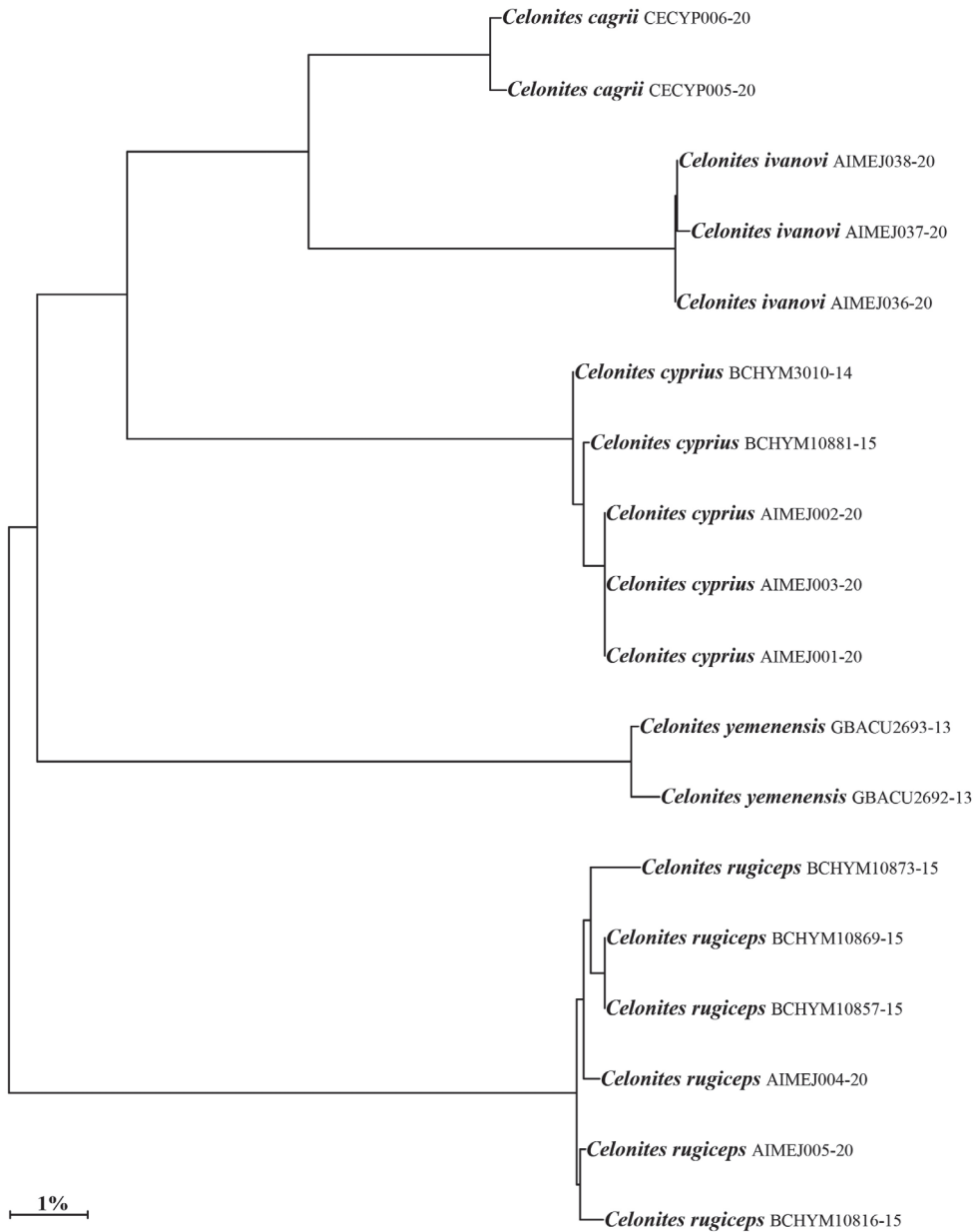


**Figure 16.** Neighbour joining BOLD taxon ID tree of 18 specimens of the *C. cyprius*-group based on COI-5P gene sequences (individually marked by BOLD process ID and assigned to species a priori by morphological characters; COI-5P gene sequence of *C. osseus* and *C. clarus* unknown).

(fused); medial margin of postero-lateral angles running in semi-circular curve medially continuing into cuticula of median lobe slightly dorsal to base of translucent lamella; posterior median lobe and postero-lateral angles nearly horizontal distinctly set off at their base by sharp bend from anteriorly adjacent rising part of tergum; posteriorly

with increasingly close and deep macropunctuation, strongest medially above sharp bend; interstices anteriorly distinctly shagreened, posteriorly smooth and more shiny, postero-medially moderately covered with tiny pale setae.

Sternum VIII acutely produced running into two pointed lancet-like tips at posterior end with deep median incision between them (Fig. 14e); convex with large longitudinal oval depression in centre, lateral margins in proximal two-third bent horizontally; cuticula shiny, postero-medially with shallow macropunctures, becoming denser towards apical end; pale postero-medially directed setae arising from macropunctures, posteriorly increasing in length, forming little tuft projecting over posterior median incision. Sparse transverse fringe of tiny setae along distal end of fused sternum VII projecting over base of sternum VIII.

Male genital as in Figs 10e, 11e, 12e, 13e. Genital comparatively narrow and elongated; in lateral view broadest at base of stipites tapering into flat distal ends of harpides, in dorsal view basal opening narrow with stipites curved towards cupula without substantial lateral enlargement. Dorsal part of stipes distally continuing into harpide, with dorsal outline of harpide nearly straight in lateral view. Harpide in ventral view with tapering spatula-like distal end with distinctly concave latero-distal margin; medial margin strongly bent in ventral direction resulting in longitudinal vertical duplication, upper margin of which curved towards longitudinal axis of harpide in addition; ventro-lateral margin continues proximally into curved sides of stipes; distally moderately covered with thin setae, short on ventral side, dorsally longer with longest setae along apical margin. Volsella continues ventro-proximally into ventral plate of stipes; medially set off from ventral plate of stipes by deep emargination of medial margin; ventrally moderately covered with strong setae that are longer apically; apically on dorsal side with strongly sclerotized large, dark tubercles. Aedoeagus with narrowly rounded distal end; thyrsos not distinctly separated from surrounding transparent soft cuticula, though clearly stronger sclerotized laterally along basal two-third of aedoeagus, converging towards distal end; each thyrsos ventrally with distinct ventro-anteriorly directed sharp process (uncus thyrsos); apodema thyrsos robust, anteriorly curved laterad. Basal region with cupula and basal sclerite; cupula fused with base of each stipes connecting both stipites dorsally, while ventro-medial ends of cupula are separated by wide gap from each other; basal sclerite forming half ring on ventral side basal to cupula; medially slightly convex in ventral direction, laterally strongly curved upwards forming vertical sides, rounded at dorsal end.

**Measurements.** Measurements of the exoskeleton are listed in Table 1.

**DNA barcoding.** COI-5P gene sequences were obtained from three specimens and entered in BOLD database (AIMEJ036-20, AIMEJ037-20, AIMEJ038-20). The intraspecific sequence divergence of *C. ivanovi* sp. nov. is low, reaching at most 0.18%. The clade is distinctly separated from the other investigated *Celonites* taxa (Fig. 16). The lowest interspecific genetic distance exists towards *C. cagrii* sp. nov. with a minimum of 6.86% (mean 7.40%).

**Etymology.** The species is named after Prof. Sergey P. Ivanov, a Crimean entomologist and the scientific advisor of A. Fateryga.

**Distribution.** Russia (Dagestan) (Fig. 17).

**Bionomics. Habitat.** Imagines were observed at roadsides with richly flowering ruderal herbaceous vegetation (Fig. 18f). The road was running along a water reservoir located at the bottom of a valley. The localities 1 and 2 were situated at 575 m and 550 m a.s.l. respectively, while the mountains surrounding them were significantly higher (up to approximately 1000 m a.s.l.). The slopes of these mountains were very dry and just sparsely covered with shrubs of *Paliurus spina-christi* Mill. (Rhamnaceae). Mean annual temperature is approximately 9.1 °C, mean precipitation 592 mm (calculated for the nearby village Untsukul by <https://de.climate-data.org>). At both localities, the most abundant flowering plants were *Heliotropium styligerum* Trautv. (Boraginaceae), as well as *Xanthium* sp. and *X. spinosum* L. (Asteraceae). In 2019 and 2021 neither *H. styligerum* nor the wasps were found at locality 1. The third locality was situated at 1345 m a.s.l. on a slope next to a road with very sparse vegetation. The most abundant plant species was *H. styligerum* followed by *Vicia alpestris* Steven (Fabaceae).

**Flower association.** Adults of *Celonites ivanovi* sp. nov. visited exclusively flowers of *Heliotropium styligerum*. A total of 36 females and 1 male were recorded on flowers of this plant (“first observations”). A female visiting a flower, stood on the corolla holding on to the margins or distal parts of the petals of the same or adjacent flowers of the inflorescence with her mid- and hind-legs, while her head was situated above the corolla opening. The fore-legs were on the level surface of the corolla postero-laterally to the sides of her head. Then she rapidly protruded the proboscis thereby inserting it into the corolla tube (Fig. 18a). The proboscis was partially pro- and retracted in a high frequency, accompanied by up and down movements of the head. Immediately thereafter, pollen was transferred from the proboscis to the fore-tarsi by moving the fore-legs characteristically parallel downwards from the lower part of the head towards the corolla opening along the simultaneously retracting proboscis, while mid- and hind-legs were still used to hold on to the flower (Fig. 18b, c). Then she placed her fore-legs back on the surface of the petals, postero-laterally to the sides of her head, protruded her proboscis again into the corolla tube, and the whole sequence started anew (Fig. 18d). After a few cycles of pollen removal and transfer to the fore-tarsi, she consumed the accumulated pollen from the fore-tarsi with her mouthparts. In the process the fore-legs were alternately drawn backwards through the opened mandibles from the proximal towards the distal end of the fore-tarsi (Fig. 18e). Nectar may have been collected simultaneously with pollen, since a discrete nectar collecting behaviour was not observed. A visit to a single flower usually took just some seconds. The females walked from flower to flower of a particular inflorescence visiting several flowers one after another. Females flew between inflorescences.

Flower visits were periodically interrupted by alighting on the ground. Standing on a stone a female repeatedly regurgitated and withdrew again a mass of pollen and nectar that became visible as a droplet of liquid between her mouthparts (Fig. 18g). This behaviour may have served to thicken the pollen and nectar mass. Occasionally, females that stood on the ground were observed to brush over their heads with their fore-legs (Fig. 18h).

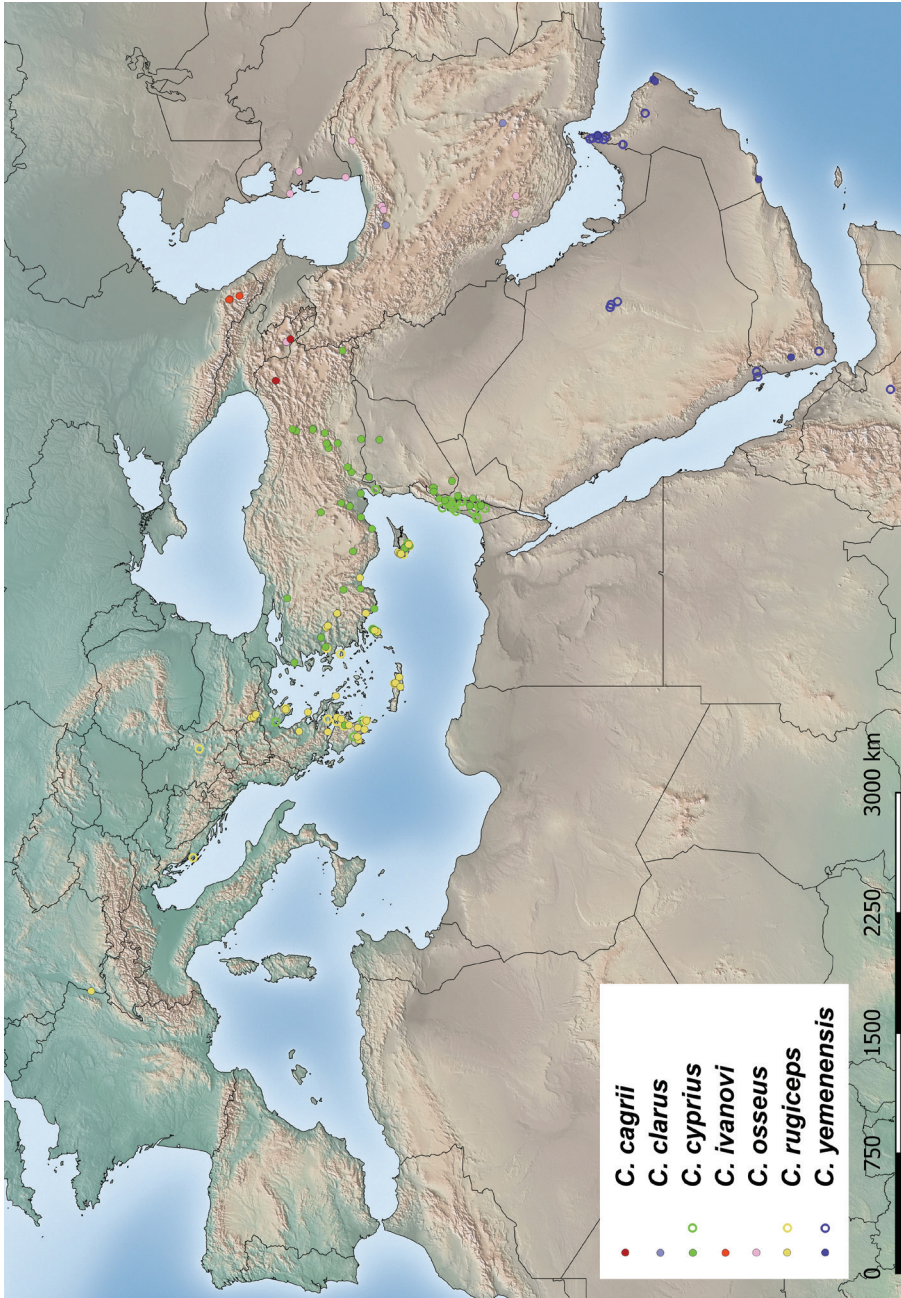


**Figure 17.** Geographic distribution of members of the *C. cyprinus*-group (full circles specimens investigated, open circles records from literature; previously published records of *C. cyprinus* from Iran and Armenia excluded; made with Natural Earth, [www.naturalearthdata.com](http://www.naturalearthdata.com)).



**Figure 18.** a–e, g, h Flower visiting behaviour of *Celonites ivanovi* sp. nov. females at flowers of *Heliotropium stylicherum* and behaviours associated with it (details see text) f habitat of *C. ivanovi* sp. nov. at locality 2 in the vicinity of Maydanskoye, Dagestan i habitat of *C. cagrii* sp. nov. near Akşar, Turkey (aspect in autumn).

**Male behaviour.** Males performed patrol flights across the area covered with *H. stylicherum* in a low constant flight. Patrolling was regularly interrupted by perching on the ground. Courtship and copulation were not observed.

## Key to the species of the *Celonites cyprius*-group

Male of *Celonites clarus* Gusenleitner, 1973 not known.

- 1 Female ..... **2**  
 – Male ..... **8**
- 2 Larger, body length approximately 7–8 mm, more sturdily built (Fig. 1). Crenulation of terga II–IV considerably stronger (Fig. 6a). Emargination between lateral lamella and postero-lateral process of propodeum in outline comparatively small, its apical end nearly circular (Fig. 7d). Gena black. ....  
 ..... ***Celonites rugiceps* Bischoff, 1928**
- Smaller, body length approximately 5–6.5 mm (Figs 1, 2). Crenulation of terga II–IV considerably weaker, sometimes almost obsolete (Fig. 6b). Emargination between lateral lamella and postero-lateral process of propodeum in outline comparatively larger, its apical end medially extended (Fig. 7a, b, e–g; except *C. cagrii* sp. nov. Fig. 7c). Gena black or with yellow marking behind compound eye ..... **3**
- 3 Postero-lateral process of propodeum with blunt apical end, outline of emargination between lateral lamella and postero-lateral process narrowly elongated (Fig. 7a). Posterior margin of sternum VI nearly transverse, with sharply bended postero-lateral corners (Fig. 8a). Mesoscutum strongly reticulate with sharply raised interstices, comb-like (Fig. 6e). Head very broad, in median 1.56 times as wide as long (1.52–1.58) (Fig. 4a) .....  
 ..... ***Celonites yemenensis* Giordani Soika, 1957**
- Postero-lateral process of propodeum and outline of emargination between lateral lamella and postero-lateral process different (Fig. 7b, c, e–g). Posterior margin of sternum VI more continuously curved, without distinct postero-lateral corners (Fig. 8b; less so in *C. cagrii* sp. nov. Fig. 8c). Mesoscutum reticulate, with interstices often less sharply raised and more bluntly rounded partly forming lines (Fig. 6c, d) or with dense macropunctuation with smooth shiny interstices (Fig. 6f). Head in some species less broad (Fig. 4c) ..... **4**
- 4 Head and especially clypeus appear less broad in frontal view, head in median 1.43 times as wide as long (1.38–1.48) (Fig. 4c). Clypeus on disk with smooth, shiny cuticula, moderately covered with fine punctures from which setae arise (Fig. 5a). Mandible on outside at base with distinct transverse depression with dull, shagreened cuticula, densely covered with pubescence of very tiny thin setae, well set off from adjacent apical smooth shiny area with few macropunctures (Fig. 5c). Fore-femur postero-ventrally only with weak carina, not produced into distinct anteriorly curved lobe in middle (Fig. 8d). Gena with extended yellow stripe behind compound eye ..... ***Celonites cyprius* Saussure, 1854**
- Head and especially clypeus appear distinctly broader in frontal view, head at least 1.45 times as wide as long (Fig. 4b, d–f). Clypeus on disk with some coarser depressions i.e. dorso-laterally, where punctures are in rows and

interstices are slightly raised forming wrinkled lines; setae arise from larger punctures (Fig. 5b). Mandible on outside at base without distinct transverse depression, basal area with shagreened cuticula extending further apically, dorsal to condylar ridge becoming distinctly longitudinally striated, basally moderately covered with pubescence of tiny thin setae (longer than in *C. cyprius*); this area contrasts to smooth shiny cuticula on condylar ridge and ventro-apical outside (Fig. 5d). Fore-femur postero-ventrally produced in middle into distinct anteriorly curved lobe that distally changes into tapering carina along ventral margin of femur (Fig. 8e, f). Gena black or with yellow marking behind compound eye..... 5

- 5 Mesoscutum with dense macropunctuation with smooth shiny interstices (Fig. 6f). A3 shorter, in median 2.1 times as long as wide (Fig. 15a). Postero-lateral process of propodeum with blunter apical end, outline of emargination between lateral lamella and postero-lateral process with narrow elongated neck (Fig. 7b). Crenulation along posterior margin of metasomal terga weak and blunt, not exceeding the lower hyaline rim of the tergum (Fig. 2). Gena with yellow marking in middle behind outside bend of compound eye and sometimes additional yellow spot close to mandible. Head very broad, in median 1.56 times as wide as long (1.55–1.56) (Fig. 4b).....

- ..... ***Celonites clarus* Gusenleitner, 1973**  
 – Mesoscutum reticulate, with distinctly raised narrow interstices partly forming lines (Fig. 6c, d). A3 longer, in median 2.5 times as long as wide (Fig. 15b). Postero-lateral process of propodeum with converging end (Fig. 7e–g). Gena black or with yellow marking..... 6

- 6 Outline of emargination between lateral lamella and postero-lateral process of propodeum with narrow short neck, its apical end small oval-shaped (Fig. 7c). Anterior pronotal carina short, forming anterior sharp edge along ventral half of crenate groove. Crenate groove straight, trough-like, its nearly vertical posterior wall separated from posterior margin of pronotum by a stripe of cuticula similarly covered with micropunctures and at same level as surface of surrounding antero-ventral area of pronotum. Bulged shiny rim of sternum VI postero-laterally strongly curved in medial direction, running obtuse to nearly transverse at posterior end resulting in blunter appearance of posterior end of sternum VI (Fig. 8c). Posterior section of bulged rim of sternum VI partly interrupted by large depressions of macropunctures (Fig. 8c). Dorso-posterior margin of sternum VI with distinct irregularly serrated crystalline horizontal lamella situated immediately above posteriorly directed stiff setae, dorso-medially fused with median spine and somewhat more protruded at postero-lateral edges (Fig. 8h, i). Light markings light yellowish-white. Head broad, in median 1.50 as wide as long (1.45–1.54) (Fig. 4f).....

- ..... ***Celonites cagrii* Mauss & Yildirim, sp. nov.**  
 – Outline of emargination between lateral lamella and postero-lateral process of propodeum with broad short neck, its apical end medially enlarged (Fig. 7f, g).

- Anterior pronotal carina starts close to posterior margin of pronotum and runs in short parabolic curve antero-laterally and then parallel to posterior margin of pronotum forming anterior margin of crenate groove. Anterior pronotal carina fairly projecting in posterior direction over anterior border of groove, especially along its ventral parabolic curve. Crenate groove posteriorly open, posteriorly adjacent cuticula gradually rising to posterior margin of pronotum. Cuticula in this lowered area differs from surrounding surface of antero-ventral area of pronotum being obliquely striated with some folds that are  $\pm$ continuing into bottom ribs of crenate groove. Bulged shiny rim of sternum VI forms regular curve postero-laterally resulting in more pointed appearance of posterior end of sternum VI (Fig. 8b). Posterior section of bulged rim of sternum VI not or barely interrupted by large depressions of macropunctures (Fig. 8b). Dorso-posterior margin of sternum VI at most with simple weak translucent cuticula crest (Fig. 8g). Light markings yellowish-white or yellow..... 7
- 7 Head in frontal view more triangular, outline of compound eye less strongly curved (Fig. 4e), in median 1.48 as wide as long (1.45–1.53). Light colouration yellowish-white, less extended, normally mesoscutum black (Fig. 6c) and outside of mid- and hind-tibia with dark ring-like markings. Dark colour of head and mesosoma deep black (Fig. 2)..... ***Celonites ivanovi* Mauss & Fateryga, sp. nov.**
- Head in frontal view more elliptic, outline of compound eye nearly semi-circular (Fig. 4d), in median 1.57 as wide as long (1.50–1.62). Light colouration more yellowish to yellow, more extended, with yellow spot on mesoscutum (Fig. 6d) and outside of mid- and hind-tibia completely yellow. Dark colour of head and mesosoma black, partly with more or less brownish to reddish shade (Fig. 2) ..... ***Celonites osseus* Morawitz, 1888**
- 8 Larger, body length approximately 7–8 mm, more sturdily built (Fig. 1). Sternum VIII semicircularly produced, not emarginated (Fig. 14a). Male genital as in Figs 10a, 11a. Harpide ventrally at base with unique ventro-medially extending sclerite (Figs 12a, 13a) ..... ***Celonites rugiceps* Bischoff, 1928**
- Smaller, body length approximately 5–6.5 mm (Figs 1, 2). Sternum VIII acutely produced, running into two tapering lobes at posterior end with deep median incision between them (Fig. 14b–f). Male genital different (Figs 10b–f, 11b–f). Harpide ventrally at base without ventro-medially extending sclerite (Figs 12b–f, 13b–f) ..... **9**
- 9 Posterior lobes of sternum VIII of medium length, wedge-shaped with acute-angled end (Fig. 14b). Male genital along posterior end of ventral plate of stipes with dense band of conspicuously long strong setae projecting well above volsella (Figs 12b, 13b). Ventral side of harpide densely covered with long setae (Figs 12b, 13b) ..... ***Celonites cyprius* Saussure, 1854**
- Posterior lobes of sternum VIII different (Figs 14c–f). Male genital on ventral plate of stipes at most with a sparse row of short setae (Figs 12c–f, 13c–f). Ventral side of harpide less densely covered with shorter setae (Figs 12c–f, 13c–f)..... **10**

- 10 Posterior lobes of sternum VIII short with blunt ending (Fig. 14c). Male genital as in Figs 10c, 11c, 12c, 13c. Lateral margin of harpide strongly and continuously concave along most of its length ..... *Celonites yemenensis* Giordani Soika, 1957
- Posterior lobes of sternum VIII long, lanceolate with pointed tip (Fig. 14d–f). Male genital as in Figs 10d–f, 11d–f, 12d–f, 13d–f. Lateral margin of harpide with concavity at most along posterior half of its length..... **11**
- 11 Male genital broader at base (Figs 10d, 11d), cupula wider, less curved (in ventral view; Figs 12d, 13d). Lateral margin of harpide without concavity near apical end, due to broad lamella along postero-lateral margin of harpide (Figs 12d, 13d). Median lobe of tergum VII broader at base between postero-lateral angles (Fig. 9c) ..... *Celonites osseus* Morawitz, 1888
- Male genital narrower at base (Figs 10e, f, 11e, f), cupula narrower, more strongly curved (in ventral view; Figs 12e, f, 13e, f). Lateral margin of harpide with shallow concavity near apical end. Median lobe of tergum VII narrower at base between postero-lateral angles (Fig. 10 d, e)..... **12**
- 12 Head in frontal view more triangular (Fig. 9a). Antennal club (A8–12) in dorsal view about 1.8–1.9 times as long as broad, asymmetrical, with evenly rounded anterior margin and weakly concave distal margin that is running obliquely upwards. At postero-distal edge distal margin curved into posterior margin forming a blunt angle (Fig. 9f); posterior margin weakly convex. Median lobe of tergum VII markedly produced, its posterior margin and adjacent posterior translucent lamella entirely convex (Fig. 9d). Sternum VIII with longitudinal depression in centre largely oval, lancet-like tips and postero-median incision between them broader (Fig. 14e). Aedoeagus with narrowly rounded distal end, its lateral sides noticeably converging. Uncus thyrsos sharp (Fig. 12e). Apodema thyrsos robust, anteriorly curved laterad (Figs 10e, 11e). Outline of emargination between lateral lamella and postero-lateral process of propodeum with broad short neck, its apical end medially enlarged (Fig. 7g). Yellowish-white stripe antero-medial on antenna restricted to A3–A7, at most with light brownish shade on adjacent proximal margin of A8..... *Celonites ivanovi* Mauss & Fateryga, **sp. nov.**
- Head in frontal view strongly oval (Fig. 9b). Antennal club (A8–12) in dorsal view about 1.68 times as long as broad, asymmetrical, with evenly rounded anterior margin and straight distal margin, that is running transverse. At postero-distal edge distal margin bent into posterior margin at nearly right angle (Fig. 9g); posterior margin nearly straight. Median lobe of tergum VII moderately produced, its posterior margin weakly concave in middle, with adjacent posterior translucent lamella fairly emarginated (Fig. 10e). Sternum VIII with longitudinal depression in centre more elongated, lancet-like tips and postero-median incision between them narrower (Fig. 14f). Aedoeagus with broadly rounded distal end, its lateral sides only weakly converging. Uncus thyrsos comparatively broad and blunt (Fig. 12f). Apodema thyrsos delicate,

anteriorly nearly straight (Figs 10f, 11f). Outline of emargination between lateral lamella and postero-lateral process of propodeum with narrow neck, its apical end small oval-shaped (Fig. 7c). Yellowish-white stripe antero-medial on antenna continues on proximal part of A8.....  
 ..... *Celonites cagrii* Mauss & Yildirim, sp. nov.

## Geographic distribution

The distribution of the members of the *C. cyprius*-group is shown in Fig. 17. All of the 20 studied specimens from collection sites in Iran and Armenia that previously had been determined as *C. cyprius smyrnensis* Richards, 1962 by J. Gusenleitner turned out to belong to *C. osseus* (dbM 4617, 5675–5679, 5778–5788) and *C. cagrii* sp. nov. (dbM 5789, 5790) respectively or even to *C. clarus* (dbM 4616). For that reason, the occurrence of *C. cyprius* is considered as doubtful in Iran and Armenia and all of the nine published records of *C. cyprius* from both countries by Gusenleitner (1973, 1997) and Ebrahimi and Carpenter (2008) were excluded from the data set. *Celonites rugiceps* seems to be absent from the whole Levant region (Fig. 17). Reinvestigation of a single specimen from Jordan (dbM 2523) previously reported by Mauss and Prosi (2013) to represent *C. rugiceps* revealed that it was misidentified and belongs to *C. cyprius* instead.

## Discussion

*Celonites cagrii* sp. nov., *C. ivanovi* sp. nov. and *C. osseus* can be assigned to *Eucelonites* and to the *Celonites cyprius*-group without contradictions since the imagines share the potential apomorphic characters of these taxa, that is the axilla is produced into a curved tapering projection which fits into a slight emargination of the tegula (Richards 1962) and the harpide has a tapering spatula-like distal end with a vertical duplication ventrally along the medial margin. Within the *Celonites cyprius*-group *C. cagrii* sp. nov., *C. ivanovi* sp. nov. and *C. osseus* are especially similar in most morphological characters. Therefore they are probably closely related and we suggest naming this group the *C. osseus*-complex. The close relationship of the members of the *C. osseus*-complex is supported by the COI-5P sequence analyses that revealed that within the *C. cyprius*-group the lowest interspecific genetic distances exist between *C. ivanovi* sp. nov. and *C. cagrii* sp. nov., while they differ from the available sequences of the other species by at least 11% (Fig. 16). However, the COI-5P gene sequence of *C. osseus* is still unknown, so that the close relationship of *C. osseus* to *C. cagrii* sp. nov. and *C. ivanovi* sp. nov. deduced from morphological data cannot be proved genetically at the moment.

*Celonites osseus* differs from *C. cagrii* sp. nov. and *C. ivanovi* sp. nov. in the shape of the harpides and the base of the male genital which is associated with different proportions of tergum VII and sterna VII+VIII of the males. Differences between *C. cagrii* sp. nov. and *C. ivanovi* sp. nov. exist in the form of the male antennal club, the proportions

of tergum VII and sternum VIII, as well as some structures of the aedeagus. All of these characteristics can be assumed to be associated with mating behaviour in *Celonites* (cf. Mauss 2006; Mauss and Müller 2014). Thus it can be hypothesized that the dissimilarity between these traits functions as a reproductive isolation mechanism between the taxa so that they probably constitute different biospecies *sensu* Mayr (1967). This hypothesis is corroborated by the measured mean interspecific genetic distance between *C. cagrii* sp. nov. and *C. ivanovi* sp. nov. of more than 7%. In Central European Apoidea and Vespoidea a level of COI sequence divergence exceeding 2% commonly signals different species, although there are a few exceptions in which maximum intraspecific genetic distances of up to 13.1% are not correlated with equally pronounced morphological characters (Schmidt et al. 2015; Schmid-Egger and Schmidt 2021).

Besides other morphological characteristics many species of the *C. cyprius*-group vary in the shape of the postero-lateral process and the lateral lamella of the propodeum resulting in different outlines of the emargination between them. Species specific differences in the shape of the postero-lateral part of the propodeum were already observed between *C. cyprius*, *C. rugiceps* and *C. clarus* (Richards 1962; Gusenleitner 1973), and also exist among another four Palearctic (Gusenleitner 1973) and four Afrotropical species of *Celonites* (Gess 2007). The function of this structure is unknown and therefore its contribution to reproductive isolation is unclear. Nevertheless, the repeated observation of species-specific differences in the postero-lateral part of the propodeum within *Celonites* suggests that the distinct structures are associated with an unknown mechanism of reproductive isolation or niche segregation. Hence, it is of note that *C. cagrii* sp. nov. differs distinctly in this character from *C. ivanovi* sp. nov. and *C. osseus* that, for their part, resemble *C. cyprius*.

The relation of *Celonites clarus* to the *C. cyprius*-group is still unresolved. It is only known from the type series collected near Teheran (Gusenleitner 1973; Rahmani et al. 2020) and the single female from Kerman province in south-east Iran assigned to this species in this study. In accordance with the description by Gusenleitner (1973) this female and two investigated paratype specimens differ distinctly from all other members of the *C. cyprius*-group in the structure of the cuticula on frons and mesoscutum and the unique postero-lateral part of the propodeum. On the other hand, *C. clarus* is otherwise quite similar to the members of the *C. osseus*-complex apart from having comparatively shorter antennae and a weaker or even absent crenulation along the posterior margins of the metasomal terga. Since the male of *C. clarus* is still unknown and genetic data are unavailable, the position of the taxon within *Eucelonites* remains uncertain and should be reinvestigated with care, when more material becomes available.

*Celonites ivanovi* sp. nov. and *C. cagrii* sp. nov. were exclusively recorded from flowers of different *Heliotropium* species. This corresponds to other members of the *C. cyprius*-group for which flower visiting records are available, that is *C. cyprius* and *C. rugiceps*, that were also found at flowers of various *Heliotropium* plants (Richards 1962; Mauss pers. obs.). The behaviour of *C. ivanovi* sp. nov. during pollen uptake from *H. styligerum* flowers is very similar to the behaviour of *C. cyprius* and *C. rugiceps* at flowers of other *Heliotropium* species (Mauss pers. obs.). Therefore, it is probably homologous.

The geographic range of *Celonites osseus* is similar to Iranian faunal elements *sensu* Lattin (1967). The adjacent small and probably endemic distribution areas of the closely related *C. ivanovi* sp. nov. and *C. cagrii* sp. nov. on the northern side of the Greater Caucasus and in East-Anatolia and Armenia respectively can be hypothesized to be relicts of a previous interglacial range expansion of their last common ancestor shared with *C. osseus*. In the following glacial epoch, range regression probably resulted in geographic isolation of small relict populations that evolved into separate biospecies. Postglacially *C. ivanovi* sp. nov. and *C. cagrii* sp. nov. remained in their glacial refuges, while *C. osseus* expanded its range again. The other species of the *C. cyprius*-group can also be assigned to different glacial refuges *sensu* de Lattin (1967) with *C. rugiceps* and *C. cyprius* being of Ponto-Mediterranean origin, while *C. yemenensis* has a distinct Syroeremial distribution and *C. clarus* seems to represent the Iranoeremial type. This distribution pattern indicates that speciation within the *C. cyprius*-group was most likely influenced by geographic isolation during glacial periods. The sympatric occurrence of *C. cyprius* with *C. rugiceps* in the west and of *C. osseus* with *C. clarus* in the east implies that some kind of niche segregation evolved between these taxa.

Just three species of pollen wasps (all in the genus *Celonites*) were previously known from Russia (Antropov and Fateryga 2017; Fateryga 2020). The present contribution increases this number to four. Since the known distribution ranges of *C. ivanovi* sp. nov. and *C. cagrii* sp. nov. are very restricted, both species may be endangered. Therefore, a systematic search for further localities of *C. ivanovi* sp. nov. in the Caucasus or *C. cagrii* sp. nov. in East Anatolia and Armenia should be carried out in suitable habitats with occurrence of *Heliotropium* plants.

## Acknowledgments

Sergey A. Belokobylskij and Yulia V. Astafurova supported the second author during his work in ZISP. Rainer Prosi kindly prepared the distribution map from our records. Christian Schmid-Egger and Stefan Schmidt provided COI Sequences of eight specimens of the *C. cyprius*-group for analysis. A. Rosenbauer identified the *Heliotropium* species from Turkey. C. Schmid-Egger, J. Gusenleitner, M. Uliana, E. Ockermüller kindly provided material from their private collections or public collections under their care. The useful and encouraging reviews by Jack Neff and Andreas Müller are sincerely acknowledged.

The work of A.V. Fateryga was a part of the State research project No. 121032300023-7.

## References

- Antropov AV, Fateryga AV (2017) Family Vespidae. In: Lelej AS, Proshchalykin MY, Loktionov VM (Eds) Annotated Catalogue of the Hymenoptera of Russia. Volume I. Symphyta and Apocrita: Aculeata. Proceedings of the Zoological Institute RAS, Supplement 6: 175–196. <https://doi.org/10.31610/trudyzin/2017.supl.6.5>

- Birket-Smith SJR (1981) The male genitalia of Hymenoptera – a review based on morphology in Dorylidae (Formicidae). *Entomologica Scandinavica Supplement* 15: 377–397.
- Bischoff H (1928) Hymenoptera (Vespidae, Scoliidae, Mutillidae, Chrysididae und Evaniidae). In: Roewer CF (Ed.) *Zoologische Streifzüge in Attika, Morea und besonders auf der Insel Kreta. II. Abhandlungen des Naturwissenschaftlicher Verein zu Bremen* 27: 85–90.
- Blüthgen P (1952) Weitere neue oder bemerkenswerte paläarktische Faltenwespen aus der Zoologischen Staatssammlung in München (Hym., Eumenidae, Masaridae). *Mitteilungen der Münchener Entomologischen Gesellschaft* 42: 1–19.
- Bytynski-Salz H, Gusenleitner J (1971) The Vespoidea of Israel (Hymenoptera). *Israel Journal of Entomology* 6: 239–299.
- Carpenter JM (1988) The phylogenetic system of the Gayellini (Hymenoptera: Vespidae; Masarinae). *Psyche* 95: 211–241. <https://doi.org/10.1155/1988/45034>
- Carpenter JM (1993) Biogeographic patterns in the Vespidae (Hymenoptera): two views of Africa and South America. In: Goldblatt P (Ed.) *Biological relationships between Africa and South America*. Yale University Press, New Haven, 139–155. <https://doi.org/10.2307/j.ctt22726mc.11>
- Carpenter JM (2001) Checklist of species of the subfamily Masarinae (Hymenoptera: Vespidae). *American Museum Novitates* 3325: 1–40. [https://doi.org/10.1206/0003-0082\(2001\)325%3C0001:COSETS%3E2.0.CO;2](https://doi.org/10.1206/0003-0082(2001)325%3C0001:COSETS%3E2.0.CO;2)
- de Lattin G (1967) *Grundriß der Zoogeographie*. Gustav Fischer, Stuttgart, 602 pp.
- Dönmez A (2008) *Heliotropium samoliflorum* subsp. *erzurumicum* (Boraginaceae), a new subspecies from Turkey. *Annales Botanici Fennici* 45: 396–399. <https://doi.org/10.5735/085.045.0509>
- Ebrahimi E, Carpenter JM (2008) Catalog of the vespid wasps of Iran (Hymenoptera, Vespidae). *Zootaxa* 1785: 1–42. <https://doi.org/10.11646/zootaxa.1785.1.1>
- Eck R (1978) Biometrische Untersuchung zur Klärung der Artunterschiede bei sozialen Faltenwespen (Hymenoptera: Vespidae). *Entomologische Abhandlungen des Staatlichen Museums für Tierkunde Dresden* 42: 315–344.
- Fateryga AV (2020) New records of *Celonites kozlovi* Kostylev, 1935 and *C. sibiricus* Gusenleitner, 2007 (Hymenoptera: Vespidae: Masarinae), with observations on their behavior at flowers. *Far Eastern Entomologist* 405: 20–32. <https://doi.org/10.25221/fee.405.4>
- Gess FW (2007) Four new species of the wasp genus *Celonites* Latreille, 1802 (Hymenoptera: Vespidae: Masarinae) from south-western Africa, designation of neotype for *C. michaelsoni* von Schulthess, 1923, species representation in Namibia, and key to species occurring in Namibia. *Journal of Hymenoptera Research* 16: 11–29.
- Gess SK, Gess FW (2010) Pollen wasps and flowers in Southern Africa. *South African National Biodiversity Institute, Pretoria, SANBI Biodiversity Series* 18, 147 pp.
- Giordani Soika A (1957) Hymenoptera: Vespidae. In: *Expedition to South-West Arabia 1937–1938. Volume 1*. British Museum (Natural History), London, 471–484. [6 figs]
- Grossheim AA (1967) *Flora Kavkaza [Flora of the Caucasus]*. Second edition. Volume VII. Nauka, Leningrad, 894 pp. [In Russian]
- Gusenleitner J (1966) Vespidae, Eumenidae und Masaridae aus der Türkei. Teil I. *Polskie Pismo Entomologiczne* 36: 343–363.
- Gusenleitner J (1973) Über Masaridae aus dem nahen Osten (Vespoidea, Hymenoptera). *Bolletino della Museo Civico di Storia Naturale di Venezia* 24: 55–69.

- Gusenleitner J (1997) Die europäischen Arten der Gattung *Celonites* Latreille 1802 (Hymenoptera, Masaridae). Linzer Biologische Beiträge 29: 109–115.
- Gusenleitner J (2002) Neue oder bemerkenswerte Vespoidea aus dem Nahen Osten (Hymenoptera: Eumenidae, Masaridae). Linzer Biologische Beiträge 34: 335–343.
- Gusenleitner J (2005) Über Faltenwespen aus dem Oman Teil 2 (Hymenoptera, Vespidae, Eumenidae, Masaridae). Linzer Biologische Beiträge 37: 1199–1201.
- Gusenleitner J (2007) Eine neue *Celonites*-Art aus Sibirien (Hymenoptera: Vespidae, Masarinae). Linzer Biologische Beiträge 39: 133–135.
- Gusenleitner J (2010) Order Hymenoptera, family Vespidae. Arthropod fauna of the UAE 3: 422–467.
- Gusenleitner J (2012) Neue Masarinae aus der paläarktischen Region (Hymenoptera: Vespidae: Masarinae). Linzer Biologische Beiträge 44: 319–326.
- Gusenleitner J (2018) Neue asiatische Faltenwespen (Hymenoptera, Vespidae: Eumeninae, Masarinae). Linzer Biologische Beiträge 50: 303–308.
- Kostylev G (1935) Materialien zur Kenntnis der Masariden-Fauna der Paläarktis. Archives du Musée Zoologique de l'Université de Moscou 2: 85–116. [In German and Russian]
- Krenn HW, Mauss V, Plant JD (2002) Evolution of the suctorial proboscis in pollen wasps (Masarinae, Vespidae). Arthropod Structure and Development 31: 103–120. [https://doi.org/10.1016/s1467-8039\(02\)00025-7](https://doi.org/10.1016/s1467-8039(02)00025-7)
- Mauss V (2006) Observations on flower association and mating behaviour of the pollen wasp species *Celonites abbreviatus* (Villers, 1789) in Greece (Hymenoptera: Vespidae, Masarinae). Journal of Hymenoptera Research 15: 266–269.
- Mauss V (2013) Description of *Celonites andreasmuelleri* sp. n. (Hymenoptera, Vespidae, Masarinae) from the Middle East with a key to the Palaearctic species of the *C. abbreviatus*-complex of the subgenus *Celonites* s. str. Journal of Hymenoptera Research 31: 79–95. <https://doi.org/10.3897/JHR.31.4235>
- Mauss V, Fateryga AV, Prosi R (2016) Taxonomy, distribution and bionomics of *Celonites tauricus* Kostylev, 1935, stat. n. (Hymenoptera, Vespidae, Masarinae). Journal of Hymenoptera Research 48: 33–66. <https://doi.org/10.3897/JHR.48.6884>
- Mauss V, Müller M (2014) First contribution to the bionomics of the pollen wasp *Celonites fischeri* Spinola, 1838 (Hymenoptera, Vespidae, Masarinae) in Cyprus. Journal of Hymenoptera Research 39: 119–153. <https://doi.org/10.3897/JHR.39.7841>
- Mauss V, Prosi R (2013) First record of the pollen wasp *Celonites rugiceps* Bischoff 1928 (Hymenoptera, Vespidae, Masarinae) from Central Europe. Linzer Biologische Beiträge 45: 697–701.
- Mauss V, Prosi R (2018) Identity and distribution of *Celonites hermon* Gusenleitner, 2002 (Hymenoptera, Vespidae, Masarinae) from the Middle East with a description of the hitherto unknown male. Journal of Hymenoptera Research 66: 55–70. <https://doi.org/10.3897/jhr.66.29795>
- Mayr E (1967) Artbegriff und Evolution. Paul Parey, Hamburg, 617 pp.
- Morawitz F (1888) Hymenoptera aculeata nova. Horae Societatis Entomologicae Rossicae 22: 224–302.
- Rahmani Z, Rakhshani E, Carpenter JM (2020) Updated Checklist of Vespidae (Hymenoptera: Vespoidea) in Iran. Journal of Insect Biodiversity and Systematics 6: 27–86. <http://zoobank.org/References/084E3072-A417-4949-9826-FB78E91A3F61>

- Richards OW (1962) A revisional study of the masarid wasps (Hymenoptera, Vespoidea). British Museum of Natural History, London, 294 pp.
- Richards OW (1984) Insects of Saudi Arabia. Hymenoptera: Fam. Masaridae (the Arabian species). Fauna of Saudi Arabia 6: 413–422.
- Schmid-Egger C (2017) Order Hymenoptera, family Vespidae. Subfamily Masarinae. In: van Harten A (Ed.) Arthropod fauna of the UAE. Volume 6. Department of The President's Affairs, Abu Dhabi, 341–349.
- Schmid-Egger C, Schmidt S (2021) Unexpected diversity in Central European Vespoidea (Hymenoptera, Mutillidae, Myrmosidae, Sapygidae, Scoliidae, Tiphiidae, Thynnidae, Vespidae), with description of two species of *Smicromyrme* Thomson, 1870. ZooKeys 1062: 49–72. <https://doi.org/10.3897/zookeys.1062.70763>
- Schmidt S, Schmid-Egger C, Morinière J, Haszprunar G, Hebert PDN (2015) DNA barcoding largely supports 250 years of classical taxonomy: identifications for Central European bees (Hymenoptera, Apoidea partim). Molecular Ecology Resources 15: 985–1000. <https://doi.org/10.1111/1755-0998.12363>
- Snelling RR (1986) The taxonomy and nomenclature of some Australian paragiine wasps (Hymenoptera, Masaridae). Los Angeles County Museum of Natural History Contributions in Science 378: 1–19. <https://doi.org/10.5962/p.208122>

## Supplementary material I

### Supplementary material

Authors: Volker Mauss, Alexander V. Fateryga, Erol Yildirim, James M. Carpenter

Data type: investigated specimens, published records, localities

Explanation note: List of all specimens, published records and localities included in the study.

Copyright notice: This dataset is made available under the Open Database License (<http://opendatacommons.org/licenses/odbl/1.0/>). The Open Database License (ODbL) is a license agreement intended to allow users to freely share, modify, and use this Dataset while maintaining this same freedom for others, provided that the original source and author(s) are credited.

Link: <https://doi.org/10.3897/jhr.89.79832.suppl1>



# All-day activity of *Dolichovespula saxonica* (Hymenoptera, Vespidae) colonies in Central Finland

Atte Komonen<sup>1</sup>, Jyrki Torniainen<sup>2</sup>

**1** Department of Biological and Environmental Science, P.O. Box 35, FI-40014 University of Jyväskylä, Jyväskylä, Finland **2** Open Science Centre, P.O. Box 35, FI-40014 University of Jyväskylä, Jyväskylä, Finland

Corresponding author: Atte Komonen ([atte.komonen@jyu.fi](mailto:atte.komonen@jyu.fi))

Academic editor: Michael Ohl | Received 13 December 2021 | Accepted 11 February 2022 | Published 28 February 2022

<http://zoobank.org/A3F4DE21-BFF0-4F38-8E8C-832DAB2A28C8>

**Citation:** Komonen A, Torniainen J (2022) All-day activity of *Dolichovespula saxonica* (Hymenoptera, Vespidae) colonies in Central Finland. Journal of Hymenoptera Research 89: 157–170. <https://doi.org/10.3897/jhr.89.79306>

## Abstract

In social vespid wasps, colony activity varies at many temporal scales. We studied the peak season activity (number of individuals entering the nest per min) of colonies of the social vespine wasp *Dolichovespula saxonica* in its native range in boreal Finland. Six colonies were monitored non-stop for a full day, starting before sunrise and ending after sunset. Shorter monitoring was carried out before and/or after the full-day monitoring. All colonies were active before sunrise and after sunset, and the overall activity was positively linked with colony size. Activity showed irregular minute-to-minute cycles in all colonies. The broader within-day dynamics were idiosyncratic among the colonies: activity varied generally between 40–100% of the peak, there were usually a few peaks per day, and the timing of the peaks varied. Ambient temperature was not related to activity dynamics consistently. Our study provides high-resolution information about the all-day activity of *D. saxonica* and underscores high among-colony variability in the dynamics of vespine wasps.

## Keywords

Nest activity, social wasps, time series, traffic rate, Vespinae

## Introduction

In social vespid wasps, colony or nest activity varies at many temporal scales: within and between days, as well as over seasons. It is well established that the consistent seasonal change in the overall activity of successful colonies is largely related to change in colony size (Kasper 2004; Archer 2012). More intriguing is the within-day variation in

activity, which apparently is linked to environmental conditions (Kasper et al. 2008) and workers' allocation of time to different activities, such as foraging and nest maintenance (Archer 2000a, 2004). Knowledge on colony activity and its variation in different environments are biologically interesting as such, provide fundamental background for other research tasks, and are needed for effective monitoring and management of wasp populations (e.g. in estimating colony size).

Colony activity can be divided in two interrelations: activity inside and outside of the nest. Studies on outside activity generally focus on flight activity, which is measured as traffic rate (i.e. the number of incoming and/or outgoing wasps). Colony-specific traffic rate and its daily variation are influenced by the developmental stage of the colony, ambient environmental conditions and time of day (Kasper et al. 2008; Archer 2012). There are also interspecific differences in overall activity of mature colonies, largely due to differences in colony sizes, but interspecific differences in within-day dynamics are poorly known. The extant studies monitored the within-day activity only for a limited and/or discontinuous time (Gaul 1952a; Potter 1964; Akre et al. 1982; Heinrich 1984; Archer 2000a, 2004; Kasper 2004), and thus were not able to capture the detailed dynamics and provide comprehensive time series analysis. Also, some older studies have studied only one colony, so it has been impossible to conclude anything general about the within-day dynamics.

Most studies on colony activities of Vespinae have focused on *Vespula* (Archer 2012); in fact, we are only aware of two activity studies of *Dolichovespula* (Brian and Brian 1952; Heinrich 1984). Furthermore, vespid activities have been little studied in the boreal region (but see Pallet and Plowright 1979), which differs from temperate and tropical regions in terms of macroclimate and photoperiodism, day length in summer in particular. Because wasp activity is closely linked with the intensity and duration of daylight as well as weather (Gaul 1952a; Potter 1964; Kasper et al. 2008; Kelber et al. 2011), within-day activity of colonies may vary in different regions. Some studies on colony activity have been done with laboratory colonies of *Vespula* (e.g. Gaul 1952a; Potter 1964; Roland and Horel 1976; Vetter and Visscher 1995), which again may lead to false generalisation to natural colonies and to *Dolichovespula*.

In boreal and temperate climates, vespid colonies are annual, each founded by a single queen (Archer 2012). The Saxon wasp, *Dolichovespula saxonica* (F., 1793), is a widespread and abundant species in Finland. It constructs aerial, free-hanging nests, which are often in buildings, cavities or bird nest boxes (Pawlikowski and Pawlikowski 2010; Archer 2012; Nadolski 2012; Broughton et al. 2015). Colonies of *Dolichovespula* (incl. *D. saxonica*) are smaller (a few hundred workers) and colony cycle is shorter than those of *V. vulgaris* (L.) and *V. germanica* F. (Douwes et al. 2012). In Finland, the colony size of *D. saxonica* typically peaks from mid-July to mid-August (Douwes et al. 2012; pers. obs.).

We studied the all-day activity of *D. saxonica* colonies in the native range of the species in boreal Finland at peak season. Flight activity was measured as traffic rate (number of ingoing individuals) with one-minute accuracy, which allowed to examine high-resolution variation in activity. We asked: 1) are the traffic rates and traffic rate dynamics similar or idiosyncratic among colonies; 2) what are the characteristics of

the traffic-rate time series; and 3) does ambient temperature influence within-day dynamics? To understand among-colony variation in traffic rate, nest characteristics and parasitism were recorded.

## Methods

### Study area and nests

The study was conducted in Jyväskylä, Central Finland, which belongs to the middle boreal zone. The studied wasp nests ( $n = 6$ ) were inside wooden bird nest boxes (1.3–2.0 m above ground; Suppl. material 1: Table S1) in semiurban broadleaved forests, 130 m to 3.5 km from each other. Wasp nests in bird nest boxes were selected, because they were easy to find and monitor, and nest boxes provide similar conditions, thus increasing comparability among nests. During monitoring, ambient temperature (8.8–28.5 °C; Suppl. material 1: Table S1) was between 2 °C and 35 °C, which are the thresholds necessary for foraging of some *Vespula* and *Dolichovespula*, and presumably close to the thresholds for *Dolichovespula saxonica* (Gaul 1952a; Blackith 1958; Potter 1964; Heinrich 1984; pers. obs.).

To allow re-monitoring, the nests were removed, dissected and their characteristics were recorded some weeks after the full-day monitoring (Suppl. material 1: Table S1). Because the nests were close to their peak size during the main monitoring, the measured characteristics represent well the situation during monitoring. Even if this would not be the case, it would only affect the correlation analysis between the nest size and mean traffic rate. The basal comb consisted always of small cells and the last, outermost comb of large cells. Because the in-between combs consisted of mixed large, intermediate and small cells, which were difficult to separate (see also Greene et al. 1976; Archer 2012), we do not provide separate counts of small and large cells. This should not affect our conclusions, because the number of small and large cells correlate in mature successful colonies (Archer 1981). The studied colonies were successful as they produced males and/or queens.

### Monitoring

In all nests, we and nine assistants did one non-stop, full-day monitoring close to the peak activity of the season (14 August 2020 in one nest and 14–23 July 2021 in five nests; hereinafter peak season). Peak season was determined based on a few shorter midday monitoring (Suppl. material 1: Fig. S1). Two of these nests were re-monitored for a full day 14 and 15 days later, and one nest for shorter time; we also aimed to re-monitor the other nests but their activity ceased. Each observer monitored the nest continuously for two hours. The full-day monitoring started at ( $n = 1$ ), or before ( $n = 7$ ; med. = 17 minutes, min.–max. = 4–41 minutes), sunrise and continued as long as wasps were active (med. = 55 minutes after sunset; min.–max. = 14–87 minutes); monitoring was done visually with a stopwatch. Colony activity was measured as the

number of individuals returning to the nest per minute (hereinafter traffic rate; see Vetter and Visscher 1995; Archer 2000a; Kasper 2004; see Gaul 1952a for discussion on using uni- vs. bidirectional traffic). During monitoring typical weather varied from half cloudy to sunny, was rainless, and the wind force at the ground level was calm to moderate breeze. In one nest (Sippula), there were 20 minutes of drizzle rain and a few stronger breezes during monitoring. Ambient temperature was recorded a few meters from the nests, 0.5–1.5 meters above the ground every half an hour, using a digital thermometer (model 210 by Suomen lämpömittarit Oy; measuring accuracy 0.1 °C) that was in the same place all day.

## Statistics

Traffic rates were expressed and analysed as individuals per minute, except in figures where longer time periods were needed for illustrative reasons. For example, within-day activity was illustrated using centered moving averages, calculated over seven 5-min periods (i.e. 35 min). Odd number of 5-min periods was used for illustrative reasons, and the 35-min moving average was used because it adequately smoothed the data and revealed underlying trends. The average full-day traffic rates were calculated between sunrise and sunset. Coefficient of Variation (**CV**) and autocorrelation analysis were used to describe variation in traffic rates. There were only 12 minutes of missing data, which were replaced with the data immediately before the gap. Linear regression was used to analyse the relationship between the mean traffic rate and colony size, and between the mean traffic rate and its variation (CV).

To identify patterns in the sequence of traffic rates over time, we used an autocorrelation analysis. First, sequence plots and the augmented Dickey-Fuller Test (**ADF**), as well as autocorrelation and partial autocorrelation plots (with a maximum number of lags = 30) were used to detect trends and seasonal effects in the time series. For subsequent autocorrelation analyses trends were removed by transforming the data using differencing ( $d = 1$ ), i.e. making the time series stationary. Transformation was needed to analyse patterns in the fine-scale, minute-to-minute variation in traffic rates.

To analyse the relationship between temperature and within-day traffic rate dynamics (i.e. the broad variation in the mean traffic rate over day), we used the Expert Modeler option in SPSS, which automatically identifies and estimates the best-fitting ARIMA or exponential smoothing models; only non-seasonal models were considered. Because temperature was measured at 30-min intervals, we made it continuous by replacing missing values using linear interpolation. In the Expert Modeler, the final model only includes those independent variables, which have a significant relationship with the dependent series. Model fit was judged by the non-significance of the Ljung-Box statistic and visual judgement of the residual autocorrelation plots; in Sippula, the non-significance was reached after automatic removal of outliers. No transformations were used.

All analyses were conducted with IBM Statistics SPSS 26.0, except the augmented Dickey-Fuller Test which was conducted with RStudio Version 1.3.1093 (library 'tseries').

## Results

During the peak season, *D. saxonica* flight activity started about half an hour before sunrise and increased sharply, whereas the evening decline was more variable (from sharp to gradual) and ended 28–77 minutes after sunset (Figs 1–8). Overall, *D. saxonica* colonies made an average of 3958 (1074–9140) trips per nest and day. The mean sunrise-to-sunset traffic rate among nests varied from 1.1 to 7.2 wasps per minute (Table 1). The number of combs varied from 3 to 7, and the total number of cells from 525 to 1784. Traffic rate was positively related to the total number of cells and combs (linear regression:  $r = 0.97$ ,  $r^2 = 0.95$ ,  $p = 0.001$ , and  $r = 0.89$ ,  $r^2 = 0.79$ ,  $p = 0.018$ , respectively,  $n = 6$ ), but not to the number of cells in the basal comb ( $r = 0.50$ ,  $r^2 = 0.25$ ,  $p = 0.32$ ).

**Table 1.** Traffic rates (number of individuals entering per minute) for the studied *Dolichovespula saxonica* colonies in Central Finland from sunrise to sunset, and colony size.

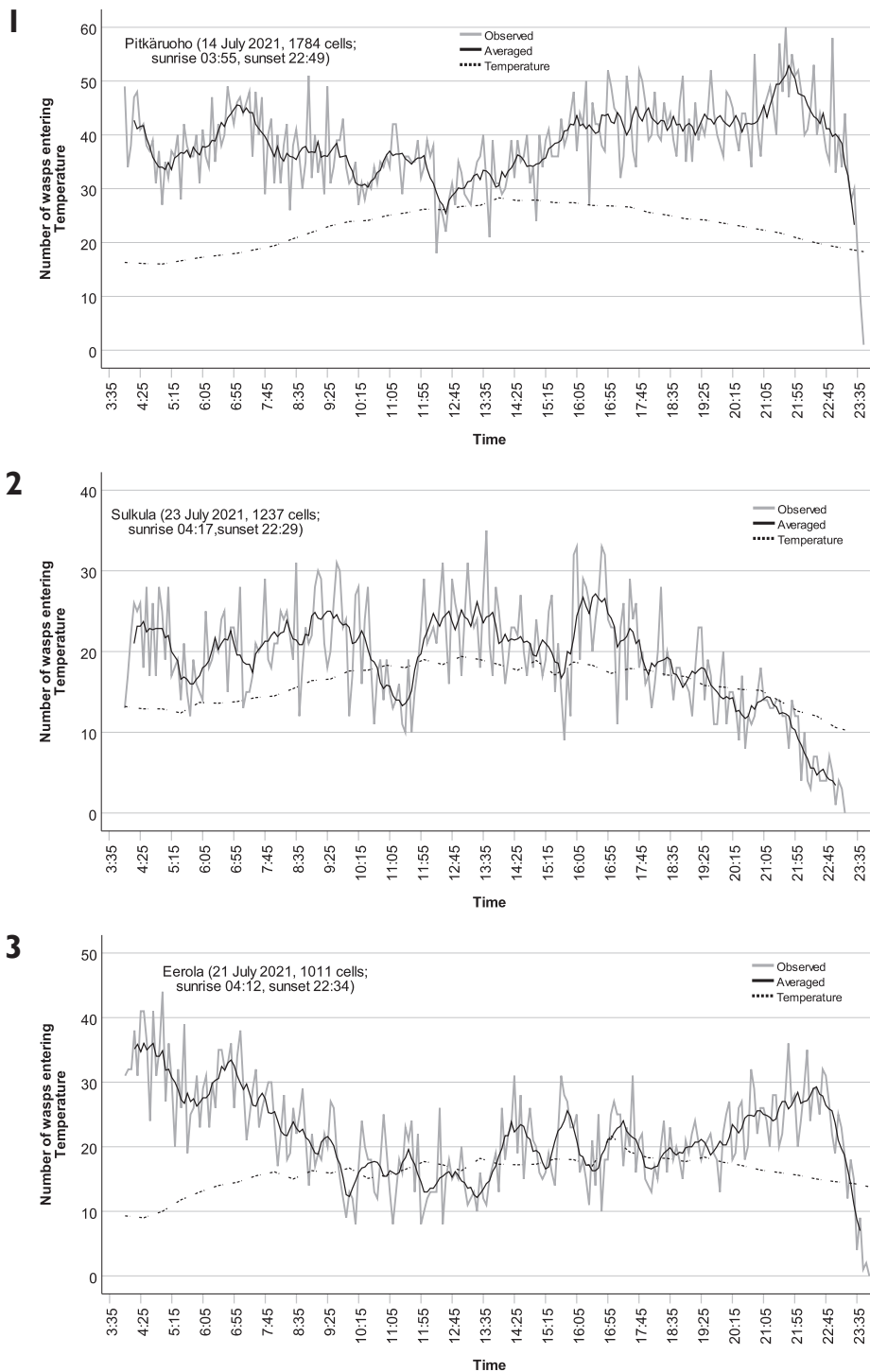
Colony	Med.	Mean	SD	CV%	Min	Max	Sum <sup>†</sup>	# of combs	# of cells
Pitkäruoho	8.0	7.76	2.80	36	0	22	8789	7	1784 <sup>‡</sup>
Sulkula	4.0	3.91	2.16	55	0	12	4279	5	1237
Eerola	4.0	4.41	2.34	53	0	16	4859	4	1011
Sippula	2.0	2.18	1.63	75	0	13	2396	3	662
Haukanniemi	1.0	1.07	1.08	101	0	6	1037	4	585
Siirtola	1.0	1.28	1.10	87	0	5	1439	3	525 <sup>‡</sup>
Sulkula re-measured	1.0	1.44	1.29	90	0	9	1456		
Eerola re-measured	1.0	1.55	1.53	98	0	10	1585		

<sup>†</sup>Total number of trips from sunrise to sunset; <sup>‡</sup>Estimated, see Suppl. material 1: Table S1.

The overall level of variation in the 35-minute traffic rate differed among nests (CV% min-max = 36–101; Table 1), and the higher the mean daily traffic rate, the lower the CV% (linear regression:  $r = 0.94$ ,  $r^2 = 0.89$ ,  $n = 8$ ,  $p < 0.001$ ). In all nests, the traffic rate was non-stationary, i.e. the mean varied during the day (Figs 1–8). Visual judgement of non-stationarity was supported by the ADF-test in all nests (ADF  $> -3.06$ ,  $p > 0.11$ , lag order = 30; ADF =  $-3.40$ ,  $p = 0.054$ , lag order = 45 in Sippula).

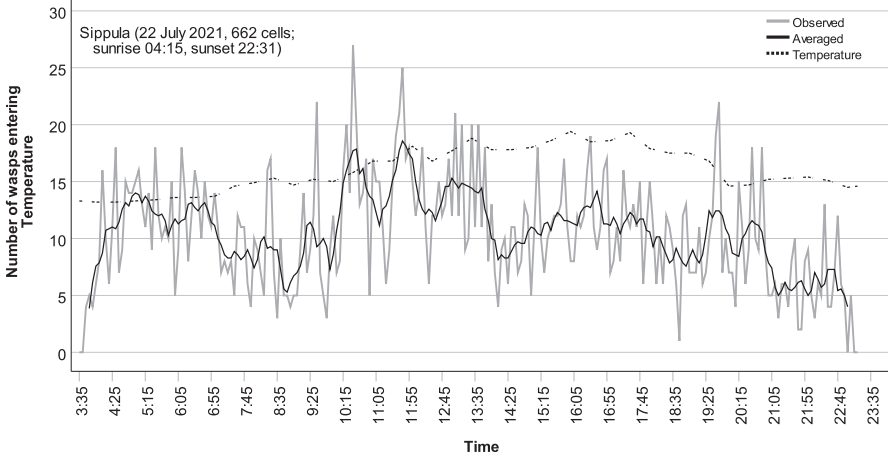
The number and timing of the peaks and lows varied among nests, and the lows of the 35-min moving average were generally about 40% of the peak (Figs 1–8). This broad variation in the mean within-day traffic rate was related to the ambient temperature only in Eerola and Siirtola but in opposite direction (Figs 1–8; Suppl. material 1: Table S2). There was also irregular cyclicity in minute-to-minute traffic rates (ACF =  $-0.52$  to  $-0.46$ ,  $p < 0.05$  at lag = 1; Suppl. material 1: Figs S2, S3).

Parasitism rate was low. No parasitoids or parasites were found in two nests. Eight cocoons of *Sphexophaga vesparum* (Curtis) (Hymenoptera: Ichneumonidae) were found in one nest, which is only 0.8% of the total number of cells. Larvae of *Aphomia sociella* (Linnaeus) (Lepidoptera: Pyralidae) were found in three nests (2, 25 and 94 individuals). (Suppl. material 1: Table S1.)

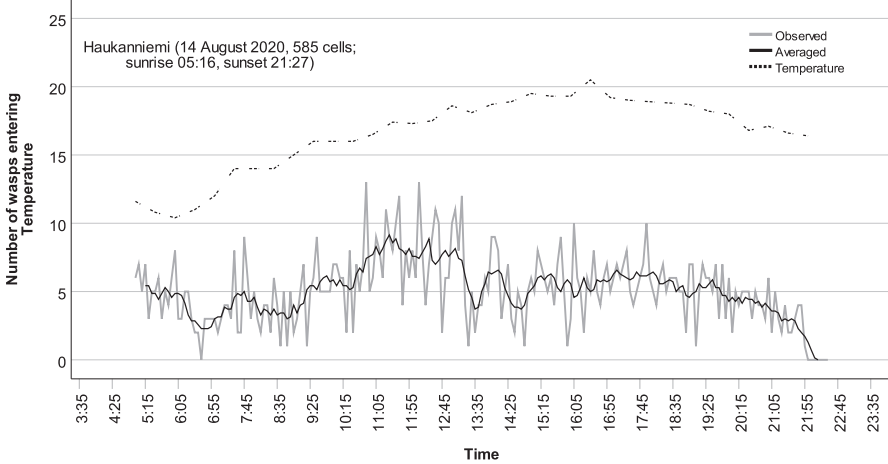


**Figures I–8.** Observed number of *Dolichovespula saxonica* individuals entering the nest per 5 min, the 35-min centered moving average, and ambient temperature (°C).

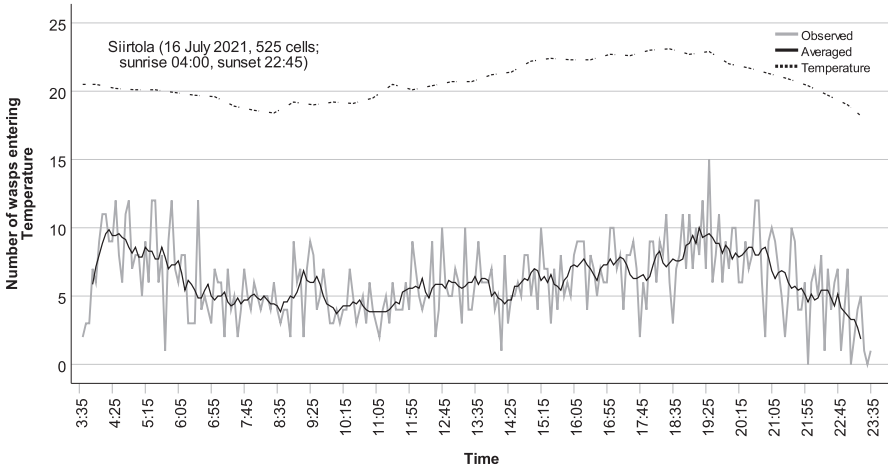
4



5

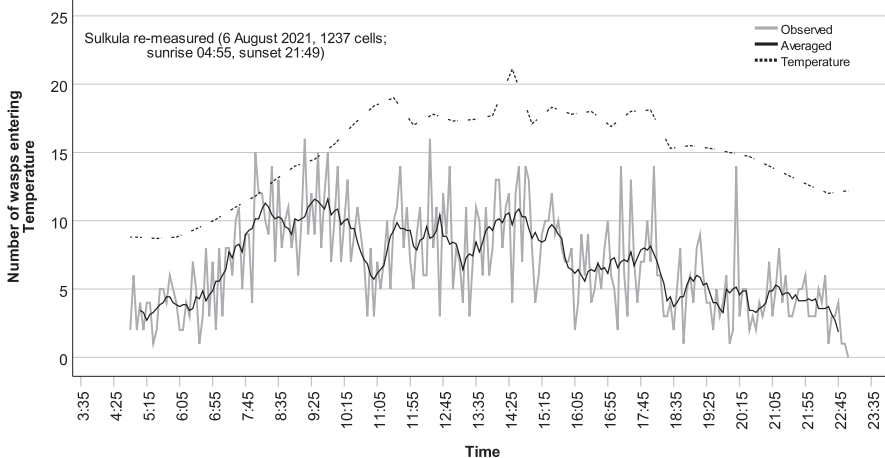


6

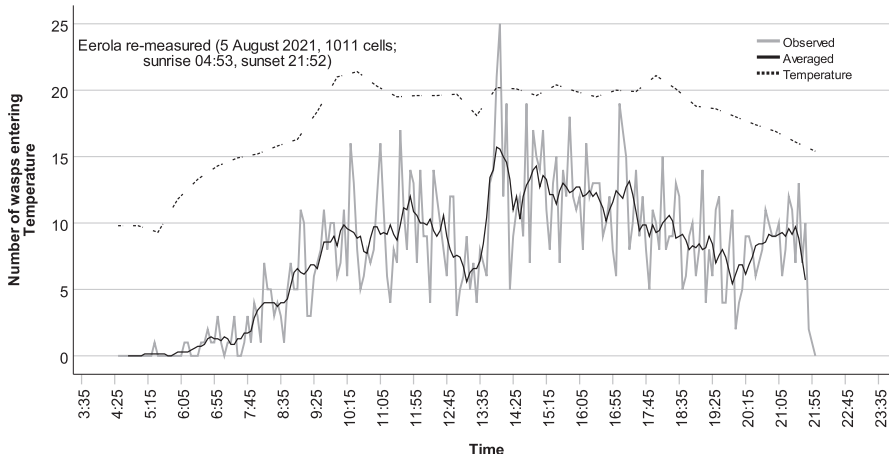


Figures I-8. Continued.

7



8



Figures 1–8. Continued.

The mean daily traffic rate as well as traffic rate dynamics changed over season. Those two nests, which were re-monitored for a full day later in the season, had then a lower traffic rate, different timing of peaks and showed a more gradual increase (over 2 to 3 hours) after sunrise; the evening decline was inconsistent among the two nests. Furthermore, the timing of the mid-day activity peaks varied over the season, but subtly (Suppl. material 1: Fig. S4).

## Discussion

Our results support the long daily activity of vespine wasps (Gaul 1952a; Archer 2004; Kasper et al. 2008 for *Vespula*; Brian and Brian 1952 and Heinrich 1984 for *Dolichovespula*). Because we generally started the monitoring at sunrise or slightly

before, after the flight had already started, it is apparent that the flight starts about half an hour before sunrise and increases rapidly. In the most extreme case, the flight continued over an hour after sunset, which is likely related to long dusk in northern latitudes. Thus, in boreal Central Finland, *D. saxonica* is active about 20 hours in July and a few hours less in August. Our results indicate that the length of the daily activity of *D. saxonica* is linked with the duration and amount of daylight, similar to *Vespula* (Gaul 1952a; Potter 1964; Kasper et al. 2008; Kelber et al. 2011). In addition to the shortening of the daily activity period after the peak season, also the dynamics change: the timing of the daily peaks was different and the increase in the morning activity became more gradual. With only two nests re-monitored for a full day, our conclusions concerning seasonal changes in the within-day activity patterns of *D. saxonica* are preliminary but do support the idea of high variability.

The sunrise to sunset traffic rates varied among nests and reflected colony sizes. Daily traffic rate is a function of worker numbers and flight activity. Worker numbers are largely related to seasonal phase of a colony, but other intrinsic and local environmental factors have a role since nearby, mature colonies vary in size (Nadolski 2012; this study). The positive relationship between traffic rate and total number of cells was much stronger and less variable than documented for invasive *V. germanica* (cf. Kasper 2004). Due to the high within-day variability in activity, traffic rate can only be used as a rough indicator of colony size in *D. saxonica* and should be estimated at least over half an hour (cf. Malham et al. 1991). The within-day variation of colony's traffic rate reflects differences in flight activity, which may be related to workers allocation of time to different activities (Archer 2000a) or variation in weather (Kasper et al. 2008). The full-day monitoring was carried out at, or near the peak activity during favourable weather (see below), we therefore assume that most trips were foraging trips and the time devoted to nest enlargement was minimal. Parasitism was unlikely to have a great effect on traffic rates (see below). As the ceased nests were removed some weeks after the main monitoring, it is possible, yet unlikely given the developmental times of *Dolichovespula* (Archer 2000b; Archer 2012), that the measured nest characteristics did not closely reflect the characteristics during monitoring.

At the peak season, *D. saxonica* activity dynamics were idiosyncratic among nests, i.e. the timing of the activity peaks, based on a 35-min moving average, varied among nests. The morning peak, which was generally not the daily peak, was followed by a variable period of lower traffic rate. The only extant study of the within-day dynamics of *Dolichovespula* (one nest of *D. maculata*) indicated early morning and late evening peaks (Heinrich 1984). Similarly, the typical daily activity of *Vespula* has often been characterised as having a sharp peak in the early morning and late evening (Spradbery 1973; Edwards 1980); yet, the more recent studies indicate high variability in the timing of the peaks (Potter 1964; Edwards 1980; Heinrich 1984; Archer 2004; Kasper 2004). Latitudinal variation in the sharpness of the morning and evening activity peaks might be related to the latitudinal variation in the length of dawn and dusk. Because we did not re-monitor the colonies during the peak season, we cannot conclude about the day-to-day variation in the dynamics of a single nest during peak

season. Yet, our study shows that there are no consistent species-specific dynamics in *D. saxonica* colonies. To disentangle the effects of colony-specific characteristics (behaviour, parasitism, nest site, environment) and daily weather on dynamics requires another study.

Traffic rate varied also at finer resolution and showed irregular cycles of a few minutes. The only study on the trip or inter-trip times of *Dolichovespula* (Brian and Brian 1952) showed rather constant times spent in the nest, even for individuals carrying out different activities (fluid, pulp or flesh collecting), whereas the times spent outside were more variable for the activities. In general, constancy in the times of in-nest or outside activities can promote regularity in cycles. Our observations about the cycle length are also in line with the mean trip times for below-ground *V. vulgaris* (Archer 2012); the in-colony time of *D. saxonica* is likely to be shorter than that of the below-ground *V. vulgaris*, because there is no need for earth removal. Cyclicity and cycle length were not conditional on a particular nest, which might be the case if availability and distribution of food were the underlying causal factors. Yet, there is evidence that wasps tend to revisit good foraging sites and might be capable of information sharing (Santoro et al. 2015) or local enhancement (D’Adamo et al. 2000) regarding food sources, which could maintain similar trip times and hence rough cyclicity in activities. Furthermore, to decrease predation risk, wasps are likely to coordinate their activities so that the nest is never left unattended.

Flight activity of wasps is affected by weather, particularly extreme temperature, rain, wind and light conditions (Gaul 1952b; Potter 1964; Kasper et al. 2008; Archer 2012). Because we monitored the activity on days when the wind was generally calm to moderate, the sky clear or half cloudy, and rainfall negligible, it is likely that these had an irrelevant effect on overall activity or activity dynamics. Temperature, in turn, might have had a larger, yet temporally inconsistent effect. Ambient temperature outside the nests was always between the lower and upper thresholds for flight activity (see Blackith 1958; Potter 1964; Heinrich 1984; Coelho and Ross 1996; Kasper et al. 2008) and remained rather stable during mid-day; thus, it neither explains the cyclicity at the scale of minutes, nor the irregular variation in mean traffic rate during the day (the statistically significant relationships between traffic rate and temperature in two colonies were in opposite directions). However, June and July 2021 were record-warm in Central Finland, and temperatures over 30 °C in the direct sunlight were regularly observed. Most of the studied nests experienced direct sunlight for some, but different time during the day, so it is possible that the in-nest temperature raised over the regulated 28–31 °C (see Heinrich 1984). This might have affected differently the within-day flight dynamics among the nests and it could explain the variation in mean traffic rate at the scale of half an hour to some hours. Indeed, a few times a buzzing sound was heard and ventilating workers were seen at the nest entrance suggesting fanning behaviour to cool the nest (see Potter 1964; Heinrich 1984). The consequences of extreme in-nest temperatures are not clear. On the one hand, fanning might decrease traffic rates, but on the other hand, high temperatures can shorten feeding times, as observed for *Vespula* (Jandt et al.

2010), and thus increase traffic rates. Because similar variation in traffic rates has been observed for under-ground colonies of *Vespula* (Kasper et al. 2008; Archer 2012; pers. obs.), which are likely to maintain more stable temperature than exposed *Dolichovespula* nests, the variation in traffic rate remains a mystery. To better resolve the effect of temperature on activity, future studies should preferably measure in-nest temperatures.

Parasitism can affect colony size and hence overall colony activity, but unlikely affect within-day dynamics. In the studied colonies, parasitism rate by *S. vesparum* and *A. sociella* was low, so the effect of parasitism on any of the measured parameters is negligible. Low parasitism rate corroborates previous observations (see Archer 2012). Furthermore, because the nests were removed 21, 17 and 19 days after the first monitoring, it is likely that the *A. sociella* infestations occurred near or after the first monitoring, and thus had little effect on traffic rates. Furthermore, *A. sociella* infested colonies can show normal development, especially if infestations occur late in colony development (Archer 2012). Only the traffic rate in the Siirtola nest (94 *A. sociella* larvae) might have been affected by parasitism, since the full-day monitoring was done after the peak activity; yet, the traffic rate was only slightly lower than at the peak and similar to the other colonies of similar size.

## Conclusions

Our study provides high-resolution information about the all-day activity of *D. saxonica* colonies. Despite the previous suggestions that vespids, or at least *Vespula*, colonies would have roughly consistent within-day dynamics, the observed idiosyncratic within-day activity among colonies challenges this idea. Together with the recent studies on *Vespula* our results suggest that the within-day dynamics of vespines as a whole are explained mainly in terms of environmental conditions rather than by any innate pattern of changes in colony needs. Furthermore, all colonies showed irregular cycles over a few minutes. This suggests that the trip and inter-trip times are roughly similar in colonies with different environmental surroundings. Future studies should verify the observed patterns in other *Dolichovespula* wasps and, even though laborious, they should combine high-resolution monitoring of colony activity with individually tagged wasps and carefully measured in-nest conditions.

## Acknowledgements

We thank the Kone foundation for a research grant to the wasp project, and Essi Järvinen, Kristiina Lindell, Lauri Viitanen, Satu Leino, Sophie Siimes, Jenna Palttala, Joonas Lähdemäki, Tatu Koponen and Joonas Hirvensalo for the help in the field.

Funding was provided by a private Kone foundation for a wasp project lead by Atte Komonen.

## References

- Akre RD, Reed HC, Landolt PJ (1982) Nesting biology and behavior of the blackjacket, *Vespula consobrina* (Hymenoptera: Vespidae). *Journal of the Kansas Entomological Society* 55: 373–405.
- Archer ME (1981) Successful and unsuccessful development of colonies of *Vespula vulgaris* (Linn.) (Hymenoptera: Vespidae). *Ecological Entomology* 6: 1–10. <https://doi.org/10.1111/j.1365-2311.1981.tb00966.x>
- Archer ME (2000a) Seasonal foraging characteristics during mid-day of successful underground colonies of *Vespula vulgaris* (Hymenoptera, Vespidae) in England. *Insectes Sociaux* 47: 117–122. <https://doi.org/10.1007/PL00001689>
- Archer ME (2000b) The life history and a numerical account of colonies of the social wasp, *Dolichovespula norwegica* (F.) (Hym., Vespinae) in England. *The Entomologist Monthly Magazine* 136: 1–14.
- Archer ME (2004) All-day foraging characteristics of successful underground colonies of *Vespula vulgaris* (Hymenoptera, Vespidae) in England. *Insectes Sociaux* 51: 171–178. <https://doi.org/10.1007/s00040-004-0731-7>
- Archer ME (2012) *Vespine wasps of the world*. Siri Scientific Press, Manchester, 352 pp.
- Blackith RE (1958) Visual sensitivity and foraging in social wasps. *Insectes Sociaux* 5: 159–169. <https://doi.org/10.1007/BF02224066>
- Brian MV, Brian AD (1952) The wasp, *Vespula sylvestris* Scopoli: feeding, foraging and colony development. *Transactions of the Royal Entomological Society of London* 103: 1–26. <https://doi.org/10.1111/j.1365-2311.1952.tb02261.x>
- Broughton RK, Hebda G, Maziarz M, Smith KW, Smith L, Hinsley SA (2015) Nest-site competition between bumblebees (Bombidae), social wasps (Vespidae) and cavity-nesting birds in Britain and the Western Palearctic. *Bird Study* 62: 427–437. <https://doi.org/10.1080/0063657.2015.1046811>
- Coelho JR, Ross AJ (1996) Body temperature and thermoregulation in two species of yellow-jackets, *Vespula germanica* and *V. maculifrons*. *Journal of Comparative Physiology B* 166: 68–76. <https://doi.org/10.1007/BF00264641>
- D'Adamo P, Corley J, Sackmann P, Lozada M (2000) Local enhancement in the wasp *Vespula germanica*, are local cues all that matter? *Insectes Sociaux* 47: 289–291. <https://doi.org/10.1007/PL00001717>
- Douwes P, Abenius J, Cederberg B, Wahlstedt U, Hall K, Starkenberg M, Reisborg C, Östman T (2012) Nationalnyckeln till Sveriges flora och fauna. Steklar: Myror–getingar. Hymenoptera: Formicidae–Vespidae. ArtDataBanken, SLU, Uppsala, 382 pp.
- Edwards R (1980) *Social wasps: their biology and control*. Rentokil Ltd., East Grinstead, 398 pp.
- Gaul AT (1952a) The awakening and diurnal flight activities of vespine wasps. *Proceedings of the Royal Entomological Society London (A)* 27: 33–38. <https://doi.org/10.1111/j.1365-3032.1952.tb00149.x>
- Gaul AT (1952b) The Flight of Vespine Wasps in Relation to Stormy Weather. *Journal of the New York Entomological Society* 60: 17–20.

- Greene A, Akre RD, Landolt PJ (1976) The aerial yellowjacket, *Dolichovespula arenaria* (Fab.): nesting biology, reproductive production, and behavior (Hymenoptera: Vespidae). *Melanderia* 26: 1–34.
- Heinrich B (1984) Strategies of thermoregulation and foraging in two vespid wasps, *Dolichovespula maculata* and *Vespula vulgaris*. *Journal of Comparative Physiology B* 154: 175–180. <https://doi.org/10.1007/BF00684142>
- Jandt JM, Taylor B, Jeanne RL (2010) Temperature and forager body size affect carbohydrate collection in German yellowjackets, *Vespula germanica* (Hymenoptera, Vespidae). *Insectes Sociaux* 57: 275–283. <https://doi.org/10.1007/s00040-010-0082-5>
- Kasper ML (2004) The population ecology of an invasive social insect, *Vespula germanica* (Hymenoptera: Vespidae) in south Australia. Ph.D. Thesis, University of Adelaide, Australia, 171 pp.
- Kasper ML, Reeson AF, Mackay DA, Austin AD (2008) Environmental factors influencing daily foraging activity of *Vespula germanica* (Hymenoptera, Vespidae) in Mediterranean Australia. *Insectes Sociaux* 55: 288–295. <https://doi.org/10.1007/s00040-008-1004-7>
- Kelber A, Jonsson F, Wallén R, Warrant E, Kornfeldt T, Baird E (2011) Hornets can fly at night without obvious adaptations of eyes and ocelli. *PLoS ONE* 6(7): e21892. <https://doi.org/10.1371/journal.pone.0021892>
- Malham JP, Rees JS, Alspach PA, Beggs JR, Moller H (1991) Traffic rate as an index of colony size in *Vespula* wasps. *New Zealand Journal of Zoology* 18: 105–109. <https://doi.org/10.1080/03014223.1991.10757956>
- Nadolski J (2012) Structure of nests and colony sizes of the European hornet (*Vespa crabro*) and Saxon wasp (*Dolichovespula saxonica*) (Hymenoptera: Vespinae) in urban conditions. *Sociobiology* 54: 1075–1120.
- Pallet MJ, Plowright RC (1979) Traffic through the nest entrance of a colony of *Vespula arenaria* (Hymenoptera: Vespidae). *The Canadian Entomologist* 111: 385–390. <https://doi.org/10.4039/Ent111385-4>
- Pawlikowski T, Pawlikowski K (2010) Nesting interactions of the social wasp *Dolichovespula saxonica* [F.] (Hymenoptera: Vespinae) in wooden nest boxes for birds in the forest reserve “Las Piwnicki” in the Chelmno Land (Northern Poland). *Ecological Questions* 13: 67–72. <https://doi.org/10.12775/v10090-010-0017-9>
- Potter NB (1964) A Study of the Biology of the Common Wasp, *Vespula vulgaris* L., with Special Reference to the Foraging Behaviour. Ph.D. Thesis, University of Bristol, England, 79 pp.
- Roland C, Horel A (1976) Étude de l’approvisionnement d’un nid de *Paravespula germanica*: Rapport entre activité, rentabilité des récoltes et conditions climatiques. *Insectes Sociaux* 23: 89–97. <https://doi.org/10.1007/BF02223843>
- Santoro D, Hartley S, Suckling DM, Lester PJ (2015) Nest-based information transfer and foraging activation in the common wasp (*Vespula vulgaris*). *Insectes Sociaux* 62: 207–217. <https://doi.org/10.1007/s00040-015-0395-5>
- Spradbery JP (1973) Wasps: an account of the biology and natural history of solitary and social wasps. University of Washington Press, Seattle, 408 pp.
- Vetter RS, Visscher PK (1995) Laboratory rearing of western yellowjackets (Hymenoptera: Vespidae) through a foundress-to-gyne colony cycle. *Annals of the Entomological Society of America* 88: 791–799. <https://doi.org/10.1093/aesa/88.6.791>

## **Supplementary material I**

### **Tables S1, S2, Figures S1–S4**

Authors: Atte Komonen, Jyrki Torniaainen

Data type: Tables and figures (docx. file)

Explanation note: Nest characteristics, seasonal activity, time series model summary, minute-to-minute dynamics and correlograms.

Copyright notice: This dataset is made available under the Open Database License (<http://opendatacommons.org/licenses/odbl/1.0/>). The Open Database License (ODbL) is a license agreement intended to allow users to freely share, modify, and use this Dataset while maintaining this same freedom for others, provided that the original source and author(s) are credited.

Link: <https://doi.org/10.3897/jhr.89.79306.suppl1>

# Assessment of an inexpensive trap design and survey method for vespine wasps (Hymenoptera, Vespidae, Vespinae)

Grady O. Jakobsberg<sup>1</sup>, Walter D. Mooney<sup>2</sup>, Jacqueline Rangel-Sanchez<sup>1</sup>

**1** US Geological Survey, Native Bee Inventory and Monitoring Lab, 12100 Beech Forest Road, Laurel, Maryland, USA **2** US Geological Survey, 345 Middlefield Rd, Menlo Park, California, USA

Corresponding author: Grady O. Jakobsberg ([gradyo99@gmail.com](mailto:gradyo99@gmail.com))

---

Academic editor: Michael Ohl | Received 8 January 2022 | Accepted 19 January 2022 | Published 28 February 2022

---

<http://zoobank.org/23F310D3-19CD-4A9E-8244-DAA2B2D43494>

---

**Citation:** Jakobsberg GO, Mooney WD, Rangel-Sanchez J (2022) Assessment of an inexpensive trap design and survey method for vespine wasps (Hymenoptera, Vespidae, Vespinae). *Journal of Hymenoptera Research* 89: 171–182. <https://doi.org/10.3897/jhr.89.80284>

---

## Abstract

The introduction of the predatory Giant Asian Hornet, *Vespa mandarinia* Smith, to North America in 2019 has motivated efforts to create early detection systems for this and other non-native social wasp species (Hymenoptera, Vespidae). Various trap and bait combinations have been used for this purpose, most of which require assembly and materials that are costly, reducing their usefulness in large-scale survey systems. This study tests an inexpensive and efficient trapping technique for detecting or surveying vespine wasps. Traps were made from reused plastic bottles containing a brown sugar and water bait. They were deployed at heights ranging from 0–6 m above ground in several configurations. Captures for traps suspended 1 m or greater above ground were, on average, nine times higher than the catch of ground-level traps. A rapid trap deployment method for large geographic areas was created, which captured seven different vespine wasp species along a 395 km east-west road transect from mountains to coastal plain in the Mid-Atlantic region of the United States. The trapping design and survey methodology described below is inexpensive and fast and could be used by land managers or citizen scientists to detect *V. mandarinia*, other exotic vespine, or conducted on a large-scale vespine diversity survey.

## Keywords

Baited trap, detection, *Dolichovespula*, exotic species, trap deployment, *Vespula*

## Introduction

Over the last several decades, there has been increased concern over the spread of exotic insect species due to international container shipping (Hulme 2009; Meurisse et al. 2019). Such species threaten native plant and insect communities both ecologically and economically. Vespid wasps are of particular concern because of the threat they pose to native pollinators. Until the appearance of *Vespa mandarinia* in the Pacific Northwest, there were no large-scale surveys for vespid species detection.

Fear over exotic wasp species introduction into North America spiked in 2019 with the arrival of the Giant Asian hornet. *V. mandarinia* is the largest bodied of any vespid (Hymenoptera, Vespidae) and is known for its ability to eradicate a bee colony in a matter of hours (Stankus 2020). Additionally, *V. mandarinia* can repeatedly deliver painful stings to humans which have caused extreme allergic reactions, resulting in 30–50 deaths per year in Japan (Stankus 2020). Models by Alaniz et al. (2020) predict damages between \$12 and \$102 million for bee-dependent products alone if *V. mandarinia* were to spread across the United States. Several established nests were found and eradicated in the Pacific Northwest, but other unverified sightings in the region have led many scientists and public officials to call for greater detection efforts (Stankus 2020; Animal and Plant Inspection Service 2021). There is a need for an inexpensive and reliable trap design that can be used for the coordinated detection of *V. mandarinia* over a large geographic range.

*V. mandarinia* has never been detected on the east coast of the United States, but other vespine species occupy the area and provide a proxy for testing *V. mandarinia* trapping methods. The most efficient way to detect vespine wasps related to *V. mandarinia* is through lethal trapping (Tripodi and Hardin 2020). Traps for vespine wasps often consist of a plastic bottle (usually a 1.5 L soda bottle or a gallon jug) filled with a liquid bait and hung from a tree branch (Dvorak 2007; Tripodi and Hardin 2020). Whether these traps are as effective when left on the ground is evaluated in this study.

Sugar-based foods are known to be effective bait for trapping some vespine species (Dvorak and Landolt 2006; Demichelis 2014; Tripodi and Hardin 2020). It is common for traps to contain a syrup or sugar mixture often with vinegar and fruit added, but a simple mix of dark brown sugar and water has proven effective if given enough time to ferment (Wegner and Jordan 2005; PDA 2020). Dark sugar bait was recommended by the Washington State Department of Agriculture in response to the first *V. mandarinia* detection (Tripodi and Hardin 2020).

In this study, a basic bottle trap with dark brown sugar bait was tested in the Mid-Atlantic region of the United States as an inexpensive and efficient method that could be used by seasonal technicians or citizen scientists to detect *V. mandarinia* or to survey other social wasp species that are attracted to fermented sugar baits. The bottle trap was tested at different heights, from ground level to 6 meters, and in different settings using a deployment method along roads in the region. Seven vespine species were detected from the genera *Vespula*, *Dolichovespula*, and *Vespa*.

## Methods

Three experiments were run with identical bottle traps and sugar bait: 1) A hanging/ground experiment with paired and unpaired trials to compare the success of suspended and standing traps; 2) an elevated trap test that compared trap success at five heights from 0 to 6 m, and 3) a 395 km long transect, with traps deployed across multiple ecoregions.

### Bottle trap design

The traps were made from recycled water or soda bottles, ranging from 0.47 to 1 L. The bottles were retrieved from recycling facilities and rinsed before use. Each trap was baited with a sugar-water mixture of the ratio of 0.47 L of dark brown sugar to 3.8 L of water. The bottles were filled halfway, to allow enough space for a large catch. For hanging traps, a string was knotted around the neck of the bottle and the trap was hung off the ground. Ground traps were placed on the ground. Over 2–4 weeks, the sugar mixture fermented, attracting wasps, hornets, and yellowjackets, which crawl through the bottle opening and are unable to navigate back out. Some by-catch of other insects occurred but was not quantified. By-catch primarily included ants, moths, and flies, with fewer than 10 individual bees trapped across all experiments. Bottles placed on the ground appeared to attract more by-catch than those that were hung. Bottle screw caps were retained for ease in transporting traps after collection. For a diagram and instructional video on trap construction, see Suppl. material 2: Fig. S1 and <https://www.youtube.com/watch?v=AonF4bqs04k>.

### Survey area

This study was conducted in the Mid-Atlantic portion of the United States, primarily in the state of Maryland. The first two experiments were conducted at the United States Geological Survey's (USGS) Native Bee Inventory and Monitoring Lab (BIML) located on the United States Fish and Wildlife Service's Patuxent Research Refuge (Laurel, Maryland, USA). Some traps were also placed in the surrounding community of Laurel, Maryland. The east-west road transect was performed on a route that started in Pennsylvania near the Maryland border (39°45'06"N, 79°23'29"W), traversed west to east, and ended in New Castle, Delaware near the Delaware River (39°39'35"N, 75°33'50"W), staying between the latitudes of 39.5°N and 39.8°N (Fig. 1). The total route was approximately 395 km long and primarily used two-lane country roads that ran parallel to larger highways.

### Hanging/ground trap experiment

Two tests were conducted to compare the yield of traps placed on the ground versus hanging traps 1.25–1.5 m above the ground. Both a paired and unpaired trap test was conducted. The paired trap test examined vespine preference when both trap heights

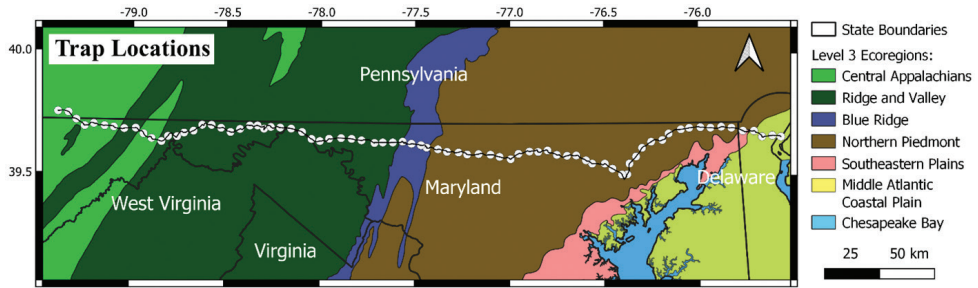


**Figure 1.** Trap locations and route of the east-west road transect. Trap locations (white dots) and route (black line) with state boundaries and level 3 ecoregions of the Environmental Protection Agency (Comeleo 2010).

are simultaneously present. The unpaired trap test shows differences in vespine attraction to traps at each height.

The paired trap test placed hanging and ground traps together, with ground traps directly under the hanging traps. Fifteen trap pairs were placed around Laurel, Maryland, primarily in the Patuxent Wildlife Refuge around the BIML. The same bottle type was used for each pair. They were left in place for three weeks between July 10<sup>th</sup> and August 16<sup>th</sup> of 2021.

The unpaired trap test placed 15 hanging and 15 ground traps at least 10 meters apart. The test was conducted in the area around the Native Bee Inventory and Monitoring Lab and the traps remained in place for three weeks, from August 2<sup>nd</sup> to August 23<sup>rd</sup>.

### Elevated trap experiment

To test the catch yield of traps at different heights, 10 lines of paracord were hung around the BIML grounds, half of which were in open fields and the other half in a deciduous forest that was approximately 70 years old. Traps were tied to each line at heights of 6 m, 3 m, 1.5 m, .6 m, and ground level. The traps were left for 3-week periods between August 17<sup>th</sup> and September 21<sup>st</sup>.

### 395 km east-west road transect

During the trap deployment, the Gaia GPS app was used to track the distance from the start of the route. The surveyor stopped every five kilometers, or the closest possible pull-off point thereof, to deploy a trap. At each survey point, a waypoint was taken on the Gaia GPS app and the current location was saved in a folder on the Google Maps app. Each waypoint/location was named after the trap number, which was written on the trap before it was placed. Ground traps were placed in a sheltered area, (e.g., higher vegetation or at the base of signs, guardrails, or telephone poles). A marking flag was placed closer to the road so the ground traps would be easier to find during collection. Hanging traps were placed 1–1.5 m off the ground, usually on telephone poles or tree

branches. For each trap, the surveyor recorded the trap number, distance from the start of the route, steps from the marking flag (for ground traps), and any additional notes for locating the trap.

The ground traps were deployed July 21<sup>st</sup> and 22<sup>nd</sup> and collected 21 days later on August 11<sup>th</sup> and 12<sup>th</sup>. The hanging traps were deployed in the same locations as the ground traps on August 19<sup>th</sup> and 20<sup>th</sup> and collected 21 days later, on September 9<sup>th</sup> and 10<sup>th</sup>. The locations saved on Google Maps were used to navigate from one trap to the next, with the surveyor spending no more than five minutes looking for the trap. During trap collection, the state of the trap was recorded as in-place, disturbed, or lost. Traps were capped and brought back to the USGS Native Bee Inventory and Monitoring Lab, Laurel MD for processing.

## Sample processing

Trap catch was processed identically for all experiments. The catch of each trap was emptied into a mesh sieve and rinsed before being transferred to a wide, white tray filled with a few centimeters of water. Each species was counted and discarded. Uncertain identifications were retained for identification at the Native Bee Inventory and Monitoring Lab.

## Data analysis

Non-parametric statistics were used for comparisons of trap results as the data weren't normally distributed. To compare the hanging/ground trap yields for statistically significant differences, non-parametric tests of two sample medians were conducted. A Mann-Whitney U test was performed to evaluate any statistical difference between two unpaired samples and a Wilcoxon test was performed to evaluate any statistical difference between two paired samples. For the hanging and ground trap comparison of the east-west road transect, paired traps included only trap locations with a usable hanging and ground trap result (thus paired by location) while unpaired traps included all usable traps from each group. To test the difference in total catch medians for the five heights of the elevated traps, a Kruskal-Wallis non-parametric ANOVA test was used. A Mann-Whitney pairwise test compared the overall catch of each combination of trap heights for statistically significant differences.

All test statistics were calculated using Paleontological Statistics Software Package (PAST), Version 4.07 (Hammer 2001), a data analysis software that performs a variety of statistical tests and data manipulation functions.

## Results

### Hanging/ground trap experiment

A Wilcoxon paired test of medians showed that hanging traps caught significantly more vespine individuals than the paired ground traps ( $p \leq .001$ ). Likewise, a Mann-

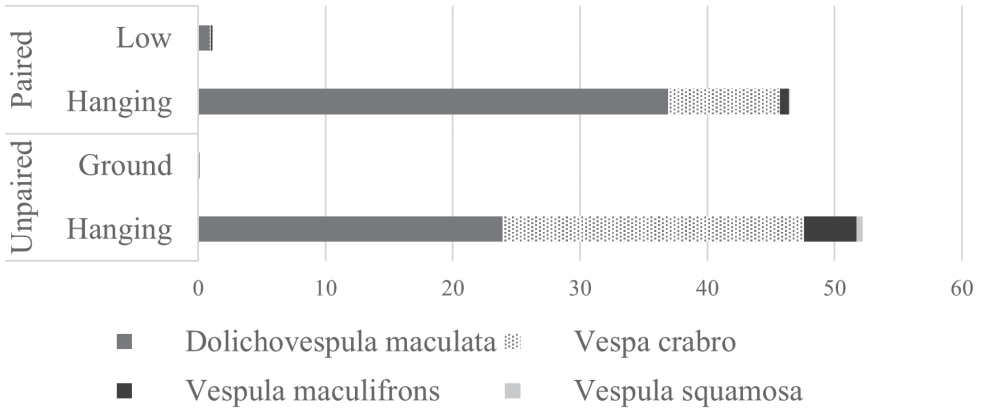


**Figure 2.** Average yield of hanging/ground trap experiment. Results are separated into paired and unpaired tests and average yield is categorized by species.

**Table 1.** Summary statistics of hanging and ground traps on the east-west road transect.

Statistics	Ground	Hanging
Number of traps set	79	77
Count of traps collected	59	72
Traps lost (%)	25	5
Minimum catch	0	0
Maximum catch	45	61
Total catch	145	942
Mean catch per trap	2.5	13.1
Std. error	0.9	1.9
Median catch per trap	0	6

Whitney U test showed the same result for the unpaired trap results ( $p \leq .001$ ). Summing across both paired and unpaired test results, hanging traps caught 98.8% of all individuals, while ground traps caught 1.2% (Fig. 2). There was a large amount of variability in overall yield amongst the hanging traps, with captures ranging from 0 to 162 individuals per trap. Four different species were found in the hanging/ground trap experiment. For more summary statistics, see Suppl. material 1: Table S1.

### Elevated trap experiment

The ground level (0 m) traps had the lowest average catch, followed by the 6 m trap, while the three highest traps averaged within two individuals of each other (Fig. 3). A Kruskal-Wallis non-parametric ANOVA test showed a statistically significant difference between the total catch sample medians ( $p = .001$ ). A Mann-Whitney pairwise test showed the total catch at the ground level was significantly lower than all other heights. There was no significant difference in total catch between the other heights.

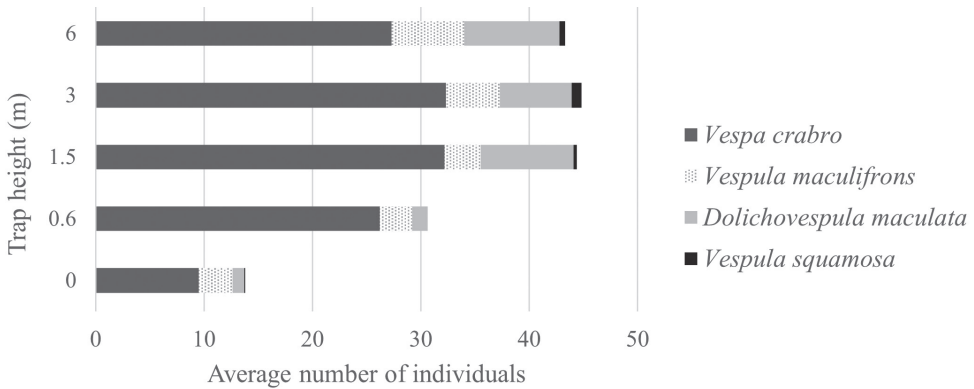


**Figure 3.** Average catch at each height of the hanging line traps. Includes the average number of individuals from each of the four species detected.

### 395 km east-west road transect

The east-west road transect intersected five EPA Level III ecoregions (Comeleo 2010), traversing from a high of 800 meters down to just above sea level, and sampled a varied landscape calculated predominantly as forested (41.1%), agricultural (29.3%), or developed (26.0%) using the 2019 National Land Cover Database.

Hanging traps had a significantly higher overall yield than ground traps for a paired test ( $p \leq .001$ ) and an unpaired test ( $p \leq .001$ ). Five percent of the hanging traps were lost (4 of 77) compared to 25 percent of the ground traps (20 of 79) (Table 1). Hanging traps had an average overall catch that was approximately five times larger than ground traps, containing seven different species compared to the five caught by ground traps (Table 2). The seven species detected include *Vespula maculifrons* (du Buysson), *Vespa crabro* (Linnaeus), *Dolichovespula maculata* (Linnaeus), *Vespula flavopilosa* (Jacobson), *Vespula germanica* (Fabricius), *Vespula squamosa* (Drury), and *Dolichovespula arenaria* (Fabricius). For more summary statistics and the original data of the east-west road transect including trap locations, landscape attributes, and catch results, see Suppl. material 1: Table S2, S3.

## Discussion

The results of this study demonstrate that a 1–1.5 m hanging trap design, consisting of a re-used plastic bottle and a dark brown sugar bait mixture, is effective at trapping a diverse group of vespine wasps. Hanging traps performed, on average, nine times better than ground-based traps in overall catch across all experiments, and five times better in trap loss as shown by the east-west road transect, with an overall trap loss of only 5%. The elevated trap test demonstrated that ground-level placements perform significantly worse than all other heights, with traps 1.5 m and above performing similarly in their total catch.

**Table 2.** Summary statistics of species found on the east-west road transect. This includes the mean number of individuals per trap (standard error in brackets), maximum in one trap, and percent occurrence, which is the percent of traps with at least one individual from that species. The median catch for all species is zero except for the *V. crabro* and *V. maculifrons* in the hanging traps, which had median values of 1 and 2 respectively.

Species	Ground			Hanging		
	Mean per trap	Max	Occurrence (%)	Mean per trap	Max	Occurrence (%)
<i>Vespula maculifrons</i>	0.83 (0.29)	12	22.0	4.96 (1.09)	56	70.8
<i>Vespa crabro</i>	1.14 (0.63)	32	8.5	4.36 (0.93)	35	51.4
<i>Dolichovespula maculata</i>	0.15 (0.09)	5	8.5	1.31 (0.29)	17	47.2
<i>Vespula flavipolosa</i>	0.07 (0.05)	3	3.4	1.06 (0.42)	26	23.6
<i>Vespula germanica</i>	0	0	0	0.74 (0.33)	18	13.9
<i>Vespula squamosa</i>	0	0	0	0.64 (0.20)	11	25.0
<i>Dolichovespula arenaria</i>	0.27 (0.14)	6	10.2	0.03 (0.02)	1	2.8

The road transect captured seven of the ten vespine species recorded in the Maryland Biodiversity Project, a non-profit citizen science project that has cataloged over 11,000 insect species in Maryland (Maryland Biodiversity Project 2021). The vespine species captured includes all but one of the species listed with more than one confirmed sighting.

The biggest asset of this trap design and deployment technique is its accessibility and cost. Assuming bottles are freely collected from a recycling facility or receptacle, as these were, the only material expenses are for the dark brown sugar and string. For those materials, we estimate the per trap cost to be approximately \$0.15. The only major expenses are gas and time. Approximately six traps spaced five km apart can be deployed or collected in an hour.

This trap design and a road transect deployment could be used to detect *V. mandarinia* and other exotic vespine species or as an inexpensive assessment of the component of regional vespine species that are attracted to fermenting sugar bait. This study demonstrated how many traps can be deployed inexpensively over a large geographic range. A small group of technicians could survey a large area using these traps and a methodology similar to the Breeding Bird Survey (Dunn et al. 2000). One example of this would be to divide the survey area into a grid of equal cell size or with cells oriented around physiographic strata. A point randomly generated within each cell and traced to the nearest road could be used as a starting point for a 25 km transect, with traps hung on the side of the road every kilometer. Two of these transects could be deployed or collected per day, meaning one technician could complete approximately 48 of these transects (1200 traps) in three months, given pick-up after three weeks and one day per week for sample transfer and storage into a freezer for later identification.

Additionally, the trap design would be ideal for a citizen science-based protocol for more large-scale surveys. Citizen science is growing in popularity as a method for surveying plants and wildlife, including exotic species. Pusceddu et al. (2019) used a verified citizen science program to monitor the spread of an invasive vespine species (*Vespa crabro*) on the island of Sardinia (Italy). The program reported high data accuracy and civil engagement.

Citizen science-based reporting could be a valuable tool for detecting and exterminating any *Vespa mandarinia* that find their way to North America. The US Department of Agriculture (USDA) called on scientists of the Pacific Northwest to assist with the detection of *V. mandarinia* after they first arrived in 2019 (Tripodi and Hardin 2020). The

Washington Department of Agriculture has launched a 2021 Asian Giant Hornet Public Dashboard to continue these efforts using citizen scientist reporting (WSDA 2021).

The hanging trap and sugar-based bait tested in this study have shown to be effective at catching vespine wasps in high densities, and they would likely be effective as a passive, lethal trap for *V. mandarinia*. We recommend that this method of trapping be explored further as a widespread, citizen scientist approach for the detection of *V. mandarinia*. Unlike similar citizen science methodology, our trap design doesn't require that land managers ship trap materials to participants (PDA 2020).

While inexpensive and accessible, these traps may not equally attract all vespine species (Dvorak 2007) and there could be high variance throughout the summer due to changes in dietary preferences (Stankus 2020; Tripodi and Hardin 2020). Similar traps have reportedly been used by Japanese farmers to capture and kill dispersing *V. mandarinia* queens in the spring and late fall (Tripodi and Hardin 2020), however future study is required to confirm the effectiveness of this trap design for *V. mandarinia*, and specifically for *V. mandarinia* queens if the design is to be used as a lethal capture to prevent species dispersal from year to year. Additionally, in any future study, we recommend that species and numbers of by-catch be recorded to assess the impact on non-target species.

## Acknowledgements

The authors thank Sam Droege and the personnel of the USGS Native Bee Inventory and Monitoring Lab for instruction in entomology and valuable advice and feedback on this research. For employment and the opportunity to conduct this research, the authors thank the USGS Cooperative Summer Field Training Program and the USGS. Reviews by Jessica Reid, Hunter Martin, and Carol Barrera-Lopez (all USGS) are gratefully acknowledged. Gabrielle Jakobsberg and Charles Lott are thanked for their assistance in constructing Suppl. material.

## References

- Alaniz A, Carvajal M, Vergara P (2020) Giants are coming? Predicting the potential spread and impacts of the giant Asian hornet (*Vespa mandarinia*, Hymenoptera: Vespidae) in the USA. *Pest Management Science* 77: 104–112. <https://doi.org/10.1002/ps.6063>
- Animal and Plant Health Inspection Service (2021) USDA: Asian Giant Hornet. <https://www.aphis.usda.gov/aphis/ourfocus/planthealth/plant-pest-and-disease-programs/honey-bees/agh/asian-giant-hornet>
- Comeleo R (2010) Level III Ecoregions of North America [vector digital data] Corvallis, OR: U.S. EPA Office of Research & Development – National Health and Environmental Effects Research Laboratory. <https://www.epa.gov/eco-research/ecoregions-north-america>
- Dewitz J (2021) National Land Cover Database (NLCD) 2019 Land Cover Conterminous United States [remote sensing image] Sioux Falls, SD: U.S. Geological Survey. <https://www.mrlc.gov/data/>

- Demichelis S, Manino A, Minuto G, Mariotti M, Porporato M (2014) Social wasp trapping in north west Italy: comparison of different bait-traps and first detection of *Vespa velutina*. *Bulletin of Insectology* 67(2): 307–317. <https://core.ac.uk/download/pdf/301963638.pdf>
- Dunn E, Johnson D, Jones S, Petit D, Pollock K, Smith C, Trapp J, Welling E (2000) A Programmatic Review of the North American Breeding Bird Survey: Report of a Peer Review Panel to USGS Patuxent. <https://www.pwrc.usgs.gov/bbs/bbsreview/bbsfinal.pdf>
- Dvorak L (2007) Social wasps (Hymenoptera: Vespidae) trapped with beer in European forest ecosystems. *Acta Musei Moraviae, Scientiae biologicae* 92: 181–204. <https://citeseerx.ist.psu.edu/viewdoc/download?doi=10.1.1.582.6189&rep=rep1&type=pdf>
- Dvorak L, Landolt P (2006) Social wasps trapped in the Czech Republic with syrup and fermented fruit and comparison with similar studies (Hymenoptera Vespidae). *Bulletin of Insectology* 59(2): 115–120. <http://www.bulletinofinsectology.org/pdfarticles/vol59-2006-115-120dvorak.pdf>
- Hammer O, Harper DAT, Ryan PD (2001) PAST: Paleontological Statistics Software Package for Education and Data Analysis. *Palaeontologia Electronica* 4(1): e9.
- Hulme PE (2009) Trade, transport and trouble: managing invasive species pathways in an era of globalization. *Journal of Applied Ecology* 46(1): 10–18. <https://doi.org/10.1111/j.1365-2664.2008.01600.x>
- Maryland Biodiversity Project (2021) Maryland Biodiversity Project. <https://www.maryland-biodiversity.com/index.php> [Accessed on 09.28.2021]
- Meurisse N, Rassati D, Hurley BP, Brockerhoff EG, Haack R (2019) Common pathways by which non-native forest insects move internationally and domestically. *Journal of Pest Science* 92: 13–27. <https://doi.org/10.1007/s10340-018-0990-0>
- PDA (2020) Annual Entomology Program Summary 2020. Pennsylvania Department of Agriculture (PDA). [https://www.agriculture.pa.gov/Plants\\_Land\\_Water/PlantIndustry/Entomology/Pages/default.aspx](https://www.agriculture.pa.gov/Plants_Land_Water/PlantIndustry/Entomology/Pages/default.aspx)
- Pusceddu M, Floris I, Mannu R, Cocco A, Satta A (2019) Using verified citizen science as a tool for monitoring the European hornet (*Vespa crabro*) in the island of Sardinia (Italy). *NeoBiota* 50: 97–108. <https://doi.org/10.3897/neobiota.50.37587>
- Stankus T (2020) Reviews of Science for Science Librarians: “Murder Hornets:” *Vespa Mandarina Japonica*. *Science & Technology Libraries* 39(3): 244–252. <https://doi.org/10.1080/0194262X.2020.1796890>
- Tripodi A, Hardin T (2020) New Pest Response Guidelines: *Vespa mandarina*, Asian giant hornet. Animal and Plant Health Inspection Service (USDA): Plant Protection and Quarantine. [https://cms.agr.wa.gov/WSDAKentico/Documents/PP/PestProgram/Vespa\\_mandarina\\_NPRG\\_10Feb2020-\(002\).pdf](https://cms.agr.wa.gov/WSDAKentico/Documents/PP/PestProgram/Vespa_mandarina_NPRG_10Feb2020-(002).pdf)
- USDA Forest Service (2019) National Land Cover Database (NLCD) 2016 Tree Canopy Cover (CONUS) [raster digital data] Salt Lake City, UT: U.S. Geological Survey. <https://www.mrlc.gov/data/>
- WSDA (2021) Asian Giant Hornet Public Dashboard. Washington State Department of Agriculture (WSDA). <https://agr.wa.gov/departments/insects-pests-and-weeds/insects/hornets/data>
- Wegner G, Jordan K (2005) Comparison of Three Liquid Lures for Trapping Social Wasps (Hymenoptera: Vespidae). *Journal of Economic Entomology* 98(3): 664–666. <https://doi.org/10.1603/0022-0493-98.3.664>

## Supplementary material I

### Tables S1–S3

Authors: Grady O. Jakobsberg, Jacqueline R. Sanchez

Data type: Tables and figures.

Explanation note: Table S1. Summary statistics of trap results for unpaired and paired hanging and ground traps, including the mean catches for the four species found. Table S2. Trap location statistics of east-west road transect. Landscape statistics are given as the percentage of each type within one kilometer of the trap location. Wetland/open water and grassland/shrubland classifications are not included due to low median percentage values of 0.20 and 0.40 respectively. Elevation data were obtained from the Gaia GPS trap location waypoints. Landscape statistics were derived in QGIS using the 2019 National Land Cover Data (Dewitz 2021), the 2016 Tree Canopy Cover (USDA Forest Service, 2019), and the EPA's Level III Ecoregions of North America (Comeleo 2010). Table S3. Trap locations, attributes, and catch statistics. Includes (from left to right): latitude coordinates, longitude coordinates, trap number, deployment date for ground traps, collection date for low traps, deployment date for high traps, collection date for high traps, usable low traps (1 means usable, 0 means unusable), usable high traps (1 means usable, 0 means unusable), elevation (in meters), level 3 ecoregion of the trap, the percentage of water/wetland within 1 km of the trap, percentage of developed land within 1 km of the trap, percentage of forested land within 1 km of the trap, percentage of grass or shrubland within 1 km of the trap, percentage of cropland or pasture within 1 km of the trap, percentage of tree canopy within 1 km of the trap, species counts for low traps (separated by species), total catch for low traps, species count for high traps, and total catch for high species. Elevation data were obtained from the Gaia GPS trap location waypoints. Landscape statistics were derived in QGIS using the 2019 National Land Cover Data (Dewitz 2021), the 2016 Tree Canopy Cover (USDA Forest Service, 2019), and the EPA's Level III Ecoregions of North America (Comeleo 2010).

Copyright notice: This dataset is made available under the Open Database License (<http://opendatacommons.org/licenses/odbl/1.0/>). The Open Database License (ODbL) is a license agreement intended to allow users to freely share, modify, and use this Dataset while maintaining this same freedom for others, provided that the original source and author(s) are credited.

Link: <https://doi.org/10.3897/jhr.89.80284.suppl1>

## Supplementary material 2

### Figure S1

Authors: Gabrielle A. Jakobsberg, Grady O. Jakobsberg

Data type: Image.

Explanation note: Illustrated diagram of hanging and ground trap placement for educational purposes. Not to scale.

Copyright notice: This dataset is made available under the Open Database License (<http://opendatacommons.org/licenses/odbl/1.0/>). The Open Database License (ODbL) is a license agreement intended to allow users to freely share, modify, and use this Dataset while maintaining this same freedom for others, provided that the original source and author(s) are credited.

Link: <https://doi.org/10.3897/jhr.89.80284.suppl2>

# An unexpected new genus of panurgine bees (Hymenoptera, Andrenidae) from Europe discovered after phylogenomic analysis

Thomas J. Wood<sup>1</sup>, Sébastien Patiny<sup>1</sup>, Silas Bossert<sup>2,3</sup>

**1** Laboratory of Zoology, University of Mons, Mons, Belgium **2** Department of Entomology, Washington State University, Pullman, Washington, USA **3** Department of Entomology, National Museum of Natural History, Smithsonian Institution, Washington, DC, USA

Corresponding author: Thomas J. Wood ([thomasjames.wood@umons.ac.be](mailto:thomasjames.wood@umons.ac.be))

---

Academic editor: Michael Ohl | Received 24 July 2021 | Accepted 19 January 2022 | Published 28 February 2022

---

<http://zoobank.org/EBFE14E0-B8CF-40DB-A143-9595D77F1D8C>

---

**Citation:** Wood TJ, Patiny S, Bossert S (2022) An unexpected new genus of panurgine bees (Hymenoptera, Andrenidae) from Europe discovered after phylogenomic analysis. *Journal of Hymenoptera Research* 89: 183–210. <https://doi.org/10.3897/jhr.89.72083>

---

## Abstract

Establishing a higher classification of bees based on morphology alone can fail to capture evolutionary relationships when morphological characters either vary very little between distantly related groups, or conversely vary greatly between closely related species. This problem is well represented in the subfamily Panurginae, for which a recent global revision based on phylogenomic data unexpectedly revealed that two Old World species previously placed in *Camptopoeum* Spinola and *Flavipanurgus* Warncke, are in fact most closely related to each other, and together form a sister group relationship to the remaining *Flavipanurgus* and *Panurgus* Panzer combined. To rectify this situation, we here establish an expanded phylogenomic data set of Old World Panurgini and re-assess generic and subgeneric concepts for the tribe. To solve the paraphyly of *Camptopoeum* and *Flavipanurgus*, we establish the new genus *Halopanurgus* **gen. nov.** containing the species *H. baldocki* (Wood & Cross), **comb. nov.** and *H. fuzetus* (Patiny), **comb. nov.**, both of which are restricted to coastal sands, saltmarshes, and inland saline lagoons in the extreme south of Portugal and south-west of Spain. Re-evaluation of four recently used subgenera in *Panurgus* strongly supports a simplified classification of two subgenera; *Pachycephalopanurgus* Patiny, **stat. rev.** including *Micropanurgus* Patiny **syn. nov.**, and *Panurgus* s. str. including *Euryvalvus* Patiny. *Pachycephalopanurgus* species seem to be oligoleges of Asteroidae (Asteraceae), whereas *Panurgus* s. str. may be oligoleges of Cichorieae (Asteraceae). Our findings reinforce the challenges of establishing a phylogenetically sound classification of Panurginae using morphology alone and illustrate that even in well-studied regions like Europe unrecognised genera can persist in underexplored corners of the continent.

**Keywords**

Asteraceae, halophile, Iberian endemic species, solitary bees, taxonomy

**Introduction**

The bee fauna of Europe boasts the longest history of study, and as such has a relatively stable system of taxonomic classification. Depending on taxonomic interpretation, 73 bee genera are known from Europe (Rasmont et al. 2017) when taking a broad approach to *Eucera* (including *Cubitalia*, *Synhalonia*, *Tetralonia*, and *Tetraloniella*; Dorchin et al. 2018) and considering *Halictus* to consist of *Halictus* s. str. and its sister group *Seladonia*, the latter including *Vestitohalictus* (Danforth et al. 1999). As a measure of this stability, only six valid genera have been described for the European bee fauna since 1955, specifically the species-poor lineages *Clavipanurgus*, *Flavipanurgus*, and *Simpanurgus* (Warncke 1972), *Hofferia* and *Senoberiades* (Tkalčú 1984), and *Chiasmognathus* (Engel 2006) (Fig. 1). In contrast, some 20 genera have been described for the broader West Palearctic region during this time.

Key to maintaining stable bee genera for the future is the use of large-scale molecular revisions to re-evaluate lineages where generic boundaries are ambiguous due to morphological intergradation (Dorchin et al. 2018), or conversely where a great deal of morphological variation has led to a proliferation of described genera that are paraphyletic (Litman et al. 2016). Integrating phylogenomic datasets with traditional morphological study allows the reciprocal illumination of morphological features in light of molecular evidence, and greatly facilitates the systematic identification of synapomorphies and homologous characters for diagnostic purposes (Bossert et al. 2020). The classification of the Panurginae presents aspects of these problems, and delineating the phylogenetic relationships between the different genera has proved challenging for several decades. This has led to numerous tribal classification schemes, as well as disagreement as to what constitutes a genus in some cases (Patiny 2001; Ascher 2004; Engel 2005; Michener 2007; Ascher and Engel 2017). For example, Engel (2005) places the Melitturgini sensu Patiny (1999a) within the Panurgini and distinct from the Meliturgulini, whereas Michener (2007) places both together in Melitturgini, and Michener (2007) takes a broad approach to *Panurgus*, including both *Flavipanurgus* and *Simpanurgus* as subgenera. Treatment of the tribe Panurgini has been particularly problematic, with some interpretations including a limited number of Old World taxa (Patiny 2001), or conversely including all Old World and even some New World taxa (Ascher 2004).

The lack of resolution from morphological analyses has recently been addressed through a phylogenomic approach using Ultraconserved Elements (UCEs; Bossert et al. 2022). An important finding of that study is that the Old World Panurginae are not a monophyletic group. The tribe Melitturgini, comprising only *Camptopoeum* and *Melitturga*, is well-separated from all other Old World genera which can be placed in

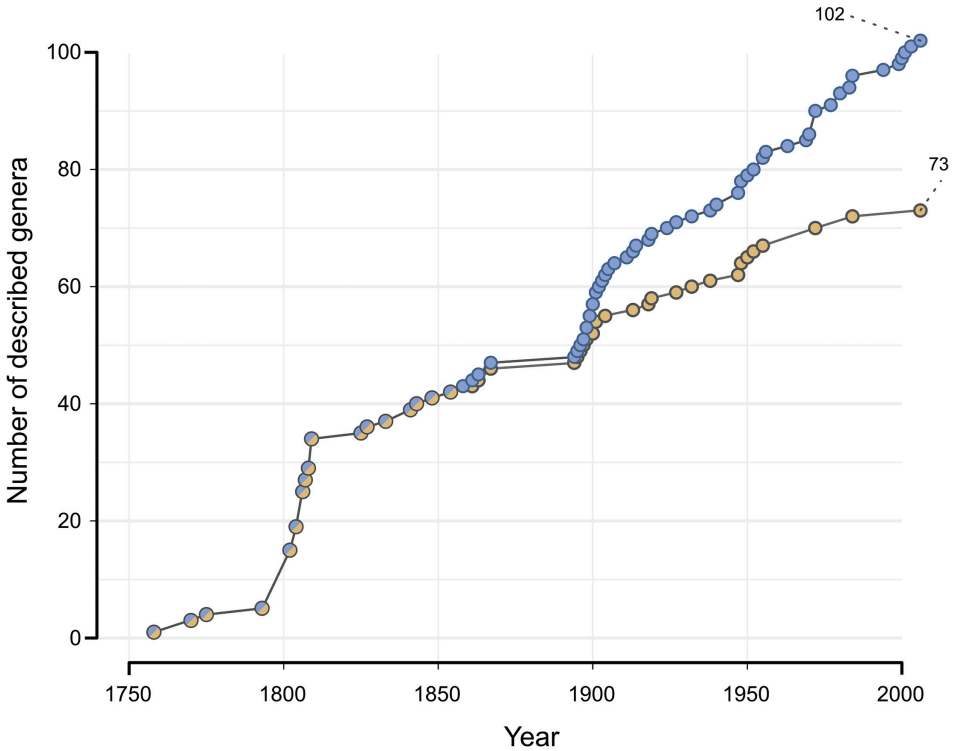


**Figure 1.** Cumulative number of valid bee genera by year of description for Europe (as defined by Rasmont et al. 2017) (yellow dots) and the wider West Palearctic region (blue dots). The recognition of genera follows Rasmont et al. (2017) with modifications as defined in the introduction.

a single large tribe, the Panurgini. Sister group to the Panurgini is the endemic North American lineage Perditiini, and both these lineages are sister group to Melitturgini: Melitturgini + (Perditiini + Panurgini). The Melitturgini likely diverged from the lineage that gave rise to the present-day Panurgini and Perditiini 46.1 million years ago (95% highest posterior density 36.8–56.1 mya, Bossert et al. 2022), shortly after their most recent common ancestor (MRCA) colonised the Palearctic. Both Panurgini and Perditiini descend from this MRCA, indicating that Panurginae only geodispersed to the Old World a single time (Bossert et al. 2022). Another surprising finding is that one species described as *Camptopoeum* (*Camptopoeum*) *baldocki* Wood & Cross, 2017 on the basis of its seemingly distinctively long glossa (Wood and Cross 2017, the glossa itself being elongate, not possessing the elongate labial palp morphology used in the division between long-tongued and short-tongued bees, see Michener (2007)) is not actually part of the lineage forming *Camptopoeum* and *Melitturga* (the Melitturgini), but instead is more closely related to the genera *Flavipanurgus* and *Panurgus*. Specifically, this species forms a sister group relationship with *Flavipanurgus fuzetus* Patiny, 1999, which has a short glossa consistent with other members of this genus (Patiny 1999b), but its placement together with *C. baldocki* renders *Flavipanurgus* paraphyletic.

Given this paraphyly, the main objectives of the current work are therefore to reassess the diagnosability of *Flavipanurgus* and *Panurgus*, re-evaluate the current usage of subgenera for *Panurgus*, and identify morphological criteria to allow for recognition of these different lineages. Considering morphological, molecular, and ecological aspects, we describe the new genus *Halopanurgus* gen. nov. to ensure that all genera are strictly monophyletic. We also take the opportunity to discuss the relationships between the different West Mediterranean genera of Panurgini, as this region is clearly a particular centre of their Old World diversity, and lastly we propose a simplified subgeneric classification for the genus *Panurgus*.

## Methodology

### Molecular methods

To better understand the phylogenetic relationships of *Panurgus* and its currently used subgenera, as well as of *Flavipanurgus*, and *Halopanurgus* gen. nov., we assembled a taxon-dense sampling of Old World Panurginae. We obtained DNA sequence data from a recently published phylogeny of Andrenidae (Bossert et al. 2022) and enriched these data with additional samples for our group of interest. Specifically, we included all *Panurgus*, *Flavipanurgus* and “*Camptopoeum baldocki*” from Bossert et al. (2022), as well as three representatives for both of the closely related tribes Melitturgini and Perditiini. Additionally, we included one representative for each of the three clades of Panurgini outside of our group of interest that were identified in Bossert et al. (2022), and chose *Neffapis longilingua* as our most distant outgroup. We combined this publicly available UCE sequence data with nine newly analysed samples for *Panurgus* and *Flavipanurgus*. We generated new sequence data for eight species of *Panurgus*, including four new samples of the previously underrepresented subgenus *Pachycephalopanurgus*. This ensures the representation of six out of seven described species of this subgenus sensu Patiny (1999c), both known species of the subgenus *Euryvalvus*, one of the three species of the subgenus *Micropanurgus* sensu Patiny (2002), and 10 out of the 22 species of *Panurgus* s. str. Lastly, we included UCE sequence data of *Flavipanurgus venustus* (Erichson, 1835), ensuring representation of five out of the seven currently recognised species of *Flavipanurgus*. Our taxon sampling totals 35 species. NCBI SRA accession numbers, collection localities and voucher depositories can be found in Table 1.

The molecular lab procedures for UCE sequencing of the nine newly analysed samples are detailed in Bossert et al. (2022), including library preparation, enrichment, and sequencing, since the newly presented data was generated jointly with this previous dataset. All newly analysed samples were enriched with the enhanced principal Hymenoptera bait set (Branstetter et al. 2017). Bioinformatic processing of these data follows the workflow detailed in Bossert et al. (2022), including the same programs and parameters for demultiplexing and sequence assembly (using SPAdes v. 3.13; Bankevich et al. 2012). After combining the new sequence data with the previously

**Table 1.** The scientific names of the included species with their collection localities and voucher depositories. NCBI SRA IDs marked with an asterisk (\*) indicate samples that are newly published. Most voucher specimens are labelled with a green coloured label which carries the voucher code. UCE assemblies of the newly generated sequence are available on the FigShare repository associated with this article (10.6084/m9.figshare.15033552). Acronyms for the collection depositories: Cornell Univ. Insect Collection (CUIC); Collection Silas Bossert (CSB); University of Mons-Hainaut, Mons, Belgium (UMH); Collection Thomas Wood, Mons, Belgium (CTW).

Taxon	Locality	Voucher depository	Collector / Identifier	Voucher Code	SRA
<i>Camptopoeum (Camp- topoeum) frontale</i>	Turkey: Agr I, Göğöglu	UMH	P. Rasmont / D. Michez	BND-1981	SRR16232743
<i>Camptopoeum (Camp- topoeum) negevensis</i>	Israel: S Negev, 13 km N Shizzafon Jct.	n/a	from Ascher (2004)	Camp 41	SRR16232742
<i>Clavipanurgus desertus</i>	Morocco: S. Anezal	CSB	Michez & Patiny / Michez & Patiny	BND-1982	SRR16232741
<i>Flavipanurgus flavus</i>	Portugal: Algarve, Aljezur	CTW	T. J. Wood / T. J. Wood	BND-2119	SRR16232720
<i>Flavipanurgus ibericus</i>	Portugal: Alentejo, Mértola	CSB	I. C. Cross / T. J. Wood	BND-2117	SRR16232718
<i>Flavipanurgus kastil- iensis</i>	Portugal: Paredelhas, Vila Real	CTW	T. J. Wood / T. J. Wood	BND-2118	SRR16232717
<i>Flavipanurgus venustus</i>	Spain: Doñana	UMH	F.P. Molina / D. Michez	BND-1926	SRR17049175
<i>Halopanurgus baldocki</i>	Portugal: Algarve, Cacela Velha	CSB	T. J. Wood / T. J. Wood	BND-1923	SRR16232744
<i>Halopanurgus fuzetus</i>	Portugal: Algarve, Cacela Velha	CTW	T. J. Wood / T. J. Wood	BND-2120	SRR16232719
<i>Macrotera (Macroter- ella) mortuaria</i>	USA: NV, Clark Co., Sacatone Wash	BBSL	T. Griswold / T. Gris- wold	BND-2005	SRR16232673
<i>Melitturga (Melitturga) clavicornis</i>	France: Hérault, Causse de la Selle	n/a	from Ascher (2004)	Mecl 73	SRR16232665
<i>Melitturgula (Melitur- gula) scriptifrons</i>	South Africa: Limpopo, 77 km S Ellisras	CUIC	B.N.D. / B.N.D. #CUIC code: 04-22	BND-1037	SRR16232644
<i>Neffapis longilingua</i>	Chile: Coquimbo Re- gion, Vicuña	RPSP	L.Packer / L. Packer	BBX-694	SRR16232638
<i>Panurgus (Pachyceph- lopanurgus) acutus</i>	Morocco/SW: 15 km NE Agadir	CSB	C. Schmid-Egger / S. Patiny	BND-1952	SRR16232763
<i>Panurgus (Pachyceph- lopanurgus) calceatus</i>	Morocco: Errachidia- Erfoud	UMH	Michez & Patiny / Michez & Patiny	BND-1931	SRR17049183
<i>Panurgus (Pachyceph- lopanurgus) canescens</i>	Spain: Sierra Nevada	UMH	J. Ortiz-Sánchez / S. Patiny	BND-1932	SSR17049182
<i>Panurgus (Pachyceph- lopanurgus) convergens</i>	Morocco: Anezal	UMH	Michez & Patiny / Michez & Patiny	BND-1933	SSR17049181
<i>Panurgus (Pachyceph- lopanurgus) farinosus</i>	Morocco: Marrakech	UMH	Michez & Patiny / Michez & Patiny	BND-1936	SSR17049180
<i>Panurgus (Pachyceph- lopanurgus) nigricopis</i>	Morocco: Drâa-Tafila- let, Ouarzazate	CSB	Michez & Patiny / Michez & Patiny	BND-1938	SRR16232758
<i>Panurgus (Pachyceph- lopanurgus) rungsii</i>	Morocco: Drâa-Tafila- let, Ouarzazate	CSB	Michez & Patiny / Michez & Patiny	BND-1943	SRR16232737
<i>Panurgus (Panurgus) avarus</i>	Morocco: Drâa-Tafila- let, Ouarzazate	CSB	Michez & Patiny / Michez & Patiny	BND-1929	SRR16232762
<i>Panurgus (Panurgus) banksianus</i>	France: Pyrénées-Or. Eyne, cabane météo	UMH	D. Michez / D. Michez	BND-1930	SRR16232761
<i>Panurgus (Panurgus) calcaratus</i>	Spain: Province of Almería	UMH	J. Ortiz-Sánchez / S. Patiny	BND-514	SSR17049179

Taxon	Locality	Voucher depository	Collector / Identifier	Voucher Code	SRA
<i>Panurgus (Panurgus) cephalotes</i>	Portugal: Trás-os-montes, Espinhosela	CTW	T. J. Wood / T. J. Wood	BND-1985	SSR17049178
<i>Panurgus (Panurgus) dentatus</i>	Morocco: Drâa-Tafilalet, Imider	UMH	Michez & Patiny / Michez & Patiny	BND-1934	SSR17049177
<i>Panurgus (Panurgus) dentipes</i>	France: Marseilles, Campus Luminy	UMH	D. Michez / D. Michez	BND-1935	SRR16232760
<i>Panurgus (Panurgus) maroccanus</i>	Morocco: Drâa-Tafilalet, Ouarzazate	CSB	Michez & Patiny / Michez & Patiny	BND-1937	SRR16232759
<i>Panurgus (Panurgus) niloticus</i>	Morocco: Drâa-Tafilalet, Ouarzazate	UMH	Michez & Patiny / Michez & Patiny	BND-1939	SRR16232757
<i>Panurgus (Panurgus) perezi</i>	Portugal: Trás-os-montes, Vila Real	CTW	T. J. Wood / T. J. Wood	BND-1940	SSR17049176
<i>Panurgus (Panurgus) pici</i>	Morocco: Drâa-Tafilalet, Ouarzazate	UMH	Michez & Patiny / Michez & Patiny	BND-1941	SRR16232740
<i>Panurgus (Panurgus) pyropygus</i>	Morocco: Drâa-Tafilalet, Ouarzazate	CSB	Michez & Patiny / Michez & Patiny	BND-1942	SRR16232738
<i>Panurgus (Panurgus) sculus</i>	Malta: Southeastern District, Ghaxaq	UMH	Michez & Balzan / D. Michez	BND-1944	SRR16232736
<i>Perdita (Hesperoperdita) trisignata</i>	USA: California	n/a	from Ascher (2004)	PeHe 77	SRR16232659
<i>Perdita (Pygoperdita) californica</i>	USA: CA, Contra Costa Co., Donner Cyn.	n/a	B. Danforth / n. a.	BND-518	SRR16232713
<i>Plesiopanurgus (Zizopanurgus) zizus</i>	Morocco: Drâa-Tafilalet, Ouarzazate	CSB	Michez & Patiny / Michez & Patiny	BND-1945	SRR16232657

published assemblies, we used the Phyluce pipeline (v. 1.7.1; Faircloth 2016) to search the assemblies for UCE sequences (with min-coverage and min-identity parameters of 80), aligned the data with MAFFT and the L-INS-i mode (v. 7.130b; Katoh and Standley 2013), and trimmed the alignments with Gblocks (Castresana 2000) and adjusted parameters ( $-b1$  0.5,  $-b2$  0.5625,  $-b3$  10,  $-b4$  5). We additionally processed the alignments with Spruceup (Borowiec 2019) and generated a concatenated sequence matrix of 80%, meaning that every individual UCE locus is represented by at least 28 taxa.

We estimated phylogenetic relationships with the maximum likelihood implementation IQ-Tree (v. 2.1.3; Minh et al. 2020). Substitution models were assigned after combining partitions of similar substitution patterns using the greedy search strategy (Lanfear et al. 2012). To ease the computational burden, we used the relaxed hierarchical clustering method (Lanfear et al. 2014) at 50% ( $-rcluster$  50). Model selection was carried out with Modelfinder (Kalyanamoorthy et al. 2017) and support was assessed with 1,000 ultrafast bootstrap approximations (UFBoot2; Hoang et al. 2018).

Newly generated SPAdes assemblies, the concatenated alignment, tree files, and the input files used to generate the phylogeny are deposited in a FigShare online repository associated with this article (10.6084/m9.figshare.15033552). Unprocessed Illumina sequence reads generated for this study are deposited in the NCBI Sequence Read Archive (SRA) under BioProject PRJNA783908 or under the individual identifiers listed in Table 1.

## Pollen analysis

Pollen was removed from *Panurgus* species whose pollen preferences have not previously been quantified to assess their pollen preferences following the methodology of Wood & Roberts (2018). The size of pollen loads on individual bees was estimated, ranging from a full load to a one-eighth load. Pollen grains were removed from the scopa using an entomological pin and transferred to a drop of water on a microscope slide. Grains were left to absorb water for a few minutes and then the slides were gently heated to allow evaporation. Molten glycerine jelly stained with fuchsin was added, and the slide was sealed with a coverslip. The percentage of the load composed of different plant taxa was estimated along three randomly selected lines across the cover slip at a magnification of  $\times 400$ . The percentage of the load was estimated by the relative area of the slide occupied by each plant species, rather than the absolute number of grains. Pollen species representing  $< 2\%$  of the load were excluded from further analysis because their presence might have arisen from contamination. The percentages of pollen collected were multiplied by the overall size of each load to give a final weighting i.e., a taxon comprising 50% of a  $\frac{3}{4}$  full pollen load would receive a weight of 37.5, whereas a taxon with 100% of a full (1/1) pollen load would receive a weight of 100.0. Pollen loads were identified to the lowest taxonomic level possible using a reference collection assembled during the project, in most cases to subfamily. Host range (dietary specialisation) was characterised following the criteria of Müller and Kuhlmann (2008).

## Terminology and imaging

Morphological terminology follows Michener (2007). Michener (2007) was also used as the baseline for taxonomic changes to the subgeneric classification of *Panurgus*, and generic and subgeneric synonymy was adapted from this work. Photographs were taken using an Olympus E-M1 Mark II with a 60 mm macro lens. Close-ups were taken with the addition of a Mitutoyo M Plan Apo 10 $\times$  infinity corrected objective lens in combination with an Olympus M.Zuiko 2 $\times$  teleconverter lens, a 10 mm Kenko DG extension tube, and a Meike MK-P-AF3B 10 mm extension tube. Photographs were stacked using Zerene Stacker 1.04 (Zerene Systems, USA) and plates were prepared in GNU Image Manipulation Program (GIMP) 2.10. Post-processing of some images was made in Photoshop Elements (Adobe Systems, USA) to improve lighting to highlight specific characters.

## Results

### Molecular phylogeny

Combining the newly presented UCE sequences of *Panurgus* with previously published data led to a concatenated sequence alignment of 1,289,627 DNA nucleotides and 35 species. The maximum likelihood analysis with IQ-Tree produced a highly supported

phylogeny that resolves the phylogenetic relationships among the examined genera and specifically of the subgenera of *Panurgus* (Fig. 2). Only the single node involving *Panurgus dentatus* Friese, 1901, *P. pici* Pérez, 1895, *P. avarus* Warncke, 1972, and *P. niloticus* Warncke, 1972 received a comparatively low bootstrap value of 53. This means that while this particular placement should be interpreted cautiously, the remaining phylogenetic relationships were resolved with high confidence. The phylogeny is congruent with the previous ML and Bayesian phylogenies of Panurgini in Bossert et al. (2022): even though the present tree includes an additional eight taxa of *Panurgus*, it is otherwise topologically identical to these previous estimates. While similar phylogenies can be expected given the shared data between these two studies, the present nucleotide matrix is nearly twice as long as the more strictly trimmed alignment of Bossert et al. (2022; 595,217 nucleotides).

Our phylogeny shows that *Flavipanurgus* in its previous sense, i.e., including “*Flavipanurgus*” *fuzetus*, is not a monophyletic group (Fig. 2). This species is not more closely related to the remaining *Flavipanurgus* than to *Panurgus*. Instead, it forms a sister group relationship with “*Camptopoeum*” *baldocki*, a lineage previously thought to be part of the genus *Camptopoeum* (Wood and Cross 2017). Recent phylogenomic analyses of the higher-level relationships of Panurginae found *Camptopoeum* to be most closely related to *Melitturga*, and hence not part of the clade investigated in the present study (Bossert et al. 2022). This means that “*Camptopoeum*” *baldocki* renders *Camptopoeum* paraphyletic, requiring taxonomic change. To rectify the paraphyly of both *Camptopoeum* and *Flavipanurgus*, we establish the new genus *Halopanurgus* gen. nov. that unites both “*Flavipanurgus*” *fuzetus* and “*Camptopoeum*” *baldocki* into one genus and ensures monophyly of both *Flavipanurgus* and *Camptopoeum*.

The presented molecular-phylogenetic relationships allow us to illuminate the subgeneric concepts of *Panurgus* with the four subgenera *Euryvalvus*, *Micropanurgus*, *Panurgus*, and *Pachycephalopanurgus* as established by Patiny (1999c). We found the subgenus *Euryvalvus* with its two species *P. banksianus* and *P. pyropygus* to be nested within the largest subgenus *Panurgus* s. str., and the included representative of the morphologically derived *Micropanurgus* renders *Pachycephalopanurgus* paraphyletic. Re-evaluating the morphological characters of these lineages in light of phylogeny, particularly of the highly informative male genitalia, we found that a simplified classification of *Panurgus* with an expanded *Panurgus* s. str. (including *Euryvalvus*) and *Pachycephalopanurgus* (including *Micropanurgus*) is most appropriate (1) to maintain readily diagnosable subgenera, (2) to ensure monophyletic groupings, and (3) to reflect the antiquity of the respective lineages. The taxonomic changes are formalised below.

## Taxonomy

### Tribe Panurgini Leach, 1815

#### *Halopanurgus* Wood, Patiny & Bossert, gen. nov.

<http://zoobank.org/D0AEA39D-BF99-406A-A439-38721C79E825>

**Type species.** *Camptopoeum baldocki* Wood & Cross, 2017

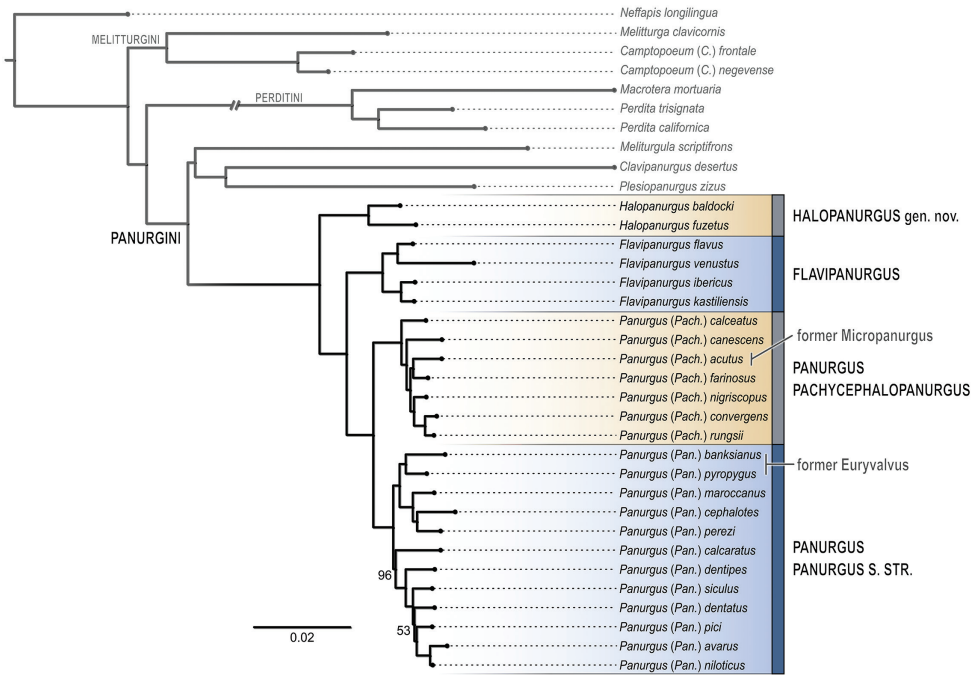


**Figure 2.** Maximum Likelihood phylogeny of *Panurgus*, *Flavipanurgus*, and the newly described genus *Halopanurgus* gen. nov., based on 2,055 ultraconserved elements. Taxonomic names reflect the nomenclatural changes proposed in this study. Node support corresponds to 100 ultrafast bootstrap support values unless indicated otherwise.

**Diagnosis.** *Halopanurgus* can be recognised as a panurgine because of its black body with yellow maculations on the head, mesosoma, and metasoma, its small size (4–5 mm), its two submarginal cells, apically truncate marginal cell, poorly developed femoral scopa, two subantennal sutures, and weak facial fovea, these shining, hairless. It is best diagnosed with reference to other similar small, yellow-marked genera with two submarginal cells, as broad characters like those used for tribal classification by Michener (2007) are not universally applicable and are not supported by the new phylogeny (Bossert et al. 2022).

*Halopanurgus* can be confused with *Camptopoeum* because of the similar structure of the male S7 and genital capsule. *Camptopoeum* has S7 as broad as long or slightly longer than broad, almost parallel sided, and with a broad apical notch (Fig. 14), and the genital capsule is parallel sided, with simple gonostyli and penis valves (Figs 6–7). In *Halopanurgus* S7 is broader, but still apically notched (Fig. 12) and the gonocoxae are produced into strong triangular points apically (Figs 3–4). In *Camptopoeum* no such points are present; the inner margin of the gonocoxae is clearly smooth and inwardly curved (in both subgenera *Camptopoeum* s. str. and *Epimethea*, Figs 6–7).

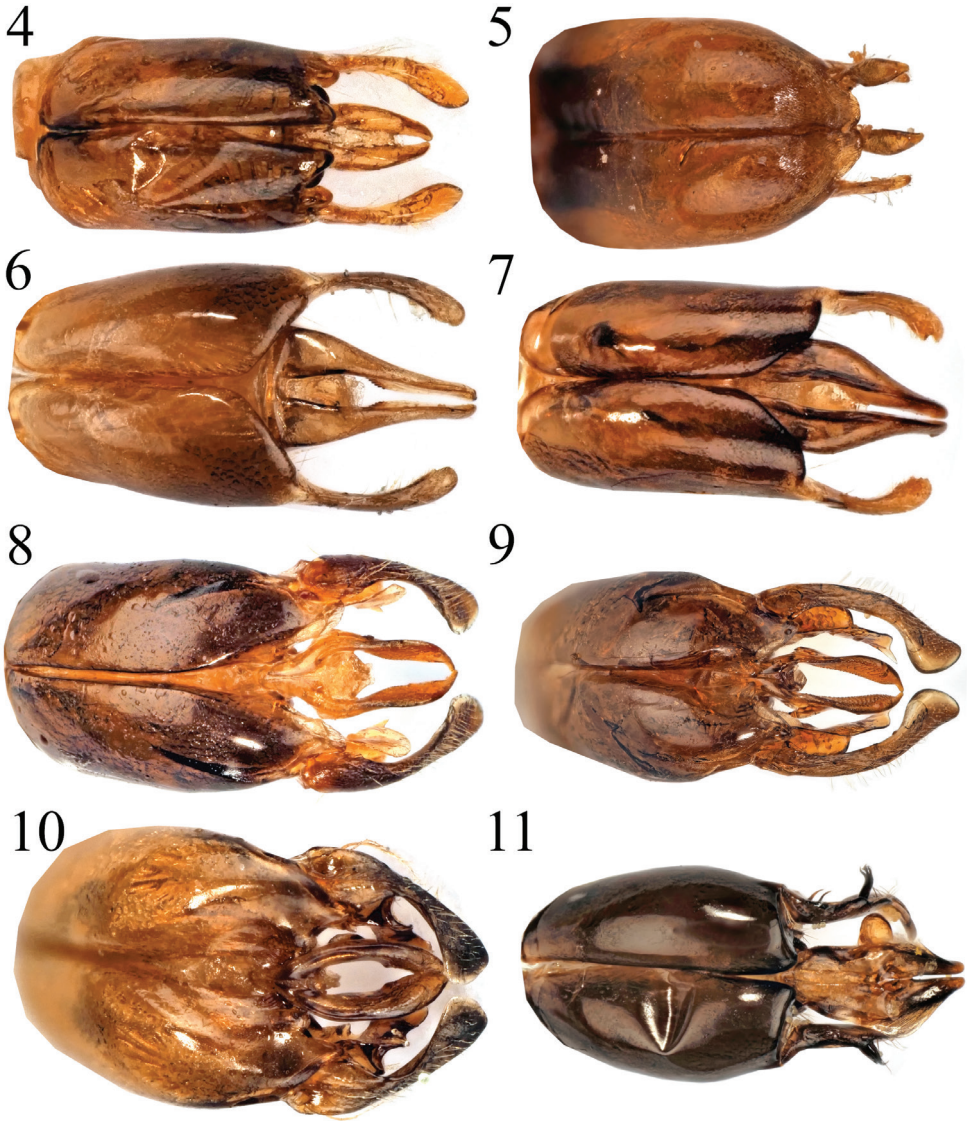
Separation from *Flavipanurgus* is simple in the male sex, as *Flavipanurgus* has S7 clearly broader than long, and deeply excavated apicomediaally (Figs 15–16). The genital capsule is also different with the gonocoxae lacking apical points and the gonostyli



**Figure 3.** Male genital capsule of *Halopanurgus baldocki*, with arrow indicating the apical part of the gonocoxa which is produced into a strong triangular point.

are flattened, apically widened, and spatulate (Figs 8–10, 31–32). In the female sex, separation is easy for *H. baldocki* because of its very long glossa (clearly longer than the length of the face, Figs 29–29, the first segment of the labial palpus exceeding the length of segments 2–4 together), but in *H. fuzetus* the length of the glossa cannot be used as the glossa is very short (clearly shorter than the length of the face, Fig. 22), with the first labial palpus not exceeding the length of segments 2–4 together. Instead, the puncturing of the face must be used, with punctures fine and weak in *Halopanurgus*, subtle, not strongly contrasting with the underlying integument. In *Flavipanurgus*, the face is strongly and clearly punctate, punctures clearly visible against the integument. This difference is most clearly seen on the frons (compare Figs 22–23).

*Halopanurgus* can be rapidly separated from *Simpanurgus* because it lacks distinctively flattened fore tarsi and clavate antennae (Figs 26–27), and from *Avpanurgus* because of its ‘Y’ shaped S7 (Fig. 13) and the genital capsule is very different, lacking the greatly expanded gonocoxae that cover almost the entire dorsal surface (Fig. 5). Note, both *Simpanurgus* and *Avpanurgus* are known only from the male sex, so diagnosis in females is not currently possible. As no genetic sequences are available for *Simpanurgus* or *Avpanurgus* their broader placement is uncertain. As *Simpanurgus* may be more closely related to *Flavipanurgus* than to *Halopanurgus*, description of the latter at a subgeneric



**Figures 4–11.** Panurgine male genitalia **4** *Halopanurgus baldocki* **5** *Avpanurgus flavofasciatus* **6** *Camptopoeum (Camptopoeum) frontale* **7** *Camptopoeum (Epimethea) variegatum* **8** *Flavipanurgus flavus* **9** *Flavipanurgus venustus* **10** *Flavipanurgus kastiliensis* **11** *Panurgus (Panurgus) calcaratus*.

level would necessitate taking a firm position on all these genera. Given this uncertainty, *Halopanurgus* is described as a genus; future studies may revise the status of these genera when suitable evidence becomes available. Lastly, *Halopanurgus* can be separated from *Panurgus* by the presence of yellow markings on the body; these are never present in *Panurgus*. Moreover, the scopae of *Halopanurgus* species are composed of simple hairs, lacking the branched hairs which are conspicuously present in *Panurgus* species.

**Description.** Small (4–5 mm) black bees with extensive yellow maculations on head, mesosoma, and metasoma; pronotal lobe, metanotum, and at least some parts of terga always yellow marked, otherwise variable. Male with at least clypeus always yellow, centrally with two small black maculations (Fig. 20). Head broader than long, compound eyes with inner margins parallel. Subantennal sutures essentially straight, outer suture only weakly arched outwards. Facial fovea narrow, slightly narrower than width of lateral ocellus, hairless, equalling length of scape. Ocellocipital distance short, subequal to width of lateral ocellus.

Face with fine and weak punctures, not strongly contrasting underlying integument (Figs 20, 22). Process of labrum square, as long as wide. Mesoscutum with scattered, fine, and short white hairs; mesepisternum and propodeum with slightly longer white hairs, equally scattered and fine. Forewing with stigma longer than wide, not parallel sided, inner margin weakly curved; two submarginal cells, first submarginal cell longer than second; first recurrent vein entering second submarginal cell; marginal cell apically truncate. Hind tibial spurs unmodified, straight. Basitibial plate present, oval, margins slightly raised; tibial scopa with simple hairs. Tarsal claws with minute inner tooth. Genital capsule simple, gonocoxae apically produced into posteriorly projecting points (Figs 3–4, see also illustrations in Wood and Cross 2017).

**Etymology.** The name is a combination of the prefix *Halo-* (Greek for salt) with the genus name *Panurgus* because of the pronounced affinity for saline soils shown by the two constituent species, both being restricted to saltmarshes, coastal sands, and inland saline lagoons (Wood & Cross 2017; Cross & Wood 2018; Fidalgo 2021; TJW unpublished data). The gender is masculine.

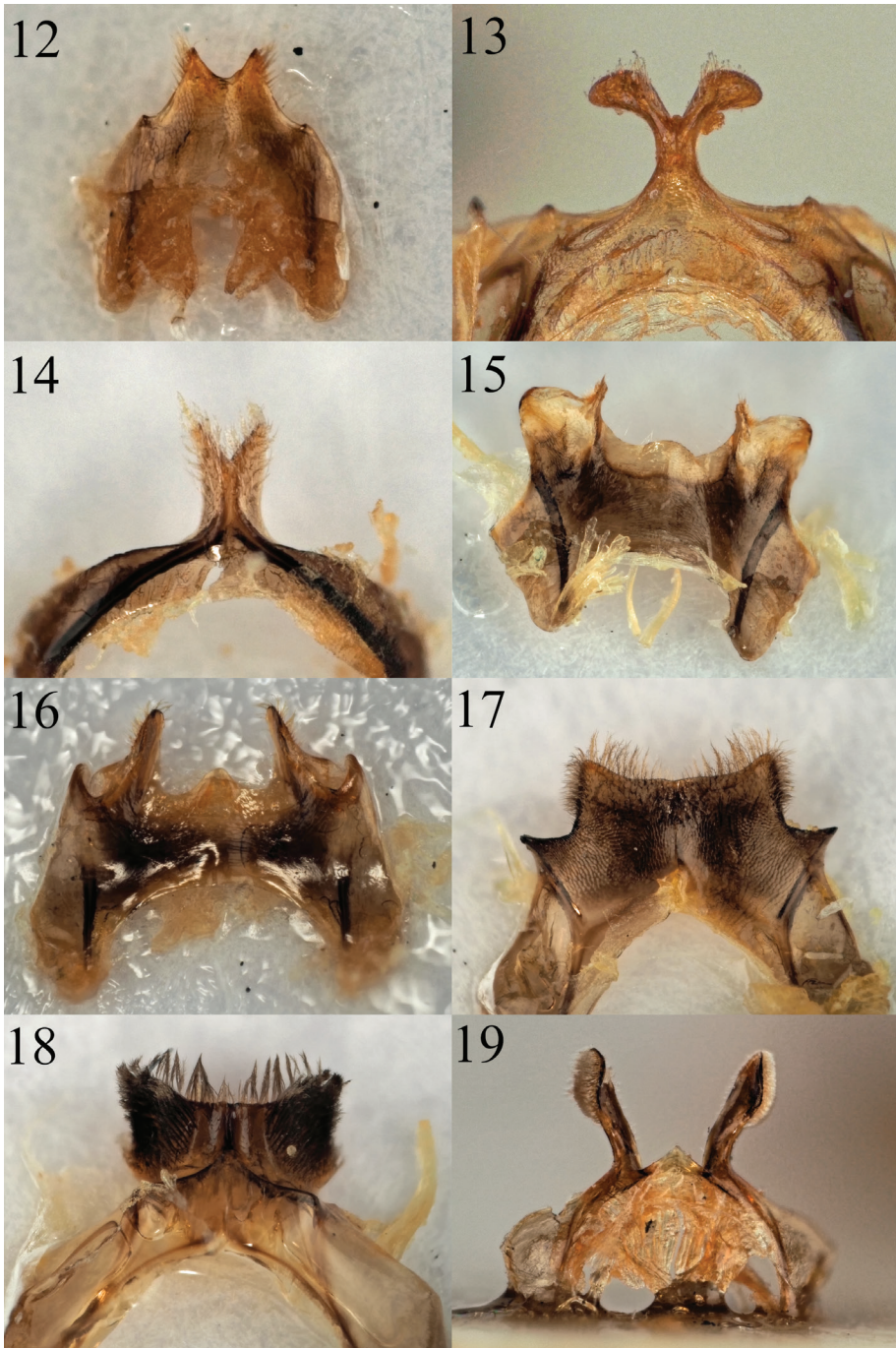
**Included species.** *Halopanurgus baldocki* (Wood and Cross, 2017) comb. nov. (Figs 28–29, Spain and Portugal, see Fidalgo 2021) and *Halopanurgus fuzetus* (Patiny, 1999) comb. nov. (Fig. 30, Spain and Portugal).

## *Flavipanurgus* Warncke, 1972

*Flavipanurgus* Warncke, 1972: 69. Type species: *Panurgus flavus* Friese, 1897

**Remarks.** No genetic samples were available for *F. granadensis* (Warncke, 1987) or *F. merceti* (Vachal, 1910). However, examination of males of these two species shows that they clearly belong in *Flavipanurgus*: *S7* is deeply excavated apicomediaally, and the genital capsule has the gonocoxae lacking apical points along with flattened and apically spatulate gonostyli (Figs 31–32).

**Included species.** Six species, *Flavipanurgus flavus* (Friese, 1897), *Flavipanurgus granadensis* (Warncke, 1987), *Flavipanurgus ibericus* (Warncke, 1972), *Flavipanurgus kastiliensis* (Warncke, 1987), *Flavipanurgus merceti* (Vachal, 1910), and *Flavipanurgus venustus* (Erichson, 1835).



**Figures 12–19.** Panurgine male sternum seven **12** *Halopanurgus baldocki* **13** *Avpanurgus flavofasciatus* **14** *Camptopoeum (Epimethea) variegatum* **15** *Flavipanurgus flavus* **16** *Flavipanurgus kastiliensis* **17** *Panurgus (Panurgus) calcaratus* **18** *Panurgus (Panurgus) dentipes* **19** *Panurgus (Pachycephalopanurgus) farinosus*.

***Panurgus* Panzer, 1806*****Panurgus* subgenus *Panurgus* s. str. Panzer, 1806**

*Panurgus* Panzer, 1806: 209. Type species: *Andrena lobata* Panzer, 1799 = *Apis calcarata* Scopoli, 1763

*Eriops* Klug, 1807: 207, 227. Type species: *Andrena lobata* Panzer, 1799 = *Apis calcarata* Scopoli, 1763, monobasic.

*Eryops* Latreille, 1811: 716, unjustified emendation of *Eriops* Klug, 1807

*Panurgus* (*Euryvalvus*) Patiny, 1999c: 316. Type species: *Apis banksiana* Kirby, 1802, by original designation.

**Diagnosis.** The subgenus can be separated from *Pachycephalopanurgus* by the shape of the male S7 which is always broad, approximately as long as wide, and never strongly apicomediaally excavated (Figs 17–18, 45–46). There may be very weak excavations, emarginations, or convexities in the apical margin (e.g. Fig. 45), but the lateral corners are never extended into long, apically produced projections (contrast Figs 19, 47–48). Genital capsule usually with gonostyli robust with strong lateral tuft of clumped hairs that diverges laterally at the midpoint of each gonostylus (Figs 11, 33–36). However, in the former group *Euryvalvus* the genital capsule is strongly divergent, lacking robust gonostyli with a strong lateral hair tuft (Figs 37–38). These can be recognised by their black, pill-like volsellae which are visible dorsally, their gonostyli which are flattened in the vertical plane, and by their S7, which as in other *Panurgus* s. str. is broad and lacks long, apically produced and extended projections (Fig. 46). Female *Panurgus* s. str. specimens cannot be consistently separated from those of *Pachycephalopanurgus*.

**Included species.** All *Panurgus* species previously placed in *Panurgus* s. str. and *Euryvalvus* (Patiny 1999c) and subsequent works; the 24 species are detailed in Table 2.

***Panurgus* subgenus *Pachycephalopanurgus* Patiny, 1999, stat. rev.**

*Panurgus* (*Pachycephalopanurgus*) Patiny, 1999c: 316. Type species: *Panurgus rungsii* Benoist, 1937, by original designation.

*Panurgus* (*Stenostylus*) Patiny, 1999c: 317. [not *Stenostylus* Pilsbury, 1898]. Type species: *Panurgus ovatulus* Warncke, 1972, by original designation syn. nov.

*Panurgus* (*Micropanurgus*) Patiny, in Ascher and Patiny 2002: 140. Replacement name for *Stenostylus* Patiny. Type species: *Panurgus ovatulus* Warncke, 1972, autobasic and by original designation syn. nov.

**Diagnosis.** The subgenus can be separated from *Panurgus* s. str. by the shape of the male S7 which has the lateral corners strongly produced into long, apical projections, these bearing a short tuft of hairs laterally (Figs 19, 47–48). S7 therefore appears to be deeply excavated. Genital capsule with gonostyli slender, the majority of species (7 out



**Figures 20–27.** Panurgine faces **20** *Halopanurgus baldocki* comb. nov. male **21** *Avpanurgus flavofasciatus* male **22** *Halopanurgus fuzetus* comb. nov. female **23** *Flavipanurgus granadensis* female **24** *Flavipanurgus kastiliensis* male **25** *Simpanurgus phyllopodus* male, including **26** male antennae and **27** male fore tarsi.

**Table 2.** Revised subgeneric classification system for the genus *Panurgus*, with all globally known species.

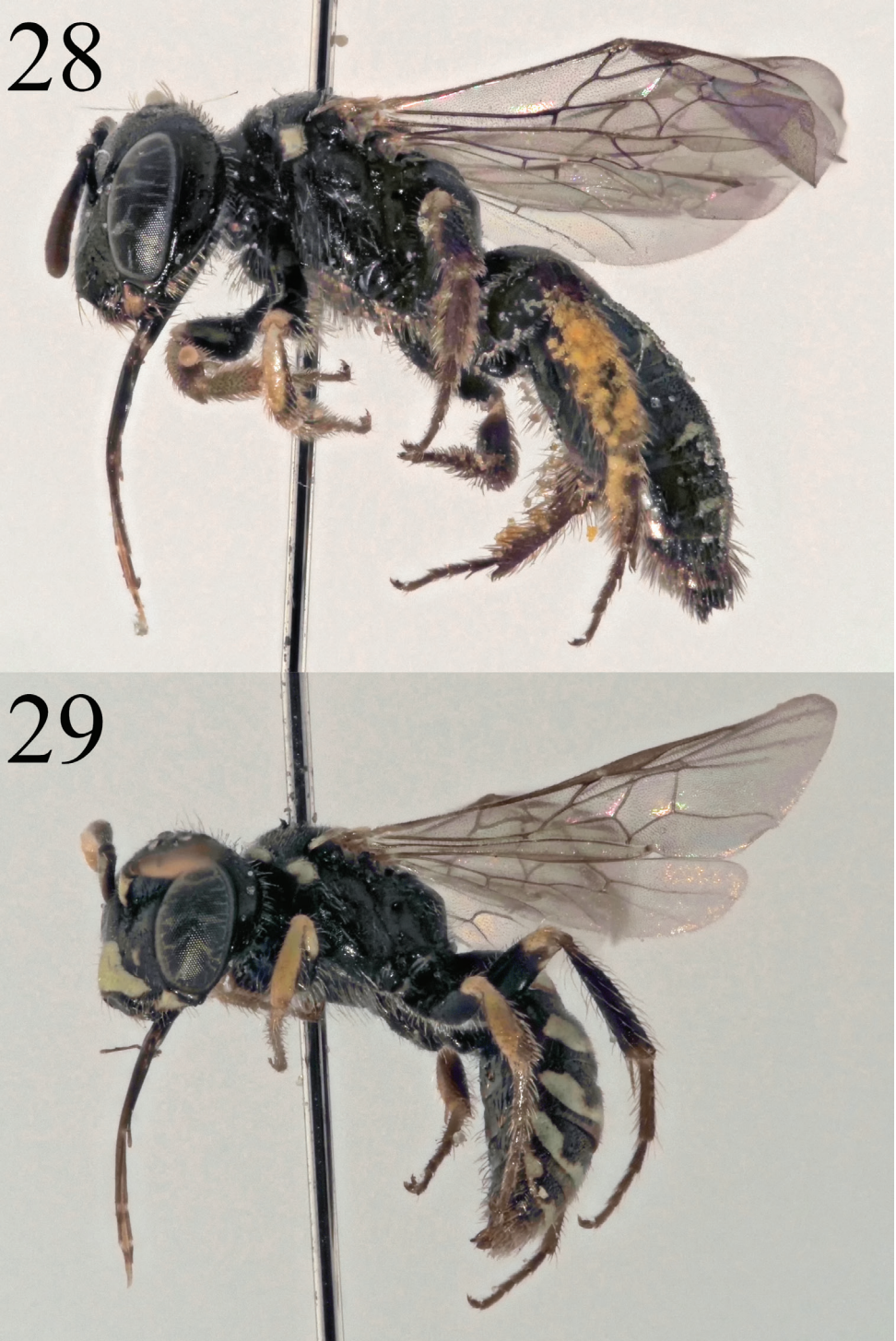
Subgenus <i>Panurgus</i> s. str. Panzer, 1806	Subgenus <i>Pachycephalopanurgus</i> Patiny, 1999 stat. rev.
<i>Panurgus afghanensis</i> Warncke, 1972	<i>Panurgus acutus</i> Patiny, 2002
<i>Panurgus avarus</i> Warncke, 1972	<i>Panurgus calceatus</i> Pérez, 1895
<i>Panurgus banksianus</i> (Kirby, 1802)	<i>Panurgus canescens</i> Latreille, 1811
<i>Panurgus buteus</i> Warncke, 1972	<i>Panurgus convergens</i> Pérez, 1895
<i>Panurgus calcaratus</i> (Scopoli, 1763)	<i>Panurgus farinosus</i> Warncke, 1972
<i>Panurgus canarius</i> Warncke, 1972	<i>Panurgus meridionalis</i> Patiny, Ortiz & Michez, 2005
<i>Panurgus cephalotes</i> Latreille, 1811	<i>Panurgus minor</i> Warncke, 1972
<i>Panurgus corsicus</i> Warncke, 1972	<i>Panurgus nigriscopus</i> Pérez, 1895
<i>Panurgus cyrenaikensis</i> Warncke, 1972	<i>Panurgus ovatulus</i> Warncke, 1972
<i>Panurgus dargius</i> Warncke, 1972	<i>Panurgus rungsii</i> Benoist, 1937
<i>Panurgus dentatus</i> Friese, 1901	
<i>Panurgus dentipes</i> Latreille, 1811	
<i>Panurgus intermedius</i> Rozen, 1971	
<i>Panurgus maroccanus</i> Pérez, 1895	
<i>Panurgus niloticus</i> Warncke, 1972	
<i>Panurgus oblitus</i> Warncke, 1972	
<i>Panurgus perezii</i> Saunders, 1882	
<i>Panurgus pici</i> Pérez, 1895	
<i>Panurgus platymerus</i> Pérez, 1895	
<i>Panurgus posticus</i> Warncke, 1972	
<i>Panurgus pyropygus</i> Friese, 1901	
<i>Panurgus siculus</i> Morawitz, 1872	
<i>Panurgus sidensis</i> Warncke, 1987	
<i>Panurgus vachali</i> Pérez, 1895	

of 10) with a clear lamelliform projection that diverges at the midpoint of each gonostylus (Figs 39–42, 44). However, in the former group *Micropanurgus* (three species), this lamelliform projection is greatly reduced and inconspicuous (Fig. 43). Gonocoxae always with strongly projecting points. Female *Pachycephalopanurgus* specimens cannot be consistently separated from *Panurgus* s. str.

**Included species.** All *Panurgus* species previously placed in *Pachycephalopanurgus* and *Micropanurgus* (Patiny 1999c; Ascher and Patiny 2002; Patiny 2002); the 10 species are detailed in Table 2.

## Genera closely related to *Panurgus*

Compared to the baseline of Michener (2007), these changes result in the elevation of *Flavipanurgus* and *Simpanurgus* from subgenera of *Panurgus*, and the re-establishment of two subgenera within *Panurgus*, *Panurgus* s. str. and *Pachycephalopanurgus*. The description of the genus *Halopanurgus* and the reorganisation of genera within panurgine tribes means that it is necessary to write a new key to facilitate their identification. Within the scope of this paper, we provide a key to the genera closely related to *Panurgus*, specifically the five genera, *Avpanurgus*, *Flavipanurgus*, *Halopanurgus*, *Simpanurgus*, and *Panurgus*. As *Avpanurgus flavofasciatus* (Warncke, 1972)



Figures 28–29. *Halopanurgus baldocki* comb. nov. profile 28 female 29 male.



Figures 31–32. *Flavipanurgus* male genitalia 31 *Flavipanurgus granadensis* 32 *Flavipanurgus merceti*.

and *Simpanurgus phyllopodus* (Warncke, 1972) are known only from the type series (comprised entirely of males), no samples were available for genetic analysis and they are therefore absent from the tree of Bossert et al. (2022). However, we retain these species in this group of related genera because of male genital morphology and for biogeographic reasons, as all genera are restricted, to or show a centre of diversity (greatest number of genera and extant taxa), in the West Mediterranean region. Specifically, the genital capsule of *Simpanurgus* resembles that of *Flavipanurgus* in its gonocoxae which lack apical points, their inner margin rounded; in its large penis valves, the blades of which are flattened in the vertical plane; and there are also similarities in the structure of S7 which is broader than long and deeply excavated medially with a tiny apicomedial tooth (see Warncke 1972, compare Figs 8–10, 15–16, 31–32, 37 of *S. phyllopodus* very similar to *F. kastiliensis*). In *Avpanurgus*, the gonostyli and penis valves are thin and delicate and have similarities with those of *Halopanurgus*, but the gonocoxae are grossly enlarged (Fig. 5). The shape of S7 is also similar, generally as long as broad, and with an apicomedial notch, though this is much more strongly pronounced, with a narrow basal stem (Fig. 13). The face is similar, being less extensively punctured (Figs 20–23) and with less yellow maculation than in *Flavipanurgus* and *Simpanurgus* (Figs 20–21, 24–25).

**Key to the genera closely related to *Panurgus***

- 1 Male S7 with extremely narrow stem, medially with apical projection that is deeply notched, forming a ‘Y’ shape, apical breadth greater than length (Fig. 13). Gonocoxae grossly enlarged, covering entire dorsal surface of capsule, only apexes of gonostyli and penis valves extend beyond its apical extent (Fig. 5).....***Avpanurgus* Warncke**
- Male S7 narrow or broad, notched or not, but never with a ‘Y’ shaped apical projection (Figs 12, 15–19, 45–48). Gonocoxae not grossly enlarged, base of both gonostyli and penis valves visible in dorsal view ..... **2**

- 2 Male antennae clavate, clearly broadened apically (Fig. 26). Fore tarsi with all segments strongly expanded and flattened (Fig. 27). Male S7 medially excavated..... ***Simpanurgus* Warncke**
- Male antennae not clavate, apical segments not noticeably broader than basal segments (e.g. Figs 20, 24). Fore tarsi normal, not noticeably expanded or flattened. Male S7 medially excavated or not ..... **3**
- 3 Male S7 comparatively narrow, slightly broader than long, medially notched (Fig. 12). Genitalia with gonocoxae apically produced into strong points (Figs 3–4). Body black with yellow markings. Face with reduced punctuation, punctures fine, superficial, not strongly standing out from underlying integument (Figs 20, 22). Tongue over twice the length of face or not (Figs 28–30) ..... ***Halopanurgus* gen. nov.**
- Male S7 broad, much broader than long, strongly excavated medially or not, but not narrowly notched (Figs 15–19). Genitalia with gonocoxae either without apical points (Figs 8–10, 31–32, 37–38), or if with apical points (Figs 11, 33–36, 39–44), then body black, never with yellow markings. Face with clear punctuation (Fig. 23). Tongue never over twice as long as face..... **4**
- 4 Body with yellow markings (except female of *F. flavus* (Friese, 1897)). Scopal hairs simple, not spiralled. Genitalia with gonocoxae lacking apical points, inner margin rounded, gonostyli flattened in lateral plane, spatulate (Figs 8–10, 31–32)..... ***Flavipanurgus* Warncke**
- Body never with yellow markings. Scopal hairs distinctively and minutely spiralled. Genitalia with gonocoxae usually with apical points (Figs 11, 33–36, 39–44), if absent then gonostyli flattened in vertical plane, never in lateral plane and never spatulate (Figs 37–38) ..... ***Panurgus* Panzer**

### Pollen preferences

A total of 93 pollen loads were analysed from nine *Panurgus* species (Table 3). All pollen was collected from Asteraceae, which is why we assume all species to be oligolectic or suspect them to be oligolectic where sample sizes were too low to be confident. *Panurgus* (*Panurgus*) showed a strong association with the subfamily Cichorioideae, whereas *P.* (*Pachycephalopanurgus*) showed a strong association with the subfamily Asteroideae, though confidence in the strength of this relationship is limited by the very low sample sizes available for North African species.

### Discussion

As demonstrated at a global scale (Pisanty et al. 2021; Bossert et al. 2022), the use of ultraconserved elements for phylogenetic analysis has considerably improved our understanding on the evolutionary relationships of andrenid bees, including the subfamily



**Figures 33–38.** *Panurgus* (*Panurgus* s. str.) male genitalia **33** *Panurgus cephalotes* **34** *Panurgus dentipes* **35** *Panurgus maroccanus* **36** *Panurgus perezi* **37** *Panurgus banksianus* **38** *Panurgus pyropygus*.

Panurginae. In the case of the Panurginae, the reciprocal analysis of morphological characters given our robust molecular phylogeny revealed that certain morphological features used to characterise genera of Old World Panurginae have been overvalued in the past and have incorrectly resulted in the association of *Halopanurgus baldocki* with the genus *Camptopoeum*.

Albeit separated by ~50 million years of divergence time (Bossert et al. 2022), certain species of Panurgini and Melitturgini share remarkably similar morphological features, leading authors to conclude close phylogenetic relationships until very recently. The most pertinent example is *Camptopoeum*, which was included with the two-celled members of the Panurgini by Michener (2007). *Halopanurgus baldocki* was described as a *Camptopoeum* (*Camptopoeum*) because of the elongate tongue, in which the first segment of the labial palpus is about as long as the second to fourth segments taken together. Indeed, based only on tongue morphology, *H. baldocki* is more similar to *Camptopoeum* (*Camptopoeum*) than it is to its sister species *Halopanurgus fuzetus*,



**Figures 39–44.** *Panurgus* (*Pachycephalopanurgus*) male genitalia **39** *Panurgus calceatus* **40** *Panurgus canescens* **41** *Panurgus convergens* **42** *Panurgus farinosus* **43** *Panurgus minor* **44** *Panurgus rungsii*.

and more similar to *Camptopoeum* (*Camptopoeum*) than to *Camptopoeum* (*Epimethea*), which have very short glossa. Tongue length within Old World panurgines is therefore clearly homoplasious.

This confusion that arose from misleading tongue morphology serves as a cautionary tale into panurgine classification. Tongue length can clearly be a labile morphological character and is not necessarily suitable for diagnosing suprageneric taxa (Danforth et al. 2019). Bee mouthparts represent a particularly intuitive example of a morphological structure facing selective pressure. All bee species examined in this study exhibit some degree of host plant specialization and most seem to be true oligoleges. It is expected that tongue length varies among species in respect to their host plant, and the appearance of bee species with physically long tongues within the short-tongued bee families such as Andrenidae (e.g. Shimizu et al. 2014), Colletidae (e.g. Laroca et al. 1989; Rozen and Wyman 2015), and Halictidae (e.g. Burger 2020) is well established, usually being associated with particular floral shapes that necessitate morphological adaptation to access particular resources. In the case of *H. baldocki*, their long tongues are used to access the



**Figures 45–48.** Sternum 7 for members of the former four subgenera of *Panurgus* **45** *Panurgus* (*Panurgus*) *cephalotes* **46** *Panurgus* (*Euryvalvus*) *banksianus* **47** *Panurgus* (*Pachycephalopanurgus*) *canescens* **48** *Panurgus* (*Micropanurgus*) *ovatulus*.

nectaries of its host *Frankenia laevis* (Frankeniaceae) which are found at the base of a tubular corolla, necessitating a long tongue for a bee of only 4 mm in length (Wood and Cross 2017). *Halopanurgus fuzetus* in turn visits species of *Spergularia* (Caryophyllaceae, Wood and Cross 2017), which have an open floral structure, and therefore do not require a long tongue to access the nectaries despite their equally small body size. The ~7.5 million years of divergence time between the two *Halopanurgus* species (Bossert et al. 2022) was sufficient to allow their tongue morphologies to diverge, and it is intuitive that they represent adaptations towards nectar uptake from different host plants. This mirrors the situation in *Camptopoeum* (*Camptopoeum*) and *Camptopoeum* (*Epimethea*), which based on the very limited number of species whose foraging niches are well understood are specialists of *Centaurea* (Asteraceae) and Apiaceae, respectively (Friese 1926, TJW unpublished data). Like *Frankenia*, *Centaurea* flowers have individual florets in which nectar is found at the bottom of a tubular corolla, whereas in the Apiaceae used by *Camptopoeum* (*Epimethea*) species, the floral structure is open and does not require a long tongue to access nectaries.

Against this context, the description of new panurgine genera from the Arabian Peninsula and Central Asia (Engel et al. 2019) based primarily on tongue morphology raises interesting questions. Placing close to *Flavomeliturgula* Patiny (now within a broad Panurgini, Bossert et al. 2022; Meliturgulina sensu Engel et al. 2019), the genus

*Belliturgula* Engel (Saudi Arabia) is diagnosed predominantly on the basis of tongue characters combined with body colouration (Engel et al. 2019), and the genus *Khuzimelissa* Engel (Iran and Pakistan) is diagnosed mainly on the basis of tongue characters and additionally on the shape of the outer antennal sulcus. Both genera are monotypic, and were described from female material only, with no male specimens known. Given the labile nature of tongue length within Panurginae, and the lack of male material that was crucial for morphologically confirming differences between the genera in the present study, it is difficult to assess the status of these genera and the relationships between the species related to *Flavomeliturgula* with confidence.

From a biogeographical perspective, the genera closely related to *Panurgus* that have been confidently placed through genetic analysis (Bossert et al. 2022) show a West Mediterranean distribution, restricted to Iberia (*Halopanurgus* and *Flavipanurgus*) or with particular diversity in the western Maghreb (*Panurgus*; Patiny and Gaspar 2000; Patiny 2001; Lhomme et al. 2020). The only known collecting localities for *Avpanurgus* and *Simpanurgus* being in Algeria and Spain, respectively (Warncke 1972; Patiny 2001), means that they align with this overall pattern; the centres of diversity for other Panurgini clades are located further east, such as Asia (taxa related to *Panurginus*), and the Middle East to sub-Saharan Africa (taxa related to *Meliturgula* and *Mermiglossa*), and also for *Camptopoeum* whose centre of diversity is the Middle East (Patiny 2001). Though the placement of *Avpanurgus* and *Simpanurgus* in the group of genera related to *Panurgus* requires additional molecular investigation and confirmation, it forms the basis of a suitable hypothesis should fresh specimens become available.

A further line of evidence that can help inform our understanding of panurgine groups are their pollen preferences. Though the division of *Panurgus* into two subgenera is justified on the basis of the strong molecular and morphological evidence in the male sex, this division between *Panurgus* s. str. and *Pachycephalopanurgus* may also be reflected in their use of Asteraceae pollen. All known *Panurgus* species are oligoleges of Asteraceae, but *Panurgus* s. str. are specialists of the subfamily Cichorioideae (Table 3, see Münster-Swendsen 1970; Westrich 1989 for *P. calcaratus*, *P. banksianus*, and *P. dentipes*; Rozen 1971 for *P. maroccanus*, *P. intermedius*, *P. pici*), whereas *Pachycephalopanurgus* appear to be specialists of the subfamily Asteroideae (Table 3, see Cross 2020 for *P. meridionalis*). Clearly, a much greater sampling effort is needed for North African *Pachycephalopanurgus* species, but a nominal specialisation on Asteroideae forms the basis of a testable hypothesis. Why these two lineages of *Panurgus* seem to divide their efforts between these two lineages of Asteraceae is unclear, but a proposed mechanism is related to their pollen-collecting behaviour. Specifically, when foraging on *Astericus* (Asteroideae), *Pachycephalopanurgus* species focus on the non-ligulate disc florets and sweep pollen into their scopae whilst rapidly pulsing and moving their metasoma, a technique that seems unlikely to be effective in the Cichorioideae where only ligulate florets are present (Cross 2020). More broadly, with their spiralled scopal hairs and specialisation on Asteraceae, *Panurgus* appear to represent another independent lineage of bees that have converged on carrying their pollen dry (Portman and Tepedino 2017), in contrast to their closest relatives *Flavipanurgus* and *Halopanurgus* which carry their pollen moistened by nectar (Wood and Cross 2017; Cross and Wood 2018).

**Table 3.** Host plant spectrum and inferred category of host use in *Panurgus* species. *n* total number of pollen loads, *N* number of pollen loads from different localities. Plant taxa AST, Asteraceae.

Species	<i>n</i>	<i>N</i>	Results of microscopic analysis of pollen grains (% pollen grains)	% Pure loads of preferred host	% Loads with preferred host	Host range
<i>P. (Panurgus)</i>						
<i>Panurgus cephalotes</i>	28	15	AST (Cichorioideae) 98.9, AST (Asteroideae) 1.1	100.0	100.0	Broadly oligolectic (Asteraceae, Cichorioideae)
<i>Panurgus maroccanus</i>	14	5	AST (Cichorioideae) 91.1, AST (Asteroideae) 9.9	100.0	100.0	Possibly broadly oligolectic (Asteraceae, Cichorioideae)
<i>Panurgus perezii</i>	23	14	AST (Cichorioideae) 100.0	100.0	100.0	Broadly oligolectic (Asteraceae, Cichorioideae)
<i>P. (Pachycephalopanurgus)</i>						
<i>Panurgus calceatus</i>	10	2	AST (Asteroideae) 65.9, AST (Cichorioideae) 26.0, AST (Carduoideae) 8.1	100.0	100.0	Broadly oligolectic (Asteraceae)
<i>Panurgus canescens</i>	12	8	AST (Asteroideae) 100.0	100.0	100.0	Broadly oligolectic (Asteraceae, Asteroideae)
<i>Panurgus convergens</i>	2	2	AST (Asteroideae) 100.0	100.0	100.0	Possibly broadly oligolectic (Asteraceae, Asteroideae)
<i>Panurgus nigricopis</i>	1	1	AST (Asteroideae) 100.0	100.0	100.0	Possibly broadly oligolectic (Asteraceae, Asteroideae)
<i>Panurgus ovatulus</i>	1	1	AST (Asteroideae) 100.0	100.0	100.0	Possibly broadly oligolectic (Asteraceae, Asteroideae)
<i>Panurgus rungsii</i>	2	2	AST (Asteroideae) 94.0, AST (Carduoideae) 6.0	100.0	100.0	Possibly broadly oligolectic (Asteraceae, Asteroideae)

## Acknowledgements

Our thanks go to Esther Ockermüller and Martin Schwarz for access to the Warncke Collection, loan of material, and hospitality at Linz, and to Ian Cross for access to his personal collection. We also thank Pierre Rasmont for substantial assistance with photography. TJW is supported by an F.R.S.-FNRS fellowship “Chargé de recherches”. This work was supported by NSF grant DEB-2127744 and a Peter Buck fellowship to SB. The authors thank Laurence Packer, Zachary Portman, and an anonymous reviewer for comments that substantially improved the manuscript.

## References

- Ascher JS, Patiny S (2002) A new name for the bee subgenus *Stenostylus* (Hymenoptera: Andrenidae). Entomological News 113: 140–140.
- Ascher J, Engel MS (2017) A new species of *Mermiglossa* from Kenya, with comments on the arrangement of Old World Panurginae (Hymenoptera: Andrenidae). Journal of Melittology 75: 1–11. <http://dx.doi.org/10.17161/jom.v0i75.6717>

- Ascher JS (2004) Systematics of the bee family Andrenidae (Hymenoptera: Apoidea). PhD thesis. Cornell University, USA.
- Bankevich A, Nurk S, Antipov D, Gurevich AA, Dvorkin M, Kulikov AS, Lesin VM, Nikolenko SI, Pham S, Pribelski AD (2012) SPAdes: a new genome assembly algorithm and its applications to single-cell sequencing. *Journal of Computational Biology* 19: 455–477. <https://doi.org/10.1089/cmb.2012.0021>
- Borowiec ML (2019) Spruceup: fast and flexible identification, visualization, and removal of outliers from large multiple sequence alignments. *Journal of Open Source Software* 4: e1635. <https://doi.org/10.21105/joss.01635>
- Bossert S, Copeland RS, Sless TJL, Branstetter MG, Gillung JP, Brady SG, Danforth BN, Policarová J, Straka J (2020) Phylogenomic and morphological reevaluation of the bee tribes Biastini, Neolarrini, and Townsendiellini (Hymenoptera: Apidae) with description of three new species of *Schwarzia*. *Insect Systematics and Diversity* 4: 1–29. <https://doi.org/10.1093/isd/ixaa013>
- Bossert S, Wood TJ, Patiny S, Michez D, Almeida EAB, Minckley RL, Packer L, Neff JL, Copeland RS, Straka J, Pauly A, Griswold T, Brady SG, Danforth BN, Murray EA (2022) Phylogeny, biogeography and diversification of the mining bee family Andrenidae. *Systematic Entomology*, in press. <https://doi.org/10.1111/syen.12530>
- Branstetter MG, Longino JT, Ward PS, Faircloth BC (2017) Enriching the ant tree of life: enhanced UCE bait set for genome-scale phylogenetics of ants and other Hymenoptera. *Methods in Ecology and Evolution* 8: 768–776. <https://doi.org/10.1111/2041-210X.12742>
- Burger R (2020) Beobachtungen zum Blütenbesuch und Pollensammeln von *Lasioglossum buccale* (Pérez 1903) (Hymenoptera: Anthophila). *Ampulex* 11: 34–40.
- Castresana J (2000) Selection of conserved blocks from multiple alignments for their use in phylogenetic analysis. *Molecular Biology and Evolution* 17: 540–552. <https://doi.org/10.1093/oxfordjournals.molbev.a026334>
- Cross I (2020) The pollen host of *Panurgus meridionalis* (Hymenoptera: Andrenidae). *Entomologist's Monthly Magazine* 156: 1–6. <https://doi.org/10.31184/M00138908.1561.4018>
- Cross I, Wood TJ (2018) New data on the Iberian endemic bee genus *Flavipanurgus* Warncke (Hymenoptera: Apoidea: Andrenidae): Ecological and genomic data reveal a hidden species. *Zootaxa* 4521: 563–572. <https://doi.org/10.11646/zootaxa.4521.4.5>
- Danforth BN, Sauquet H, Packer L (1999) Phylogeny of the bee genus *Halictus* (Hymenoptera: Halictidae) based on parsimony and likelihood analyses of nuclear EF-1a Sequence Data. *Molecular Phylogenetics and Evolution* 13: 605–618. <https://doi.org/10.1006/mpev.1999.0670>
- Danforth BN, Minckley RL, Neff JL (2019) The solitary bees: biology, evolution, conservation. Princeton University Press, Princeton, 488 pp. <https://doi.org/10.2307/j.ctvd1c929>
- Dorchin A, López-Urbe MM, Praz CJ, Griswold T, Danforth BN (2018) Phylogeny, new generic-level classification, and historical biogeography of the *Eucera* complex (Hymenoptera: Apidae). *Molecular Phylogenetics and Evolution* 119: 81–92. <https://doi.org/10.1016/j.ympev.2017.10.007>
- Engel MS (2005) Family-group names for bees (Anthophila). *American Museum Novitates*, 3476: 1–33. [https://doi.org/10.1206/0003-0082\(2005\)476\[0001:FNFBA\]2.0.CO;2](https://doi.org/10.1206/0003-0082(2005)476[0001:FNFBA]2.0.CO;2)

- Engel MS (2006) A new genus of minute ammobatine bees (Hymenoptera: Apidae). *Acta Entomologica Slovenica* 14: 113–121.
- Engel MS (2019) New genera of meliturguline bees from Saudi Arabia and Persia, with notes on related genera and a key to the Arabian fauna (Hymenoptera: Andrenidae). *Journal of Hymenoptera Research* 69: 1–21. <https://doi.org/10.3897/jhr.69.32561>
- Faircloth BC (2016) PHYLUCE is a software package for the analysis of conserved genomic loci. *Bioinformatics* 32: 786–788. <https://doi.org/10.1093/bioinformatics/btv646>
- Fidalgo PA (2021) First record of *Camptopoeum* (*Camptopoeum*) *baldocki* Wood & Cross, 2017 from Spain (Hymenoptera, Apoidea, Andrenidae). *Boletín de la Sociedad Entomológica Aragonesa (S.E.A.)* 68: 433–434.
- Friese H (1926) *Die Bienen, Wespen, Grab- und Goldwespen Insekten Mitteleuropas*. Franckh'sche Verlagshandlung, Stuttgart, 192 pp.
- Hoang DT, Chernomor O, von Haeseler A, Minh BQ, Vinh LS (2018) UFBoot2: improving the ultrafast bootstrap approximation. *Molecular Biology and Evolution* 35: 518–522. <https://doi.org/10.1093/molbev/msx281>
- Kalyaanamoorthy S, Minh BQ, Wong TKF, von Haeseler A, Jermin LS (2017) ModelFinder: fast model selection for accurate phylogenetic estimates. *Nature Methods* 14: e587. <https://doi.org/10.1038/nmeth.4285>
- Katoh K, Standley DM (2013) MAFFT multiple sequence alignment software version 7: improvements in performance and usability. *Molecular Biology and Evolution* 30: 772–780. <https://doi.org/10.1093/molbev/mst010>
- Lanfear R, Calcott B, Ho SYW, Guindon S (2012) PartitionFinder: Combined selection of partitioning schemes and substitution models for phylogenetic analyses. *Molecular Biology and Evolution* 29: 1695–1701. <https://doi.org/10.1093/molbev/mss020>
- Lanfear R, Calcott B, Kainer D, Mayer C, Stamatakis A (2014) Selecting optimal partitioning schemes for phylogenomic datasets. *BMC Evolutionary Biology* 14: e82. <https://doi.org/10.1186/1471-2148-14-82>
- Laroca S, Michener CD, Hofmeister RM (1989) Long mouthparts among “short-tongued” bees and the fine structure of the labium in *Niltonia* (Hymenoptera: Colletidae). *Journal of the Kansas Entomological Society* 62: 400–410.
- Lhomme P, Michez D, Christmann S, Scheuchl E, Abdouni IE, Hamroud L, Ihsane O, Sentil A, Smaili MC, Schwarz M, Dathe HH, Straka J, Pauly A, Schmid-Egger C, Patiny S, Terzo M, Müller A, Praz C, Risch S, Kasperek M, Kuhlmann M, Wood TJ, Bogusch P, Ascher JS, Rasmont P (2020) The wild bees (Hymenoptera: Apoidea) of Morocco. *Zootaxa* 4892: 1–159. <https://doi.org/10.11646/zootaxa.4892.1.1>
- Litman JR, Griswold T, Danforth BN (2016) Phylogenetic systematics and a revised generic classification of anthidiine bees (Hymenoptera: Megachilidae). *Molecular Phylogenetics and Evolution* 100: 183–196. <https://doi.org/10.1016/j.ympev.2016.03.018>
- Michener CD (2007) *The Bees of the World*. 2<sup>nd</sup> edn. John Hopkins University Press, Baltimore, 953 pp.
- Minh BQ, Schmidt HA, Chernomor O, Schrempf D, Woodhams MD, von Haeseler A, Lanfear R (2020) IQ-TREE 2: New models and efficient methods for phylogenetic inference in the

- genomic era. *Molecular Biology and Evolution* 37: 1530–1534. <https://doi.org/10.1093/molbev/msaa015>
- Müller A, Kuhlmann M (2008) Pollen hosts of western palaeartic bees of the genus *Colletes* (Hymenoptera: Colletidae): the Asteraceae paradox. *Biological Journal of the Linnean Society* 95: 719–733. <https://doi.org/10.1111/j.1095-8312.2008.01113.x>
- Münster-Swendsen M (1970) The nesting behaviour of the bee *Panurgus banksianus* Kirby (Hymenoptera, Andrenidae, Panurginae). *Insect Systematics & Evolution* 1: 93–101. <https://doi.org/10.1163/187631270X00113>
- Patiny S (1999a) Etude phylogénétique des Panurginae de l'ancien monde (Hymenoptera, Andrenidae). *Linzer biologische Beiträge* 31: 249–275.
- Patiny S (1999b) Description d'une nouvelle espèce de *Flavipanurgus* Warncke, 1972. *Notes fauniques de Gembloux* 37: 57–61.
- Patiny S (1999c) Révision des Panurginae ouest-paléarctiques n'appartenant pas à la tribu des Melitturgini Michener, 1944, Partie I: *Panurgus* Panzer, 1806 et *Camptopoeum* Spinola, 1843. *Entomofauna* 20: 309–328.
- Patiny S (2001) Monographie des Panurginae de l'ancien monde (Hymenoptera: Apoidea, Andrenidae). PhD thesis, Faculté universitaire des sciences agronomiques de Gembloux, Belgium, 278 pp.
- Patiny S (2002) Nouvelles espèces de Panurginae (Hymenoptera, Apoidea, Andreninae) du sud de l'Ouest-Paléarctique. *Notes fauniques de Gembloux* 47: 41–46.
- Patiny S, Gaspar C (2000) Premier aperçu de la biodiversité des Panurginae (Hym.: Andrenidae) de l'Anti-Atlas (Maroc). *Notes fauniques de Gembloux* 41: 33–41.
- Pisanty G, Richter R, Martin T, Dettman J, Cardinal S (2021) Molecular phylogeny, historical biogeography and revised classification of andrenine bees (Hymenoptera: Andrenidae). *Molecular Phylogenetics and Evolution* *in press*. <https://doi.org/10.1016/j.ympev.2021.107151>
- Portman ZM, Tepedino V (2017) Convergent evolution of pollen transport mode in two distantly related bee genera (Hymenoptera: Andrenidae and Melittidae). *Apidologie* 48: 461–472. <https://doi.org/10.1007/s13592-016-0489-8>
- Rasmont P, Devalez J, Pauly A, Michez D, Radchenko VG (2017) Addition to the checklist of IUCN European wild bees (Hymenoptera: Apoidea). *Annales de la Société entomologique de France* 53: 17–32. <https://doi.org/10.1080/00379271.2017.1307696>
- Rozen JG (1971) Biology and immature stages of Moroccan panurgine bees (Hymenoptera, Apoidea). *American Museum Novitates* 2457: 1–37.
- Rozen JG, Wyman ES (2015) The Chilean bees *Xeromelissa nortina* and *X. sielfeldi*: their nesting biologies and immature stages, including biological notes on *X. rozeni* (Colletidae: Xeromelissinae). *American Museum Novitates* 3838: 1–20. <https://doi.org/10.1206/3838.1>
- Shimizu A, Dohzono I, Nakaji M, Roff DA, Miller DG, Osato S, Yajima T, Niitsu S, Utsugi T, Yoshimura J (2014) Fine-tuned bee-flower coevolutionary state hidden within multiple pollination interactions. *Scientific Reports* 4: e3988. <https://doi.org/10.1038/srep03988>
- Tkalců B (1984) Neue paläarktische Arten der Gattungen *Pseudoheriades* und *Archeriades* mit Beschreibung von *Hofferia* gen. n. (Hymenoptera, Apoidea, Megachilidae). *Annotationes Zoologicae et Botanicae* 158: 1–22.

- Warncke K (1972) Westpaläarktische Bienen der Unterfamilie Panurginae (Hym., Apidae). *Polskie Pismo Entomologiczne* 52: 53–108.
- Westrich P (1989) *Die Wildbienen Baden-Württembergs*. Eugen Ulmer, Germany, 972 pp.
- Wood TJ, Cross I (2017) *Camptopoeum* (*Camptopoeum*) *baldocki* spec. nov., a new panurgine bee species from Portugal and a description of the male of *Flavipanurgus fuzetus* Patiny (Andrenidae: Panurginae). *Zootaxa* 4254: 285–293. <https://doi.org/10.11646/zootaxa.4254.2.9>
- Wood TJ, Roberts SPM (2018) Constrained patterns of pollen use in Nearctic *Andrena* (Hymenoptera: Andrenidae) compared with their Palaearctic counterparts. *Biological Journal of the Linnean Society* 124: 732–746. <https://doi.org/10.1093/biolinnean/bly080>

# Discovery of *Mourecotelles* (Hymenoptera, Apidae, Colletinae) in Brazil: nesting biology and pollen preferences of a remarkable new species of the genus

Rafael R. Ferrari<sup>1</sup>, Maria L. T. Buschini<sup>2</sup>, Mary E. R. Diniz<sup>2</sup>,  
Chao-Dong Zhu<sup>1,3,4</sup>, Gabriel A. R. Melo<sup>5</sup>

**1** Key Laboratory of Zoological Systematics and Evolution, Institute of Zoology, Chinese Academy of Sciences, 1 Beichen West Road, Chaoyang District, Beijing 100101, China **2** Universidade Estadual do Centro-Oeste, Rua Simeão Camargo Varela de Sá 03, Vila Carli, Guarapuava, PR, 85040-080, Brazil **3** University of Chinese Academy of Sciences, 19A Yuquan Road, Shijingshan District, Beijing 10049, China **4** State Key Laboratory of Integrated Pest Management, Institute of Zoology, Chinese Academy of Sciences, 1 Beichen West Road, Chaoyang District, Beijing 100101, China **5** Departamento de Zoologia, Universidade Federal do Paraná, PB 19020, 81531-980, Curitiba, PR, Brazil

Corresponding author: Rafael R. Ferrari ([raf\\_ferrari@hotmail.com](mailto:raf_ferrari@hotmail.com))

Academic editor: Jack Neff | Received 2 November 2021 | Accepted 10 January 2022 | Published 28 February 2022

<http://zoobank.org/68DFCDDC-0598-46FB-9058-53581A512753>

**Citation:** Ferrari RR, Buschini MLT, Diniz MER, Zhu C-D, Melo GAR (2022) Discovery of *Mourecotelles* (Hymenoptera, Apidae, Colletinae) in Brazil: nesting biology and pollen preferences of a remarkable new species of the genus. Journal of Hymenoptera Research 89: 211–231. <https://doi.org/10.3897/jhr.89.77485>

## Abstract

*Mourecotelles* Toro & Cabezas (Hymenoptera, Apidae, Colletinae) currently includes only nine valid species of cellophane bees found mostly in relatively-dry regions of western South America (Chile, Argentina, Bolivia, and Ecuador). In this paper, we describe and illustrate a new species of the genus – *M. braziliensis* Ferrari & Melo, **sp. nov.** – based on individuals of both sexes captured through trap-nesting in an environmental protection area (Araucárias Municipal Natural Park) and in flowers in different localities in southern Brazil. In total, we obtained 16 nests of *M. braziliensis*, each consisting of two to eleven brood cells arranged horizontally and lined with a cellophane-like substance. Of the 57 adult bees that emerged, 41 were male (mean weight 46.5 mg) and 16 were female (mean weight 58.9 mg), resulting in biased sex and investment ratios of 2.56:1 and 2.02:1, respectively. Both the numbers of provisioned cells and mortality rate were higher for trap nests with the narrowest bore diameter, although the differences in relation to other trap nests were not statistically significant. Pollen of nine different

plant families were found in brood cells of *M. braziliensis*, but the species showed a clear preference for Fabaceae and Polygalaceae. Indeed, some of the specimens were collected while foraging in flowers of an unidentified species of *Monnina* Ruiz & Pav. (Polygalaceae) growing in swampy areas. The evolutionary and biogeographical implications of our discovery are briefly discussed.

### Keywords

Bee, Colletini, floral host, Neotropical region, sex ratio, trap nest

## Introduction

Nesting biology has historically been one of the most widely studied aspects of the natural world of bees (e.g. Michener 1964; Houston 1975; Rozen 1984; Roubik 2006; Martins et al. 2019; Vivallo et al. 2021), presumably due to its remarkable diversity across taxa. For instance, despite the fact that most species of bees are ground nesters (Cane 1991; Cane and Neff 2011), several other substrates are also exploited, such as twigs, dead soft stems, termite nests and previously-established cavities in concrete walls (Roubik 1989; Camargo and Pedro 2003; Fortel et al. 2016). The Colletinae are unique among bees in producing a cellophane-like waterproof substance, which is composed mainly of a mixture of macrocyclic lactones (produced by Dufour's gland) and salivary gland secretions (Albans et al. 1980; Duffield et al. 1980), to line their brood cells (Batra 1980; Torchio et al. 1988). This process is facilitated by their specialized (bilobed or bifid) glossa, a character not found in any other group of bees (McGinley 1980; Michener and Brooks 1984; Michener 2007; Ferrari and Packer 2021).

The tribe Colletini (Hymenoptera: Apidae: Colletinae; sensu Melo and Gonçalves 2005) includes approximately 540 valid species of cellophane bees (Ascher and Pickering 2021) that are divided into four genera: *Colletes* Latreille, *Hemicotelles* Toro & Cabezas, *Mourecotelles* Toro & Cabezas and *Xanthocotelles* Toro & Cabezas (Toro and Cabezas 1977, 1978; Ferrari et al. 2000; Ferrari and Packer 2021). In alternative classifications, however, only *Colletes* and *Mourecotelles* are recognized at the generic level, the latter including *Hemicotelles* and *Xanthocotelles* as subgenera (Michener 1989, 2007; Ascher and Pickering 2021). All species of Colletini are ground nesters, except *M. mixtus* Toro & Cabezas and *M. rubicola* (Benoist), which nest in dead stems (Claude-Joseph 1926 (as *C. biciliatus* Cockerell); Benoist 1942 (as *C. rubicola*)), as well as *C. rufipes* Smith and *M. triciliatus* Toro & Cabezas, which were observed nesting in trap nests (Garófalo et al. 2004; Gazola and Garófalo 2009; Dorado and Vázquez 2016). On the other hand, most species of the closest allies of the Colletini – i.e. the Euryglossini, Hylaeini, Scapterini, and Xeromelissini (Almeida and Danforth 2009) – nest in the ground, soft wood or cavities previously excavated by other animals (see Almeida 2008 and references therein). Unlike most ground-nesting bees, females of Colletini do not possess basitibial and pygidial plates (Michener 1989), which is intriguing given that these structures are typically used in the construction of brood cells in the soil (Michener 2007). This may explain why many *Colletes* species tend to

nest in sandy soils (Batra 1980) that can be excavated with less effort and thus with less energy expenditure.

*Mourecotelles* currently comprises nine valid species found mostly in temperate, often xeric regions of western South America (Toro and Cabezas 1977). While the nesting biology of many *Colletes* species has already been studied and described in detail – e.g. *C. cunicularius* (Linnaeus) (Malyshev 1927), *C. michenerianus* Moure (Michener and Lange 1957), *C. ciliatoides* Stephen (Torchio 1965), *C. compactus* Cresson (Rozen and Fraveau 1968), *C. daviesanus* Smith (Scheloske 1974), *C. xerophilus* Timberlake (Batra and Schuster 1977), *C. kincaidii* Cockerell (Torchio et al. 1988) – very little is known about the other genera of Colletini (Almeida 2008).

The main goals of this paper are to describe a new species of *Mourecotelles* from southern Brazil and to document relevant aspects of its nesting biology and pollen preferences.

## Methods

### Study area

This study was conducted in Araucárias Municipal Natural Park (AMNP), an environmental protection area of approximately 1 km<sup>2</sup> located in the municipality of Guarapuava, Paraná state, Brazil (25°21'06"S, 51°28'08"W; Fig. 1A, B). The location of AMNP falls within the humid subtropical climate zone (Köppen 1900, 1918), which is characterized by warm and humid summers (mean temperature ~25 °C) and mild winters (mean temperature ~12 °C); precipitation is relatively evenly distributed over the year, with an annual mean of about 1900 mm (IDR-Paraná 2019).

AMNP's vegetation consists predominantly of *Araucaria* forest (43%), but also includes gallery forest (10%), grassland (7%), swamp (7%) and anthropized areas (33%). The *Araucaria* forest remnants found at AMNP, although represented mostly by *Araucaria angustifolia* (Bertol.) Kuntze (Araucariaceae), are particularly diverse, comprising approximately 100 species of woody plants belonging to 73 genera in 41 families, most notably: Myrtaceae, Lauraceae, Bignoniaceae, Salicaceae, Sapindaceae, and Solanaceae (Cordeiro 2005). The grassland areas are surrounded by the *Araucaria* forest remnants and are characterized by the predominance of short species of Compositae, Cyperaceae, Leguminosae, Umbelliferae, and Verbenaceae. The swampy area is located at the lowest parts of AMNP and is primarily covered with grasses and asters (Buschini and Fajardo 2010).

### Bee sampling

The studied bees were captured within AMNP through wooden trap nests between December 2001 and December 2007, following the collection methodology outlined in detail in Buschini (2006). Data from December 2001 and December 2003 were originally obtained by that author, while data from the remaining collection period

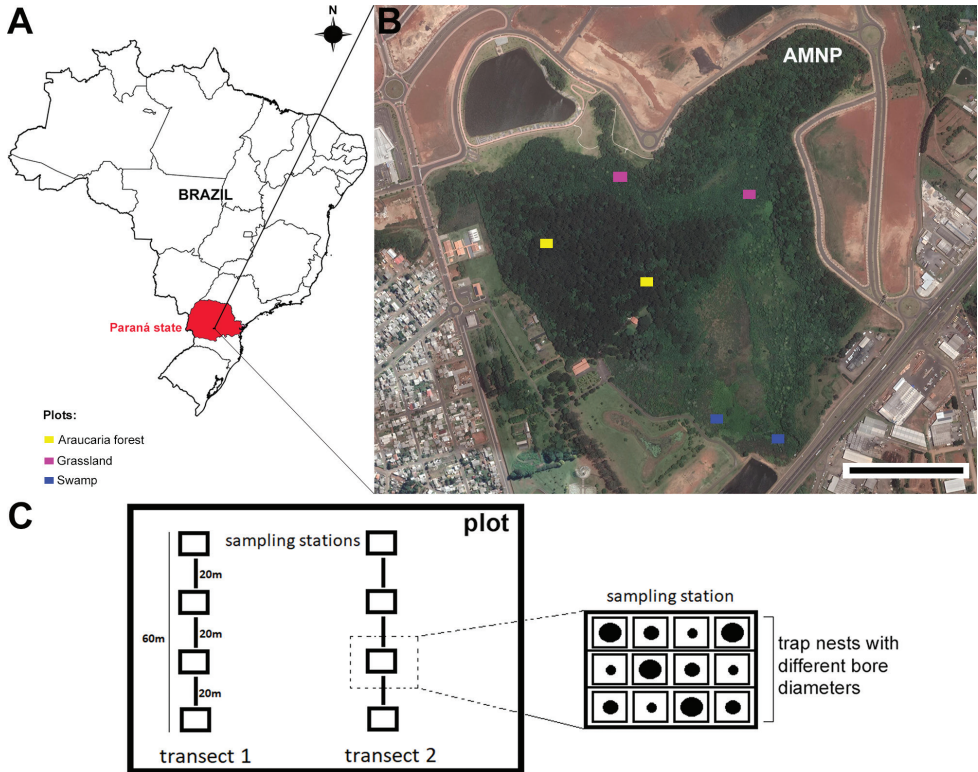


**Figure 1.** Study site and schematic representation of our trap-nest experiment **A** Map showing the exact location of AMNP within Paraná state, Brazil **B** Satellite image of AMNP with color-coded rectangles pointing to where the collecting plots were set up within each environment **C** Line art depicting that plots consisted of two 60-meter transects, each containing four sampling stations with 12 trap nests of different bore diameters. Scale bar: 250 m.

are new. Sampling was carried out in two plots within each of the major natural environments found at AMNP: *Araucaria* forest, grassland and swampy area. In each plot, we set eight sampling stations with 12 trap nests each along two 60-meter transects (i.e. four sampling stations per transect), totaling 96 trap nests (Fig. 1B, C). Therefore, a total of 192 trap nests were placed within each environment, 576 overall.

The trap nests were built from 120 × 25 × 20 mm (length × width × height) wooden blocks as follows. First, each block was drilled to create a one-opening cavity of 90 mm in depth. Drills of 7 mm, 10 mm and 13 mm in diameter were used to produce trap nests with different bore diameters (henceforth TN07, TN10 and TN13, respectively). Next, blocks were sawed mid-longitudinally and the resulting halves held together with adhesive tape. This allowed for ease of inspection of the interior of the trap nests both in the field and laboratory later.

The ready-to-use trap nests were placed 1.5 m above the ground mounted on natural vegetation, mostly tree branches. They were then inspected every two weeks; all colonized trap nests were removed for subsequent examination in the laboratory and replaced with new ones in order to keep the number of trap nests per sampling area constant. In the laboratory, the trap nests were re-inspected and those housing nests with immature bees were placed in rearing containers (two-liter PET bottles sealed with cotton balls) to allow for ease of capture of recently-emerged adults. The terminology used in the descriptions of nests and brood cells followed Almeida (2008).

### Bee species description

All adult bees that emerged in the laboratory were killed with ethyl acetate, weighed with a precision digital scale and then pinned. Next, they were examined under a Nikon SMZ1000 stereomicroscope (maximum magnification of 112×) equipped with fluorescent light. To dissect the terminalia (i.e. genital capsule, seventh and eighth metasomal sterna) of males, we first kept them inside a sealed plastic container with cotton balls soaked in water for 12 hours to relax their soft tissues. We then severed the conjunctival membrane of the metasomal apex and removed the loose terminalia from the mostly-hollow cavity with fine-tipped forceps. We subsequently cleared the terminalia of each male within separate wells of a ceramic plate containing a ~10% solution of potassium hydroxide for six hours. Using an insect pin, we separated the three structures from one another and stored them in glycerin in glass genital vials to facilitate comparative study and imaging.

We identified the bees to genus (*Mourecotelles*) using the keys of Ferrari and Packer (2021). We then attempted to identify them to species with the keys of Toro and Cabezas (1977), with special reference to the terminalia of males. Because the bees clearly did not match any of the previously known *Mourecotelles*, they are herein described as belonging to a new species. The terminology employed in this paper follows Michener (2007) for general bee morphology and Aguiar and Gibson (2010) for spatial orientation of legs. Puncture spacing is given in terms of the relative sizes of the interspaces (i) and puncture diameters (d), for example,  $i=2\times d$ . Antennal flagellomeres, metasomal terga and sterna are abbreviated as F1, F2, etc., T1, T2, etc. and S1, S2, etc., respectively.

The collection data in the labels of the holotype are reproduced exactly as they are given there, as follows: data in a single label are provided between quotation marks, and the end of each line in a label is indicated by an inverted bar (\). For paratypes, data are given in the following format: country, state, municipality, collection date as dd/mm/yyyy, collector(s), number of individuals per sex [repository]. Acronyms of repositories mentioned herein are: DZUP, Coleção Entomológica Padre Jesus Santiago Moure, Universidade Federal do Paraná (Curitiba, Brazil); UNICENTRO, Universidade Estadual do Centro Oeste (Guarapuava, Brazil); PCYU, Packer Collection at York University (Toronto, Canada).

The habitus images presented in this paper were taken with a Leica DFC295 camera attached to a Leica M125 stereomicroscope. Stacking of multiple images was made using Zerene Stacker 1.4 (Zerene Systems, LLC) software. Terminalia of males were imaged with the addition of a Canon Extender EF 2× lens for a higher magnification. In all cases, we used a P-51Cam-Lift high precision Linear Actuator, which is operated by the program P51 Camlift Controller v.2.6, to take pictures from different planes of focus. First, individual pictures were imported with Adobe Lightroom v4.4 and then exported to Helicon Focus v.5.3.3, where they were stacked to produce multifocus composite images. We added scale bars and mounted the final images into plates in Adobe Photoshop CS6 v.13.0 (Adobe Inc.).

### Statistical tests

Mann-Whitney nonparametric tests were performed to determine whether the bore diameters of trap nests influenced the number of brood cells constructed. The same test was used to compare whether there were statistical differences in (i) cell length, (ii) development time or (iii) body mass between males and females. The development time of bees was calculated as the time interval between the collection of trap nests from the field and the emergence of adults. Chi-square tests were performed to see whether bore diameter affected (i) the sex ratio and (ii) mortality rate. All statistical analyses were carried out in BioEstat 3.0 (Ayres et al. 2003).

### Pollen analysis

The pollen samples examined for the purpose of the present study were collected from three of the nests studied by Buschini (2006). In that study, the samples were obtained from the cells containing dead immatures wherein the food provision had not yet been fully consumed. Five pollen grain slides were prepared from each nest (totaling 15 slides), following the acetolysis protocol outlined in Erdtman (1960). We also harvested pollen from known flowering plants (Cordeiro 2005) within a 500-meter radius from transects and then prepared one pollen slide for each sampled plant, following the same protocol. Next, the nest pollen provisions were identified to the lowest Linnean category possible by a palynologist (see acknowledgements) based on comparisons with pollen obtained directly from flowers under a light microscope. The Missouri Botanical Garden's online database (available at <http://www.tropicos.org/>) was also largely consulted. The higher-level botanical classification adopted herein follows the World Flora Online (available at <http://www.worldfloraonline.org/>).

To quantify the pollen from brood cell provisions, 400 grains were randomly identified per slide, totaling 1200 grains per nest. Some pollen grains were photographed with an Olympus BX 50 photomicroscope equipped with a video camera using CellSens. All pollen slides are deposited in the palynotheca of UNICENTRO.

## Results

### Taxonomy

#### *Mourecotelles braziliensis* Ferrari & Melo, sp. nov.

<http://zoobank.org/3807CBF0-7470-4AE8-9A5A-3B3CE1F8502B>

Figures 2A–D, 3A–C

**Diagnosis.** Both sexes of *M. braziliensis* can be readily diagnosed by having the mesosoma covered almost entirely with dark-orange pubescence (Fig. 2A–F), whereas in all other species of the genus the mesosomal pubescence is off-white to pale-yellow, which may or may not include sparse black hairs. Females of *M. braziliensis* are also unique in having the marginal zone of T6 forming a raised lip (Ferrari and Packer 2021: fig. S9E), while in females of all other *Mourecotelles* the T6 is entirely subvertical (Ferrari and Packer 2021: fig. S9E). Males of *M. braziliensis* can be further differentiated from their congeners by having the volsella with a convex digitus (Ferrari and Packer 2021: fig. S4A), whereas the digitus is always concave in the other *Mourecotelles* (Ferrari and Packer 2021: fig. S4B). *Mourecotelles braziliensis* is most similar to the sister species *M. moldenkei* Toro & Cabezas and *M. spinolae* (Crawford & Titus), but females of the former species have the gena devoid of tomentum (Fig. 2B), while the gena of females of the latter two species is covered with dense pale tomentum. Males of *M. braziliensis* have the mandible with a narrowly rounded apical tooth (Ferrari and Packer 2021: fig. S15A), thus making them very distinct from males of both *M. moldenkei* and *M. spinolae*, in which the apical tooth is broadly truncate (Ferrari and Packer 2021: fig. S15B).

**Description. Female** (Holotype, Fig. 2A, B, D). **Dimensions (mm).** Approximate body length 11.0; head width 3.9; head length 2.9; intertegular distance 3.2; forewing length 7.1.

**Colouration.** Black, except dark-brown on wing venation (except veins C and R of forewing black), distitarsi, tarsal claws distally; pale reddish-brown on tegula, tibial spurs, tarsal claws proximally, marginal zones of S1–S5; reddish-brown on tarsal claws distally.

**Structure.** Labrum with longitudinal subellipsoidal concavities. Malar area 1.4× longer than broad. Inner margins of compound eyes subparallel. F1 2.1× as long as its apical width. Facial fovea narrowly rounded below, more broadly rounded above. Dorsolateral angle of pronotum obtusely angled. Tibial spurs ciliate. Hind basitarsus 3.6× longer than broad. Marginal zone of T6 forming a raised lip.

**Pubescence.** Head with long, erect, off-white and black hairs intermixed; equivalent hairs longer on vertex; mandible with a fringe of long, pale-yellow setae oriented mesad; clypeus with short, suberect, pale-yellow setae concentrated below. Mesosoma with long, erect, dark-orange plumose hairs; equivalent hairs longer and paler on mesepisternum, metepisternum and lateral surface of propodeum; mesoscutum with dark-orange and black hairs intermixed anteriorly. Legs mostly with moderately long,

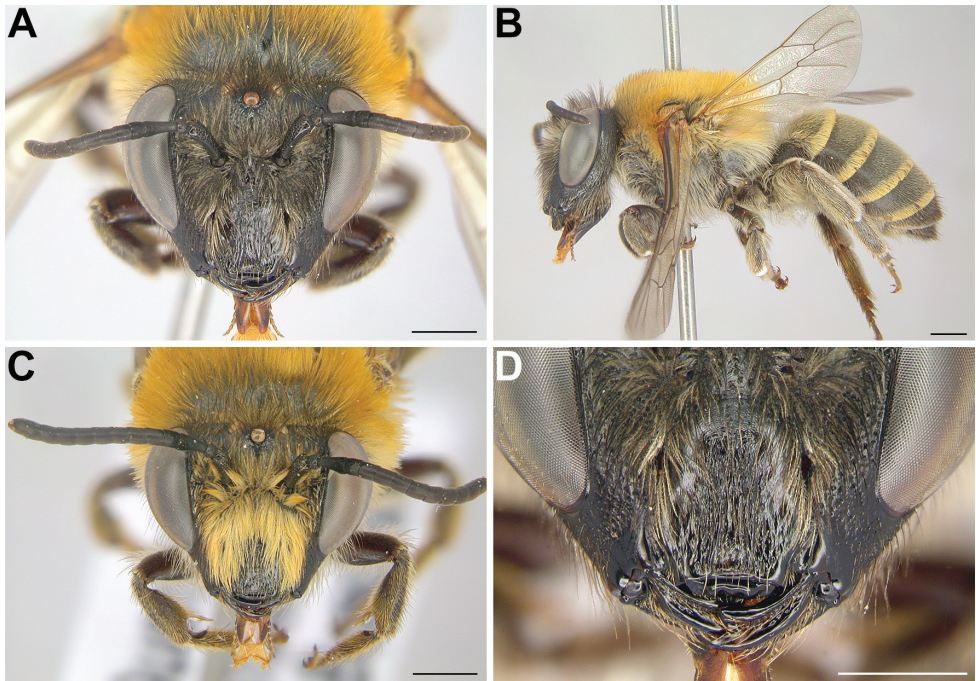


**Figure 2.** *Mourecotelles braziliensis* **A** head of female holotype, frontal view **B** habitus of female holotype, lateral view **C** head of male paratype, frontal view **D** lower half of head of female holotype, frontal view. Scale bars: 1 mm.

suberect, pale-yellow branched hairs; front trochanter and femur with long, erect, off-white and black hairs intermixed posteriorly; mid femur and mid and hind coxae and trochanters with very long, erect off-white hairs ventrally; mid tibia with short, erect, bright-orange thick setae forming a longitudinal line along proximal third ventrally; mid and hind tibiae and basitarsi with short, suberect, pale-yellow setae dorsally; femoral and tibial scopae with very long, pale-yellow apically-branched hairs. Metasomal terga with short, erect, pale-yellow setae on discs; T1 with very long, erect, pale-orange plumose hairs; T1–T5 apical bands with pale-orange tomentum; T6 with short, suberect, black thick setae. Metasomal sterna with minute, suberect, pale-yellow setae.

**Sculpture.** Clypeus with subparallel longitudinal coarse striae. Malar area unevenly punctate ( $i=0.5\text{--}2.0d$ ); several punctures elongate and poorly delimited; interspaces finely imbricate. Paraocular area finely and very densely punctate ( $i<0.5d$ ). Supraclypeal area largely impunctate; integument finely imbricate. Frons moderately coarsely and densely punctate ( $i=0.5\text{--}1.0d$ ). Vertex finely punctate; punctures sparser ( $i=1.0\text{--}3.0d$ ) medially, denser ( $i=0.5\text{--}1.0d$ ) towards upper summit of eye. Mesosomal dorsum coarsely punctate; punctures sparsest ( $i>3d$ ) on mesoscutum medially, densest ( $i=0.5\text{--}1.0d$ ) on scutellum posteriorly, finer on metanotum; interspaces smooth, except finely imbricate on anterior third of mesoscutum. Mesepisternum coarsely and unevenly punctate, punctures densest ( $i=0.5\text{--}1.0d$ ) near scrobe, sparsest ( $i=1.0\text{--}2.0d$ ) towards ventral surface; interspaces finely imbricate throughout. Lateral surface of propodeum with minute

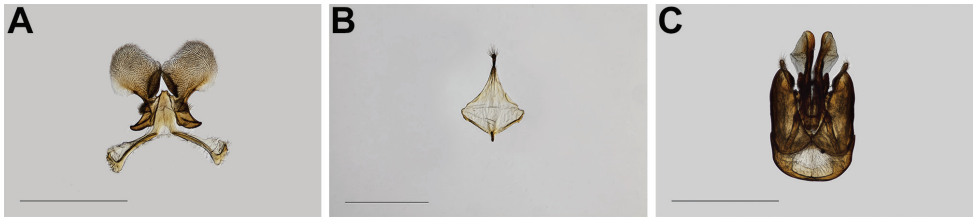


**Figure 3.** Terminalia of *Mourecotelles braziliensis* **A** S7, ventral view **B** S8, ventral view **C** genital capsule, dorsal view. Scale bars: 1 mm.

punctures; interspaces coarsely imbricate. Metapostnotum mostly smooth, with many short carinae along anterior margin. Metasoma minutely and sparsely ( $i=1.0-2.0d$ ) punctate; interspaces corrugated on terga, finely imbricate on sterna.

**Male** (Fig. 2C): As in female, except for secondary sexual features and as follows.

**Dimensions (mm).** Approximate body length 9.4; head width 3.6; head length 2.6; intertegular distance 3.2; forewing length 6.9.

**Colouration.** Tegula dark brown; metasomal sterna with black marginal zones.

**Structure.** Malar area  $1.5\times$  as long as basal width of mandible. F1  $1.8\times$  as long as its apical width. Hind basitarsus  $3.8\times$  longer than broad. S7, S8 and genital capsule as in Fig. 3A–C, respectively.

**Pubescence.** Face with mostly pale-yellow hairs, black hairs restricted to paraocular area and vertex. Supraclypeal area, gena near proboscoidal fossa and lateral surface of propodeum with very long hairs. Mesoscutum with only dark-orange hairs, black hairs absent.

**Sculpture.** Malar area with convex interspaces. Clypeal striae somewhat finer and more irregularly oriented. Supraclypeal area more densely punctate ( $i=1.0-1.5d$ ).

**Type material. Holotype** ♀: “DZUP\ 028459”. “Buschini, M.L.T\ Guarapuava – PR\ Brasil – 22/11/02”. “N. 283 (1)\ 22/11/02\ 30/10/03\ (0,7)”. “HOLOTYPE \ *Mourecotelles\ braziliensis\* Ferrari & Melo, 2021”. [DZUP 028459].

**Paratypes.** Brazil, Paraná, Guarapuava, 24/10/2002, M.L.T. Buschini leg., 1♀ [UNICENTRO]; same data as for preceding, except 22/11/2002, 1♂ [UNICENTRO], 1♀ and 1♂ [DZUP 028460, 028462]; same data as for preceding, except 06/12/2002, 1♂ [PCYU]; same data as for preceding, except 19/12/2002, 1♂ [UNICENTRO]; same data as for preceding, except 11/10/2003, 1♀ [UNICENTRO]; same data as for preceding, except 27/10/2003, 1♀ [DZUP 028465]; same data as for preceding, except 18/12/2003, 1♀ [PCYU], 1♀ [DZUP 028461]; same data as for preceding, except 19/10/2005, 2♂ [DZUP 028463, 028464]; Brazil, Paraná, Palmas, 18/11/2009, G. Melo, K. Ramos & V. Kanamura leg., 1♀ and 1♂ [DZUP 028395, 028468]; Brazil, Rio Grande do Sul, Rio Grande, 11/2004, FURG leg., 1♀ and 1♂ [DZUP 028466, 028467].

**Etymology.** The only species of *Mourecotelles* currently known to occur in Brazil.

**Comments.** The species described herein has been referred to in several previous publications, including Buschini (2006) (as *Colletes* sp.), Diniz and Buschini (2009) (as *Rhynchocolletes* sp.), Almeida et al. (2019) (as *Mourecotelles* sp.) and Ferrari and Packer (2021) (as *Mourecotelles* sp.1).

## Nesting activity

In total, females of *M. braziliensis* nested in 16 of the 576 trap nests (2.8%) placed in the field. The number of bees that emerged from each nest varied from one to ten, totaling 57 individuals (3.6 bees/nest on average).

*Mourecotelles braziliensis* nidified in 13 TN07 and three TN10; no nest was built in TN13. All 16 nests were founded in either the austral spring or summer, in the years of 2002 (n=10, 62.5%), 2003 (n=2, 12.5%), 2004 (n=1, 6.25%) and 2006 (n=3, 18.75%). No nest was founded in 2001, 2005 and 2007, although the year of 2001 was surveyed only in December. Of the 16 nests, 13 were founded in the sampling stations placed in the grassland area (81.25%) and three in the swampy area (18.75%).

## Nest and brood cell structures

All nests founded by *M. braziliensis* are very alike in terms of general architecture. Specifically, each consisted of a series of cells arranged horizontally and separated from one another by walls built with the same cellophane-like substance used in the lining of the nest (Fig. 4A–C). Overall, the nests founded in TN10 were slightly longer ( $82.1 \pm 0.5$  mm in length) than the ones founded in TN07 ( $81.5 \pm 0.5$  mm in length). Regardless of the trap nest used, cells were fairly similar in shape: tubular chambers with truncate ends on both sides, except the innermost cell, the inner end of which was rounded due to the rounded end of trap-nest's bores. The mean lengths of the brood cells from which males and females emerged (irrespective of the nest's bore diameter) were  $10.84 \pm 0.04$  mm and  $10.71 \pm 0.06$  mm, respectively; however, the difference between them were not statistically significant ( $p=0.4274$ ). After the outermost cell was constructed and provisioned, the nest entrance was plugged with a layer of the cellophane-like substance of approximately 3 mm in thickness (Fig. 4D). Larval food provisioned by *M. braziliensis* was soupy as is typical in Colletinae, although the Neopasiphaeini are known for producing semi-solid provisions (see Michener 1960). Brood cells were initially bright orange due to the color of the fresh provisions (Fig. 4A); then they gradually turned dark brown (~26 days after hatch; Fig. 4B) and subsequently black (~31 days after hatch; Fig. 4C) as the result of the accumulation of larval feces.

The number of cells constructed in each nest of *M. braziliensis* varied from two to 11, totaling 78 cells in 16 nests (4.9 cells/nest on average). Of these, 55 cells were from the 13 TN07 (4.2 cells/nest on average) and 23 from the three TN10 (7.5 cells/nest on average). This difference, however, was not statistically significant ( $p=0.2482$ ). Of the 16 nests, 14 (87.5%) had at least one vestibular cell. The number of vestibular cells constructed in TN07 and TN10 was 22 and four, respectively (1.8 and 2.0 vestibular cells/nest on average, respectively).

## Development time and sex/investment ratios

Overall, males ( $333 \pm 16.4$  days) developed faster than females ( $345 \pm 16.7$  days), although the difference between their mean development times was not statistically

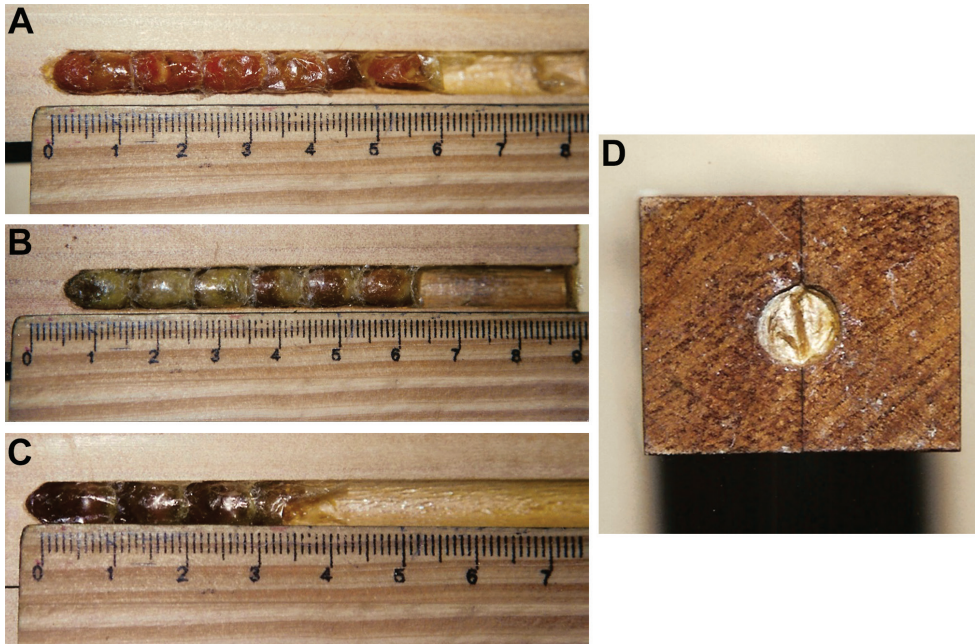


**Figure 4.** Nests of *Mourecotelles braziliensis* built in wooden trap nests **A** food provision looks bright orange when relatively fresh **B** brood cells become darker as larvae start to defecate (~26 days after hatch) **C** brood cells turn nearly black due to accumulation of larval feces (~31 days after hatch) **D** entrance of a TN07 plugged with cellophane-like material.

different ( $p=0.0341$ ). On the other hand, females ( $58.9 \pm 5.8$  mg) were significantly heavier than males ( $46.5 \pm 7.8$  mg) ( $p<0.001$ ).

Of the 57 bees of *M. braziliensis* that emerged in the laboratory, 41 were male (72%) and 16 were female (28%), resulting in a biased sex ratio towards males of 2.56:1. This is significantly different from an unbiased (i.e. 1:1) sex ratio ( $p<0.001$ ). When the mean weight of individuals of each sex was accounted for, the calculated investment ratio was lower (2.02:1), albeit still statistically significant ( $p<0.05$ ). The sex ratio was particularly more male biased when only TN10 was considered: 16 of the 20 bees that emerged were male (80%) and only four were female (20%), thus resulting in a sex ratio of precisely 4:1, which is also statistically different from a 1:1 sex ratio ( $p<0.05$ ). The investment ratio related to only TN10 (3.15:1) was also statistically significant ( $p<0.05$ ). Finally, 25 of the 37 bees that were reared from TN07 were male (67.5%) and 12 were female (31.5%), yielding sex and investment ratios of 2.08:1 and 1.64:1, respectively, both significantly different from a 1:1 ratio ( $p<0.05$ ).

### Mortality rate and natural enemies

No bee emerged from 20 of the 78 constructed cells, resulting in an overall mortality rate of about 26%. Of these, 13 cells contained dead larvae (65%), three were completely empty (15%), three contained dead adults (15%) and one was found with an

unidentified meloid beetle inside (5%). Although the mortality rate was, on average, higher for TN07 (17 of 55, 31%) than TN10 (three of 23, 13%), the difference between the two types of trap nests was not statistically significant ( $\chi^2=2.715$ ;  $p=0.0994$ ).

## Pollen preferences

Microscopic examination of the brood cell content obtained from the nests of *M. braziliensis* revealed 11 pollen morphotypes belonging to nine different plant families: Campanulaceae (*Lobelia* sp.), Commelinaceae (Commelinaceae sp.), Compositae (Compositae sp.1 and Compositae sp.2), Fabaceae (*Crotalaria* sp. and Fabaceae sp.), Lauraceae (*Cinnamomum* sp.), Myrtaceae (Myrtaceae sp.), Poaceae (Poaceae sp.), Polygalaceae (Polygalaceae sp.) and Styracaceae (Styracaceae sp.).

Two morphotypes, Fabaceae sp. (Fig. 5A) and Polygalaceae sp. (Fig. 5B), were largely dominant and together corresponded to roughly 98.5% of the pollen content examined (51.08% and 47.41%, respectively). However, when their relative amounts are adjusted by pollen grain size, it is revealed that the pollen mass of Polygalaceae sp. (64  $\mu\text{m}$  in diameter) seemingly consumed by the larvae of *M. braziliensis* was nearly 2.5 $\times$  as much as that of Fabaceae sp. (24  $\mu\text{m}$  in diameter). The relative amounts of the other nine pollen morphotypes – *Crotalaria* sp. (0.55%), *Lobelia* sp. (0.25%), Myrtaceae sp. (0.16%), Styracaceae sp. (0.16%), Commelinaceae sp. (0.13%), *Cinnamomum* sp. (0.08%), Compositae sp.1 (0.08%), Compositae sp.2 (0.08%), and Poaceae sp. (0.02%) – were all negligible and most likely not actively collected by *M. braziliensis*.

## Discussion

Almost all of what was previously known about the nesting biology of the Colletini was related to the widespread genus *Colletes* (e.g. Malyshev 1927; Stephen 1954; Michener and Lange 1957; Torchio 1965; Rozen and Fraveau 1968; Scheloske 1974; Batra and Schuster 1977; Torchio et al. 1988; Zhao et al. 2010). Thus, information on the other genera, including *Mourecotelles*, has remained comparatively much scarcer in the literature (Almeida 2008). In an early paper, females of *M. mixtus* (as *C. ciliatus*; see Toro and Cabezas 1977 for further details) were found nesting inside abandoned galleries seemingly built by xylophagous insects in dead wood in Santiago, Chile (Claude-Joseph 1926). Later, Benoist (1942) observed *M. rubicola* (as *C. rubicola*) building nests in dry twigs of brambles (Rosaceae: *Rubus*) in Quito, Ecuador. More recently, the species described herein as new was captured with wooden trap nests during two different field experiments at AMNP (Buschini 2006 [as *Colletes* sp.]; Diniz and Buschini 2009 [as *Rhynchocolletes* sp.]). In the latest publication on the nesting biology of *Mourecotelles*, Dorado and Vázquez (2016) obtained nests of *M. triciliatus* founded in trap nests near Mendoza, Argentina. There seems to be an undescribed species of *Mourecotelles* found in northern Chile that also nests in twigs (L. Packer, pers. comm.). Therefore, the evidence accumulated so far indicates that the *Mourecotelles* are fundamentally (if not strictly) cavity-nesting bees, although this finding may change with further investigation.



**Figure 5.** The two most abundant pollen types found in the food provisions of *Mourecotelles braziliensis* **A** Fabaceae sp.1 **B** Polygalaceae sp.1. Scale bars: 10  $\mu\text{m}$  (**A**); 20  $\mu\text{m}$  (**B**).

Assuming that the genus-level relationships recovered by Ferrari and Packer (2021) are correct, *i.e.* *Mourecotelles* plus *Xanthocotelles* and *Colletes* plus *Hemicotelles* as sister taxa, then the most parsimonious interpretation for the evolution of nesting behavior within Colletini is as follows. The ancestor of all Colletini might have been either a cavity- or stem-nesting species, a behavior that would have later been inherited by the ancestral *Mourecotelles* but evolved to a ground-nesting condition in the ancestral *Colletes*. This scenario, however, can only be confirmed through a rigorous ancestral trait phylogenetic reconstruction in light of additional nesting behavior data of both *Hemicotelles* and *Xanthocotelles*, which unfortunately remain unavailable. It was previously suggested that the ancestral *Colletes* may have arisen as a stem-nesting species (Almeida 2008), although this possibility was raised prior to the more recent discoveries (Dorado and Vázquez 2016).

*Mourecotelles braziliensis* stands out for being the sister species to the remaining species of the genus and the only one found in eastern South America (Ferrari and Packer 2021), which raises questions regarding the origin of *Mourecotelles*. Based on the available phylogenetic evidence, the ancestral *Mourecotelles* may have inhabited southern South America about 30 million years ago (Mya; see Ferrari et al. 2020), where it would have likely been relatively widespread. At that time, South America was experiencing a remarkable vegetation transformation, in which beech forests were taking over a tropical forest that had remained as the dominant biome throughout most of the Palaeocene, while drier open biomes were appearing in central portions of the continent (Iglesias et al. 2011; Meseguer et al. 2015). In the biogeographical literature, it is well established that emerging biomes may act as either corridors or dispersal barriers for some taxa (see Luebert 2021). Thus, it is possible that a dramatic change in vegetation may have resulted in a vicariant cladogenetic event that would have given rise to the lineage leading to *M. braziliensis* plus the ancestor of the remaining extant species. We argue that shedding further light on the phylogeny of *Mourecotelles* would be crucial for a better understanding of the evolution and historical biogeography of the Colletini as a whole.

Over the six-year experiment conducted by us, *M. braziliensis* nidified in trap nests that were placed only in the open environments (grassland and swampy areas), while

no nest was founded within the *Araucaria* forest remnants. Given that the forested area covers 43% of AMNP, it seems obvious that *M. braziliensis* prefers nesting in sun-exposed environments. This actually corresponds to a nesting behavior that has long known to be predominant among solitary bees (e.g. Sakagami and Hayashida 1960; Potts and Willmer 1997). Some bees nonetheless have a clear preference for nesting in rather shaded situations, such as *Bicolletes iheringi* (Schrottky) and *Neocorynura laevis-triata* Gonçalves (Michener et al. 1958; as *N. polybioides* (Ducke)), as well as various species of *Centris* Fabricius (Frankie et al. 1988). It has been demonstrated that the development rate of immature bees is positively correlated with temperature, provided an upper limit is not exceeded (Bosch and Kemp 2000), above which high temperatures typically decrease development rate (Frankie et al. 1988) or may even be lethal to immatures (Undurraga and Stephen 1980).

The average number of cells constructed by *M. braziliensis* in our experiment (4.9 cells/nest) is very close to that reported for the Argentina-endemic *M. triciliatus* (5.7 cells/nest on average; see Dorado and Vázquez 2016). This information is relevant, among other reasons, from a conservation standpoint (see Paini and Roberts 2005; Huang et al. 2021). Note that the available report on *M. triciliatus* was based on merely three nests containing only 17 cells in total, therefore this comparison needs to be interpreted with caution. Even though the nests founded in TN07 contained less brood cells on average (4.9 cells/nest) than those founded in TN10 (7.5 cells/nest), the difference was not statistically significant. A preference for narrower cavities is further supported by the fact that *M. braziliensis* built no nest in TN13 over the experiment conducted by us. This is actually not surprising given that the head width (3.8–4.0 mm) of females, which in turn is a good proxy for body size, is more compatible with the bore diameter TN07 (i.e. 7 mm). Previous studies on the nesting biology of other bee and wasp species showed that body size is probably the most important factor influencing the selection of bore diameters of potential nesting cavities by females (Fricke 1991; Pereira et al. 1999; Aguiar and Garófalo 2004; Buschini and Farjardo 2010). It is not possible to conclude, however, that 7 mm is in fact the optimum cavity diameter for *M. braziliensis* because our experiments did not include trap nests with narrower bores.

Even though we have identified 11 different pollen morphotypes in brood cells of *M. braziliensis*, the nine least abundant of them constituted merely 1.57% of the total examined. These likely were involuntarily accumulated by females while drinking nectar or picked up as pollen secondarily deposited by other flower visitors, rather than being actively collected to nourish the larvae (see Diniz et al. 2021). Since roughly 98.5% of the observed grains belong to only two pollen morphotypes (Polygalaceae sp. and Fabaceae sp.), it appears that *M. braziliensis* may be a specialist in the order Fabales (Bello et al. 2012). However, it has been shown that even slight disparities in size among different pollen types can lead to critical differences in their respective volumes in samples (Buchmann and O'Rourke 1991). Thus, when pollen size is taken into consideration it is possible to conclude that pollen of Polygalaceae sp. corresponded to over two thirds (71%) of the total pollen mass that larvae of *M. braziliensis* apparently

consumed, which suggests a potential oligolecy. To our knowledge, no datum on floral hosts of *Mourecotelles* is currently available in the literature, although the primary author (RRE, *pers. obs.*) has observed several species of the genus visiting *Adesmia* (Fabaceae) in central Chile. It is also worth mentioning that the female and male paratypes from Palmas (Paraná state) were collected while visiting flowers of an unidentified species of *Monnina* (Polygalaceae) growing in a swampy area situated in a region of native grasslands. The female had its scopae loaded with pollen and presumably was not harvesting only nectar (GARM, *pers. obs.*).

An overall, male-biased investment ratio of roughly 2:1 observed for *M. braziliensis* in our study is intriguing and its causes are unclear. Investment ratio is an important concept in behavioral ecology, which can be defined as the relative amount of energy allocated in the production of males *vs.* females (Danforth 1990), typically calculated from the weight ratio of the emerging offspring (Paini and Bailey 2002). It has been reasoned that an investment ratio of 2:1 in favor of males would imply that the production of a female would demand twice the effort expended for the production of a male (Fisher 1930; see also Torchio and Tepedino 1980). If Fisher's rational is correct, then the investment ratio of species whose females are heavier than males (as in most hymenopterans) should always be biased towards the latter—in fact, it is well known that the amount of food provisioned for female larvae is higher than for male larvae across Hymenoptera (e.g. Frohlich and Tepedino 1986; Johnson 1990; Arvidson et al. 2018; Farder-Gomes et al. 2018; Fawcett et al. 2019). As resources become scarcer, solitary bees tend to produce even more males because decrease in body size in female offspring has a proportionally higher negative impact on maternal fitness (Peterson and Roitberg 2006). Possibly, resource availability was relatively low either during the time period when this study was conducted, or, in AMNP in comparison with surrounding areas, which may have affected the sex ratio of *M. braziliensis*. This possibility is based on the well-established understanding that resource availability plays a major role in the determination of investment ratios in solitary bees (see Kim 1999). Testing this conjecture, however, was beyond the scope of our study.

## Conclusions

The remarkable new species of *Mourecotelles* described in this paper represents not only the first record of the genus in Brazil but also the first outside western South America (Chile, Argentina, Bolivia, and Ecuador). *Mourecotelles braziliensis* is morphologically very distinct from its congeners and can be easily recognized, among other features, due to its unique dark-orange mesosomal pubescence. We showed that trap-nesting is a useful method for studying relevant aspects about the nesting biology of *Mourecotelles* as the genus seems to comprise fundamentally cavity-nesting bees. Although we have found 11 different pollen morphotypes in brood cells of *M. braziliensis*, the species seems to be a specialist in the family Polygalaceae.

## Acknowledgements

We thank Fundação Araucária for the financial support, without which this study would not have been possible. We are very grateful to both Cláudia Inês Silva (São Paulo State University) and Cynthia Luz (“Maria Eneyda P. Kaufmann Fidalgo” Herbarium) for the identifications of the pollen samples. We are also indebted to Laurence Packer for allowing us to use his photographic equipment, which was purchased through a Canadian Foundation for Innovation award through Canadensys. RRF was supported by a President’s International Funding Initiative postdoctoral fellowship (grant 2020PB0130) and a National Natural Science Foundation of China research grant (grant 41761144068). GARM thanks Conselho Nacional de Desenvolvimento Científico e Tecnológico – CNPq for financial support (grant 309641/2016-0).

## References

- Aguiar CM, Garófalo CA (2004) Nesting biology of *Centris* (*Hemisiella*) *tarsata* Smith (Hymenoptera, Apidae, Centridini). *Revista Brasileira de Zoologia* 21: 477–486. <https://doi.org/10.1590/S0101-81752004000300009>
- Aguiar AP, Gibson GAP (2010) The spatial complexity in describing leg surfaces of Hymenoptera (Insecta), the problem and a proposed solution. *Zootaxa* 2415: 54–62. <https://doi.org/10.11646/zootaxa.2415.1.5>
- Albans KR, Aplin RT, Brehcist J, Moore JF, O’toole C (1980) Dufour’s gland and its role in secretion of nest cell lining in bees of the genus *Colletes* (Hymenoptera: Colletidae). *Journal of Chemical Ecology* 6: 549–564. <https://doi.org/10.1007/BF00987667>
- Almeida EAB (2008) Colletidae nesting biology (Hymenoptera: Apoidea). *Apidologie* 39: 16–29. <https://doi.org/10.1051/apido:2007049>
- Almeida EAB, Danforth BN (2009) Phylogeny of colletid bees (Hymenoptera: Colletidae) inferred from four nuclear genes. *Molecular Phylogenetics and Evolution* 50: 290–309. <https://doi.org/10.1016/j.ympev.2008.09.028>
- Almeida EAB, Packer L, Melo GAR, Danforth BN, Cardinal SC, Quintero FB, Pie MR (2019) The diversification of neopasiphaeine bees during the Cenozoic (Hymenoptera: Colletidae). *Zoologica Scripta* 48: 226–242. <https://doi.org/10.1111/zsc.12333>
- Ayres M, Ayres Jr M, Ayres DL, Santos ADA (2007) Aplicações estatísticas nas áreas das ciências bio-médicas. Instituto Mamirauá (Belém): 1–364.
- Ascher JS, Pickering J (2021) Discover Life bee species guide and world checklist (Hymenoptera: Apoidea: Anthophila). <https://www.discoverlife.org>
- Batra SWT (1980) Ecology, behavior, pheromones, parasites and management of the sympatric vernal bees *Colletes inaequalis*, *C. thoracicus* and *C. validus*. *Journal of the Kansas Entomological Society* 53: 509–538.
- Batra SWT, Schuster JC (1977) Nests of *Centris*, *Melissodes*, and *Colletes* in Guatemala (Hymenoptera: Apoidea). *Biotropica* 9: 135–138. <https://doi.org/10.2307/2387670>

- Bello MA, Rudall PJ, Hawkins JA (2012) Combined phylogenetic analyses reveal interfamilial relationships and patterns of floral evolution in the eudicot order Fabales. *Cladistics* 28: 393–421. <https://doi.org/10.1111/j.1096-0031.2012.00392.x>
- Benoist R (1942) Les hyménoptères qui habitent les tiges de ronce aux environs de Quito (Equateur). *Annales de la Société entomologique de France* 111: 75–90. <https://doi.org/10.1080/00378941.1943.10837496>
- Bosch J, Kemp WP (2000) Development and Emergence of the Orchard Pollinator *Osmia lignaria* (Hymenoptera: Megachilidae). *Physiological and Chemical Ecology* 29: 8–13. <https://doi.org/10.1603/0046-225X-29.1.8>
- Buchmann SL, O'Rourke MK (1991) Importance of pollen grain volumes for calculating bee diets. *Grana* 30: 591–595. <https://doi.org/10.1080/00173139109427817>
- Buschini MLT (2006) Species diversity and community structure in trap-nesting bees in Southern Brazil. *Apidologie* 37: 58–66. <https://doi.org/10.1051/apido:2005059>
- Buschini MLT, Fajardo S (2010) Biology of the solitary wasp *Trypoxylon (Trypargilum) agamemnon* Richards 1934 (Hymenoptera: Crabronidae) in trap-nests. *Acta Zoologica* 91: 426–432. <https://doi.org/10.1111/j.1463-6395.2009.00429.x>
- Camargo JMF, Pedro SRM (2003) Meliponini neotropicais: o gênero *Partamona* Schwarz, 1939 (Hymenoptera, Apidae, Apinae)-bionomia e biogeografia. *Revista Brasileira de Entomologia* 47: 311–372. <https://doi.org/10.1590/S0085-56262003000300001>
- Cane JH (1991) Soils of ground-nesting bees (Hymenoptera: Apoidea): texture, moisture, cell depth and climate. *Journal of the Kansas Entomological Society* 64: 406–413.
- Cane JH, Neff JL (2011) Predicted fates of ground-nesting bees in soil heated by wildfire: thermal tolerances of life stages and a survey of nesting depths. *Biological Conservation* 144: 2631–2636. <https://doi.org/10.1016/j.biocon.2011.07.019>
- Claude-Joseph F (1926) Recherches biologiques sur les Hyménoptères du Chili (Mellifères). *Annales des Sciences Naturelles, Zoologie* 10: 113–268.
- Cordeiro J (2005) Levantamento florístico de plantas lenhosas e caracterização fitossociológica de um remanescente de Floresta Ombrófila Mista em Guarapuava, PR. Master Thesis. Universidade Federal do Paraná (Curitiba), 1–144.
- Danforth BN (1990) Provisioning behavior and the estimation of investment ratios in a solitary bee, *Calliopsis (Hypomacrotera) persimilis* (Cockerell) (Hymenoptera: Andrenidae). *Behavioral Ecology and Sociobiology* 27: 159–168. <https://doi.org/10.1007/BF00180299>
- Diniz MR, Silva AG, Carreira LMM, Almeida EBD, Rêgo MMC (2021) Pollen Spectrum of Honey from the Bee *Melipona subnitida* Ducke (1910) in Restinga in Maranhão State. *Floresta e Ambiente* 28: e20200068. <https://doi.org/10.1590/2179-8087-floram-2020-0068>
- Diniz MER, Buschini MLT (2009) Biologia de nidificação de *Rhynchocolletes* sp. (Hymenoptera; Apoidea; Colletidae; Colletinae). *Anais do IX Congresso de Ecologia do Brasil, São Lourenço (Brazil), September 2009. Sociedade de Ecologia do Brasil, São Paulo*, 1–2.
- Dorado J, Vázquez DP (2016) Flower diversity and bee reproduction in an arid ecosystem. *PeerJ* 4: e2250. <https://doi.org/10.7717/peerj.2250>
- Duffield RM, Fernandes A, McKay S, Wheeler JW, Snelling RR (1980) Chemistry of the exocrine secretions of *Hylaesus modestus* (Hymenoptera; Colletidae). *Comparative Biochemistry and Physiology B* 67: 159–162. [https://doi.org/10.1016/0305-0491\(80\)90287-4](https://doi.org/10.1016/0305-0491(80)90287-4)

- Erdtman G (1960) The acetolysis method—a revised description. *Svensk Botanisk Tidskrift* 54: 516–564.
- Farder-Gomes CF, da Silva VP, Pereira TPL, Serrão JE, Pires EM, Oliveira MA (2018) Parasitism, sexual dimorphism and effect of host size on *Apocephalus atrophilus* offspring, a parasitoid of the leaf-cutting ant *Atta bisphaerica*. *Plos One* 13: e0208253. <https://doi.org/10.1371/journal.pone.0208253>
- Fawcett F, Minckley RL, Neff JL (2019) Foraging and provisioning behavior. In: Danforth BN, Minckley RL, Neff J (Eds) *The solitary bees: biology, evolution, conservation*. Princeton University Press (Princeton): 187–223. <https://doi.org/10.2307/j.ctvd1c929.11>
- Ferrari RR, Packer L (2021) Morphological phylogeny and review of the generic classification of Colletinae (Hymenoptera: Colletidae). *Zoological Journal of the Linnean Society* 193: 199–216. <https://doi.org/10.1093/zoolinnean/zlaa128>
- Fisher RA (1930) *The Genetical Theory of Natural Selection*. Clarendon Press (Oxford), 597 pp. <https://doi.org/10.5962/bhl.title.27468>
- Fortel L, Henry M, Guilbaud L, Mouret H, Vaissiere BE (2016) Use of human-made nesting structures by wild bees in an urban environment. *Journal of Insect Conservation* 20: 239–253. <https://doi.org/10.1007/s10841-016-9857-y>
- Frankie GW, Vinson SB, Newstrom LE, Barthell JF (1988) Nest site and habitat preferences of *Centris* bees in the Costa Rican dry forest. *Biotropica* 20: 301–310. <https://doi.org/10.2307/2388320>
- Fricke JM (1991) Trap-nest design for small trap-nesting Hymenoptera. *The Great Lakes Entomologist* 24: 121–122.
- Frohlich DR, Tepedino VJ (1986) Sex ratio, parental investment, and interparent variability in nesting success in a solitary bee. *Evolution* 40: 142–151. <https://doi.org/10.1111/j.1558-5646.1986.tb05725.x>
- Garófalo CA, Martins CF, Alves-dos-Santos I (2004) The Brazilian solitary bee species caught in trap nests. In: Freitas BM, Pereira JO (Eds) *Solitary Bees: Conservation, Rearing and Management for Pollination*. Imprensa Universitária (Fortaleza), 77–84.
- Gazola AL, Garófalo CA (2009) Trap-nesting bees (Hymenoptera: Apoidea) in forest fragments of the State of São Paulo, Brazil. *Genetics and Molecular Research* 8: 607–622. <https://doi.org/10.4238/vol8-2kerr016>
- Houston TF (1975) Nests, behaviour and larvae of the bee *Stenotritus pubescens* (Smith) and behavior of some related species (Hymenoptera: Apoidea: Stenotritinae). *Journal of the Australian Entomological Society* 14: 145–154. <https://doi.org/10.1111/j.1440-6055.1975.tb02016.x>
- Huang D, Kou R, Orr MC, Li H, Dou F, Zhu C (2021). Comparison of two criteria on the essential number calculation of *Andrena camellia*. *Bulletin of Entomological Research* 111: 364–370. <https://doi.org/10.1017/S0007485320000747>
- Iglesias A, Artabe AE, Morel EM (2011) The evolution of Patagonian climate and vegetation from the Mesozoic to the present. *Biological Journal of the Linnean Society* 103: 409–422. <https://doi.org/10.1111/j.1095-8312.2011.01657.x>
- Instituto de Desenvolvimento Rural do Paraná (2019) *Dados Meteorológicos Históricos e Atuais*. <http://www.idrparana.pr.gov.br/Pagina/Dados-Meteorologicos-Historicos-e-Atuais>

- Johnson MD (1990) Female size and fecundity in the small carpenter bee, *Ceratina calcarata* (Robertson) (Hymenoptera: Anthophoridae). *Journal of the Kansas Entomological Society* 63: 414–419.
- Kim JY (1999) Influence of resource level on maternal investment in a leaf-cutter bee (Hymenoptera: Megachilidae). *Behavioral Ecology* 10: 552–556. <https://doi.org/10.1093/beheco/10.5.552>
- Köppen W (1900) Versuch eine Klassifikation der Klimate vorzugsweise nach ihren Beziehungen zur Pflanzwelt. *Geographische Zeitschrift* 6: 593–611.
- Köppen W (1918) Klassifikation der Klimate nach Temperatur, Niederschlag und Jahreslauf. *Petermann's Mitteilungen* 64: 193–203.
- Luebert F (2021) The two South American dry diagonals. *Frontiers of Biogeography* 13: e51267. <https://doi.org/10.21425/F5FBG51267>
- Malyshev SI (1927) Lebensgeschichte des *Colletes cunicularius* L. *Zeitschrift für Morphologie und Ökologie der Tiere* 9: 390–409. <https://doi.org/10.1007/BF00408703>
- Martins CF, Neto VIS, Cruz RDM (2019) Nesting biology and mating behavior of the solitary bee *Epicharis nigrita* (Apoidea: Centridini). *Journal of Apicultural Research* 58: 512–521. <https://doi.org/10.1080/00218839.2019.1584963>
- McGinley RJ (1980) Glossal morphology of the Colletidae and recognition of the Stenotritidae at the family level (Hymenoptera: Apoidea). *Journal of the Kansas Entomological Society* 53: 539–552.
- Melo GA, Gonçalves RB (2005) Higher-level bee classifications (Hymenoptera, Apoidea, Apidae sensu lato). *Revista Brasileira de Zoologia* 22: 153–159. <https://doi.org/10.1590/S0101-81752005000100017>
- Meseguer AS, Lobo JM, Ree R, Beerling DJ, Sanmartín I (2015) Integrating fossils, phylogenies, and niche models into biogeography to reveal ancient evolutionary history: The case of *Hypericum* (Hypericaceae). *Systematic Biology* 64: 215–232. <https://doi.org/10.1093/sysbio/syu088>
- Michener CD (1960) Notes on the behavior of Australian colletid bees. *Journal of the Kansas Entomological Society* 33: 22–31.
- Michener CD (1964) Evolution of the nests of bees. *American Zoologist* 4: 227–239. <https://doi.org/10.1093/icb/4.2.227>
- Michener CD (1989) Classification of American Colletinae (Hymenoptera, Apoidea). *University of Kansas Science Bulletin* 53: 22–703.
- Michener CD (2007) *Bees of the World*. Second Edition. Johns Hopkins University Press (Baltimore): 1–1016.
- Michener CD, Brooks RW (1984) A comparative study of the glossae of bees (Apoidea). *Contributions of the American Entomological Institute* 22: 1–73.
- Michener CD, Lange RB (1957) Observations on the ethology of some Brazilian colletid bees (Hymenoptera, Apoidea). *Journal of the Kansas Entomological Society* 30: 71–80.
- Michener CD, Lange RB, Bigarella JJ, Salamuni R (1958) Factors influencing the distribution of bees' nests in earth banks. *Ecology* 39: 207–217. <https://doi.org/10.2307/1931865>
- Moure JS, Urban D, Melo GAR (2007) Colletini Lepeletier, 1841. In: Moure JS, Urban D, Melo GAR (Eds) *Catalogue of Bees (Hymenoptera, Apoidea) in the Neotropical Region*. *Sociedade Brasileira de Entomologia (Curitiba)*: 677–691.

- Paini DR, Bailey WJ (2002) Seasonal sex ratio and unbalanced investment sex ratio in the Bank-sia bee *Hylaeus alcyoneus*. *Ecological Entomology* 27: 713–719. <https://doi.org/10.1046/j.1365-2311.2002.00459.x>
- Paini DR, Roberts JD (2005) Commercial honey bees (*Apis mellifera*) reduce the fecundity of an Australian native bee (*Hylaeus alcyoneus*). *Biological Conservation* 123: 103–112. <https://doi.org/10.1016/j.biocon.2004.11.001>
- Pereira M, Garófalo CA, Camillo E, Serrano JC (1999) Nesting biology of *Centris (Hemisiella) vittata* Lepeletier in southeastern Brazil (Hymenoptera, Apidae, Centridini). *Apidologie* 30: 327–338. <https://doi.org/10.1051/apido:19990409>
- Peterson JH, Roitberg BD (2006) Impact of resource levels on sex ratio and resource allocation in the solitary bee, *Megachile rotundata*. *Environmental Entomology* 35: 1404–1410. <https://doi.org/10.1093/ee/35.5.1404>
- Potts S, Willmer PAT (1997) Abiotic and biotic factors influencing nest-site selection by *Halictus rubicundus*, a ground-nesting halictine bee. *Ecological Entomology* 22: 319–328. <https://doi.org/10.1046/j.1365-2311.1997.00071.x>
- Roubik DW (2006) Stingless bee nesting biology. *Apidologie* 37: 124–143. <https://doi.org/10.1051/apido:2006026>
- Rozen Jr JG (1984) Nesting biology of diphaglossine bees (Hymenoptera, Colletidae). *American Museum Novitates* 2786: 1–33.
- Rozen Jr JG, Favreau MS (1968) Biological notes on *Colletes compactus compactus* and its cuckoo bee, *Epeolus pusillus* (Hymenoptera: Colletidae and Anthophoridae). *Journal of the New York Entomological Society* 76: 106–111.
- Sakagami SF, Hayashida K (1960) Biology of the primitive social bee, *Halictus duplex* Dalla Torre II. Nest structure and immature stages. *Insectes Sociaux* 7: 57–98. <https://doi.org/10.1007/BF02225757>
- Scheloske HW (1974) Untersuchungen über das Vorkommen, die Biologie und den Nestbau der Seidenbiene *Colletes daviesanus* Sm. *Zoologische Jahrbücher: Abteilung für Systematik, Ökologie und Geographie der Tiere* 101: 153–172.
- Stephen WP (1954) A revision of the bee genus *Colletes* in America north of Mexico (Hymenoptera, Colletidae). *University of Kansas Science Bulletin* 36: 149–527.
- Torchio PF (1965) Observations on the biology of *Colletes ciliatoides* (Hymenoptera: Apoidea, Colletidae). *Journal of the Kansas Entomological Society* 38: 182–187.
- Torchio PF (1984) The nesting biology of *Hylaeus bisinuatus* Forster and development of its immature forms (Hymenoptera: Colletidae). *Journal of the Kansas Entomological Society* 57: 276–297.
- Torchio PF, Tepedino VJ (1980) Sex ratio, body size and seasonality in a solitary bee, *Osmia lignaria propinqua* Cresson (Hymenoptera: Megachilidae). *Evolution* 34: 993–1003. <https://doi.org/10.1111/j.1558-5646.1980.tb04037.x>
- Torchio PF, Trostle GE, Burdick DJ (1988) The nesting biology of *Colletes kincaidii* Cockerell (Hymenoptera: Colletidae) and development of its immature forms. *Annals of the Entomological Society of America* 81: 605–625. <https://doi.org/10.1093/aesa/81.4.605>
- Toro H, Cabezas V (1977) Nuevos generos y especies de Colletini sudamericanos, segunda parte. *Anales del Museo de Historia Natural de Valparíso* 10: 45–64.

- Toro H, Cabezas V (1978) Nuevos generos y especies de Colletini sudamericanos (Apoidea Colletidae). Segunda parte. Anales del Museo de Historia Natural de Valparíso 11: 131–148.
- Undurraga JM, Stephen WP (1980) Effect of temperature on development and survival in post-diapausing leafcutting bee pupae (*Megachile rotundata* (F.)). II. Low temperature. Journal of the Kansas Entomological Society 53: 677–682.
- Vivallo F (2021) Nesting behavior of the oil-collecting bee *Epicharis* (*Triepicharis*)  *analis* Lepeletier (Hymenoptera: Apidae) in an urban area of Rio de Janeiro, RJ, Brazil. Journal of Apicultural Research 60: 135–142. <https://doi.org/10.1080/00218839.2020.1820150>
- Zhao Y, Ding L, Yuan F, Zhang Y, Tu L, Zhu C (2010) Nesting biology of *Colletes gigas* Cockerell (Hymenoptera: Colletidae). Acta Entomologica Sinica 53: 1287–1294.



# First report of a gynandromorph of *Florilegus condignus* (Cresson, 1878) (Hymenoptera, Apidae), with notes on phenology and abundance

Katherine A. Parys<sup>1,2</sup>, Kendal A. Davis<sup>2</sup>, Sharilyn T. James<sup>1,3</sup>,  
J. Brian Davis<sup>3</sup>, Heather Tyler<sup>4</sup>, Terry Griswold<sup>5</sup>

**1** USDA Agricultural Research Service, Pollinator Health in Southern Crop Ecosystems Research Unit, Stoneville, MS, USA **2** USDA Agricultural Research Service, Southern Insect Management Research Unit, Stoneville, MS, USA **3** Mississippi State University Department of Wildlife, Fisheries and Aquaculture, Mississippi State, MS, USA **4** USDA Agricultural Research Service, Crop Production Management Research Unit, Stoneville, MS, USA **5** USDA Agricultural Research Service, Pollinating Insect – Biology, Management, Systematics Research Unit, Logan, UT, USA

Corresponding author: Katherine A. Parys ([katherine.parys@usda.gov](mailto:katherine.parys@usda.gov))

Academic editor: Christopher K. Starr | Received 27 September 2021 | Accepted 27 January 2022 | Published 28 February 2022

<http://zoobank.org/FFAFADAA-E976-45B2-B166-1448B1DF4E87>

**Citation:** Parys KA, Davis KA, James ST, Davis JB, Tyler H, Griswold T (2022) First report of a gynandromorph of *Florilegus condignus* (Cresson, 1878) (Hymenoptera, Apidae), with notes on phenology and abundance. Journal of Hymenoptera Research 89: 233–244. <https://doi.org/10.3897/jhr.89.75857>

## Abstract

Gynandromorphs are individuals that exhibit aspects of both males and females simultaneously and are the most commonly reported sexual anomalies in bees. We describe the first known specimen of a gynandromorph of the specialist pollinator *Florilegus condignus* (Cresson, 1878) (Hymenoptera: Apidae: Eucerini) collected in an agricultural field in northwestern Mississippi, USA. Additionally, we include and discuss phenological data from collections made in Mississippi and the Mid-Atlantic region of the United States.

## Keywords

Development, morphology

## Introduction

Gynandromorphs are individuals that exhibit both male and female characteristics at the same time and are the most commonly reported sexual anomalies in bees (Hinojosa-Díaz et al. 2012). Several general overviews listing known gynandromorphs of bees have been previously published (Dalla Torre and Friese 1899; Wolf 2001, 2006; Wcislo et al. 2004; Michez et al. 2009; Hinojosa-Díaz et al. 2012). As of the latest comprehensive review published in 2012, over 150 gynandromorphs have been described from most bee families representing over thirty genera and are more frequently observed in *Andrena* (Andrenidae) and *Megachile* (Megachilidae). Other recent review papers have focused on gynandromorphs within individual genera of bees including *Megachile* (Sommaggio et al. 2021), *Osmia* (Kratochwil 2021), and *Xylocopa* (Lucia and Gonzalez 2013). Gynandromorphs are broadly divided into several categories following Wcislo et al. (2004) and Dalla Torre and Friese (1899): bilateral (divided left to right), transverse (divided dorsal to lateral), anterior-posterior (divided front to back), and mixed (mosaics, or combinations of the other types).

*Florilegus condignus* (Cresson, 1878) (Hymenoptera: Apidae: Eucerini) is the sole North American representative of its genus. LaBerge and Ribble (1966) describe the range within the United States as encompassing the east coast from New Jersey to Florida, west to Colorado, and south to the Mexico border. *Florilegus condignus* is considered a specialist pollinator across its entire range in the USA (Fowler 2020a, b; Fowler and Droege 2020), and is reported to be oligolectic on pickerelweed (*Pontederia* sp.). It has also been reported as an important pollinator for production of watermelon (*Citrullus lanatus* (Thunb.) Matsum. & Nakai) and alfalfa (*Medicago sativa* L.) (Mitchell 1962; LaBerge and Ribble 1966; Brewer 1974). Individuals were also collected in cotton fields in both Mississippi and Texas (Parys et al. 2020). Additional floral visitation records include sweet clover (*Melilotus* sp.), prairie milkweed (*Asclepias sullivantii* Engelm. ex A.Gray), common milkweed (*Asclepias syriaca* L.), wood mint (*Blephilia hirsute* (Pursh) Benth.), partridge pea (*Chamaecrista fasciculata* (Michx.) Greene), common buttonbush (*Cephalanthus occidentalis* L.), water willow (*Justicia americana* (L.) Vahl), lanceleaf frogfruit (*Phyla lanceolata* (Michx.) Greene), French grass (*Psoralea onobrychis* Nutt.), Appalachian mountain mint (*Pycnanthemum flexuosum* (Walter) Britton, Sterns & Poggenb.), mountain mint (*Pycnanthemum virginianum* (L.) T.Durand & B.D.Jacks. ex B.L.Rob. & Fernald), and hoary vervain (*Verbena stricta* Vent.) (Robertson 1928). The species is primarily observed from May through August in most eastern states of the USA, but records from April and September have been noted from Florida (Mitchell 1962). Here we describe the first known gynandromorph of the species *F. condignus* (Cresson, 1878), also the first known from the genus *Florilegus* along with information about phenology in two regions of the USA.

## Materials and methods

Specimens of *F. condignus* in Mississippi were collected through widespread sampling across Mississippi between 2015 and 2018 as part of ongoing pollinator studies at the USDA Agricultural Research Service located in Stoneville, MS. Additional data from

2017 was provided by a project at the Mississippi State University Department of Wildlife, Fisheries and Aquaculture in Mississippi State, MS. These projects used a variety of collecting techniques including directed netting, malaise traps (BugDorm, Taiwan), blue and yellow vane traps (BanfieldBio Inc./Springstar, Seattle, WA, USA), bee bowls (modified pan traps), and examining bycatch from other studies. Bee bowls were constructed and used following previously published protocols (Droege 2015; Parys et al. 2020).

Observations from the Mid-Atlantic region were obtained from the United States Geological Survey's Bee Inventory and Monitoring Lab (BIML) based at the Patuxent Wildlife Research Center in Maryland. The original dataset included 191 specimen records of *F. condignus*. We eliminated records all records with no collection dates and those that were beyond the Mid-Atlantic region of the United States (this left records from Delaware, District of Columbia, Maryland, and Virginia), leaving 187 records for analysis. Some of these records are included in a recently published data set that only included pan trapping efforts from BIML (Kammerer et al. 2020).

The gynandromorph specimen in our Mississippi study was collected in a blue vane trap filled with propylene glycol between 9–16 June, 2016. The trap was placed in a commercially farmed sunflower field (*Helianthus annuus* L.) planted for recreational hunting purposes, which was surrounded by cotton (*Gossypium hirsutum* L.) and soybean (*Glycine max* (L.) Merr.) production. Photographs of external morphology were taken using a Keyence VHX-7000, and the images were cropped and shadows removed using an airbrush in GNU Image Manipulation Program (GIMP v2.1). The specimen is currently housed at the Parys Laboratory (USDA Agricultural Research Service, Pollinator Health in Southern Crop Ecosystems Research Unit, Stoneville, MS). For identification the specimen was keyed out using Mitchell (1962).

Specimen data were only used in phenology analyses when greater than 10 specimens including both sexes were collected in any given year and region. The first and last two observations of each calendar year were used ( $n = 8$  per year per sex). Collection dates were converted to date within the calendar year (1–365) for use in analyses. Data sets were tested for normality using a Shapiro-Wilk test and for homogenous variances using an F-test (Box 1953; Shapiro and Wilk 1965). When the data were normally distributed and variances were similar, phenology between genders within a state or region was analyzed using Welch's two-sample t-tests (Murtaugh et al. 2012). When data were not normally distributed, a Mann-Whitney-Wilcoxon test was used (Mann and Whitney 1947). All statistical analyses were completed in R version 4.0.4 "Lost Library Book" (R Core Team 2019).

## Results

### Gynandromorph: *Florilegus (Florilegus) condignus* (Cresson, 1878)

**Descriptive remarks:** Specimen appears primarily female with the head bilaterally split and having both male and female characters. The specimen shows wear and some loss of hair, similar to most specimens collected in vane traps and washed.

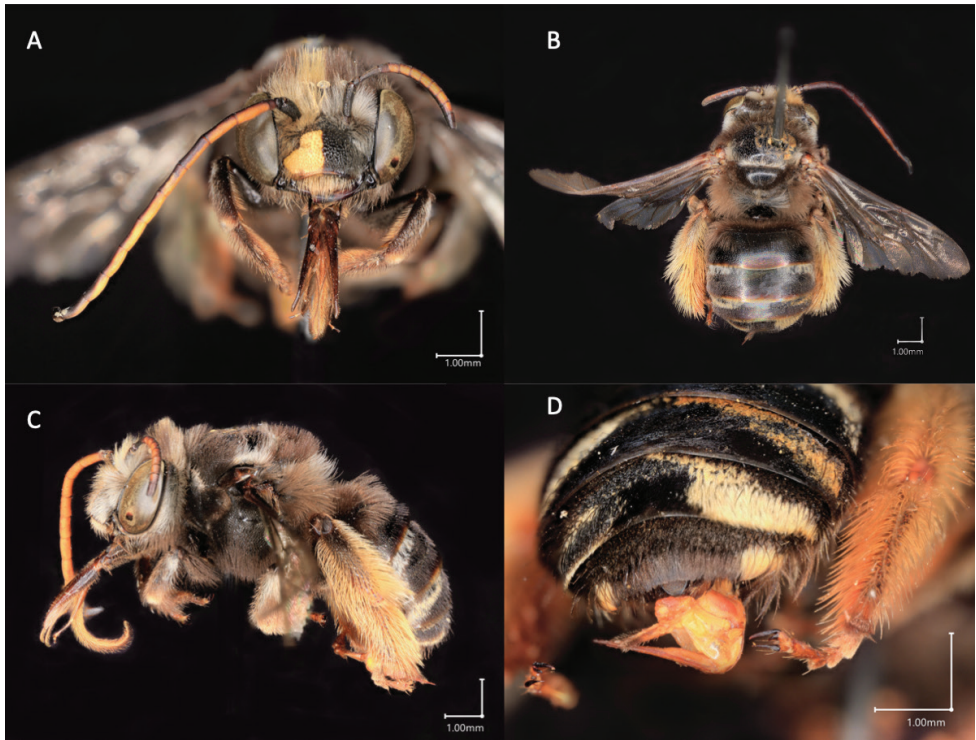


**Figure 1.** Images of the gynandromorph of *Florilegus condignus* **a** front view of the head and antennae **b** dorsal view **c** lateral view **d** final tergites of the abdomen with ovipositor.

**Head:** Bilaterally asymmetrical, right side with only male features as listed (Fig. 1A): right side of clypeus bright yellow. Flagellum of right antennae elongate, 13 segments and 11 flagellomeres as in other male Eucerini, median segments brown beneath and piceous above. Hairs along right side of face and vertex yellow as in typical male specimens. Left side of head typically female (Fig. 1A), as follows: dark clypeus, left antennal flagellum not elongate with 12 segments and 10 flagellomeres as in other female Eucerini, median segments brown beneath and black above. Hairs along left side of face and vertex brown as in typical female specimens. Both mandibles appear similar and are dark.

**Mesosoma and metasoma:** The mesosoma and metasoma present as fully female with ovipositor visible (Fig. 1B–D). Integument and legs black, tegulae brown, scutum shining with coarse punctures. Legs all appear as female, with light colored plumose scopa on both hind legs. Abdominal terga punctate almost to rim, with apical rim of terga alone impunctate. Terga are slightly iridescent. Full description of typical specimens available in Mitchell (1962).

**Material examined:** SIMRU5775, USA: Mississippi: Sunflower Co., Holly Ridge Plantation Sunflowers, 33.462079, -90.707222, 9–16 June 2016 – Blue Vane Trap, coll. Parys et. al.

**Table 1.** Collection methodology and abundance of *F. condignus* specimens collected in two regions.

Collection type	Mississippi			Mid-Atlantic/BIML		
	Female	Male	Total	Female	Male	Total
Pan Traps (no color given)	-	-	-	10	12	32
Pan Trap (Blue)	126	70	196	-	-	-
Pan Trap (White)	8	6	14	-	-	-
Pan Trap (Yellow)	12	0	12	-	-	-
Vane Trap (no color given)	-	-	-	25	8	33
Vane Trap (Blue)	387	167	554	-	-	-
Vane Trap (Yellow)	3	1	4	-	-	-
Malaise Trap	5	2	7	-	-	-
Agricultural Sweeping	1	1	2	-	-	-
Lepidopteran Pheromone Trap	1	0	1	-	-	-
Netting	8	3	11	12	109	121
Pitfall Trap	-	-	-	1	0	1

### *F. condignus* phenology

Overall, 999 specimen records were used from Mississippi and the Mid-Atlantic regions of the USA. Across both regions, the specimens were collected by various methods; most specimens (96%) were collected with pan and vane traps in Mississippi while the specimens from the Mid-Atlantic were primarily collected by netting (64.7%) (Table 1).

Between May 3 and November 10, 2018 a total of 812 specimens of *F. condignus* were collected from 12 counties in northern Mississippi (Fig. 2). There was no significant difference in date of first collected specimens between males and females ( $W = 29$ ,  $P = 0.79$ ), or in last date of specimen collection ( $t = 1.22$ ;  $df = 14$ ;  $P = 0.24$ ) (Fig. 3a, c).

An additional 187 specimens of *F. condignus* were collected from seven counties across three states: Virginia, Maryland, and the District of Columbia between 2003 and 2020. Of these 187 records, nine were included in the clean and publicly available dataset released by Kammerer et al. (2020). All individuals were collected between June and August (Fig. 4). There was no significant difference in date of first collected specimens between males and females ( $W = 45$ ;  $P = 0.18$ ), or in last date of specimen collection ( $W = 39.5$ ;  $P = 0.46$ ) (Fig. 3b, d).

### Discussion

The sexual dimorphism present in many species of bees offers unique opportunities to study gynandromorphs while using morphology to positively associate males and females of the same species in which only one sex is distinctive. Several theories of the occurrence of gynandromorphs have been proposed, especially in honeybees (*Apis mellifera* L.). Jones et al. (2021) provide a recent review of developmental mechanisms and the production of gynandromorphs. Multiple studies have suggested that extreme temperatures can increase the incidence of this phenomenon in bees and other

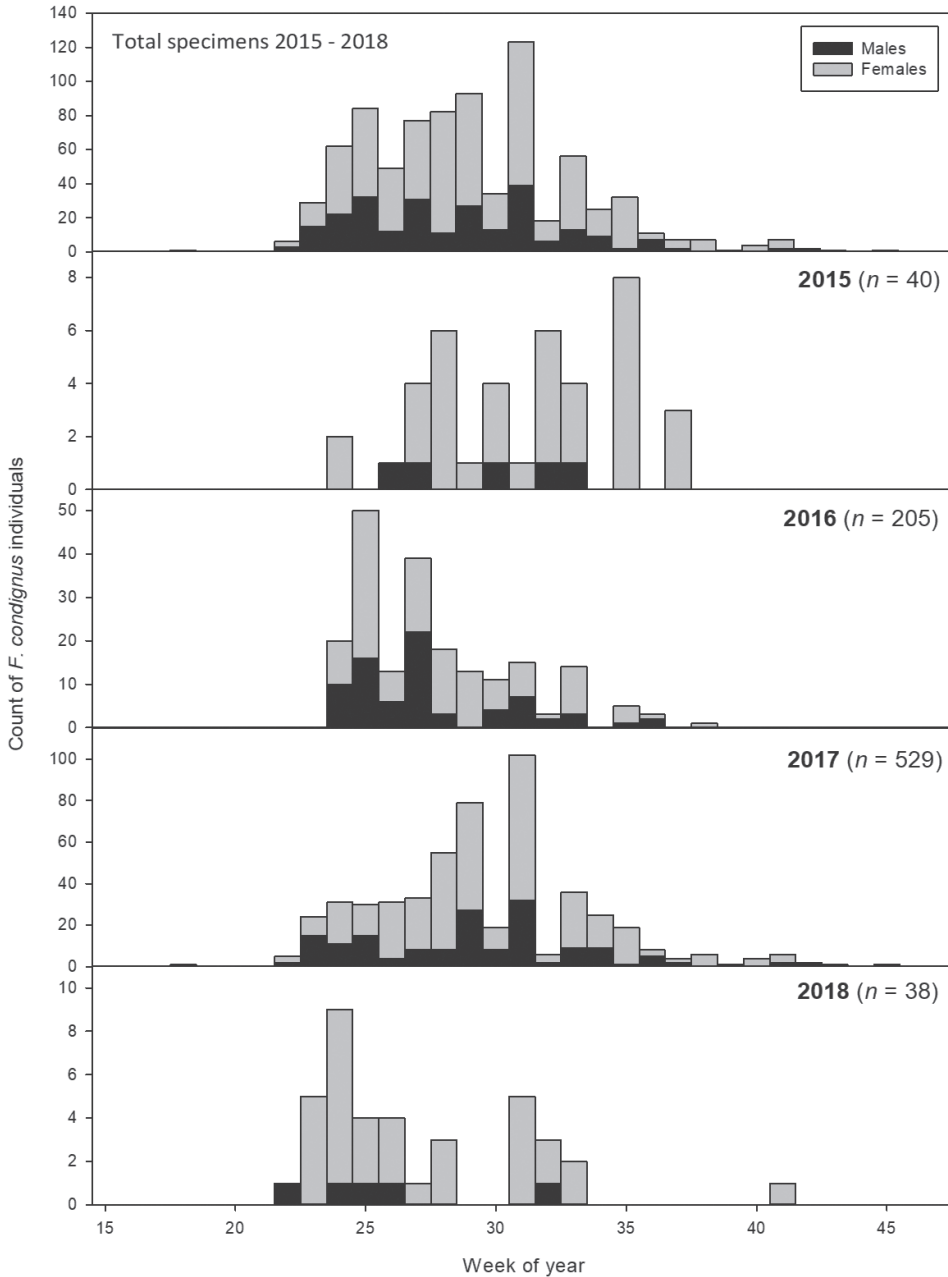


**Figure 2.** Total collections of *F. condignus* specimens in Mississippi in total by week of the year (top), and by individual years below.

hymenopterans (Drescher and Rothenbuhler 1963; Berndt and Kremer 1981; Kamping et al. 2007). Bees in the genus *Andrena* are known to be more likely intersex or gynandromorph if parasitized by stylopids (Salt 1931). Other studies suggest that bee gynandromorphs, at least in the genus *Megachile*, could have epigenetic origins

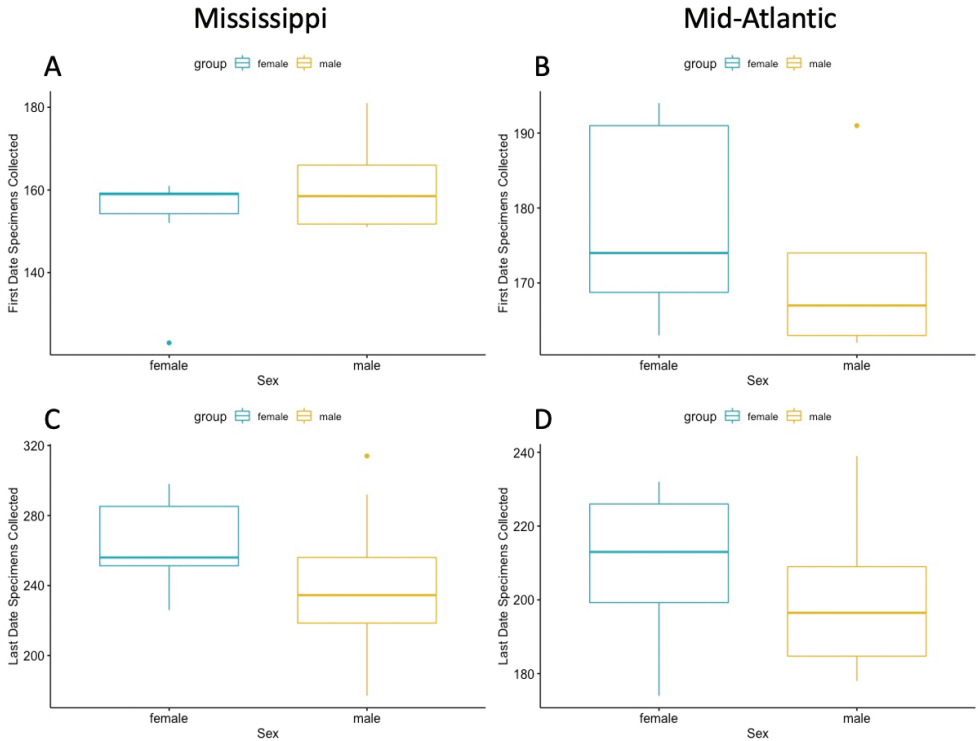


**Figure 3.** Box plots showing average first and last specimen collections of each year from two regions for four year (2015–2018).

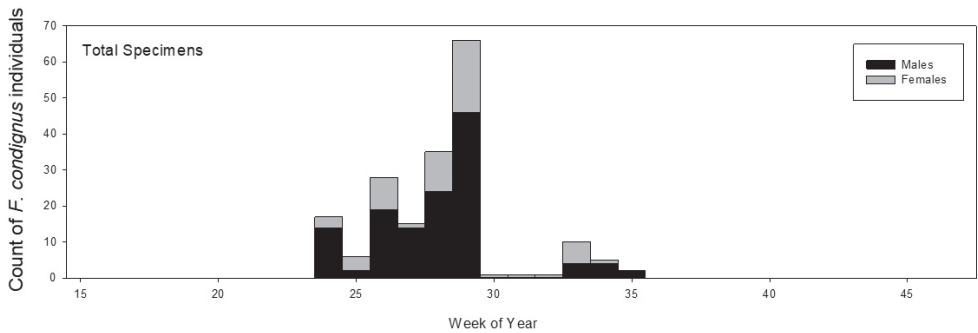


**Figure 4.** Total collections of *F. condignus* specimens in the Mid-Atlantic in total by week of the year.

(Sommaggio et al. 2021). Since gynandromorphs are rarely collected, especially in wild populations of bee species, little is known about the developmental mechanism or causes. Further research is needed, along with updated documentation of known occurrences of deviant phenotypes and their distribution across the phylogenetic landscape of bees and other Hymenoptera.

In addition to gynandromorphs, a variety of other mutations and deformities are known from bees including: variation in submarginal cells and other wing deformities

(Schneider and Feitz 2003; Sheffield and Heron 2017; Scarpulla 2018), missing antennae (Portman and Griswold 2016), eyes or ocelli (Lohrmann and Engel 2015), and malformed mouthparts (Orr and Tripodi 2017). Additionally, many of the newer observations available since the last comprehensive review are either citizen science records from platforms like bugguide and iNaturalist or observations published online alone from the USGS' Bee Monitoring and Inventory Lab (Kelly 2020; USGS BIML 2014). Such specimens are rare given the number of insects regularly collected and the recent worldwide focus on pollinator research.

*Florilegus condignus* is not commonly encountered in either Mississippi or the Mid-Atlantic region of the USA. Between 2015 and 2018, the USDA and MSU labs collected roughly 50 thousand specimens of bees across the northern part of the state as part of other studies, making *F. condignus* only 1.6% of specimens collected during that time frame. Kammerer et al. (2020) contains 99,053 specimen records from BIML pan traps in Maryland, Delaware, and the District of Columbia and only has nine *F. condignus* records suggesting that this species is only a fraction of the overall community that exists within the larger Mid-Atlantic region as well. Despite being overall uncommon, this is the first record of a specimen of *F. condignus* displaying morphological characteristics of both sexes. Additional records of gynandromorphs in the Eucerini are known from *Alloscirtetica* (Urban 1999), *Eucera* (Dalla Torre and Friese 1899; Morice 1903; Masuda 1940; Levchenko 2011; Jones et al. 2021), *Melissodes* (Cockerell 1906), and *Tetraloniella* (Dalla Torre and Friese 1899).

*Florilegus condignus* was active as early as May 3 and as late as November 10 during in Mississippi during the period of this study. In Nebraska, LaBerge and Ribble (1966) suggested a much shorter period of activity from July 3 to August 13, with peak abundance occurring in late July, while Mitchell (1962) noted early and late records of April and September from Florida. Other studies note protandrous patterns with male *F. condignus* emerged before females in Nebraska (LaBerge and Ribble 1966), our data appears to suggest that males were collected prior to females but the difference in collection dates between males and females were not statistically significant. Total data from the Mid-Atlantic region appear bimodal in Fig. 4, but that pattern was not seen in the total specimens in Fig. 2. These patterns are likely an artifact of sampling since this is aggregate data from many separate studies and collection methods. While we've only examined collection dates here, phenology and emergence of many wild or native non-*Apis* bee species are often strongly tied to temperature (Forrest and Thompson 2011; Ovaskainen et al. 2013; Kehrberger and Holzschuh 2019), and further studies should be done on this species.

As noted above, this species appears to be oligolectic, but additional studies are needed to determine whether it is narrowly specialized on pickerelweed and only visits other plants for nectar. The possibility remains that it is, in fact, polylectic and has been incorrectly reported as a specialist. Within the Southeastern US, some habitats or landcover types of western Mississippi, for example, may provide important resources for this species as many of the plant species listed by Robertson (1928) as visited by *F. condignus* are frequently present in or amid wetland habitats in western Mississippi (Gunn et al. 1980). *Florilegus condignus* was also recently detected in Arkansas

wetlands, across the Mississippi River from where collections were made in Mississippi (Stephenson et al. 2018). The phenological findings included in this paper alongside the description of a gynandromorph of *F. condignus* in Mississippi add to the generally limited knowledge about this species.

## Acknowledgements

Thank you to G. Chad Roberts, Leslie Price, Elizabeth Hanson, Raven Alison, KeAndrea Brown, Raksha Chatakondi, Megan Clark, and Shawnee Gundry for field and lab assistance. Special thanks to Sam Droege for providing data from the Mid-Atlantic United States. The manuscript was greatly improved following reviews from William T. Wcislo and an additional anonymous reviewer. This research was supported by the U.S. Department of Agriculture, Agricultural Research Service (USDA ARS). Mention of trade names or commercial products in this publication is solely for the purpose of providing specific information and does not imply recommendation or endorsement by the USDA. USDA is an equal opportunity provider and employer.

## References

- Berndt K-P, Kremer G (1981) Heat shock-induced gynandromorphism in the pharaoh's ant, *Monorium pharaonis* (L.). *Experientia* 38: 798–799. <https://doi.org/10.1007/BF01972277>
- Box GEP (1953) Non-normality and tests on variance. *Biometrika* 40: 318–335. <https://doi.org/10.1093/biomet/40.3-4.318>
- Brewer JW (1974) Pollination requirements for watermelon seed production. *Journal of Apicultural Research* 13: 207–212. <https://doi.org/10.1080/00218839.1974.11099780>
- Cockerell TDA (1906) XLVI. Descriptions and records of Bees. X. *The Annals and Magazine of Natural history, Zoology, Botany, and Geology* 102: 359–369. <https://doi.org/10.1080/00222930608562537>
- Dalla Torre KWv, Friese H (1899) Die hermaphroditen und gynandromorphen Hymenopteren [The hermaphrodite and gynandromorphic Hymenoptera]. 96 pp.
- Drescher W, Rothenbuhler WC (1963) Gynandromorph production by egg chilling: Cytological mechanisms in honey bees. *Journal of Heredity* 54: 194–201. <https://doi.org/10.1093/oxfordjournals.jhered.a107247>
- Forrest JRK, Thompson JD (2011) An examination of synchrony between insect emergence and flowering in Rocky Mountain meadows. *Ecological Monographs* 81: 469–491. <https://doi.org/10.1890/10-1885.1>
- Fowler J (2020a) Pollen specialist bees of the central United States. [https://jarrodflower.com/bees\\_pollen.html](https://jarrodflower.com/bees_pollen.html) [accessed 20 September 2021]
- Fowler J (2020b) Pollen specialist bees of the Western United States. [https://jarrodflower.com/pollen\\_specialist.html](https://jarrodflower.com/pollen_specialist.html) [accessed 20 September 2021]

- Fowler J, Droege S (2020) Pollen specialist bees of the Eastern United States. [https://jarrod-fowler.com/specialist\\_bees.html](https://jarrod-fowler.com/specialist_bees.html) [accessed 20 September 2021]
- Gunn CR, Pullen TP, Chandler JM, Barnes J (1980) Vascular flora of Washington County, Mississippi, and environs. Agricultural Research (Southern Region), Science and Education Administration, US Department of Agriculture, New Orleans, LA, 150 pp.
- Hinojosa-Díaz IA, Gonzalez VH, Ayala R, Mérida J, Sagot P, Engel MS (2012) New orchid and leaf-cutter bee gynandromorphs, with an updated review (Hymenoptera, Apoidea). *Zoosystematics and Evolution* 88: 205–214. <https://doi.org/10.1002/zoos.201200017>
- iNaturalist (2021) iNaturalist observations: *Xylocopa sonorina*. <https://www.inaturalist.org/observations/53282807>; <https://www.inaturalist.org/observations/53283045>; <https://www.inaturalist.org/observations/54525336> [accessed 28 October 2021]
- Jones LJ, Kilpatrick SK, López-Urbe MM (2021) Gynandromorph of the squash bee *Eucera (Peponapis) pruniosa* (Hymenoptera: Apidae: Eucerini) from an agricultural field in western Pennsylvania, USA. *Journal of Melittology* 100: 1–10.
- Kammerer M, Tooker JF, Grozinger CM (2020) A long-term dataset on wild bee abundance in Mid-Atlantic United States. *Scientific Data* 7: e240. <https://doi.org/10.1038/s41597-020-00577-0>
- Kamping A, Katju V, Beukeboom LW, Werren JH (2007) Inheritance of gynandromorphism in the parasitic wasp *Nasonia vitripennis*. *Genetics* 175: 1321–1333. <https://doi.org/10.1534/genetics.106.067082>
- Kehrberger S, Holzschuh A (2019) Warmer temperatures advance flowering in a spring plant more strongly than emergence of two solitary spring bee species. *PLoS ONE* 14: e0218824. <https://doi.org/10.1371/journal.pone.0218824>
- Kratochwil A (2021) First record of a gynandromorph of *Osmia submicans* MORAWITZ, 1870 (Hymenoptera, Megachilidae) – characterisation by morphological and morphometric parameters and critical note on gynander classification. *Linzer Biologische Beiträge* 53: 3–31.
- LaBerge WE, Ribble DW (1966) Biology of *Florilegus condignus* (Hymenoptera: Anthophoridae), with a description of its larva, and remarks on its importance in alfalfa pollination. *Annals of the Entomological Society of America* 59: 944–950. <https://doi.org/10.1093/aesa/59.5.944>
- Levchenko TV (2011) Materiali po faune pchel (Hymenoptera: Apoidea) Moskovskoi oblasti. 2. Semeistvo Apidae. Podsemeistva Apinae (кrome *Bombus* Latr.) i Xylocopinae [Contributions to the fauna of bees (Hymenoptera: Apoidea) of Moscow Province. 2. Family Apidae. Subfamilies Apinae (excluding *Bombus* Latr.) and Xylocopinae.]. *Eversmannia* 27–28: 87–104.
- Lohrmann V, Engel MS (2015) A quadriocellar scoliid wasp (Hymenoptera, Scoliidae) from Mallorca, with a brief account of supernumerary ocelli in insects. *Zoosystematics and Evolution* 91: 191–197. <https://doi.org/10.3897/zse.91.5463>
- Lucia M, Gonzalez VH (2013) A new gynandromorph of *Xylocopa frontalis* with a review of gynandromorphism in *Xylocopa* (Hymenoptera: Apidae: Xylocopini). *Annals of the Entomological Society of America* 106: 853–856. <https://doi.org/10.1603/AN13085>
- Mann HB, Whitney DR (1947) On a test of whether one of two random variables is stochastically larger than the other. *Annals of Mathematical Statistics* 18: 50–60. <https://doi.org/10.1214/aoms/1177730491>

- Masuda H (1940) シロスチヒゲナガバチ (*Eucera difficillis* Perez) と その寄生蜂キマラバナバチ (*Nomada japonica* Smith) (附: シロスチヒゲナガバチの1雌雄型) [Biological notes on *Eucera difficillis* Perez and whose parasitic bee, *Nomada japonica* Smith, with description of a gynandromorphic *Eucera*]. *Kontyû* 14: 45–60.
- Michez D, Rasmont P, Terzo M, Vereecken NJ (2009) A synthesis of gynandromorphy among wild bees (Hymenoptera: Apoidea), with an annotated description of several new cases. *Annales de la Société entomologique de France (NS)*45: 365–375. <https://doi.org/10.1080/00379271.2009.10697621>
- Mitchell TB (1962) Bees of the Eastern United States (II). North Carolina Agricultural Experiment Station Technical Bulletin 152: 1–557.
- Morice FD (1903) Exhibitions. The Proceedings of the Entomological Society of London for the Year 1903: i–ii.
- Murtaugh PA, Emerson SC, McEvoy PB, Higgs KM (2012) The statistical analysis of insect phenology. *Environ Entomol* 41: 355–361. <https://doi.org/10.1603/EN11260>
- Orr M, Tripodi A (2017) Stiff upper lip: Labrum deformity and functionality in bees (Hymenoptera, Apoidea). *Journal of Hymenoptera Research* 57: 89–101. <https://doi.org/10.3897/jhr.57.12510>
- Ovaskainen O, Skorokhodova S, Yakovleva M, Sukhov A, Kutenkov A, Kutenkova N, Shcherbakov A, Meyke E, Delgado Mdel M (2013) Community-level phenological response to climate change. *Proceedings of the National Academy of Sciences of the United States of America* 110: 13434–13439. <https://doi.org/10.1073/pnas.1305533110>
- Parys KA, Esquivel IL, Wright KW, Griswold T, Brewer MJ (2020) Native pollinators (Hymenoptera: Anthophila) in cotton grown in the Gulf South, United States. *Agronomy* 10(5): e698. <https://doi.org/10.3390/agronomy10050698>
- Portman ZM, Griswold T (2016) An anomalous specimen of *Perdita wasbaueri* Timberlake with only one antenna (Hymenoptera: Andrenidae). *Journal of the Kansas Entomological Society* 89: 267–269. <https://doi.org/10.2317/0022-8567-89.3.267>
- R Core Team (2019) R: A language and environment for statistical computing (<https://www.R-project.org/>). 4.0.4 “Lost Library Book” ed. R Foundation for Statistical Computing, Vienna.
- Robertson C (1928) Flowers and Insects, Lists of visitors of four hundred and fifty-three flowers. The Science Press Printing Company, Carlinville. <https://doi.org/10.5962/bhl.title.11538>
- Salt G (1931) A further study of the effects of stylopization on wasps. *Journal of Experimental Biology* 59: 133–166. <https://doi.org/10.1002/jez.1400590107>
- Scarpulla EJ (2018) Four submarginal cells on a forewing of *Melitoma taurea* (Say) (Hymenoptera) Apidae, and a summary of known records of atypical and variable numbers of submarginal cells. *Insecta Mundi* 0667: 1–28.
- Schneider N, Feitz F (2003) Malformations observées chez quatre abeilles et neuf guêpes du Luxembourg (Hymenoptera, Aculeata). *Bulletin (Société des naturalistes luxembourgeois)* 104: 95–98.
- Shapiro SS, Wilk MB (1965) An analysis of variance test for normality (complete samples). *Biometrika* 52: 591–611. <https://doi.org/10.1093/biomet/52.3-4.591>
- Sheffield CS, Heron J (2017) An unusual specimen of the subgenus *Lasioglossum* Curtis from British Columbia, Canada (Hymenoptera, Halictidae). *Journal of the Entomological Society of British Columbia* 114: 87–92.

- Sommaggio D, Fusco G, Uliana M, Minelli A (2021) Possible epigenetic origin of a recurrent gynandromorph pattern in *Megachile* wild bees. *Insects* 12(5): e437. <https://doi.org/10.3390/insects12050437>
- Stephenson PL, Griswold TL, Arduser MS, Dowling APG, Kremetz DG (2018) Checklist of bees (Hymenoptera: Apoidea) from managed emergent wetlands in the lower Mississippi Alluvial Valley of Arkansas. *Biodiversity Data Journal* 6: e24071. <https://doi.org/10.3897/BDJ.6.e24071>
- The Very Handy Manual (2015) The Very Handy Manual: How to Catch and Identify Bees and Manage a Collection. [http://www.pwrc.usgs.gov/nativebees/Handy%20Bee%20Manual/The\\_Very\\_Handy\\_Manual.pdf](http://www.pwrc.usgs.gov/nativebees/Handy%20Bee%20Manual/The_Very_Handy_Manual.pdf) [accessed 15 July 2015]
- Urban D (1999) Ginandromorfia em *Alloscirtetica brethesi* (Jorgensen) (Hymenoptera, Anthophoridae) [Gynandromorph of *Alloscirtetica brethesi* (Jorgensen) (Hymenoptera, Anthophoridae)]. *Revista Brasileira de Zoologia* 16: 171–173. <https://doi.org/10.1590/S0101-81751999000500008>
- USGS BIML [USGS Bee Inventory and Monitoring Lab] (2021) *Anthidium oblongatum*. <https://www.flickr.com/photos/usgsbiml/albums/72157663081604293> [accessed 28 October 2021]
- Wcislo WT, Gonzalez VH, Arneson L (2004) A review of deviant phenotypes in bees in relation to brood parasitism, and a gynandromorph of *Megalopta genalis* (Hymenoptera: Halictidae). *Journal of Natural History* 38: 1443–1457. <https://doi.org/10.1080/0022293031000155322>
- Wolf H (2001) Bemerkungen zu zwittern unter den Stechimmen (Hymenoptera: Aculeata). *Linzer Biologische Beiträge* 33: 579–581.
- Wolf H (2006) Bemerkungen zu zwittern unter den Stechimmen (Hymenoptera: Aculeata) II. *Linzer Biologische Beiträge* 38: 1725–1726.

## Book review: Ichneumonid wasps (Hymenoptera, Ichneumonidae): their classification and biology

Mostafa Ghafouri Moghaddam<sup>1</sup>, Diana Carolina Arias-Penna<sup>2</sup>,  
Minoo Heidari Latibari<sup>3,4</sup>

**1** *Yas com., Zahedan, Sistan and Baluchestan, P. O. Code: 98169-87383, Iran* **2** *Bogotá D. C., Cundinamarca, Colombia* **3** *Department of Plant Protection, College of Agriculture, Ferdowsi University of Mashhad, Mashhad, P. O. Box: 91779-48974, Iran* **4** *Czech Academy of Sciences, Biology Centre, Institute of Entomology, České Budějovice, Czech Republic*

Corresponding author: Mostafa Ghafouri Moghaddam ([m.ghafourim@yahoo.com](mailto:m.ghafourim@yahoo.com))

---

Academic editor: Michael Ohl | Received 5 February 2022 | Accepted 13 February 2022 | Published 28 February 2022

<http://zoobank.org/591E0195-82D5-4329-9D58-7BC34AB4C06D>

---

**Citation:** Ghafouri Moghaddam M, Arias-Penna DC, Heidari Latibari M (2022) Book review: Ichneumonid wasps (Hymenoptera, Ichneumonidae): their classification and biology. *Journal of Hymenoptera Research* 89: 245–247. <https://doi.org/10.3897/jhr.89.81731>

---

Many of us have encountered the difficulty of identifying a specimen due to the paucity and scattered availability of specialized papers and books. This shortage of information applies to all hierarchical levels. However, things are changing for good that allied to a rather fluid taxonomy as our knowledge has evolved. The handbook entitled *Ichneumonid Wasps (Hymenoptera: Ichneumonidae): their Classification and Biology* (Broad et al. 2018; Fig. 1) made its debut four years ago. This comprehensive and highly detailed manual is part of the Royal Entomological Society (RES) handbooks series. It encompasses roughly 418 pages making it a treasure trove of information about Darwin wasps. It constitutes an up-to-date and thoughtful review of ichneumonid. The handbook is divided into four main sections. Firstly, it includes aspects of classification, biology, conservation, collecting, rearing, and preservation; secondly, functional morphology; thirdly, identification key. The largest part is the last section, which consists of individual treatment for each subfamily.

This manual offers a massive amount of information for the identification of ichneumonid wasps circumscribed to the United Kingdom of Great Britain and Ireland. Nevertheless, the identification keys and the detailed account for each of the 35 subfamilies are useful to identify ichneumonids from surrounding areas as well as world-



**Figure 1.** Front/back covers and authors of the present book. Left to right: Mark. R. Shaw, Michael G. Fitton and Gavin R. Broad (Photo credit: Lucy Broad).

wide, data that are seldom brought together in one place. Despite the rapidly changing concepts of higher classification of this family, the authors, Dr. Broad, Dr. Shaw, and Dr. Fitton (Fig. 1), made a substantial effort for providing a comprehensive review of current knowledge on systematic, biology, host relations, and most relevant species-level identification. They also present this complex information in a straightforward language appropriate for academics and non-specialists to unlock a huge treasure chest of species that were reputation for being 'difficult' to identify. The manual incorporates a large number of high-resolution colored images and black/white line drawings that allow an easy understanding of the morphological characteristics presented both in keys and in each subfamily taxonomic treatment. Another aspect that embraces the handbook is host associations. This kind of information is extremely convenient for field entomologists that try to emulate the rigorous techniques for rearing Hymenoptera parasitoids. Each chapter is complemented with relevant references making it an excellent source for finding specialized literature and subsequently will give readers an opportunity for exploring this economically important group.

In summary, *Ichneumonid Wasps (Hymenoptera: Ichneumonidae): their Classification and Biology* is a valuable acquisition especially if you are an amateur hymenopterologist. The handbook can be purchased through online bookstores and although the high price (£70, including shipping cost) might be a deterrent for many students, the investment pays off in the long run. It is already a benchmark publication, for that reason its addition to a personal library from any broad-minded entomologist or naturalist is more than welcome. It should also be part of the libraries of universities and museums.

## Acknowledgements

We gratefully acknowledge Edward Baker (Diversity and Informatics Division of the Natural History Museum, London, UK), who checked and improved the draft manuscript linguistically. We greatly appreciate to Jose L. Fernandez-Triana (Canadian National Collection of Insects, Ottawa, Canada), whose careful reading and freely offered and helpful suggestions resulted in many improvements to the paper. We would also like to thank subject editor, Michael Ohl (Museum für Naturkunde, Berlin, Germany), who put forward the valuable comments to this paper.

## Reference

- Broad GR, Shaw MR, Fitton MG (2018) *Ichneumonid Wasps (Hymenoptera: Ichneumonidae): their Classification and Biology*. *Handbooks for the Identification of British Insects* 7(12): 1–418.

